

The Development of an *In vitro* Model using Equine Hepatocytes and Liver Microsomes for the Study of Drug Metabolism in the Horse

By

Khaled Ayad Shibany

DVM, MSc

Thesis submitted to the University of Nottingham for the degree of Doctor of Philosophy

Division of Comparative Medicine

School of Veterinary Medicine and Science

The University of Nottingham

Abstract

Horses are extensively exposed to various kinds of medication. However, limited information is available about how these medications are metabolised in this species. Hence, the development of strategies and methods that provide a better understanding of different metabolic pathways for different drugs is of major importance.

Although, the horse is considered as a monogastric animal, it is also a hind gut fermenting animal, i.e. most of the feed is degraded in the cecum and colon. Thus, it is hypothesised that this could result in an evolutionary difference in xenobiotic metabolising enzymes between human and horses which may lead to different pharmacokinetics.

Therefore, the main aim of this study is to develop an *in vitro* model as a preclinical testing system of newly developed substances for horses using freshly isolated, cryopreserved equine hepatocytes and liver microsomes.

Fresh hepatocytes were isolated and liver microsomes were prepared using livers which were obtained from horses, post slaughter. Part of the freshly isolated hepatocytes were cryopreserved.

A comparison metabolic study was carried out to compare the three *in vitro* systems. The intrinsic clearance (Cl_{int}) of three drugs used in equine medicine omeprazole, flunixin and phenylbutazone, was determined via the substrate depletion method. The determined Cl_{int} values were extrapolated to *in vivo* hepatic clearance (Cl_H) using two *in vitro* liver models, namely, well stirred and parallel tube models. To perform the extrapolation step, the values of microsomal protein per gram of liver (MPPGL) and the number of hepatocytes per gram of liver in the horse (HPGL), also known as the hepatocellularity, key scaling factors in both the well-stirred and parallel tube models, were obtained for horse. These scaling factors were determined by comparing the CYP P450 content in microsomes and cryopreserved hepatocytes against the CYP P450 content of the liver.

Additionally, HPGL was also calculated from the ratio of liver protein concentration to matched hepatocyte suspension protein concentration.

Effects of ageing on CYP P450 content, MPPGL and HPGL values were also investigated. Furthermore, chloramphenicol's potential effect on the *in vivo* AUC for omeprazole was predicted using microsomes.

In the present study, freshly isolated equine hepatocytes were successfully cryopreserved and the viability of recovered cells, after a 30% Percoll gradient, was 77 ± 11% and estimated recovery rate was approximately 27%. MPPGL and HPGL values ranged 41-73 mg/gram of liver (mean= 57 mg/gram of liver, n=39) and 146 - 320 × 10^6 cells/g of liver (Average = 227× 10^6 cells/g of liver, n=18) using CYP P450 method; and 156 - 352 × 10^6 cells/g of liver (Average = 232× 10^6 cells/g of liver) using protein method. It was found that increase in age had no effect on CYP P450/mg microsomal protein content.

This study successfully predicted the *in vivo* clearance for omeprazole, flunixin and phenylbutazone using, both, freshly isolated and cryopreserved equine hepatocytes. Meanwhile, microsomes significantly underpredicted the *in vivo* hepatic clearance Cl_H. However, microsomes were used in present study to perform drug-drug interaction (DDI) *in vitro* study between omeprazole and chloramphenicol. The average of IC_{50} and the inhibitor constant K_i of the three horses were 17.7±5.8 μM and 15.4±5 μM, respectively.

The work presented in this thesis paves the way to develop *in vitro* models using equine hepatocytes and liver microsomes, which are reproducible, scalable and compatible with screening platforms. These models can be applied to the improvement of predicted detection times (DT) in horse racing which may aid veterinarians to estimate accurate withdrawal times; hence, the horse welfare will be improved. Moreover, further phase II metabolism, drug induction and comparative studies can be performed.

The following published paper contain work undertaken for this thesis:

Shibany, K. A., Tötemeyer, S., Pratt, S. L., & Paine, S. W. (2016). Equine hepatocytes: isolation, cryopreservation, and applications to in vitro drug metabolism studies. *Pharmacology Research & Perspectives*, *4*(5), 1–8.

Declaration

I declare that the work presented in this thesis was carried out in accordance with the requirements of the Nottingham University Regulations.

The work is original except where indicated by specific reference in the text, and has not been submitted for any other academic award at the University of Nottingham or any other institution.

Name: Khaled Ayad S. Shibany

Signed:

Date:

Conferences, Posters and Oral Presentations:

1. Khaled A. Shibany, Sabine Tötemeyer and Stuart Paine, 2014. The Development of an *In vitro* Model using Isolated Equine Hepatocytes and Equine Live Microsomes for the Study of Drug Metabolism in the Horse, (the social, economic and scientific impact of the project) Faculty Postgraduate Research Forum (Medicine and Health Sciences Faculty) University of Nottingham, (25/06/2014, Nottingham, UK). (Poster and oral presentation).

2. Khaled A. Shibany, Sabine Tötemeyer and Stuart Paine, 2015. Determination of a Horse Hepatic Microsomal Scaling Factor for Predicting In vivo Metabolic Clearance, 13th European Meeting of the International Society for the Study of Xenobiotics (Strathclyde University, Glasgow, UK). (Poster presentation).

3. The British Equine Veterinary Association (BEVA) Congress 2014 (10th to 13th of September 2014 – Birmingham. UK). (Attendance).

4. Postgraduate Research Day (Second Year); Oral Presentation, in Veterinary Medicine and Science, Nottingham University; 8 January 2015.

5. The Development of an *In vitro* Model using Equine Hepatocytes and Liver Microsomes for the Study of Drug Metabolism in the Horse. Invited oral presentation. LGC, Newmarket, Cambridgeshire, UK, 29 January 2015.

6. Prediction of *in vitro* equine hepatic metabolic clearance values for omeprazole, flunixin and phenylbutazone. Invited oral presentation. LGC, Newmarket, Cambridgeshire, UK, 25 July 2016.

7. Khaled A. Shibany, Sabine Tötemeyer and Stuart Paine 2017. Cryopreserved Equine Hepatocytes: A potential alternative for animal experimentation. East Midlands 3Rs Symposium (2017) (19th September 2017, The University of Nottingham, Nottingham, UK) (Poster presentation).

This thesis is dedicated to the memory of my father, Ayad S. Shibany, who passed away in March 2014. I miss him every day, and I wish if he saw this process through to its completion.

Acknowledgements

First and foremost, thanks to the God Almighty, the most merciful and the most beneficial for being with me all the way. With his silent blessings, each day was a new chapter of hope. Second, I must thank my parents for their love and support throughout my life. Thank you both for giving me strength to reach for the stars and chase my dreams. My sisters and brothers deserve my wholehearted thanks as well.

I would like to sincerely thank my supervisors, Dr. Stuart W. Paine and Dr. Sabine Tötemeyer for all their support, patience, valuable discussions and advice, constant supervision and, mainly, for believing in me in tough times.

Most of the results described in this thesis would not have been obtained without close help from people and laboratories. I owe a great deal of appreciation and gratitude to Mr Wayne Sanders, Biobank, Faculty of Medicine & Health Sciences, University of Nottingham, for sample collection, Prof. Andy Salter, food science, University of Nottingham, for help in preparation of equine liver microsomes, Mr. Michael Goengresh, physiology department, Medical School, University of Nottingham, for CYP P450 measurments and Miss Stefannie Pratt for assistance in omeprazole kinetic studies and optimisation of purification of recovered crypreserved equine hepatocytes protocol.

I wish to express my unqualified thanks to my wife, SEHAM, I could never have accomplished this thesis without her love, support, and understanding. I also wish to thank my sons ABDULMUHAIMEN and MOHAMED and my daughters ARWA, RAGHD and HLA for doing their best to understand a father who had to be confined to his study for such a long time, making the Sutton Bonington Campus his home.

Last but certainly not least, thanks to people and the government of my country, Libya. I could not have gone through the doctoral program overseas

without their financial support. I would like to express my full appreciation to the staff of the Department of Scholarship, Ministry of Higher Education and scientific research of Libya and Cultural Attaché in the Libyan Embassy-London for their generous support, both financial and moral.

Table of contents

Abstract i
Aknowledgments vii
1 Introduction 1
1.1 Pharmacokinetics 2
1.1.1 Absorption 2
1.1.2 Distribution 3
1.1.2.1 Membrane transport 3
1.1.3 Metabolism/biotransformation 4
1.1.3.1 Metabolism and Transport Interplay 6
1.1.3.2 Equine Drug Metabolism 7
1.1.4 Cytochrome P450 Enzyme 9
1.1.4.1 Nomenclature of CYP P450 10
1.1.4.2 Equine CYP P450 10
1.1.5 Excretion 11
1.1.6 Elimination 12
1.1.6.1 Plasma Clearance 12
1.2 Drugs used in equine medicine 13
1.3 Drug detection time and withdrawal time in the context of Equine Sports Competition 15
1.4 The liver 20
1.4.1 Liver anatomy and architecture 20
1.4.2 Hepatic lobule and hepatocyte 22
1.4.2.1 Liver extracellular matrix 24
1.4.3 Liver *in vitro* pharmacology systems 24
1.4.3.1 Liver microsomes 25
1.4.3.2 Isolated hepatocytes 26
1.4.4 Hepatocyte isolation 27
1.4.5 Cryopreserved hepatocytes 27
1.4.5.1 Requirements for successful cryopreservation protocol 28
1.5 Tissue like *in vitro* systems 30
1.6 *In vitro* Kinetics 31
1.6.1 Chemical Kinetics 31
1.6.2 First Order Reaction 31
1.6.3 Zero Order Reactions 33
1.6.4 Enzyme kinetics 34
1.6.4.1 Enzyme catalysis 34

1.6.4.2 Michaelis-Menten kinetics 35
1.6.4.3 The Significance of $\boldsymbol{Vmax}$ and $\boldsymbol{Km}$ 43
1.7 Predictions of hepatic xenobiotic clearance 43
1.8 *In vitro-in vivo* extrapolation (IVIVE) 46
1.8.1 Drug binding 48
1.9 Drug-Drug interactions 49
1.9.1 Enzyme inhibition 50
1.9.1.1 Reversible inhibition 50
1.9.1.2 Quasi-irreversible inhibition 53
1.9.1.3 Irreversible inhibition 54
1.9.1.4 Substrate auto inhibition 54
1.9.2 Cytochrome P450 induction 55
1.10 Hypothesis and Aims 55
2 Materials and Methods 58
2.1 Preparation of equine liver homogenates and microsomes 58
2.1.1 Horse liver tissue 58
2.1.2 Homogenisation of liver samples 58
2.1.3 Preparation of microsomes 58
2.1.4 Protein determination 59
2.1.5 Cytochrome P450 determination 59
2.1.6 Correction for loss of microsomal protein 60
2.2 Isolation of primary equine hepatocytes 60
2.2.1 Equipment and reagents 60
2.2.2 Source of liver samples 61
2.2.3 Hepatocyte preparation 61
2.2.4 Purification of the initial cell suspension 62
2.2.5 Determination of hepatocytes yield and viability 63
2.2.6 Cryopreservation of equine hepatocytes 63
2.2.7 Thawing of cryopreserved hepatocytes 64
2.2.8 Storage 64
2.2.9 Percoll purification 65
2.2.10 Measurement of viability in cultured hepatocytes 65
2.2.10.1 Attachment efficiency 66
2.2.10.2 Determination of horse HPGL 67
2.2.10.3 Homogenization of hepatocyte suspensions 67
2.2.10.4 Determination of Hepatocellularity 67
2.2.10.5 The operator (researcher) influence on estimated 67
2.3 Age related alteration in the size of equine hepatocytes 68

2.3.1 Preparation of histological sections 68
2.4 Determination of Michaelis-Menten parameters for omeprazole, flunixin and phenylbutazone 69
2.4.1 Linearity of initial reaction rate with respect to mg microsomal protein or number of hepatocytes per ml 69
2.4.2 Microsomes 70
2.4.3 Fresh hepatocytes 70
2.4.4 Cryopreserved hepatocytes 71
2.4.5 LC/MS method development 71
2.4.6 LC/MS Analysis 72
2.4.7 Enzyme Kinetic Analysis 72
2.4.8 Estimating blood hepatic clearance 72
2.4.9 Drug-Drug interaction study 73
2.5 Statistical analysis 73
3 Preliminary studies 76
3.1 Introduction 76
3.1.1 Why use primary hepatocytes 76
3.1.2 Cryopreservation and recovery of equine hepatocytes 77
3.1.3 Comparison of Enzyme activity in fresh and cryopreserved equine hepatocytes 77
3.2 Results 78
3.2.1 Isolation of equine hepatocytes 78
3.2.2 Cryopreservation and recovery of equine hepatocytes 79
3.2.3 Effect of storage in liquid nitrogen 80
3.2.4 Cell viability and attachment 80
3.2.5 Percoll Purification 80
3.2.6 Comparison of intrinsic clearance and metabolite formation between fresh and cryopreserved equine hepatocytes 81
3.2.7 Optimisation of incubation conditions 81
3.3 Discussion 86
4 91
4.1 Introduction 91
4.1.1 Variability of microsomal protein per gram of liver and the effect of age 92
4.1.2 Age-related alterations in the number and size of equine hepatocytes 93
4.2 Results 94
4.2.1 Hepatocyte scaling factor (Hepatocellularity) 94
4.2.2 Inter-Individual Variability of horse MPPGL and HPGL and the effect of age 100

4.2.3 Age-Related alterations in the size and number of equine hepatocytes 103
4.3 Discussion 106
5 111
5.1 Introduction 111
5.1.1 Drug-drug interactions 113
5.2 Results 114
5.2.1 LCMS method development 114
5.2.2 Linearity of initial reaction rate with respect to number of cells or mg microsomal protein 116
5.2.3 Omeprazole Metabolism by Freshly Isolated Equine Hepatocytes 117
5.2.4 Omeprazole Metabolism by Cryopreserved Equine Hepatocytes 119
5.2.5 Omeprazole Metabolism by Equine Liver Microsomes 121
5.2.6 Metabolite appearance 123
5.2.7 *In vitro* comparison of Cl_{int} 127
5.2.8 *In vitro in vivo* extrapolation 128
5.2.9 Drug interaction study 129
5.3 Discussion 132
6 138
6.1 Introduction 138
6.2 Results 141
6.2.1 Flunixin 141
6.2.1.1 LCMS analysis of flunixin 141
6.2.1.2 Linearity of initial reaction rate with respect to number of cells or mg microsomal protein 141
6.2.1.3 Flunixin metabolism in freshly isolated equine hepatocytes 142
6.2.1.4 Cryopreserved hepatocytes 144
6.2.1.5 Equine liver microsomes 146
6.2.1.6 Metabolite appearance 148
6.2.1.7 *In vitro* comparison of Cl_{int} 151
6.2.1.8 *In vitro in vivo* extrapolation 151
6.2.2 Phenylbutazone 153
6.2.2.1 LCMS analysis of phenylbutazone 153
6.2.2.2 Linearity of initial reaction rate with respect to number of cells or mg microsomal protein 154
6.2.2.3 Phenylbutazone metabolism in freshly isolated equine hepatocytes 154
6.2.2.4 Cryopreserved hepatocytes 156

6.2.2.5 Equine liver microsomes 158
6.2.2.6 Metabolite appearance 160
6.2.2.7 *In vitro* comparison of Cl_{int} 166
6.2.2.8 *In vitro in vivo* extrapolation 167
6.3 Discussion 169
7 General discussion 173
Reference 169

List of tables

Table 3.2.1: Overview of the results of the 18 horse liver perfusions 79
Table 3.2.2: Summary of equine liver perfusions and Cell viabilities and yield, pre, and post cryopreservation. 81
Table 3.2.3: Kinetic incubation method trialled and outcomes..... 84
Table 5.2.1: Kinetic parameters from fresh hepatocyte incubations at 1 million cells/mL 119
Table 5.2.2: Kinetic parameters from cryopreserved equine hepatocyte incubations at 1 million cells/mL 121
Table 5.2.3: Microsome kinetic parameters 123
Table 5.2.4: K_m determined from metabolite formation in freshly isolated equine hepatocytes for 3 horses. 125
Table 5.2.5: K_m determined from metabolite formation in cryopreserved equine hepatocytes for 3 horses. 126
Table 5.2.6: K_m determined from metabolite formation in equine liver microsomes for 3 horses..... 126
Table 5.2.7: The average of K_m determined from drug disappearance and metabolite formation in microsomes, fresh and cryopreserved hepatocytes (n=3). 126
Table 5.2.8: Cl_{int} correction for unbound fraction in incubation and unit standardisation for equine microsomes, fresh and cryopreserved hepatocytes 127
Table 5.2.9: Hepatic clearance in microsomes, fresh and cryopreserved hepatocytes following scaling to liver Cl_{int} using both models 128
Table 5.2.10: Plasma hepatic clearance for in vitro and in vivo studies . 129
Table 5.2.11: IC_{50} and K_i determined from an interaction study performed on equine microsomes (n=3) 131
Table 6.2.1: Kinetic parameters from fresh hepatocyte incubations at 1 million cells/mL 144
Table 6.2.2: Kinetic parameters from cryopreserved hepatocyte incubations at 1 million cells/mL 146
Table 6.2.3: Cl_{int} from equine liver microsome incubations at 1 mg protein/mL..... 148
Table 6.2.4: Cl_{int} unit standardisation for fresh, cryopreserved hepatocytes and equine liver microsomes 151
Table 6.2.5: Hepatic clearance in microsomes, fresh and cryopreserved hepatocytes following scaling to liver Cl_{int} and Cl_H using both models 152
Table 6.2.6: Blood and plasma hepatic clearance for in vitro and in vivo studies 153
Table 6.2.7: Cl_{int} obtained from freshly isolated hepatocyte incubations at 1 million cells/mL 156
Table 6.2.8: Cl_{int} obtained from cryopreserved hepatocyte incubations at 1 million cells/mL 158
Table 6.2.9: Cl_{int} obtained from equine liver microsome incubations at 1 mg protein/mL..... 160
Table 6.2.10: Oxyphenbutazone formation Cl_{int} in liver microsome incubations at 1 mg protein/ml..... 166
Table 6.2.11: Cl_{int} unit standardisation for equine microsomes, fresh and cryopreserved hepatocytes 166
Table 6.2.12: Cl_{int} unit standardisation for equine microsomes..... 167
Table 6.2.13: Enzyme kinetics in microsomes, fresh and cryopreserved hepatocytes following scaling to liver Cl_{int} and Cl_H..... 167

Table 6.2.14: Enzyme kinetics in microsomes following scaling to liver Cl_{int} and CL_H 168
Table 6.2.15: Plasma hepatic clearance for in vitro and in vivo studies . 169

List of figures

Figure 1.4.1: Liver of the horse, schematic, visceral surface (cited from Bragulla et al. (2004) 21
Figure 1.4.2: Hepatic lobules in relation to afferent and efferent vessels, three-dimensional, schematic (cited from Bragulla et al., 2004). 22
Figure 1.4.3: Liver lobule 23
Figure 1.4.4: Location of CYPs in the cell. The Figure shows increasingly microscopic levels of detail, sequentially expanding the areas within the black boxes. Cited from Brunton et al. (2012). 26
Figure 1.6.1: Graphical presentation of initial velocity against substrate concentration 32
Figure 1.6.2: Mono-exponential Decay Curve. The mono-exponential decay curve describes first-order elimination when plotted as concentration versus time. 33
Figure 1.6.3: Energy change for an uncatalysed reaction and a catalysed reaction. Enzymes decrease the Gibbs free energy of activation, but they have no effect on the free energy ΔG of reaction. 34
Figure 1.6.4: Graphical presentation of velocity against substrate concentration in an enzyme catalysed reaction. The graphical segments showing first-order and zero-order kinetics are marked. This Figure, also, shows the relationship between the rate of reaction for a simple Michaelis-Menten rate law. The reaction rate reaches a limiting value (saturates) at the $\boldsymbol{Vmax}$. $\boldsymbol{Km}$ is the substrate concentration that gives half the maximum rate. 35
Figure 1.6.5: A double-reciprocal plot, between velocity (v) and [S]. 40
Figure 1.6.6: Eadie-Hofstee plot 41
Figure 1.6.7: Hanes-Wolf plot 42
Figure 1.8.1: In vitro to in vivo scaling 47
Figure 1.8.2: Schematic diagram of the liver. The "Well stirred" model (A) describes the liver as a single well stirred compartment. The difference between the rate of presentation of drug to and its rate of exit from the liver at steady state is represents the rate of drug elimination. The dashed line represents the unbound hepatic drug concentration. The "Parallel tube" model (B) views the liver as a series of identical and parallel cylinders; each cylinder represents a sinusoid with enzymes distributed evenly in hepatocytes lining the tubes. The dashed line represents the declining unbound hepatic drug concentration along the direction of blood flow. Adapted from Pang and Rowland (1977). 48
Figure 1.9.1: The scheme of competitive inhibition 51
Figure 1.9.2: Non-competitive inhibition 52
Figure 1.9.3: Uncompetitive inhibition 53
Figure 2.2.1: (a) Perfusion setup. [A] Peristaltic pump, [B] water bath, [C] glass jacketed condenser, [D] bubble trap. (b) Liver piece with curved irrigation cannulae with olive tips inserted in blood vessels on a Büchner funnel. (c) Digested liver tissue: the digested areas appear bulged and pale in colour (left side). 63
Figure 2.3.1: HE staining, 200X – liver normal structure in 1-year-old (1), 19-year-old (2) and <21-year-old horse (3). High magnification (400X) shows microscopic view of a portal triad; small hepatic arterial (A), portal vein (V), bile duct (B), Lymph vessel (L) (1a), mononuclear, binuclear and polynuclear hepatocytes (arrow) and Kupffer cells (K). 69

Figure 3.2.1: Effect of storage time on equine hepatocyte post-thaw viability. Cryopreserved hepatocytes were stored in liquid nitrogen from 2 days to 480 days. 80
Figure 3.2.2: Comparison of intrinsic clearance between fresh and cryopreserved horse hepatocytes (average presented by dash line) for omeprazole (A), flunixin (B) and phenylbutazone (C) (n=3 horse for each drug). The results show that there is no significant difference between fresh and cryopreserved equine hepatocytes, p>0.5..... 83
Figure 3.2.3: HPLC–MS chromatograms of oxidation metabolites of omeprazole in extracellular medium of fresh (A=0 min and B=30min) and recovered cryopreserved (C=0 min and D= 30 min) equine hepatocytes. $1x10^6$ freshly isolate and recovered cryopreserved equine hepatocytes/ml were incubated with omeprazole as described under Materials and Methods during 30 min. The ratio between the peak areas of M1, M2 and M3 was 2:1:1, respectively in both fresh and cryopreserved hepatocytes. 85
Figure 3.2.4: HPLC–MS chromatogram of metabolites of phenylbutazone in extracellular medium of fresh (A=0 min and B=30min), and recovered cryopreserved (C=0 min and D= 30 min) equine hepatocytes. $1x10^6$ freshly isolated and recovered cryopreserved equine hepatocytes/ml were incubated with omeprazole as described under Materials and Methods during 30 min. 85
Figure 4.2.1: Relationship between whole homogenate P450 (nanomoles per gram liver) and microsomal P 450 (nanomoles per milligram protein). There is a statistically significant ($r^2 = 0.533$) ($p=0.05$) relationship between these metrics. 94
Figure 4.2.2: Effect of operator (researcher) on MPPGL (a) and HPGL (b) values. There was no correlation between measurements and time for a 21-month period ($p > 0.05$). 95
Figure 4.2.3: (A) Relation between nmol P450/g of liver and horse age (n=39). (B) Comparisons of the three different age groups were made using a one-way ANOVA followed by Tukey's multiple comparison test. ** = P<0.05, ***=P<0.01 101
Figure 4.2.4: (A) Relation between nmol P540/mg of liver microsomal protein and horse age. Each value represents the average±SD for triplicate of one horse. (n=39). (B) Comparisons of the three different age groups were made using a one-way ANOVA followed by Tukey's multiple comparison test. 101
Figure 4.2.5: (A) Correlation between CYP P450 content per 10^6 hepatocytes and horse age. (B) Comparisons of the three different age groups were made using a one-way ANOVA followed by Tukey's multiple comparison test * = P<0.05 101
Figure 4.2.6: Effect of increasing age on protein in liver microsomes (A). (n=39). Comparisons of the three different age groups were made using a one-way ANOVA followed by Tukey's multiple comparison test (B). ** = P<0.05..... 102
Figure 4.2.7: Relationship between HPGL and horse age. (n=18). Each value represents the average ± SD for 3-9 horses. Comparison of the three different age groups was made using a one-way ANOVA followed by Tukey's multiple comparison test. ** = P<0.05, ***=P<0.01... 102
Figure 4.2.8: Relationship between HPGL and CYP P450 content per 10^6 cells for 18 equine livers. There is statistically significant ($p<0.05$) inverse relationship ($r^2 = 0.3926$), between these values. 103

Figure 4.2.9: (A) The age-related changes in the size of hepatocytes is presented in this graph. There is a decline in cell size between 0 and 19 years, followed by a significant increase between 19 and 29 years ($p<0.05$). Each value represents the average ± SD for 3 horses. (B) Comparison of the three different age groups was made using a one-way ANOVA followed by Tukey's multiple comparison test. *= $P<0.05$ 104
Figure 4.2.10: (A) The age-related changes in the number of cells of hepatocytes per unit area is presented in this graph. There is a significant increase in number of cells between 0 and 19 years, followed by a significant decline between 19 and 29 years ($p>0.05$) (a). Each value represents the average ± SD for 3 horses. (B) Comparison of the three different age groups was made using a one-way ANOVA followed by Tukey's multiple comparison test. * and ** = $P<0.05$. 104
Figure 4.2.11: (A) Relationship between HPGL and number of cells and (B) cell size (b). There is a strong ($r^2 = 0.8294$ and 0.7323), statistically significant ($p<0.05$) relationship between these values, respectively. 105
Figure 5.1.1: Structure of omeprazole (Chung et al., 2004) 111
Figure 5.2.1: Mass chromatograms for omeprazole standard (a) and microsomes incubation for 25 µM omeprazole at t=0, with internal standard lansoprazole (b). Peaks were observed at m/z 346 and 370 for omeprazole, lansoprazole, respectively. 114
Figure 5.2.2 Mass chromatograms showing omeprazole (m/z 346) disappearance and metabolite (M1, M2 and M3) (m/z 362) appearance with internal standard (lansoprazole) (m/z 370) in microsomes at the following time points; 0, 10, 20 and 60 minutes. 115
Figure 5.2.3: Linearity of initial reaction rate with respect to number of hepatocytes in 1 ml incubation (A). Linearity of initial reaction rate with respect to microsomal protein concentration in 1 ml incubation (B and C). 116
Figure 5.2.4: depletion concentration-time profile in freshly isolated equine hepatocytes. Data was plotted as the natural logarithm (Ln) of substrate concentration over initial concentration against time. Only time points fall within the linear time period of the reaction and allow the assumption of initial rate conditions were chosen. K_{dep} is represented by the slope of the line (refer to table A.III.3, horse 1). 118
Figure 5.2.5: Michealis-Menten curve for freshly isolated equine hepatocytes with omeprazole. Initial rate (µM/min) is plotted against substrate concentration. 119
Figure 5.2.6: depletion concentration-time profile in cryopreserved equine hepatocytes. Data was plotted as the natural logarithm (Ln) of substrate concentration over initial concentration against time. Only time points fall within the linear time period of the reaction and allow the assumption of initial rate conditions were chosen. K_{dep} is represented by the slope of the line (refer to table A.III.3, horse 1). 120
Figure 5.2.7: Michealis-Menten curve for cryopreserved equine hepatocytes with omeprazole. Initial rate (µM/min) is plotted against substrate concentration. 121

Figure 5.2.8: data gathered using various omeprazole concentrations with equine microsomes. Data was plotted as the natural logarithm (Ln) of substrate concentration over initial concentration against time. Only time points fall within the linear time period of the reaction and allow the assumption of initial rate conditions were chosen. K_{dep} is represented by the slope of the line (refer to table A.III.3, horse 1). 122
Figure 5.2.9: Michaelis-Menten plot demonstrating omeprazole metabolism by equine microsomes. 123
Figure 5.2.10: Omeprazole metabolites appearance in freshly isolated (A), cryopreserved (B) equine hepatocytes and microsomes (C) at 25 µM omeprazole. 124
Figure 5.2.11: Michaelis-Menten plots demonstrating omeprazole metabolites appearance in freshly isolated (A), cryopreserved (B) equine hepatocytes and microsomes (C) (Refer to Table A.III.4, horse 1). 125
Figure 5.2.12: K_m Values determined using drug disappearance and metabolite formation. Each value represents the average ± SD (n=3). Comparison of the three different systems was made using a two-way ANOVA followed by Tukey's multiple comparison test. *= $p<0.05$, **=$p<0.01$. 127
Figure 5.2.13: Hepatic clearances of omeprazole determined from microsomes, fresh and cryopreserved equine hepatocytes (well stirred model). Significant difference between three systems was tested using one-way ANOVA with Tukey's test. *=$p < 0.05$, **=$p<0.01$. 129
Figure 5.2.14: data gathered using various chloramphenicol concentrations with equine microsomes and omeprazole as the substrate. Data was plotted as the natural logarithm (Ln) of substrate concentration against time. K_{dep} is represented by the slope of the line. 130
Figure 5.2.15: Dose-response curve demonstrating chloramphenicol inhibition of omeprazole metabolism in microsomes (refer to Table A.III.7). 131
Figure 5.2.16: The predicted effect of increasing concentrations of chloramphenicol on the AUC for *in vivo* omeprazole pharmacokinetics 132
Figure 6.1.1: Metabolism of flunixin to 5'hydroxyflunixin. Adapted from "Determination and confirmation of 5-hydroxyflunixin in raw bovine milk using liquid chromatography tandem mass spectrometry" by Boner et al. (2003). 139
Figure 6.1.2: Phase I metabolism of phenylbutazone in the horse. Adapted from Scarth et al. (2011). 140
Figure 6.2.1: Chromatogram for monitoring flunixin disappearance. The ion of mass 297.26 was monitored at a retention time of 4.75 minutes. 141
Figure 6.2.2: Linearity of initial reaction rate of flunixin with respect to number of hepatocytes in 1 ml incubation (A). Linearity of initial reaction rate with respect to microsomal protein concentration in 1 ml incubation (B and C). 142
Figure 6.2.3: Metabolism of flunixin by freshly isolated hepatocytes. Data was plotted as the natural logarithm (Ln) of substrate concentration against time. Only time points fall within the linear time period of the reaction and allow the assumption of initial rate conditions were

chosen. K_{dep} is represented by the slope of the line (refer to table A.IV.3, horse 1)..... 143
Figure 6.2.4: Michaelis-Menten plot demonstrating flunixin metabolism by fresh hepatocytes 144
Figure 6.2.5: metabolism of flunixin by cryopreserved hepatocytes. Data was plotted as the natural logarithm (Ln) of substrate concentration against time. Only time points fall within the linear time period of the reaction and allow the assumption of initial rate conditions were chosen. K_{dep} is represented by the slope of the line (refer to table A.IV.1.3, horse 1)..... 145
Figure 6.2.6: Michaelis-Menten plot demonstrating flunixin metabolism by cryopreserved hepatocytes 146
Figure 6.2.7: Metabolism of flunixin by equine liver microsomes. Data was plotted as the natural logarithm (Ln) of substrate concentration against time. Only time points fall within the linear time period of the reaction and allow the assumption of initial rate conditions were chosen. K_{dep} is represented by the slope of the line (refer to table A.IV.1.3, horse 1)..... 147
Figure 6.2.8: Michaelis-Menten plot demonstrating flunixin metabolism by equine liver microsomes. 148
Figure 6.2.9: Graphs derived from flunixin metabolite appearance in equine liver microsomes at 50 µM flunixin..... 149
Figure 6.2.10: Flunixin metabolite appearance in microsomes at various flunixin concentrations (refer to A.IV.1.3, horse 1)..... 150
Figure 6.2.11: Michaelis-Menten plot demonstrating flunixin metabolite appearance in microsomes..... 151
Figure 6.2.12: Hepatic clearances (well stirred model) of flunixin in microsomes, fresh and cryopreserved equine hepatocytes. Significant difference between three systems was tested using one-way ANOVA with Tukey's test. **= $p < 0.05$. 152
Figure 6.2.13: Chromatogram for monitoring phenylbutazone disappearance. The ion of mass 209.19 was monitored at a retention time of 2.11 minutes..... 153
Figure 6.2.14 Linearity of initial reaction rate with respect to number of hepatocytes in 1 ml incubation (A). Linearity of initial reaction rate with respect to microsomal protein concentration in 1 ml incubation (B and C)..... 154
Figure 6.2.15: Metabolism of phenylbutazone by freshly isolated hepatocytes. Data was plotted as the natural logarithm (Ln) of substrate concentration against time. Only time points fall within the linear time period of the reaction and allow the assumption of initial rate conditions were chosen. K_{dep} is represented by the slope of the line (refer to A.IV.2.3, horse 1). 155
Figure 6.2.16: Michaelis-Menten plot demonstrating phenylbutazone metabolism by fresh hepatocytes..... 156
Figure 6.2.17: Metabolism of phenylbutazone by cryopreserved hepatocytes. Data was plotted as the natural logarithm (Ln) of substrate concentration against time. Only time points fall within the linear time period of the reaction and allow the assumption of initial rate conditions were chosen. K_{dep} is represented by the slope of the line (refer to Table. A.IV.2.3, horse 1)..... 157
Figure 6.2.18: Michaelis-Menten plot demonstrating phenylbutazone metabolism by cryopreserved hepatocytes..... 158

Figure 6.2.19: Metabolism of phenylbutazone by equine liver microsomes. Data was plotted as the natural logarithm (Ln) of substrate concentration against time. Only time points fall within the linear time period of the reaction and allow the assumption of initial rate conditions were chosen. K_{dep} is represented by the slope of the line (refer to table A.IV.2.3, horse 1). 159
Figure 6.2.20: Michaelis-Menten plot demonstrating phenylbutazone metabolism by equine liver microsomes. 160
Figure 6.2.21: Graphs derived from phenylbutazone metabolite appearance in equine liver microsomes at 50 µM. 161
Figure 6.2.22: Data for oxyphenbutazone production with freshly isolated hepatocytes. Concentration was determined using a stock of oxyphenbutazone of known concentration to convert mass spectrometry response into µM. Data was plotted as the concentration (in µM) against time (refer to table A.IV.2.4). 162
Figure 6.2.23: Data for oxyphenbutazone production with cryopreserved equine hepatocytes. Data was plotted as the concentration (in µM) against time. Concentration was determined using a stock of oxyphenbutazone of known concentration to convert mass spectrometry response into µM (refer to table A.IV.2.4) 163
Figure 6.2.24: Data for oxyphenbutazone production with equine liver microsomes. Concentration was determined using a stock of oxyphenbutazone of known concentration to convert mass spectrometry response into µM. Data was plotted as the concentration (in µM) against time (refer to table A.IV.2.4, horse 1). 165
Figure 6.2.25: Velocity obtained from oxyphenbutazone formation by equine liver microsomes as a function of phenylbutazone concentration, fit to a substrate inhibition model. 166
Figure 6.2.26: Hepatic clearances (well stirred model) of phenylbutazone in microsomes, fresh and cryopreserved equine hepatocytes. Significant difference between three systems was tested using one-way ANOVA with Tukey's multiple comparisons test. *= $p < 0.05$. 168

List of equations

1.1 12
1.2 16
1.3 16
1.4 17
1.5 17
1.6 17
1.7 18
1.8 19
1.9 19
1.10 19
1.11 19
1.12 20
1.13 31
1.14 31
1.15 32
1.16 32
1.17 33
1.18 33
1.19 33
1.20 36
1.21 36
1.22 37
1.23 37
1.24 37
1.25 37
1.26 37
1.27 37
1.28 38
1.29 38
1.30 38
1.31 38
1.32 38
1.33 38
1.34 39
1.35 39
1.36 40
1.37 40
1.38 41
1.39 44
1.40 44
1.41 44
1.42 45
1.43 45
1.44 45
1.45 47
1.46 47
1.47 49
1.48 51
1.49 51
1.50 51
1.51 51

1.52 52
1.53 55
2.1 60
2.2 60
2.3 67
2.4 72
2.5 73

Abbreviations

BSA	Bovine serum albumin
°C	Degree Celsius
Cl_H	Hepatic clearance
Cl_{int}	Intrinsic clearance
CYP	Cytochrome P450
2D	Two-dimensional
3D	Three-dimensional
DMSO	Dimethyl sulphoxide
ECM	Extracellular matrix
EGTA	Ethylene glycol-bis (β-aminoethylether)-N, N, N', N'-tetraacetic acid
FCS	Foetal calf serum
fu_{inc}	unbound fraction in the incubation medium
fu_p	unbound fraction in plasma
g	Gram
HPGL	Hepatocellularity Per Gram of Liver
HBSS	Hank's Balanced Salt solution
KCs	Kupffer cells
l	Litre
mg	milligram
µg	microgram
ml	millilitre
µl	microliter
mM	millimolar
µM	micromolar
MPPGL	Microsomal Protein per Gram of Liver
nm	nanometre
NADPH	Nicotinamide adenine dinucleotide phosphate
NaCl	Sodium chloride

PBS	Phosphate buffered Saline
pmol	Pico mole
RER	Rough endoplasmic reticulum
SD	Standard deviation
SER	Smooth endoplasmic reticulum
UDPGT	Uridine diphosphate-glucuronosyltransferase
UW	University of Wisconsin
WEM	Williams' medium E

Chapter 1
Introduction and Aims

1 Introduction

Horses are considered as companion animals, but also as a food producing species in certain countries. Furthermore, according to the British Horseracing Authority (BHA), the British racing industry has an overall impact of £3.45bn on the British economy (British Horseracing Authority, 2013). Horses are extensively exposed to different kinds of medication (Nebbia et al., 2003; Scarth et al., 2011). However, limited information is available about how drugs are metabolised in this species. Thus, a better understanding of equine drug metabolism is important for optimal drug dosing regimens and to predict potential drug-drug interaction (DDI). Consequently, equine veterinary surgeons will be better informed with regard to the outcomes of administered drugs and as a result, potential DDIs may be avoided. This will ultimately lead to improved welfare of the horse population. Furthermore, with a greater understanding of how drugs are metabolised the detection of drug abuse in equine sports such as horseracing and equestrian eventing will be better regulated. Consequently, the development of strategies and methods that provide better understanding of different metabolic path-ways for different drugs is of major importance.

The liver is considered the predominant organ of metabolism for the majority of endogenous chemicals and xenobiotics. This has led to the development of a set of liver-based approaches that can be used to study drug metabolism *in vitro* (Brandon et al., 2003). In the last three decades, *in vitro* metabolism has gained significant popularity in the drug discovery process. Primarily, this has been due to a number of factors, including the controversial ethical issues involved with studies using animals, because, first it wrongly violates the "rights" of animals, and second, it wrongly imposes on sentient creatures much "avoidable suffering" (Cohen, 1987). Thus, for many decades people have continued to debate, defend and protest animal use in these kind of

experiments and research. On the other hand there is a questionable applicability of the data to human; also there are significant financial costs associated with *in vivo* studies (Ferdowsian and Beck, 2011). Isolated hepatocytes and microsomes are considered as the most common and practical systems used to study drug metabolism *in vitro* (Brown and Houston 2007).

1.1 Pharmacokinetics

Pharmaceutical compounds act on different molecular targets inside the body. The desired pharmacological effect can only be achieved when a specific concentration of unbound drug reaches the site of action. Hence, the drug concentration at different sites is a key element of the pharmacological efficiency of any drug therapy.

Pharmacokinetics (PK) is defined as ''the study of kinetics of absorption, distribution, metabolism and excretion (ADME) of drugs and their corresponding pharmacologic, therapeutic, or toxic responses in man and animals'' (American Pharmaceutical Association 1972). Hence, pharmacokinetics enables to quantify the drug absorption, distribution, metabolism and excretion (ADME) (Ionescu and Caira 2005; Alsanosi et al. 2014).

1.1.1 Absorption

The movement of drugs from the site of administration to the systemic circulation, most often irreversible, is known as absorption. Except intravenous or intra-atrial injection directly into blood, all systemically acting drugs that are administered via any extravascular routes such as oral, sublingual, inhalational, sub-cutaneous, transdermal, intradermal and rectal needs to be absorbed to the blood (Jambhekar and Breen 2009).

1.1.2 Distribution

When a drug is distributed it moves from one location (usually the blood) to another (usually organ or tissue) within the body. The rate and extent of drug distribution is reliant on three factors; 1) how well the tissue and/or organs are perfused with blood. 2) the capability of the drug to bind to blood plasma proteins and tissue constituents, and 3) the tissue membrane permeability to the drug molecules (Jambhekar and Breen, 2009). These variations lead to most drugs being distributed unequally to all parts of the body.

1.1.2.1 Membrane transport

Drugs can be transported via cellular membranes by diverse ways, this include: passive transcellular diffusion, paracellular transport, endocytosis or carrier-mediated transport. The most common route by which drugs passes the enterocytes in the intestinal mucosa is passive diffusion. This process is driven by the concentration gradient, which indicates that the compound moves towards regions of lower concentration (or by an electrochemical gradient) (Sugano et al., 2010). On the other hand, there are several carrier-mediated transport mechanisms; 1) facilitated diffusion occurs when the compounds are transported across the membrane in the direction of the concentration gradient, despite the transport has a saturable behaviour, 2) Primary active transporters, which utilise ATP to maintain a gradient across the membrane, 3) Secondary active transporters use energy from ion gradients (often Na+, Ca+ and H+ gradients) generated by primary active transporters. Membrane transporters are divided into two main super families, ATP-Binding Cassette (ABC) and SoLute Carrier (SLC) superfamily (Schinkel and Jonker 2003; Hediger et al., 2004; Mooij et al., 2016). Transporters comprise several transmembrane domains and one or more binding domain(s) which enable the translocations of drugs over the cell membrane. However, numerous drugs undergo both passive diffusion and

active transport. The ABC transporters (efflux transporters) are ATP-dependent and pump the drugs out from the cell. Whereas, the SLC transporters may work in both direction and are driven by electrochemical gradients or gradients of counter-substrates or co-substrates (Endres et al. 2006; Vasiliou et al., 2009). Furthermore, uptake of compounds from the blood into tissue or organs such as liver and kidney as well as absorption from the gastrointestinal tract or lung tissue into the peripheral circulation is mediated by the SLC transporters (Sai and Tsuji, 2004). The phase II conjugates often have poor membrane permeability. Therefore, carrier-mediated transport is essential for biliary excretion and secretion from hepatocytes into sinusoidal blood as well as for the excretion of drug metabolites from tubular cells of the kidney into the urine (Zamek-Gliszczynski et al., 2006).

1.1.3 Metabolism/biotransformation

Metabolism or biotransformation is the process of converting a drug to another molecule which mainly occurs in the liver. Usually these metabolites are inactive, however, there are some exceptions where metabolites produce a pharmacological effect (Ionescu and Caira 2005; Jambhekar and Breen 2009). Certain compounds, known as prodrugs are inactive and need to be metabolised to another form to become an active drug; e.g. valacyclovir which is an oral prodrug of the, antiviral agent, acyclovir (Zovirax®) (Garré et al., 2007). Water-soluble substances are secreted by the kidneys, whereas lipophilic substances must be transformed in the hepatocytes into water-soluble compounds by increasing their polarity to allow secretion. Biotransformation can be divided into phase I and II reactions (Grijalva and Vakili, 2013).

(A) Phase I reaction

Phase I reactions are also called activation reactions or "functionalisation reactions", which involves oxidation, reduction, and hydrolytic reactions. In this stage, the polarity of lipophilic substances is enhanced by adding or unmasking the chemically reactive group, e.g. $-NH_2$, -COOH, -OH or –SH groups. This can be done in different ways, such as the introduction of the functional group (e.g., aromatic and aliphatic hydroxylation) or by modifying existing functionalities (e.g., reduction of ketones and aldehydes to alcohols; oxidation of alcohols to acids; hydrolysis of ester and amides; reduction of azo and nitro compounds; oxidative N - , O - , and S - dealkylation) (Penner et al., 2012).

(B) Phase II reaction

The phase II reaction or detoxification reaction mostly refers to conjugation. In this phase, a substance or its metabolites from a phase I reaction are bound with a water-soluble endogenous molecule (conjugation) to form more water-soluble derivatives that can be excreted in the urine or bile. Phase II enzymes are located in the smooth endoplasmic reticulum (that forms microsomes), cytosol and mitochondria. These conjugative enzymes include glucuronosyltransferases (UGTs), sulfotransferase (SULTs), glutathione-S-transferase (GSTs) and methyl (N - methyl -, thiomethyl -, and thiopurinemethyl-) transferases. Phase II reactions include many types, namely glucuronidation, sulfation, glutathaione conjugation, acetylation, methylation and conjugation with amino acids (e.g. glycine and glutamic acid). In most of cases, the outcome of phase II reactions is an increase in a compound's hydrophilicity and decrease in volume of distribution; hence excretion can be increased (Gibson and Sket 2001; Nebbia, 2001; Ionescu and Caira 2005).

1.1.3.1 Metabolism and Transport Interplay

In several cases, same drug may be eliminated by both transporters and metabolising enzymes. This can complicate the evaluation and understanding of drug-drug interactions studies in vitro and in vivo. Uptake transporters may take up the drug into the hepatocyte; hence the drug will be metabolised by phase I and/or phase II enzymes; eventually, the parent drug and/or the metabolite(s) may be transported back to the blood and/or into bile. All these enzymes and transporters are potential sites of drug-drug interactions (Endres et al., 2006). DDIs at the level of hepatic cytochrome P450 is well characterised and there are many examples in the literature (Lin and Lu 1998; Park et al., 2003; Mukoyoshi et al., 2008). On the other hand, changes in the concentration of the drug in the cells or in the circulation can also occur by either inhibition or induction of relevant transporter proteins in the liver (Shitara et al., 2003; Wu and Benet 2005). For example, it was found that rifampicin, which is both inhibits OATP uptake transporters and induces P450 enzymes, where interacted with the OATP/P450 substrate glyburide. The AUC of glyburide was increased after the first intravenous dose of rifampicin, most likely due to inhibition of organic anion–transporting polypeptide OATP family. Whereas multiple doses of rifampicin decreased the AUC of glyburide, possibly due to induction of P450 enzymes (Zheng et al., 2009). Similarly, it was found that administration of rifampin for five days prior phenylbutazone into horses, resulted in a significant increase in both the rate of distribution (α) overall rate of elimination (β) as well as the body clearance rate (ClB). Whereas, the plasma half-life was decreased (t1/2 β) (Burrows et al., 1989). However, the occurrence of OATP in horse tissues is not evident in the literature.

Several in vitro systems have been developed to study the uptake kinetic of drugs and the biliary efflux in human and rat (Ansede et al. 2010; Cantrill and Houston 2017). Human epithelial Caco-2 cells (colorectal

adenocarcinoma cells) can be used as a model to study hepatic efflux transporter-mediated interactions (Hu et al., 2004; Zou et al., 2012). Whereas, the evaluation of uptake activity of important hepatic drug transporter requires more liver like models or cell lines. Hence, primary hepatocytes which possess a complete set of metabolising enzymes and transporters involved in hepatic drug clearance and are considered as the best in prediction relevant *in vivo* clearance parameters are used in this type of studies (Jigorel and Houston 2012). However, fresh human hepatocytes exhibited an extensive reduction in transporters activity 6 h after plating (Ulvestad et al., 2011). Therefore, sandwich cultured human hepatocyte system was developed and can be used if longer incubation times are required (Swift et al., 2010). Moreover, cryopreserved human hepatocytes represents a potential alternative for freshly isolated hepatocytes since the activities of important hepatic drug uptake transporters have been reported to be present in cryopreserved hepatocytes (Umehara et al., 2007; Soars et al., 2009) . In this context, immerging of Biopharmaceutics Drug Disposition Classification System (BDDCS), which categorises drugs into four classes according to their solubility and permeability, may help in: predicting effects of efflux and absorptive transporters on oral absorption when transporter-enzyme interplay will yield clinically significant effects such as low bioavailability and drug-drug interactions, understand the direction and importance of food effects, and transporter effects on post-absorption systemic levels following oral and intravenous dosing (Wu and Benet 2005).

1.1.3.2 Equine Drug Metabolism

The effect of physiological differences between horse and human has not been completely understood due to the lack of relevant data. However differences in digestive tracts between the two species are expected to have some impact on drug metabolism (Scarth et al., 2011). For example, the

equine caecum can produce substantial amounts of monoamines. When absorbed into the body these monoamines may have directed the evolution of certain drug metabolising systems (levels of monoamine oxidases and certain CYPs/Flavin monooxygenase [FMOs]) over many thousands of generations. Moreover, it has been found that the detected concentrations of monoamines in the blood of horses vary with their diet according to the season. This suggested that any enzymes responsible for monoamines metabolism may show similar seasonal fluctuations through adaptive induction (Bailey et al., 2003).

Generally, within the equine field most of the published literature is obtained from the detection of drug abuse in horseracing (Toutain and Lassourd, 2002). This could be due to metabolism data needed for drug approval regulations having less importance in the veterinary drug industry however, a vast number of drugs are prohibited in horse racing. On the other hand, some countries consider horses as a food-producing animal. This has an impact on therapeutic drug usage and consequently on drug metabolism research due to legislations regarding the residues of veterinary drugs entering the food chain (Blanca et al. 2013; Boison et al. 2016). However, as popular companion and athletic animals, horses are frequently administered a wide range of medications where drug-drug interaction are more likely to occur. It was reported that, phenylbutazone metabolism was faster when administered after rifampicin; moreover, renal clearance of digoxin was decreased when dosed along with quinidine (Scarth et al., 2011). In this context, doping control is a major concern in the horseracing industry and many substances, such as anabolic steroids, are banned within racehorses due to potential performance-enhancing effects (Scarth et al., 2011). In racehorses, like human athletes, doping control comprises of searching for certain metabolites in plasma and urine; however, due to the lack of details of the specific enzymes involved in drug metabolism in the

horse, most of the data concerning horse-dosing and potential drug-drug interactions is based on other species. However, many species differences have been reported regarding drug metabolism suggesting that it may not be ideal to extrapolate metabolism data between species (Chauret et al., 1997; Nebbia et al., 2003). Unlike other species, *in vivo* metabolism studies in the horse are not easy to conduct because of their size, cost, difficulty to obtain large sample numbers and the associated regulations around large mammal research (Animals in Science Regulation Unit 2014). Recently, *in vitro* drug metabolism studies have been used in equine surveillance laboratories to compliment the *in vivo* studies and to determine possible routes of metabolism (Ho et al., 2005; Ho et al., 2007; Scarth et al., 2010). Furthermore, *in vitro* studies may help in the identification of drug metabolites *in vivo* by producing a more concentrated sample and the generation of metabolite reference standards.

1.1.4 Cytochrome P450 Enzyme

Cytochrome (CYP) P450s represent one of the largest and most ancient superfamily of mainly microsomal and mitochondrial haemoproteins. They are containing a haem cofactor in their reactive site, and are involved in electron transfer reactions (Gray and Winkler, 1996). CYP P450s were first discovered in rat liver microsomes by Klingenberg (1958), who noticed that a prominent optical peak at 450 nm appeared when carbon monoxide was added to the microsomal suspension reduced with dithionite or NADH.

CYP P450 enzymes are considered as the main contributor in drug metabolism followed by Uridine diphospho-glucuronosyl transferase (UGTs) and esterases. Generally, more than 95% of the top marketed drugs in human are metabolised to some extent by this group of enzyme (Williams et al., 2004). CYP P450 enzymes are located on the smooth endoplasmic reticulum of number of tissues such as liver and lungs (Ogu and J. L. 2000).

Their mechanism of action is quite complex, however the result of the reaction is relatively simple: the formation of a hydroxyl group by inserting one atom of molecular oxygen into the substrate while reducing the other atom of oxygen to water (Penner et al., 2012).

1.1.4.1 Nomenclature of CYP P450

Reduction of the oxidised form of cytochrome P450 (Fe^{+3}) to the ferrous (Fe^{+2}) state, gives it the ability to bind ligands such as O_2 and CO. The term 'cytochrome P450' refers to a coloured substance in the cell. This pigment, when reduced and bound with carbon monoxide, forms a complex with the maximal absorbance between 447 and 452 nm (with an average of 450 nm) (Klingenberg 1958).

The nomenclature system is based on an evolutionary relationship between CYP450 enzymes and not on similarity in substrate phenotype. The drug metabolising P450s are confined to subfamilies 1, 2, 3, and 4 (Mckinnon et al., 2008).

Generally, P450 sequences that display greater than 40% amino acid identity are placed in the same family. Similarly, those sequences that are greater than 70% identical are placed in the same subfamily (Mckinnon et al., 2008).

In human liver, there are at least 18 distinct P450s, while only 10 from families 1, 2, and 3 (CYP1A2, CYP2A6, CYP2B6, CYP2C8, CYP2C9, CYP2C19, CYP2D6, CYP2E1, CYP3A4, and CYP3A5) are responsible for the hepatic metabolism of most marketed drugs (Furge and Guengerich 2006).

1.1.4.2 Equine CYP P450

An equine CYP named P450-(h-1) was purified and partially characterised by Komori et al. (1993). The cross-reactivity of an antibody generated against P450-(h-1) with rat 2C P450s suggested that P450-(h-1) belonged to the CYP2C subfamily.

CYP enzymes in subfamily 1, 2 and 3, which play a major role in drug metabolism, have been characterized in horses and studies have revealed metabolic activity in equine liver microsomes for various substrates such as testosterone (Schmitz et al., 2014). Many species differences have been identified regarding CYP activities (Chauret et al., 1997; Nebbia et al., 2003). A comparison between horse, dog, human and cat using microsomes revealed that troleandomycin, an inhibitor of CYP3A4 in humans, did not affect the metabolism of testosterone in the horse; however, inhibitors of other CYPs did affect the metabolism of specific compounds (Chauret et al., 1997). Furthermore, it has recently been shown that the CYP2B6A subfamily is involved in testosterone metabolism in horse and human but not dog, and sulfaphenazole inhibited metabolism in human more than in horse (Zielinski and Mevissen, 2015).

Differences in CYP P450 activities could lead to significant pharmacokinetic differences between humans and horses. For example, non-steroidal anti-inflammatory drugs are used frequently in horses to treat inflammation and pain (Kollias-Baker 2005). However, few studies have been conducted regarding the pharmacokinetics of these compounds in horses (Chay et al., 1982; Sams et al., 1999; Rehman et al., 2012; Friebe et al., 2013). Furthermore, monensin, an ionophoric coccidiostat used in poultry may cause fatal intoxication in horses. Comparative studies with microsomes from various animal species, including pigs, horses, cattle, broiler chickens, and rats, revealed that the horse had the lowest catalytic ability to demethylate (and hence detoxify) monensin (Nebbia, 2001).

1.1.5 Excretion

Even though the kidney is considered as a primary site for elimination of drugs and their metabolites, the liver is the primary organ where drug metabolism occurs which can be excreted via bile. On the other hand,

substances of high vapour pressure such as gaseous anaesthetics and alcohol are excreted via lungs. Breast milk is also considered as a potential route for drug elimination (Jambhekar and Breen 2009).

1.1.6 Elimination

Elimination is defined as an irreversible removal of drug from the body (Ionescu and Caira 2005; Jambhekar and Breen 2009). This is normally performed either by excretion and/or by metabolism. In this context, among many terms related to drug pharmacokinetics (PK), the parameters of clearance and volume of distribution have the highest importance. The volume of distribution (V) of a drug represents the amount left in blood after the drug has been absorbed and distributed. It is usually expressed in either litres, or litres/kg of body weight. The larger the V, the more the drug has been widely distributed in the body (Jambhekar and Breen 2009).

1.1.6.1 Plasma Clearance

Plasma clearance is often defined as the plasma volume which is totally cleared of drug per unit of time. It is one of the most important PK parameter values because it determines dosage rate (Jambhekar and Breen 2009). The relationship between the dosing rate and the plasma clearance is expressed in the following equation:

$$Dosing\ rate = \frac{Plasma\ clearance\ x\ therapeutic\ plasma\ concentration}{Bioavailability} \qquad 1.1$$

Where 'Dosing rate' is the dose per dosing interval (amount/time), 'Clearance' is the plasma clearance expressed for the given dosing interval (e.g. per day), 'therapeutic concentration' is the average effective target plasma concentration required to obtain the desired response, and 'Bioavailability' is defined as the actual percentage of drug that reaches the systemic circulation after administration by an extravascular route.

1.2 Drugs used in equine medicine

There are different classes of drugs used in or has an importance in horses and particularly in horseracing; these include: anabolic-androgenic steroids (AAS) (such as testosterone, nandrolone, and boldenone), stimulants (such as amphetamine), sedatives/tranquilizers (such as xylazine, barbiturates and acepromazine), β_2-agonists, local anaesthetics, non-steroidal anti-inflammatory analgesics (NSAIDS)/cyclooxygenase-2 (COX-2) inhibitors (such as phenylbutazone, meloxicam and flunixin, opioid analgesics (such as morphine, codeine and diacetylmorphine), diuretics (such as furosemide), beta-blockers, anti-ulcerative drugs, anti-infective drugs (Scarth et al., 2011).

Both anabolic-androgenic steroids and stimulants are banned by many horseracing authorities (Federation Equestre Internationale 2017). The other classes of drugs such as NSAIDS and anti-ulcerative drugs are frequently used to improve the horse welfare; however, because of their potential to affect horse performance all these drugs are controlled by most of horse race authorities. Therefore, most of these drugs has been subject to metabolism and pharmacokinetic studies. For example, it was found that 55% of radio-labelled phenylbutazone dose administered to horses was excreted into urine, and the remaining of the radio-labelled dose was recovered in faeces. The same study reported that about 80% of the radioactivity in plasma could be ascribed to parent phenylbutazone; whereas, the remining percentage being divided equally between the unconjugated phase I metabolites oxyphenbutazone and γ-hydroxyphenylbutazone. On the other hand, parent phenylbutazone represent only approximately 7% of the urinary products with presence of unconjugated phenylbutazone metabolites. However, other study found that a considerable animal to animal variation was encountered in tested horses when on oral dose of phenylbutazone was administered. This could be due

to phenylbutazone being recirculated i.e. secreted in the bile and subsequently reabsorbed (Gerring et al., 1981).

Other commonly medications being frequently used in performance horses are anti-ulcer medications such as cimetidine, ranitidine, and omeprazole. They are used to treat gastric and duodenal ulcers (Knych et al., 2016). The disposition of this class of drugs has been extensively studied in horses. It was reported that there is a degree of individual variation with bioavailability, and healing of the squamous mucosa consistently observed (Sykes et al., 2015) which may has a direct impact on drug efficacy and horse welfare. This variation in the efficacy of omeprazole has been observed in human and it is linked to mutations in the CYP2C19 gene and changes in the rate of elimination (Ma et al., 2012). Despite relative scarcity of sequenced enzyme data compared to many other species, but availability of *in vitro* models that being used for study drug disposition and development in human medicine may represent a suitable alternative for better understanding of drug deposition in horses. In this context, conducting prop substrates studies may help to understand drug metabolism in horses and in identify different metabolic pathways. For example, chloramphenicol which is considered as potent inhibitor of CYP P450 isoform CYP2C19 can be used to conduct drug-drug interaction in horses using both equine liver microsomes or isolated equine hepatocytes. Furthermore, sandwich cultured hepatocytes between collagen and matrigel can form an intact canalicular networks and polarised excretory function (Bi et al., 2006; Kim et al., 2010). This will help to understand the drug metabolism in horses allowing to make better pharmacokinetic prediction. This is crucial since pharmacokinetic parameters having a key role in determining the dosage rate of a therapeutic substance. Clearance, for example, can be used to determine the therapeutic plasma concentration when the dosage rate is known which can be applied to medication control in sport's competitions.

1.3 Drug detection time and withdrawal time in the context of Equine Sports Competition

Sport horses, as athletes, and to reach their full potential need to be fed, trained and treated correctly. However, horse treatment represents the major challenge for a veterinarian, because of the substantial number of drugs in everyday use. These drugs are administered to horses at different doses and are eliminated at widely different rates. Therefore, these medications have to be given under controlled protocols to prevent medication violations and protect the welfare of the horse (medication control) (Toutain, 2010b).

In Europe, for instance, there is a committee responsible for harmonising sample testing and polices for racing in Europe, which is called the European Horse-race Scientific Liaison Committee (EHSLC). A general policy that discriminates the control of drug effects of therapeutic substances (medication control) and the control of any drug exposure for all illegal substances (doping control) has been established by this committee (Barragry 2006; Dowling 2002; Toutain 2010a). Regarding medication control, the central mission of the EHLSC is to establish agreed harmonised screening limits (HSL) for all nations involved in the EHLSC programme. From a technical prospective, within the EHLSC, the HSL is known as the recognised limit of detection. It can be defined as a confidential instruction to laboratories from racing authorities to screen for the presence of drugs commonly used in equine medication. The presence of these medications in plasma and urine should not be at a level that can be a threat to the welfare of the horse, alter its racing performance or compromise the integrity of racing (Toutain, 2010a). Thus, veterinarians must inform owners or trainers on appropriate withholding times after a treatment to avoid the risk of facing a positive drug test. This is crucial for sport horses because some medication can be given to improve the health and welfare interest of the animal

(legitimate medication). Simultaneously these medications can be abused to alter or restore horse performance (the illegitimate use of therapeutic drugs).

On the other hand, doping control is aimed at detecting any trace of drug exposure (parent drug or metabolites) from substances banned at all times using state of art powerful analytical techniques i.e. chromatographic/mass spectrometric techniques (Toutain, 2010b). This is not appropriate for medical control due to the high level of sensitivity of the screening methods which allows the detection of totally irrelevant plasma or urine concentrations. The irrelevant plasma drug concentration (IPC) and irrelevant urine drug concentration (IUC) are defined as "plasma or urine concentrations which guarantee the absence of any relevant drug effect and for which there will be no regulatory action" (Toutain and Lassourd, 2002). Hence, a novel approach based upon a pharmacokinetic/pharmacodynamic (PK/PD) has been developed for legitimate therapeutic compounds. In this approach, both IPC and IUC are calculated using retrieved published parameters and variables as follows: taking into account that an effective dose is a PK/PD hybrid variable calculated by two PK parameters i.e. plasma clearance and bioavailability, and one PD parameter i.e. the effective plasma concentration (EPC) (equation 1.2) (Toutain and Lassourd, 2002).

$$Effective\ dose\ rate = \frac{Plasma\ clearance\ x\ effective\ plasma\ concentration}{bioavailability} \quad 1.2$$

EPC can be estimated by rearranging (equation 1.2 as 1.3):

$$EPC = \frac{standard\ dose\ (per\ dosing\ interval)\ x\ F}{plasma\ clearnce\ (per\ dosing\ interval)} \quad 1.3$$

Where standard dose is the generally recommended dose per dosing interval, plasma clearance is the pharmacokinetic parameter which

expresses the body's capacity to eliminate the drug, F is the bioavailability factor lying between 0 and 1. However, the EPC is calculated using IV data only so that F = 1, as the EPC is the same whatever the route of drug administration. Hence, (equation 1.2) can be reduced to (equation 1.4):

$$EPC = \frac{standard\ dose\ (per\ dosing\ interval)}{plasma\ clearnce\ (per\ dosing\ interval)} \quad 1.4$$

The irrelevant plasma concentration (IPC) can be determined from EPC by applying a safety factor (SF) to EPC (equation 1.5):

$$IPC = EPC/SF \quad 1.5$$

The selection of an SF is both a policy and scientific decision. The regulatory authorities are responsible on a determination that is acceptable (or unacceptable) in terms of drug effect (Toutain and Lassourd, 2002).

The irrelevant urine concentration (IUC) can be derived from the IPC using (equation 1.6):

$$IUC = IPC\ x\ Rss \quad 1.6$$

Where R_{ss} is the steady-state urine to plasma concentration ratio.

Generally, the IPC and IUC are used as HSLs in plasma and urine respectively, however, for some drugs the IPC or IUC are below the current limit of detection (LOD) and the HSL is simply set as the LOD.

The EHLSC defines the detection time (DT) for plasma or urine as the interval between the time of the last drug administration and the time at which the observed plasm (or urine) concentrations of all investigated horses (during an experiment conducted according to EHSLC recommendations) are below the HSL with the routine analysis method. In other words, DT is a raw experimental observation and represents the only information released by

the authorities to stakeholders to help veterinarians to recommend a suitable WT for a given horse. In this context, the WT is a recommendation of the treating veterinarian and completely relies on their professional judgement (Toutain 2010a). Accordingly, the WT should be longer than the DT, since all sources of animal variability (age, sex, breed, training, and racing) and those of the administered medicinal product (formulation, route of administration, dosage regimen, duration of treatment) should be considered to avoid a positive test.

The biological variabilities between horses represents a major obstacle in making drug withdrawal time recommendations (Tobin, 1986; Toutain 2010b). Moreover, providing a rather robust DT is the major challenge for both, the horserace committees and veterinarians. This requires two conditions: 1) the horses being investigated should be representative of the target horse population, and 2) number of horses involved in the study should be appropriate to get a "grip" on the skewedness of a plasma level distribution (Tobin, 1986). However, the first condition is not easy to fulfil due to the lack of information regarding horse pharmacogenetics. The second condition examined using Monte Carlo Simulations (MCSs) (Toutain 2010a). An MCSs is a numerical method with a built-in random process that involves combining variability due to source diversity (Bonate, 2010). Toutain (2010a), used MCSs to extrapolate a WT from a DT by simultaneous combining all sources of variability mentioned above; hence a large hypothetical population of DTs can be generated. In the presence of a suitable PK model that can provide the numerical value of the DT, the variability of DT can be determined using MCSs. A mono-exponential decay is usually used for medication control to describe the elimination phase of interest (equation 1.7):

$$C(t) = Y_z \; x \; Exp(-\lambda_z \; x \; time) \qquad 1.7$$

Where C(t) is the plasma/urine concentration at time t after administration (single dose), Y_z is the intercept (a concentration) of the terminal (elimination) phase and λ_z is the slop of the terminal phase. Whereas, the time corresponding to any fixed concentration C(t) as an HSL is given by (equation 1.8)

$$Time = \left[Ln\ \frac{C(t)}{Y_Z}\right]/\lambda_z \qquad 1.8$$

If C(t) is the HSL, then time is a DT equation 1.9

$$Time = \left[Ln\ \frac{HSL}{Y_Z}\right]/\lambda_z \qquad 1.9$$

In equation 1.8, Y_z and λ_z are hybrid PK parameters e.g. the slope of the terminal (elimination) phase has only 2 physiological factors, plasma clearance (Cl_{plasma}) and terminal volume of distribution (V_z). Hence, the slope of λ_z is given by (equation 1.10):

$$\lambda_z = CL_{plasma}/V_z \qquad 1.10$$

Meanwhile, the intercept Y_z represents the dose, bioavailability and volume of distribution, and for urine, the urine-to-plasma ratio as given by (equation 1.11):

$$Y_z = [F\ x\ BW\ x\ Dose\ x\ R_{ss}]/V_z \qquad 1.11$$

Where F is bioavailability, BW is the body weight in kg, Dose is the nominal dose expressed by kg of BW, R_{ss} is the urine to plasma ratio and V_z as defined above.

If Y_z and λ_z in equation 1.8 were replaced by their physiological determinants, i.e. by combining (equations 1.8, 1,9 and 1.10), the DT is given by (equation 1.12):

$$DT = \left[Ln \frac{HSL}{[F \; x \; BW \; x \; Dose \; x \; R_{ss}]/V_Z}\right] \Big/ \left[\frac{Cl_{plasma}}{V_z}\right] \quad 1.12$$

From (equation 1.12), the effect of all mentioned variables on DT can be observed by simply changing the model input of these variables.

Therefore, the proportion of horses achieving a given DT value can be determined. This may make MCSs as a candidate to replace large population surveys designed to generate a WT experimentally. However, lack of information on the actual statistical distributions of PK parameters (plasma clearance, volume of distribution, urine-to-plasma ratio and systemic bioavailability) in horses represents the major obstacle to apply this approach. This leads to the conclusion that the number of investigated horses should be increased to at least 8 (Tobin 1986; Toutain 2010a).

1.4 The liver

1.4.1 Liver anatomy and architecture

The liver is the largest internal organ in the body, constituting 2-5% of the adult body weight, depending on the species and age (Bragulla et al., 2004; Vekemans and Braet 2005).

The liver is located in the thoracic part of the abdomen, behind the diaphragm, and lies to the right of the median plane. It has a strongly convex surface towards the diaphragm and a concave surface facing towards the other abdominal organs. In most species the liver is grossly divided into four main lobes by fissures that extend into the organ from the ventral border; however, in the horse the left lobe is subdivided into medial and lateral lobes, while the right lobe remains undivided (Figure 1.4.1). The liver is both endocrine and exocrine in function, and plays a major role in different metabolic processes in the body. It is, for example, responsible for glycogenesis, production of plasma proteins, clotting factors and urea. Furthermore, the liver transforms, detoxifies and accumulates metabolites

and as a result can be considered as a barrier between the digestive tract and the rest of the body. Endocrine products are released into the blood stream; whereas, the exocrine product (bile) is drained into the intestinal tract and is essential for fatty compounds emulsification. In human and most animal species the bile is stored and concentrated in the gallbladder; however some species such as horse are lacking a gallbladder, hence bile is transported directly into duodenum by bile ducts (Bragulla et al 2004). The liver performs all these activities effectively because of its unique architecture. The peritoneum covers almost completely the free surface of the liver to form its serous coat. The peritoneum is fused to the underlying fibrinous Glisson's capsule, which encloses the whole organ. The finer trabeculae of the hepatic connective tissue divide the liver parenchyma into innumerable small units hepatic lobules (Bragulla et al., 2004; Chapman and Eagles 2007).

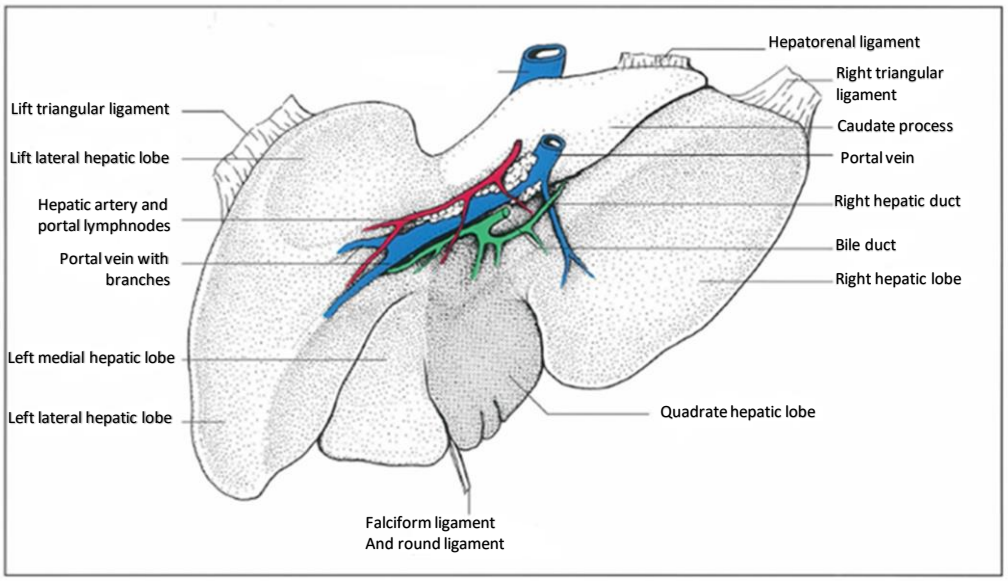


Figure 1.4.1: Liver of the horse, schematic, visceral surface (cited from Bragulla et al. (2004)

Unlike other organs, the liver receives a substantial blood supply through two sources, the hepatic artery and the portal vein. The hepatic artery, a branch of the celiac artery, carries blood with high oxygen content. The hepatic arteries supply the liver framework, the capsule, the interahepatic

biliary duct system, the walls of the blood vessels and the nerves before they finally drain-together with the branches of the portal vein into the liver sinusoids. The portal vein has three branches: the splenic vein, the cranial and the caudal mesenteric veins; they collect blood from all unpaired organs of the abdomen (stomach, pancreas, intestines and spleen). The portal blood is enriched with nutrients absorbed by the intestine. However, the hepatocytes are immersed by mixed blood from the hepatic artery and the portal vein, so they actually receive nutrients from both (Figure 1.4.2) (Bragulla et al., 2004; Ishibashi et al., 2009).

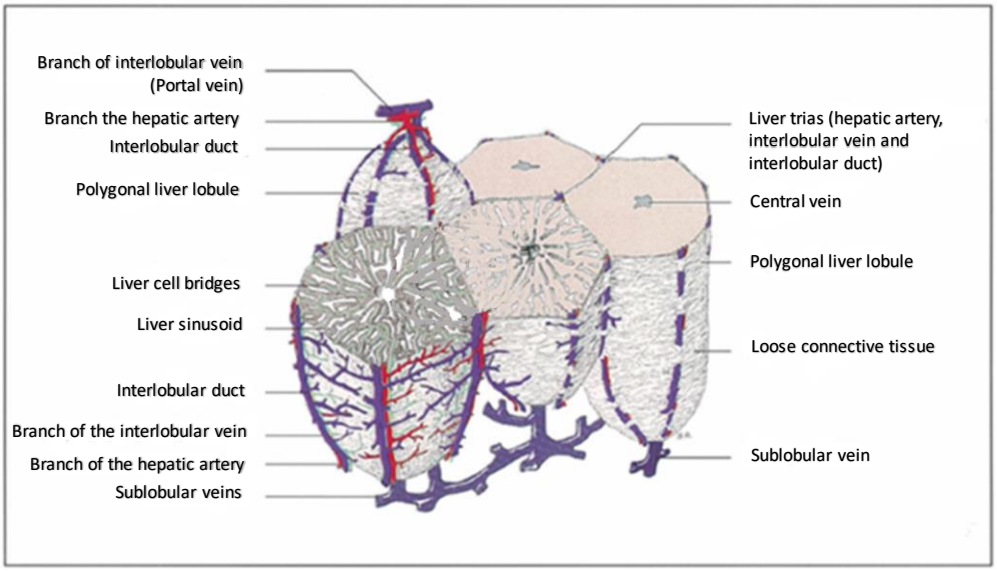


Figure 1.4.2: Hepatic lobules in relation to afferent and efferent vessels, three-dimensional, schematic (cited from Bragulla et al., 2004).

1.4.2 Hepatic lobule and hepatocyte

The hepatic lobule is considered as the structural and functional unit of the liver. It is composed of curved sheets of hepatocytes which extend to form one-cell- thick liver cell plates 15-20 hepatocytes in length, forming a hexagonal shape (Figure 1.4.3).

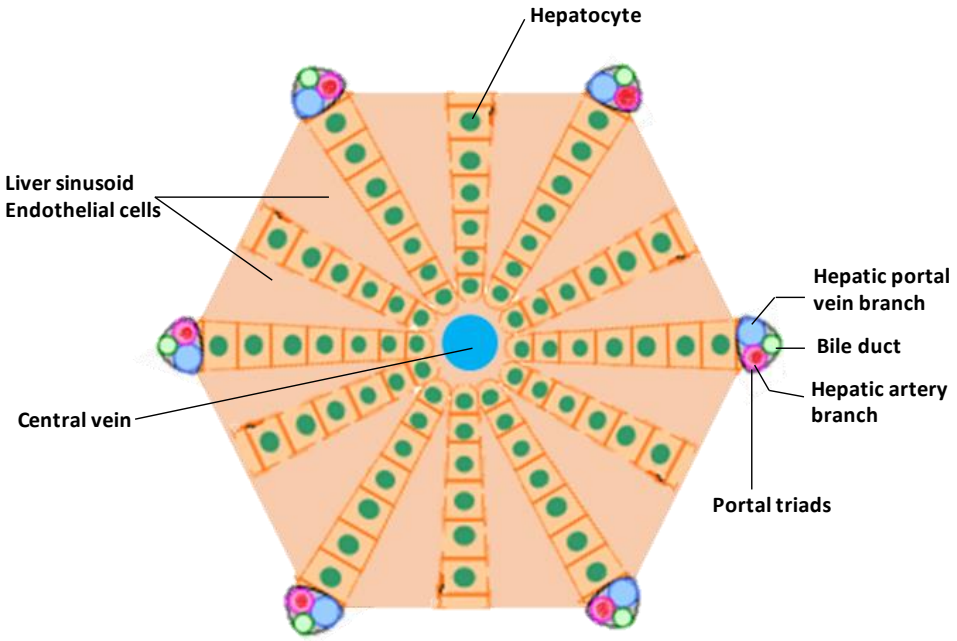


Figure 1.4.3: Liver lobule

The tissue space between hepatocytes and sinusoidal endothelium is named the space of Disse. The space of Disse contains a network of reticular fibres such as collagen type IV, which bring hepatocytes together (Reid et al., 1992; Godoy et al., 2013). As there is no epithelial basement membrane, the hepatocyte is the only epithelial cell in the body not separated from the vasculature by two continuous basement membranes. Hence, the blood plasma passes freely into the space of Disse which facilitates rapid bidirectional macromolecular exchange between plasma and hepatocytes (Wisse et al., 1996).

Hepatocytes (Parenchymal cells), represent up to 80% of the entire liver mass and account for about 60% of the total liver cell count. They are metabolically very active and perform uptake, transport, synthesis, biotransformations and degradation of proteins, lipids, hormones and xenobiotics (Gebhardt et al., 2003; Godoy et al., 2013). A large proportion of these cells are mononuclear, whereas, approximately 30-40% of the cell population are bi- or multi-nucleate. Polyploidization seems to be an important restriction mechanism for hepatocyte proliferation (Gupta 2000).

Hepatocytes have an eosinophilic cytoplasm, which reflects numerous mitochondria, where a number of metabolic processes take place such as oxidative phosphorylation. Moreover, hepatocytes contain large amounts of rough endoplasmic reticulum and free ribosomes, which are often located near the mitochondria and are performing the synthesis of specific proteins, especially albumin (Ramadori et al., 2008). Detoxification of many xenobiotics is performed by smooth endoplasmic reticulum (SER) mainly through the cytochrome P450-dependent monooxygenase system. Steroids such as cholesterol and bile acids are synthesized in the SER (Schaffner, 1975).

1.4.2.1 Liver extracellular matrix

Extracellular matrix ECM comprises up to 3% of the relative area of a normal liver section; however, it plays a significant role, both, in liver physiology and pathology. It acts as a physical scaffold of the liver and as a modulator of biologic processes; including cell attachment, migration, differentiation, repair and development.

In normal liver, ECM consists of four major components which are collagens, elastin, structural glycoprotein and proteoglycans and is restricted, to the portal tracts, sinusoid walls, central veins and the Glisson's capsule (Xu et al., 2012). Collagens are the most abundant components in liver ECM acting as scaffolding that support the parenchyma and maintains hepatic integrity (Marttinez-Hernandez and Sepastian. 1995).

1.4.3 Liver *in vitro* pharmacology systems

Within the drug development process, toxicity is one of the major limiting factors. The success rate in bringing a drug to market in the USA and/or Europe was less than 11% in the period 1964 to 2000 (Astashkina et al., 2012). Hence, studies of efficacy and the safety of drugs in human as well as in horses are critical prior to clinical trials. For this reason several *in vitro*

pharmacological and toxicological models have been established to determine these factors,; in addition to, interspecies differences between animals and humans (Brandon et al., 2003; Hewitt et al., 2007). A number of *in vitro* human liver systems have been developed in the last few decades, such as microsomes, cytosol, S9 fraction, liver slices, primary hepatocytes, and perfused liver and recombinant enzymes ((Groneberg et al., 2002; Mazzoleni and Steimberg 2012).

1.4.3.1 Liver microsomes

Because of their large availability and ease of use,microsomes provide relatively a simple method to give a good indication of the CYP and UGT metabolic profile of a drug. Therefore, they are considered as the first-line high throughput screening model.

Liver microsomes comprise vesicles of the hepatocyte endoplasmic reticulum and contain mainly CYP and UGT enzymes (Figure 1.4.4) (Brandon et al., 2003). The CYP P450 can be quantefied using the P450 spectral assay. This assay is based on that the ferrus form of the hemeprotein reacts with carbon monoxide (CO) to form a complex that specifically produces a spectrum with a wavelength at ~450 nm (Groneberg et al., 2002).

The main disadvantage of microsomes is that there is a significant variation between individuals; however, poolingmicrosomes from different donors can overcome this issue and results in representative population enzyme activity (Brandon et al., 2003; Plant 2004).

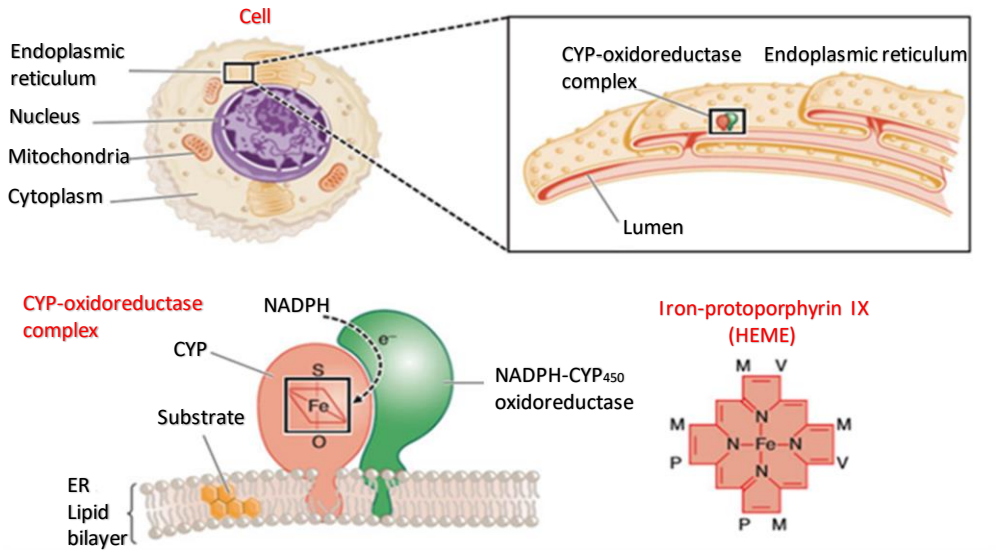


Figure 1.4.4: Location of CYPs in the cell. The Figure shows increasingly microscopic levels of detail, sequentially expanding the areas within the black boxes. Cited from Brunton et al. (2012).

1.4.3.2 Isolated hepatocytes

Primary hepatocytes are the most commonly used *in vitro* liver cell model (Brandon et al., 2003). Primary hepatocyte culture has been considered a gold standard in the study of drug metabolism *in vitro* (Hewitt et al., 2007; Van Summeren et al., 2013).. Despite the fact that, during classical monolayer culture, the primary hepatocytes undergo a series of morphological and functional changes such as loss of their cuboidal morphology and become flattened; reduction of the expression of several CYP enzymes and a loss of response to well-known inducers of these enzymes are observed. Significant progress has been achieved regarding the methodology of *in vitro* hepatocyte maintenance over the last decade. For instance, the introduction of three-dimensional spheroids has improved the preservation of the native liver structure and introduction of a bioreactor system overcomes the lack of oxygen and nutrient exchange in classic 2D cultures. Hence, unlike the isolated perfused organ and liver slices, well-differentiated hepatocytes in 3D cell-based models would have a potential

advantage for drug metabolism studies (Brandon et al. 2003, Godoy et al. 2013).

1.4.4 Hepatocyte isolation

Hepatocyte isolation was performed for the first time in the mid-1960s; rat hepatocytes was isolated by using a combined mechanical/enzymatic digestion technique (Howard et al. 1967). Significant progress has been achieved by introducing the two-step isolation procedure in which the liver is first perfused with calcium free medium containing EDTA prior to being perfused with collagenase-containing media, which allowed to obtain higher yeild and viability (Selgen 1976).

Due to high potential research applications of isolated hepatocytes, beside human, livers from species such as mouse, rat, pig, sheep, cattle and horses have been perfused in order to obtain fresh hepatocytes (Berry and Edwards 2001; Bakala et al., 2003).

Technically, freshly isolated hepatocytes represent a readily available and easy to handle *in vitro* system that can be used to study drug metabolism. These cells have the capacity for biotransformation. However, freshly isolated hepatocytes have a limited viability in suspension which is not more than 4 hours (Soldatow et al., 2013). This period is long enough to determine the metabolic stability of a drug and to allow identification of a major metabolite, but may be too short to generate some minor, especially phase II metabolites. Therefore, hepatocyte culture systems or bioreactors are used in order to increase time span of cell viability (Gebhardt et al., 2003).

1.4.5 Cryopreserved hepatocytes

Cryopreservation refers to the process of cell preservation by cooling to subzero tempratures in liquid nitrogen for long-term storage. Cryopreservation methods are based on preventing cellular damage, due to

ice crystal formation and chemical changes in cells as they cool and eventually freeze.

The viability before cryopreservation is one of the main determinants of thawed cell function. Generally a drop in overall viability of cryopreserved hepatocytes by 25-53% of the original number was reported (Dou et al., 1992). Moreover, the attachment efficiency of cryopreserved hepatocytes can be reduced compared with freshly isolated hepatocytes (Li et al., 1999; Li 2007; Grondin et al., 2009). However, there is no difference between fresh and cryopreserved cells in terms of morphology and CYP P450 activities (Madan et al., 1999).

1.4.5.1 Requirements for successful cryopreservation protocol

Several factors have been determined for a successful cryopreservation protocol such as type of cryoprotectant, rate of freezing and storage, cell density, and storage temperature (Diener et al., 1993; Kasai and Mito 1993; De Loecker et al., 1998; Madan et al., 1999; Wu et al., 2000; Sosef et al., 2005; Stéphenne et al., 2010).

Many different types of cryoprotectant, such as glycerol, polyvinylpyrrolidine, dextran and DMSO, have been used and a number of studies were conducted in order to compare between these different formulas (Loretz et al. 1989; Diener et al., 1993; Kasai and Mito 1993). Most of these studies demonstrate that DMSO is the cryoprotectant of choice because of its superior properties to other cryoprotectants (Lawrence and Benford 1991; Diener et al., 1993).

In addition to the type of cryoprotectant, a number of studies have investigated the impact of concentrations of hepatocytes per ml in cryopreservation vials and most of the published data recommend that hepatocytes should be cryopreserved at a low cell density (less than 10^7cells/ml) (Diener et al., 1993; Kasai and Mito 1993; De Loecker et al.,

1998; Madan et al., 1999; Wu et al. 2000). The slow, controlled freezing rate controls the process of intracellular ice formation which consequently will affect hepatocyte outcome following cryopreservation (Harris et al., 1991). In this slow, controlled freezing strategy a constant temperature decrease (usually -1°C/min) is used (Coundouris et al., 1993). The controlled drop in temperature is achieved by either placing freezing tube in a Styrofoam rack or a specially designed isopropanol-cell cooler ("Mr Frosty" cell cooler unit) at -80 °C for 24h before transfer to liquid nitrogen. The storage temperature of cryopreserved hepatocytes has been studied, and most studies found that storage of hepatocytes at -20°C or -80°C is harmful for cell functions since the number of proteases might be active at those temperatures. Whereas, the minimum acceptable temperature for long-term storage of cryopreserved hepatocytes is -140°C/-150°C (Li et al., 1999; Rijntjes et al., 1986; Chesne and Guillouzo 1988; Sosef et al., 2005; Stéphenne et al., 2010).

1.4.5.1.1 Enrichment of viable cells post-thawing via Percoll gradient

Cryopreservation leads to an overall drop in cellular viability (Dou et al., 1992). To overcome this limitation, Percoll® a density gradient medium (composed of colloidal silica particles coated with polyvinylpyrrolidone), is used for cell purification (Pertoft et al., 1978). It works based on the principle that the sedimentation rate of the particles is dependent on centrifugal force, particle size, density in proportion to its media and viscosity (Amersham Biosciences, 2013). Several early studies suggested that Percoll® enriched viable cells; hence, CYP P450 activity and attachment (Lawrence and Benford, 1991; Dou et al., 1992; Utesch et al., 1992). It was found that use of Percoll increased the activities of Glutathione S-transferase (GST) and Sulfotransferase Enzymes (ST) to the level of freshly isolated hepatocytes (Diener et al., 1993). On the other hand, use of a Percoll® gradient could

lead to the loss of many healthy cells during the process which reduces the overall yield (Utesch et al. 1992). However, recently a post-thaw viability of 88±3% with an acceptable loss of cells was obtained after a Percoll® step (McGinnity et al., 2004).

1.5 Tissue like *in vitro* systems

As mentioned earlier, isolated hepatocytes are used in most liver *in vitro* studies in drug development because of their ability to perform the full range of known *in vivo* drug biotransformation pathways and retain many of the functions of liver cells. The two-dimensional 2D cell culture (monolayer culture) is traditionally used for *in vitro* drug metabolism studies. However, alternative methods should be considered since 2D cultures have many limitations (Acikgöz et al., 2013; Breslin and O'Driscoll 2013). The main disadvantage of 2D experimental systems is the early de-differentiation of primary hepatocytes in cultures which result in the decrease of metabolic competency and other liver specific functions, and eventually will compromise the effective biotransformation of drugs (Hewitt et al. 2007; Godoy et al., 2013). Therefore, it seems that 3D cellular assays would be more similar to and predictive of *in vivo* events compared to more simplified 2D cultures.

In this context, a number of *in vitro* models that provide physiologically relevant conditions and preserve *in vivo* like phenotype and biological activity of hepatocytes include microfluidic platforms, co-cultures, flow based hollow fibres, spheroids and bioreactors (Dittrich and Manz 2006; De Bartolo et al., 2007; Khetani and Bhatia, 2007; De Bartolo et al., 2009 Schmelzer et al., 2009; Leite et al., 2011; Prot et al., 2011; Acikgöz et al. 2013; Bachmann et al., 2015). Some of these new culturing approaches have been successful in retaining intracellular functions and hepatocyte polarity by forming 3D structure, cell-cell contact and providing a constant

medium flow and oxygen supply (Tilles et al., 2001; Bioreactors et al., 2004; Schmelzer et al., 2009; Vinci et al., 2011; Ishikawa et al., 2011). It has been observed that foetal liver hepatocytes cultured in rotating wall vessels were able to form 3D spheroids that were capable of producing albumin, store glycogen and the formation of bile canaliculi between hepatocytes (Ishikawa et al. 2011).

The use of 3D *in vitro* systems in drug research has therefore been considered as a forward step to bridge the gap between monolayer cultures and animal model studies (Nussler et al. 2001; Godoy et al. 2013).

1.6 *In vitro* Kinetics

1.6.1 Chemical Kinetics

Chemical reaction kinetics is the study of the rates of chemical processes and mechanisms by which they occur. Any chemical process consists of a sequence of one or more single-step processes known either as elementary processes, elementary steps, or elementary reactions. Chemical reaction can be classified according to their order i.e. first, second, or zero order (Cornish-Bowden 2012).

1.6.2 First Order Reaction

The spontaneous conversion of a substrate, S, into a product, P, such as in radioactive decay is considered as the simplest chemical reaction (Cornish-Bowden, 2012):

$$S \overset{k_1}{\rightarrow} P \qquad 1.13$$

Therefore, the velocity, v , of this reaction is the amount of S consumed or amount of P produced per unit of time (t) and is directly proportional to the quantity of S:

$$v = -\frac{d[S]}{dt} = \frac{d[P]}{dt} \qquad 1.14$$

The relationship between reaction rate, and concentration of reaction, [S], is:

$$v = k_1 [S] \quad 1.15$$

Therefore, the rate is proportional to the concentration of S multiplied by k_1. The first order rate constant (k_1) is concentration-independent and has units of time^{-1} (Figure 1.6.1b).

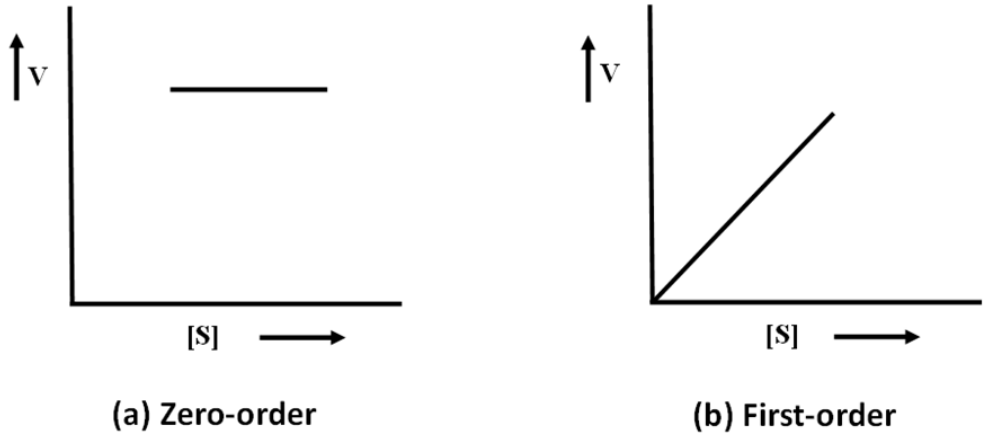


Figure 1.6.1: Graphical presentation of initial velocity against substrate concentration

A first order reaction can be visualised as a mono-exponential decay curve. The plot in (Figure 1.6.2) shows the exponential decline in substrate concentration with respect to time. Equation (1.16) describes this curve, where [S] is the substrate concentration, $[S]_0$ is the initial substrate concentration (y-intercept), k is the elimination rate constant and t is time.

$$[S] = [S]_0 . e^{-k_1 t} \quad 1.16$$

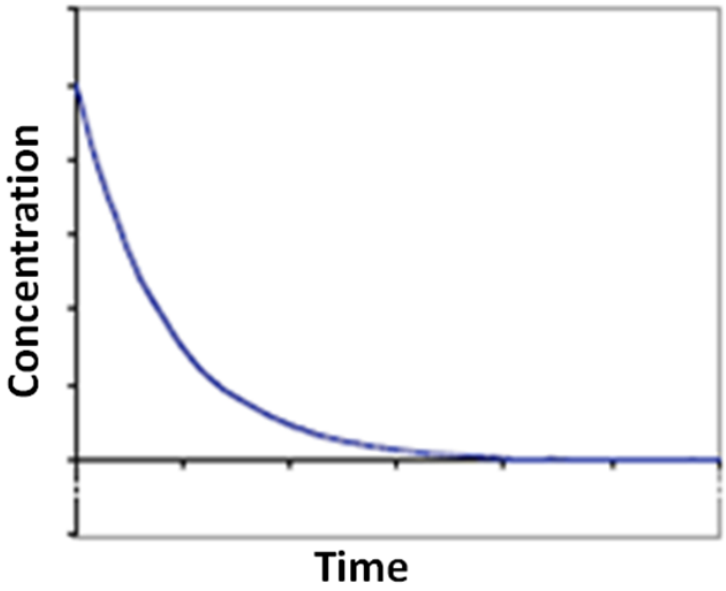


Figure 1.6.2: Mono-exponential Decay Curve. The mono-exponential decay curve describes first-order elimination when plotted as concentration versus time.

This type of curve can be linearized according to Eq. (1.17) by plotting the logarithmic entry of substrate or product concentrations versus time.

$$\ln[S] = \ln[S]_0 - k_1\, t \qquad 1.17$$

1.6.3 Zero Order Reactions

A Zero-order reaction describes the process where the rate of reaction is independent of the substrate concentration i.e. a fixed amount of reactant is eliminated per unit of time (Cornish-Bowden, 2012) (Figure 1.6.1a):

$$v = -\frac{d[S]}{dt} = \frac{d[P]}{dt} = k \qquad 1.18$$

Where k is zero order rate constant and has units of mol/time

Integration with respect to time gives a linear relation:

$$[S] = [S]_0 - kt \qquad 1.19$$

1.6.4 Enzyme kinetics

Enzyme kinetics deals with time-dependent enzyme reactions which aid to explain mechanisms of enzyme catalysis regulation (Bisswanger, 2008).

1.6.4.1 Enzyme catalysis

Reactant molecules must contain sufficient energy to cross a potential energy barrier (the activation energy) to enable a reaction to occur. Living cells exist at relatively low temperature (between 0°C and 100°C). However, most exogenic and endogenic metabolism reactions occur at elevated temperatures that are not suitable for cell maintenance and growth. On the other hand, enzymes allow cells to operate under relatively mild environmental conditions by selectively lowering the energy of activation of the vital chemical reactions. Hence, enzymes are catalysts which upsurge the rate of a reaction without itself being consumed during the process (Figure 1.6.3) (Segel, 1975).

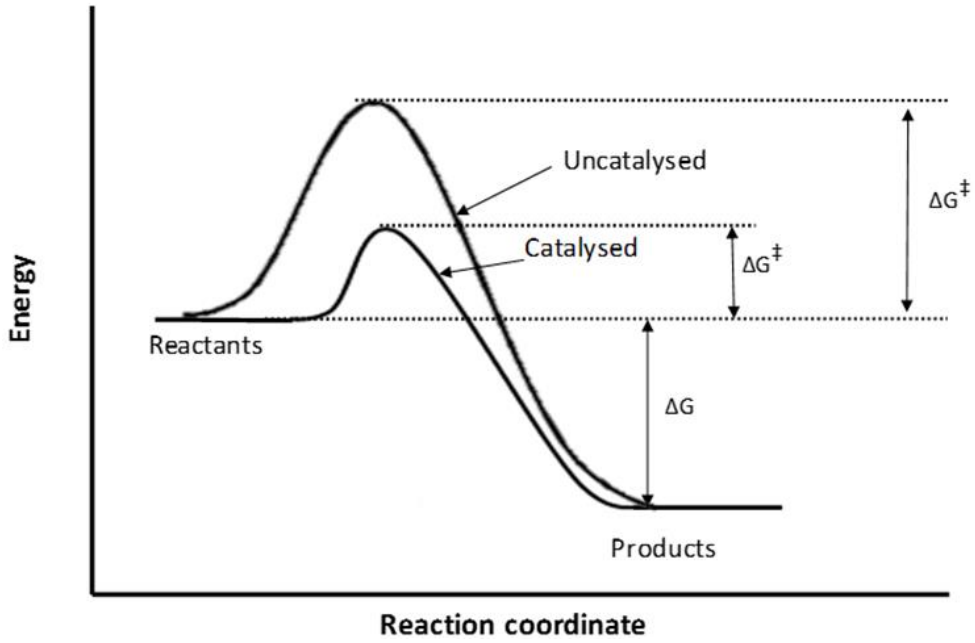


Figure 1.6.3: Energy change for an uncatalysed reaction and a catalysed reaction. Enzymes decrease the Gibbs free energy of activation, but they have no effect on the free energy ΔG of reaction.

For the enzyme catalysed reactions involving a single substrate, at low substrate concentrations, v is proportional to [S] as is normally expected for a first-order reaction. However, at high substrate concentration, v does not increase in proportion to the increase in [S] but instead levels off, and at high substrate concentration v is independent of [S] and reaches a maximum level i.e. V_{max}. Therefore, at these high [S] concentrations where the rate of enzyme catalysed reaction is no longer dependent on [S] the kinetics is zero-order (Segel, 1975) (Figure 1.6.4).

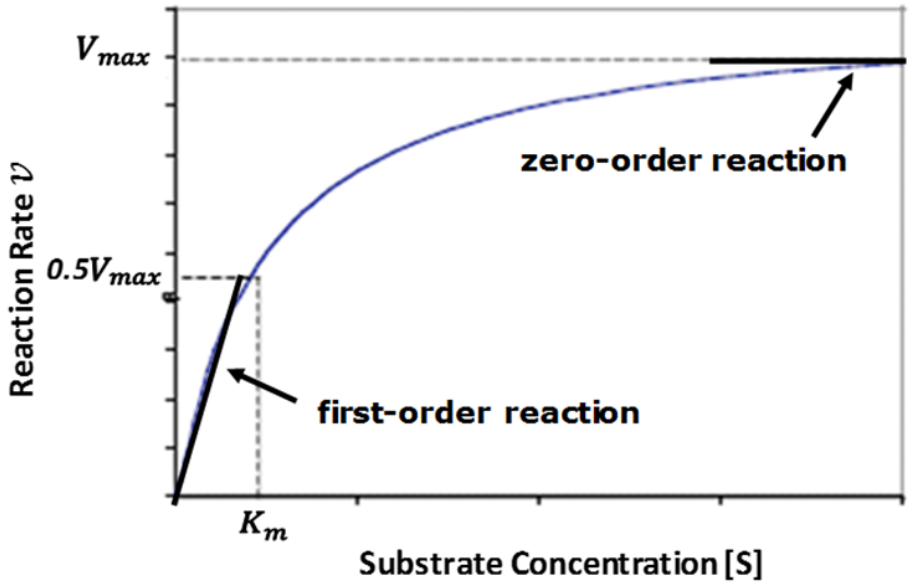


Figure 1.6.4: Graphical presentation of velocity against substrate concentration in an enzyme catalysed reaction. The graphical segments showing first-order and zero-order kinetics are marked. This Figure, also, shows the relationship between the rate of reaction for a simple Michaelis-Menten rate law. The reaction rate reaches a limiting value (saturates) at the V_{max}. K_m is the substrate concentration that gives half the maximum rate.

1.6.4.2 Michaelis-Menten kinetics

This model was established in 1913 by the German biochemist Leonor Michaelis (1875-1949) and the Canadian biochemist Maud L. Menten (1879-1960), based on French chemist Victor Henri's (1872-1940) discovery that enzyme activity could be saturated; it suggests that free enzyme binds to the reactant (substrate) forming an enzyme-reactant complex. This complex

undergoes a transformation resulting in a product and free enzyme is released. The free enzyme can be used in another round of binding to new reactant (Bisswanger, 2008). This mechanism is often written as:

$$E + S \underset{k_{-1}}{\overset{k_1}{\rightleftharpoons}} ES \xrightarrow{k_2} E + P \qquad 1.20$$

Here, E represents the free enzyme, S the substrate of the enzyme catalysed by the reaction, ES the enzyme-substrate complex, and P the product of the enzyme-catalysed reaction, k_1 the rate constant of the forward reaction of E+S, k_{-1} the rate constant of the reverse reaction where the enzyme-substrate complex, ES, separated to E+S and k_2 the rate constant of the forward reaction of ES forming E+P. In this model, it is assumed that none of the product reacts with the enzyme to form the enzyme-substrate complex, ES (this is the case during the initial stage of the reaction when product [P] is low, whereas towards the end of the reaction when [P] is high this may no longer be correct).

From equation 1.20, an expression that relates the reaction velocity, v, to the enzyme substrate complex concentration, [ES] and the rate constant of the forward reaction of product formation, k_2 , of the individual step can be derived. Thus, v can be expressed as:

$$v = (\frac{d[P]}{dt}) = k_2[ES] \qquad 1.21$$

Since ES is an intermediate, its concentration cannot be measured easily, however [ES] can be expressed in terms of known values. As the enzyme can either be unbound (E) or bound (ES) to the substrate, the fraction of bound enzyme can be expressed as follows:

The rates at which [ES] is formed and broken-down are:

Rate of formation:

$$[ES] = k_1[E][S] \quad 1.22$$

Rate of breakdown:

$$[ES] = (k_{-1} + k_2)[ES] \quad 1.23$$

There is a quasi-equilibrium state which is retained, however, only for a limited period. This state is termed as steady-state. Under the steady-state estimation, the concentration of the intermediate [ES] stays constant, while the concentrations of reactants and product change (Chang, 2005). The steady state occurs when eq. 1.22= eq. 1.23 i.e.

$$k_1[E][S] = (k_{-1} + k_2)[ES] \quad 1.24$$

Rearranging,

$$[ES] = \frac{[E][S]k_1}{k_{-1} + k_2} \quad 1.25$$

This leads to define a new constant, the Michaelis-Menten constant (K_m), as follows in eq (1.26):

$$K_m = \frac{K_{-1+}K_2}{K_1} \quad 1.26$$

Substituting 1.26 into 1.25

$$[ES] = \frac{[E][S]}{K_m} \quad 1.27$$

Since in most situations the enzyme concentration is very small ([E] << [S]), the binding of substrate to enzyme is in equilibrium i.e. the concentration of the unbound S is almost equal to the total concentration of S_0. The concentration of unbound E is equal to the total enzyme concentration [E_0] minus the concentration of the complex [ES].

$$[E] = [E_0] - [ES] \quad 1.28$$

Substituting (1.28) into (1.27)

$$[ES] = \frac{([\mathrm{Eo}] - [ES])[S]}{K_m} \quad 1.29$$

Solving (1.29) for [ES],

$[E_0]$ [S] - [ES] [S] = [ES] K_m

or

$[E_0]$ [S] = [ES] (K_m+ [S])

Or

$$[ES] = [E_0]\ \frac{[\mathrm{S}]}{[S] + K_m} \quad 1.30$$

Substituting (1.30) into $v = (\frac{d[P]}{dt}) = k_2[ES]$

$$v = k_2[E_0]\ \frac{[\mathrm{S}]}{[S] + K_m} \quad 1.31$$

The maximum reaction velocity, V_{max}, is reached when all enzyme sites are saturated with the substrate. This will occur when [S]>> K_m, so that [S]/([S]+ K_m) approaches 1. In this limit, V_{max} can be expressed from (1.32) as:

$$V_{max} = k_2\ [E_0] \quad 1.32$$

Substituting (1.32) into (1.31),

$$v_0 = \frac{V_{max} \cdot [S]}{[S] + K_m} \quad 1.33$$

The most appropriate rate to experimentally measure is the initial rate (v_0). If v_0 vs [S] is plotted, the resulting plot will have a shape as shown in (Figure 1.5.4). Therefore, equation (1.33) describes the kinetic behaviour of an enzyme as modelled by the scheme in equation (1.19). Analysis of (equation 1.33) at very low substrate concentrations, when [S] <<K_m, v_0 approximates to,

$$v_0 = \frac{V_{max}}{K_m} \qquad 1.34$$

The rate is proportional to [S] describes the linear region of the plot in (Figure 1.5.4). At high substrate concentrations, when [S] >>K_m, v=V_{max} and hence independent of [S] (the "plateau" region of the plot in (Figure 1.5.4).

The three most common methods, available in the literature, for determining the V_{max} and K_m are Lineweaver-Burk plot (the double reciprocal plot), Eadie-Hofstee plot, and Hanes-Woolf plot. All three of these methods are linearised models that convert the original Michaelis-Menten equation into a form which can be graphed as a straight line (Marasovi et al., 2017).

The first linearization method has been named after American Chemists H. Lineweaver (1907-2009) and Dean Burk (1904-1988), and it is based on the plot of 1/ v vs. 1/[S] (Chang, 2005). Therefore, the equation (1.33) can be re-arranged as:

$$\frac{1}{v_0} = \frac{1}{V_{max}} + \frac{K_m}{V_{max}} \frac{1}{[S]} \qquad 1.35$$

The reciprocal of the rate data plotted against the reciprocal of the substrate concentration (1/ v vs. 1/[S]), will give a straight line with a y-intercept = 1/V_{max} and a slope = K_m/V_{max} (Figure 1.6.5).

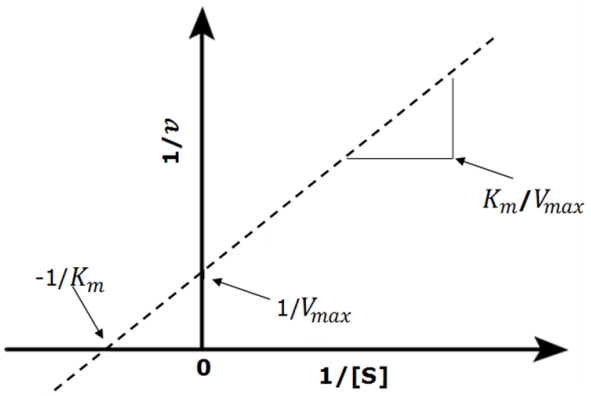


Figure 1.6.5: A double-reciprocal plot, between velocity (v) and [S].

The limitation of the Lineweaver-Burk plot is that when using a wide substrate concentration range, the majority of the data will be obscured i.e. linear regression of data transformed in this way effectively weights/skews the line to the lowest concentration data, which is more than likely to be the least accurately determined (Chang, 2005); (Bisswanger, 2008). The second method is named the Eadie-Hofstee plot ((Bisswanger, 2008), and is based on multiplying both sides of (equation 1.35) by $v_0 V_{max}$ to obtain:

$$V_{max} = v_0 + \frac{v_0 K_m}{[S]} \qquad 1.36$$

Rearrangement of (eq. 1.36) gives:

$$v_0 = V_{max} - \frac{v_0 k_m}{[S]} \qquad 1.37$$

The Eadie-Hofstee transformation yields a linear regression line with slope equal to $-K_m$, V_{max} as the y-axis intercept and V_{max}/K_m as x-axis intercept (Figure 1.6.6).

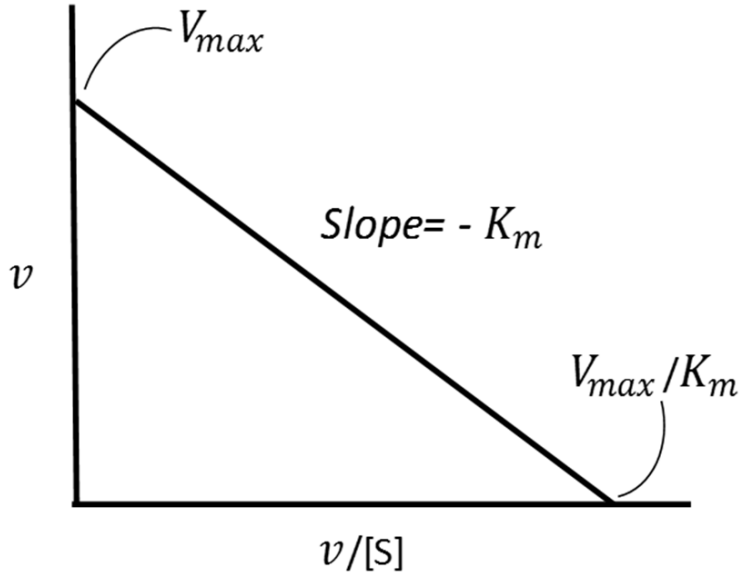


Figure 1.6.6: Eadie-Hofstee plot

The disadvantages of this method are that values plotted on the x-axis (v /[S]) are not independent from those on the y-axis (v) and any error which occurs in the experiment will therefore be present on both axes. However, the error in this plot is lower than Lineweaver-Burk plot. The third approach is called the Hanes-Wolf method (Bisswanger, 2008) (eq. 1.38):

$$\frac{[S]}{v_0} = \frac{K_m}{V_{max}} + \frac{[S]}{V_{max}} \qquad 1.38$$

Eq 1.38 gives a straight line when [S]/ v_0 is plotted against [S] with $1/V_{max}$ as slope, K_m/V_{max} as y-axis intercept and $-K_m$ as x-axis intercept (Figure 1.6.7).

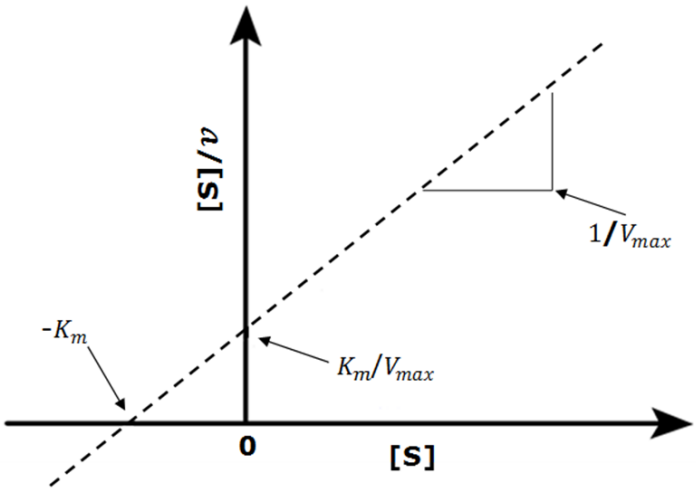


Figure 1.6.7: Hanes-Wolf plot

K_m and V_{max} can be derived using this method with smaller error than the two previous approaches. Moreover, the Hanes-Wolf plot avoids the problem of the Eadie-Hofstee plot of having velocity (dependent) data affecting the data on the x-(independent) axis (Bisswanger, 2008). However, with the entering of the computers era, nonlinear regression techniques are used to determine parameters. Wilkinson (1961) suggested the use of least-squares nonlinear regression for more precise estimation of enzyme kinetic parameters. Nonlinear regression permits direct determination of K_m and V_{max} from untransformed data points. The procedure starts with initial estimates and then continually concurs on parameter estimates that provide the best fit of the underlying model to the actual data points (Motulsky and Christopoulos 2003; Marasovi et al., 2017). The algorithms used include the Levenberg-Marquardt method, the Gauss-Newton method, the steepest-descent method, and simplex minimization. Several software packages, such as Excel, MATLAB, and Graph Prism, nowadays include readily available routines and scripts to perform nonlinear least-squares fitting (Nelatury et al., 2014; Kemmer and Keller 2010).

1.6.4.3 The Significance of V_{max} and K_m

V_{max} represents the maximum rate at which the total enzyme concentration is present as the enzyme-substrate complex, ES. From equation (1.33), when [S] = K_m , then v_0 = V_{max}/2. Hence, K_m is equal to the substrate concentration at which the reaction rate is half its maximum value. Therefore, an enzyme that has a small value of K_m , will achieve its maximum catalytic efficiency at low substrate concentrations, which averages the smaller the value of K_m , the more efficient is the catalyst. K_m , also, usually describes the affinity of substrate for the free enzyme (k_{-1}>>k_2) i.e. the smaller the value of K_m, the higher the affinity of enzyme for that substrate. The value of K_m for an enzyme depends on the particular substrate, the pH of the solution and the temperature at which the reaction is carried out (Fersht 1999; Chang 2005).

1.7 Predictions of hepatic xenobiotic clearance

The biotransformation of a drug to more polar metabolites is a crucial step in drug elimination. Without this process, the drug will persist in the body and drug accumulation could occur. The structure of the drug moiety plays a key role in the way in which drugs are transformed. Biotransformation is performed mainly in the liver; however, the liver also possesses excretory functions in which drug or metabolic products are excreted into bile (Grijalva and K. 2013).

From the kinetic prospective, hepatic clearance for the metabolism of compounds comprises two main features: intrinsic (metabolic) clearance for the unbound compound in hepatocytes and unbound (free) fraction of compound in the blood (or plasma when corrected by the blood-to-plasma partition) (Shibata et al., 2002). Intrinsic (metabolic) clearance (Cl_{int}) can be defined as the liver capacity to remove a drug in the absence of other confounding factors i.e. hepatic blood flow (Q_H) and drug binding to cells or

proteins in the blood (Hakooz et al., 2006). The Cl_{int}, when the drug concentration << K_m, can be calculated from the maximum velocity (V_{max}) and the Michealis-Menten constant (K_m) of the suitable eliminating enzyme(s) involved (Iwatsubo et al. 1997; Nikolic and Agababa 2009) using the following (equation 1.39).

$$Cl_{int} = \frac{V_{max}}{K_m} \quad 1.39$$

Experimentally, the parameters V_{max} and K_m can be determined by quantifying the initial production of metabolite with time for a range of drug concentrations in a liver *in vitro* metabolising system e.g. microsomes, hepatocytes etc. From (equation 1.40) the initial linear increase in metabolite concentration (Δ[M]) divided by time period elapsed (ΔT) will approximate to the initial rate (v_0)

$$v_0 = (\frac{d[P]}{dt}) \sim \frac{\Delta[M]}{\Delta T} \quad 1.40$$

However, one of the major issues with measuring metabolite production is that the molarity of the metabolite is required in order to give appropriate units that can be compared across laboratories. Without an authentic metabolite standard, neither the metabolite species can be confirmed, nor the molar concentration be determined. An alternative approach in determining V_{max} and K_m is by monitoring drug depletion (Nath and W. M. 2006). When substrate depletion displays apparent first-order kinetics, substrate concentration as a function of time can be described by the following single exponential.

$$[D]_t = [D]_0 e^{-k_{dep}t} \quad 1.41$$

Where $[D]_t$ represents the drug concentration at transient time (t), $[D]_0$ is the initial drug concentration and k_{dep} is the apparent first-order rate constant of substrate depletion. Taking the first derivative of (eq. 1.41) gives:

$$-\frac{d[D]_t}{dt} = k_{dep}\,[D]_t \qquad 1.42$$

Under the steady-state assumption

$$-\frac{d[D]_t}{dt} = \frac{d[M]_t}{dt} \qquad 1.43$$

Where $[M]_t$ is the metabolite concentration at transient time (t). However, close to the start of the reaction

$$\frac{\Delta[M]}{\Delta T} \sim v_0 \sim k_{dep}\,[D]_0 \qquad 1.44$$

This assumption means that only data from the beginning of each reaction, where $[D]_t$ is close to its initial value, should be used in the calculation of k_{dep} and ultimately V_0.

The advantage of using the depletion method is that the initial rate v_0 in appropriate units can be determined without knowing the change in molar drug concentration because determining k_{dep} only requires a rate of change from an arbitrary quantification e.g. arbitrary area under a mass spectrum peak. k_{dep} is determined from the slope of a natural logarithm (Ln) of drug response versus time plot. Once V_o has been determined, from either metabolite appearance or drug depletion, V_{max} and k_m can be determined as long as significant saturation has been reached. However, if sufficient saturation has not been reached then V_{max} and hence k_m will be highly extrapolated. This is often the case; however, Cl_{int} can still be determined

accurately by calculating the initial slope of the V_o verses initial drug concentration, $[D]_0$, Michalis-Menten plot.

Generally, the intrinsic clearance for the unbound compound is measured *in vitro* by the incubation of isolated hepatocytes or subcellular fractions such as S-9 and microsomes in the protein-free medium (Wilson et al., 2003). The *in vitro* data obtained using liver tissue needs to be scaled to predict the *in vivo* metabolic clearance (Cl_{int} per liver).

1.8 *In vitro-in vivo* extrapolation (IVIVE)

In vitro-in vivo extrapolation (IVIVE) requires a knowledge of the amount of microsomal protein per gram of liver (MPPGL) or hepatocellularity per gram of liver (HPGL), and the size of the liver. For hepatocytes, the intrinsic (metabolic) clearance data are expressed per million cells and can be scaled to *in vivo* intrinsic (metabolic) clearance by multiplying the former by hepatocellularity of the entire liver. For hepatic microsomes the intrinsic (metabolic) clearance data are expressed per milligram of microsomal protein. In order to scale the microsomal intrinsic (metabolic) clearance data to the *in vivo* intrinsic (metabolic) clearance the MPPGL must be determined. To determine the MPPGL and HPGL a marker within the microsomes must be employed and is usually taken as the ratio of the nanomoles of P450 per gram of liver (obtained from a whole-homogenate analysis) divided by the nanomoles of P450 per milligram of microsomal protein and has units of milligrams of microsomal protein per gram of liver (Iwatsubo et al., 1997, Hakooz et al., 2006).

The obtained kinetic parameters from the *in vitro* incubation needs to be scaled up to a whole-liver capacity (Cl_{int} per liver) (Figure 1.7.1). However, there are other physiological determinants that should be taken into account in the IVIVE procedure such as hepatic blood flow (Q_H) and the fraction of drug unbound in blood (f_u) (Pang and M. 1977).

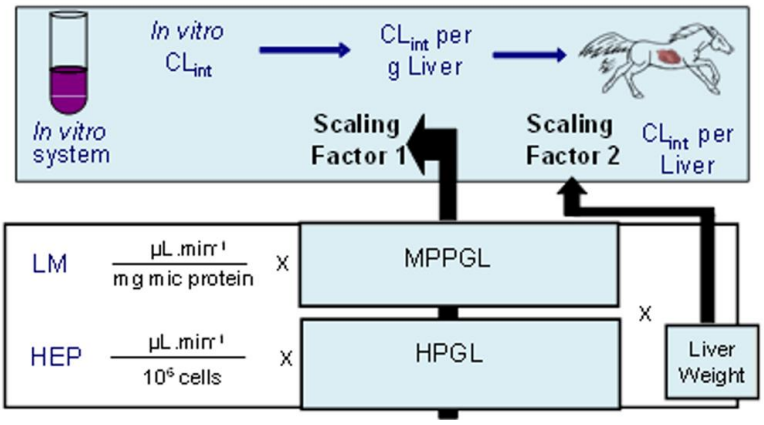


Figure 1.8.1: *In vitro to in vivo* scaling

The two most important models that have been used to explain and predict quantitatively the influence of these physiological parameters on blood clearance are: the well-stirred and parallel tube models (Pang and M. 1977). The well-stirred model assumes that the liver is a single well-stirred compartment and that the concentration of unbound drug in the emergent blood is in equilibrium with that within the liver (Figure 1.7.2a). Therefore, hepatic clearance can be calculated using the following equation:

$$CL_H = \frac{Q_H * fu * CLint}{Q_H + fu * CLint} \qquad 1.45$$

The parallel tube model assumes that the liver is composed of number of identical and parallel tubes with enzymes distributed evenly in each cross section of the sinusoidal vascular and perisinusoidal space. The total liver enzymatic activity (V_{max}) is the sum of the individual enzymatic activities for each tube (Pang and Rowland 1977) (Figure 1.7.2b). Therefore, hepatic clearance can be calculated using the following equation:

$$Cl_H = Q_H - Q_H * \exp\left(-fu * \frac{CLint}{Q_H}\right) \qquad 1.46$$

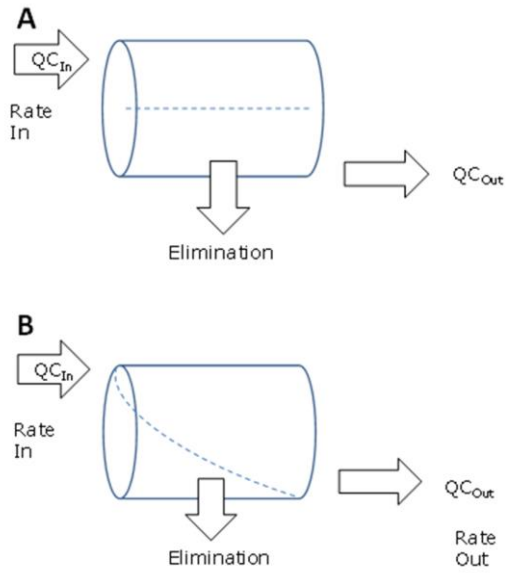


Figure 1.8.2: Schematic diagram of the liver. The "Well stirred" model (A) describes the liver as a single well stirred compartment. The difference between the rate of presentation of drug to and its rate of exit from the liver at steady state is represents the rate of drug elimination. The dashed line represents the unbound hepatic drug concentration. The "Parallel tube" model (B) views the liver as a series of identical and parallel cylinders; each cylinder represents a sinusoid with enzymes distributed evenly in hepatocytes lining the tubes. The dashed line represents the declining unbound hepatic drug concentration along the direction of blood flow. Adapted from Pang and Rowland (1977).

Prediction of human population clearance using the *in vitro-in vivo* extrapolation (IVIVE) has become a key tool in both discovery and preclinical phases of the drug development process (Naritomi et al., 2001). In human IVIVE, the common values of MPPGL and HPGL used are 45 mg/g of liver and 120×10^6 cell/g of liver, respectively. However, several studies revealed that age may has a negative effect on these values and subsequently on hepatic drug-metabolising capacity. (Barter et al., 2008; Kwak et al., 2014),

1.8.1 Drug binding

Binding of drugs to plasma proteins is a significant element affecting their pharmacokinetic and pharmacodynamic properties. Several studies have suggested that unbound fraction of drug in blood or plasma should be taken into account for determining Cl_H and are included in the well stirred and

parallel tube models discussed previously (Wilkinson and Shand 1975; Pang and Rowland 1977). However, it has been found that as well as binding of drug to blood *in vivo*, binding of the drug to non-specific proteins in the *in vitro* studies has a significant impact on the Cl_H extrapolation (Obach 1997; Obach 1999). This seems to be reasonable since *in vitro* assays are not pure systems; hence, as bound drug is unavailable for metabolism, the K_m measured in the *in vitro* assays is assumed to be free drug concentration (Obach 1997; Obach 1999). Consequently, a K_m correction should be made for this nonspecific binding of drug in the assay using the unbound fraction of drug in the incubation. This factor can be implemented into (equation 1.45) and the result is Equation 1.47 for Cl_H (Obach 1996; Austin et al. 2002).

$$CL_H = \frac{Q_H * fu * \frac{Cl_{int,in\ vitro}}{Fu_{inc}}}{Q_H + fu * \frac{Cl_{int,in\ vitro}}{Fu_{inc}}} \qquad 1.47$$

1.9 Drug-Drug interactions

When drugs are co-administered a drug-drug interaction (DDI) may occur where the drug may either inhibit or induce the metabolism of the second drug (Gibson and P. 2001). Competition between two drugs, metabolised by the same CYP, may result in that only one will be metabolised. Also, some drugs are metabolised by two enzyme systems; therefore, inhibition or induction of one enzyme system may or may not cause clinically significant interactions. On the other hand, the elevation in the total amount of CYP enzyme via induction, by a specific drug could lead to a marked decrease in plasma concentration of this drug. This can have significant consequences in the pharmacokinetics and toxicity of drugs (Ito et al., 1998; Gibson and Sket 2001).

1.9.1 Enzyme inhibition

Competitive binding at the enzyme's binding site is the most common cause of CYP inhibition. Competitive binding depends on the affinity of the substrate for the enzyme, the concentration of substrate needed for inhibition, and the half-life of the inhibitor drug. The duration of enzyme inhibition relies on the half-life and time to steady state of the inhibitor drug. The mechanism of CYP inhibition can be divided into three categories (a) reversible inhibition, (b) quasi-irreversible inhibition and (c) irreversible inhibition. Of these, reversible inhibition is considered as the most common cause of documented drug interactions. Both quasi-irreversible and irreversible inhibitions are caused by the formation of reactive metabolites (Badyal and Dadhich 2001; Hollenberg, 2002).

1.9.1.1 Reversible inhibition

In the reversible inhibition of CYPs, the enzymes will resume their normal metabolic functions after removal of the inhibitors from the body. Nitrogen-containing drugs, such as imidazoles, pyridines and quinolines are one of the most potent reversible CYP inhibitors (Lin and A. Y. 1998). This type of inhibition can be classified as competitive, non-competitive, or uncompetitive (Chang 2005).

a) Competitive inhibition

In competitive inhibition substrate binding to the active site of the enzyme is prevented by the interaction between the inhibitor and the enzyme (Figure 1.9.1). Therefore, the simple Michaelis-Menten equation that describes reactions involving one substrate, (equation 1.48) will be expressed as follows:

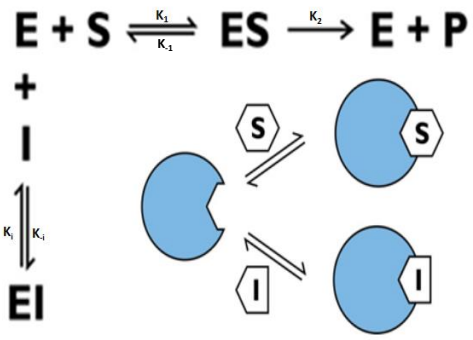


Figure 1.9.1: The scheme of competitive inhibition

$$v_i = \frac{V_{max} * [S]}{K_m\left(1 + \frac{[I]}{K_i}\right) + [S]} \qquad 1.48$$

Where V_i is the velocity in the presence of inhibitor; E is the enzyme, S is the substrate, ES is the enzyme-substrate complex, P is the product, I, is the inhibitor, EI, is the enzyme-inhibitor complex and K_i, is the inhibition constant for I.

When $V_0 = 2V_i$ (the conditions for an inhibitor decreasing V_0 by 50% also known as the IC_{50}), then the value for the K_i is:

$$\frac{2V_{max}*[S]}{K_m\left(1+\frac{[IC_{50}]}{K_i}\right)+[S]} = \frac{V_{max}*[S]}{K_m+[S]} \qquad 1.49$$

By rearrangement:

$$IC_{50} = K_i(1 + \frac{S}{K_m}) \qquad 1.50$$

Hence,

$$K_i = \frac{IC_{50}}{(\frac{S}{K_m} + 1)} \qquad 1.51$$

According to Equation 1.51, if $S=K_m$ then $Ki=IC_{50}/2$, If $S>>K_m$ then $K_i<<IC50$ and if $S<<K_m$ then $K_i \cong IC_{50}$.

Malonic acid, $CH_2(COOH)_2$, represents the best example for competitive inhibition. It competes with succinic acid in the dehydrogenation reaction catalyzed by succinic dehydrogenase. In normal cases, succinic acid is converted to fumaric acid by succinic dehydrogenase. However, in the presence of Malonic acid which has, almost, the same structure as succinic acid, it can combine with the enzyme, although no product is formed in this reaction (Chang 2005).

b) Non-competitive inhibition

In noncompetitive inhibition, the inhibitor does not bind to the active site; it binds to another site of the enzyme (Figure 1.9.2). This enzyme-substrate-inhibitor complex is, catalytically, non-functional and has no direct effect the binding of substrate, but it reduces the enzyme activity (Chang 2005).

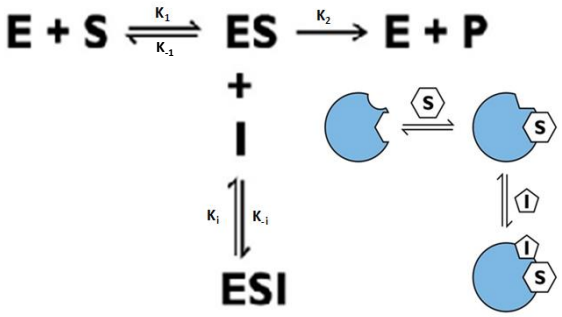


Figure 1.9.2: Non-competitive inhibition

The K_i can be expressed by the following equation:

$$K_i = \frac{IC_{50}}{(\frac{K_m}{S} + 1)} \qquad 1.52$$

According to Equation 1.50 if $S=K_m$ then $K_i=IC_{50}/2$, If $[S]>>K_m$ then $K_i \cong IC_{50}$ and if $[S]<<K_m$ then $K_i<<IC_{50}$.

An example of noncompetitive reversible inhibitor is digitalis, which blocks the activity of Na^+-K^+ ATPase which is used for the treatment of cardiac arrhythmia.

c) Uncompetitive inhibition

In this type of inhibition, the inhibitor binds to both enzyme and enzyme-substrate complex and consequently a non-productive enzyme-substrate-inhibitor complex will be formed (Figure 1.9.3) (Hollenberg, 2002).

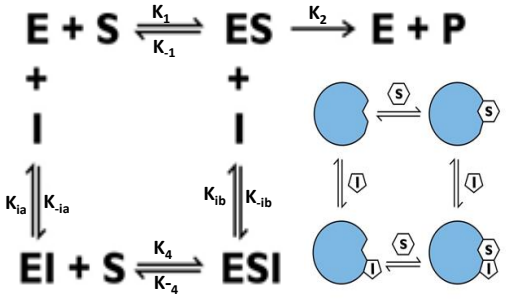


Figure 1.9.3: Uncompetitive inhibition

The K_i is expressed by:

$K_i = IC_{50}$ when $S = K_m$ or $S >> K_m$ or $S << K_m$

Oxalate, which inhibits lactate dehydrogenase is one of the best examples of an uncompetitive reversible inhibitor (Mohan et al., 2013).

1.9.1.2 Quasi-irreversible inhibition

Quasi-irreversible inhibition involves the formation of a non-covalent, but tight quasi-irreversible complex. In the case of CYP P450 enzymes a tight complex is formed with the iron of the heme prosthetic group. Despite the fact that this tight metabolic intermediate (MI) complex does not destroy the enzyme; the MI complex is so stable *in vivo* that the enzyme involved in the complex is unavailable for drug metabolism. Thus, any new enzyme biosynthesis process will be interrupted. In a practical sense, the MI complex can be considered as irreversible inhibition *in vivo* (Hollenberg, 2002; Riley

et al., 2007). However, Quasi-irreversible inhibition can be reversed in experimental conditions, for instance, by incubation with highly lipophilic drugs that displace the metabolic intermediate from the active site of the enzyme, by irradiation at 400 to 500 nm, or by ferricyanide (Ullrich and Schnabel, 1973; Dickins et al., 1979).

1.9.1.3 Irreversible inhibition

In this category of inhibitors, the enzyme is inactivated (destroyed) by binding of reactive intermediates to the heme and/or protein of the CYP. Enzyme activity cannot be resumed even after elimination of the inhibitor, and *de novo* biosynthesis of enzymes is the only way to restore the functional activity (Hollenberg, 2002). Because of their ability to bind by stable covalent bonds with the active site of the enzyme or destroy an essential functional group of the active sites, irreversible inhibitors are often used to identify functional groups of the enzyme's active sites (Chang 2005; Sharma 2012). For example, iodoacetamides and maleimides act as irreversible inhibitors to the sulfhydryl groups of lactate dehydrogenase enzyme (Barthová et al., 1977). Moreover, organophosphorus nerve gases such as Sarin and Tabun and other organophosphorus toxins such as the insecticides malathion, parathion and chlorpyrifos inhibit acetylcholine esterase (ACE), which leads to the accumulation of acetylcholine that overstimulates the autonomic nervous system (including heart, blood vessels, and glands). Hence poisoning symptoms of vomiting, abdominal cramps, nausea, salivation, and sweating will appear on the victim (Sharma, 2012).

1.9.1.4 Substrate auto inhibition

Substrate auto-inhibition can occur at high substrate concentrations as a result of the substrate blocking the enzyme's activity, or alternatively the product (metabolite) produced by the enzyme inhibiting the enzyme's

activity. For both mechanisms of substrate inhibition, a typical Michaelis-Menten analysis may not be possible for the data (Lu and A. P. 2010). The inhibition constant (K_i) can be used to determine the reaction velocity rate via (equation 1.53).

$$v_0 = \frac{V_{max} * [S]}{K_m + [S]\left(1 + \frac{[S]}{K_i}\right)} \quad 1.53$$

1.9.2 Cytochrome P450 induction

Induction can be described as a slow regulatory process that increases the intracellular enzyme concentration and in most cases due to transcriptional gene activation. Cytochrome P450 1A1 and 1A2 are the main targets of induction; however, other metabolising enzymes are also increased such as glutathione S-transferases (GSTs). Generally, CYP induction is considered as an important part of the defense system since it increases the capability for metabolic detoxification and elimination (Fuhr, 2000; Tompkins and Wallace, 2007).

The advances achieved in sequencing of equine CYP P450 isoform and comparing their activity to human isoforms allows to indicate some differences in drug metabolism between the two species. In addition to, availability of equine tissue that needs less resource requirement and ethical consideration have led to the use of *in vitro* techniques using *ex vivo* liver is gaining popularity in equine metabolism research (Scarth et al., 2010).

1.10 Hypothesis and Aims

As mentioned earlier, several *in vitro* models have been developed successfully using human and rat hepatocyte and microsomes. However, it is hypothesised that the presence of any evolutionary difference in xenobiotic metabolising enzymes between human and horses may lead to different pharmacokinetics. Therefore, the main aim of this research is to

develop an *in vitro* approach that mimics the *in vivo* pharmacokinetic clearance of a drug in horse and can be used for equine drug metabolism studies. With the following objectives:

- Isolation of fresh equine hepatocyte with high viability
- Cryopreservation of the freshly obtained hepatocytes
- Preparation of equine liver microsomes
- Determination of microsomal protein per gram of liver (MPPGL) and hepatocellularity (HPGL) for horses.
- Generation of enzyme kinetic parameters for commonly used equine drugs using hepatocytes and microsomes and the prediction of their hepatic metabolic plasma clearance.
- Detection of horse specific drug metabolites.

Chapter 2
General Materials and Methods

2 Materials and Methods

2.1 Preparation of equine liver homogenates and microsomes

2.1.1 Horse liver tissue

Samples of fresh horse liver were obtained from F. Drury and Sons Ltd, Swindon except for two samples, which were obtained from the Animal Health trust (AHT) Newmarket. The ages of horses (n=39) range from 1 to 29 years. All horses were slaughtered in accordance with the Welfare of Animals at the Time of Killing (UK) Regulation 2015. After the chosen liver being inspected by the veterinarian, small cubes were excised, immediately put into a labelled bag and then flash frozen using dry ice.

2.1.2 Homogenisation of liver samples

Tissue samples (approximately 5 g), previously stored at -80 °C, were thawed on ice and weighed accurately. The samples were finally chopped and homogenized using a blender (ASDA, UK) for 60s in 0.15 M potassium chloride buffer pH 7.4 (10 ml/gram of liver). The homogenised samples were filtered through a nylon mesh (pore size= 250 µm) (Fisher scientific, UK). The aliquots were stored at -80 °C.

2.1.3 Preparation of microsomes

Microsomes were prepared according to a protocol described by Wilson et al. (2003). Briefly, the homogenates were centrifuged at 10,000g for 20 minutes at approximately 4 °C and the supernatant (S24 fraction) retained. The supernatant was then centrifuged at 100,000g for 60 minutes and the resulting supernatant was discarded, and the pellet re-suspended in ice cold 0.1 M phosphate buffered saline (PBS), before being centrifuged at 100,000g for a further 60 minutes. The final pellet was then re-suspended in a volume of PBS equivalent to two thirds the weight of the original tissue. Samples of

all fractions were stored at – 80 °C pending CYP P450 and total protein determination.

2.1.4 Protein determination

The total concentration of the protein of homogenate and microsomal samples (both diluted 10 and 20-fold) were measured according to Bradford (1976).

The linear calibration curve was made with Bovine Serum Albumin BSA (Fisher, UK). A 2 mg/ml BSA solution was prepared in elution buffer (1× Phosphate Buffer Solution, PBS) and this was used to make a calibration standard curve of serial dilutions (0, 0.1, 0.5, 1.0, 1.4 and 2 mg/ml).

20 µl of each standard dilution and sample was mixed in a microcentrifuge tube with 1 ml of Bradford reagent (Sigma Aldrich, UK). 20 µl of the liver microsomes was mixed with 1 ml of Bradford reagent. Samples were left for 5 min at room temperature, and then transferred to cuvettes (Fisher, UK) to determine the Optical density (OD) at 595 nm using a Biochrom Libra S22 spectrophotometer (Scientific Laboratory supplies, UK).

The protein concentration was determined by comparing the OD of the liver microsomes against the standard calibration curve. The total concentration of protein present in the original sample of equine liver microsomes was calculated by multiplying the determined protein concentrations for the diluted samples with the dilution factor.

2.1.5 Cytochrome P450 determination

A dithionite difference spectroscopy method (Matsubara et al. 1976) was used to determine the P450 content of the microsomes and homogenate fractions using a Unicam UV/Vis Spectrometer UV4 (Unicam, Cambridge, UK). The samples were exposed to carbon monoxide for one minute, at the rate of one bubble per second. Each sample was divided in two cuvettes and the baseline recorded. Sodium dithionate (Sigma-Aldrich, UK) was added to

one cuvette and the spectral difference between the two samples was determined. The CYP P450 content in both microsomes and homogenate was calculated using (equation 2.1).

$$nmol\ P450\ per\ ml = \frac{(A450 - A490)}{0.091} \quad 2.1$$

Where 0.091 mL/nmol/cm is the CYP450 molar extinction coefficient, A450 is absorbance at 450nm and A490 is absorbance at 490nm.

2.1.6 Correction for loss of microsomal protein

Calculation of total P450 content of both the homogenate and microsomes can be used to correct for any losses in microsomal protein in the preparation process (Wilson et al., 2003) as over 96% of the 450 content of the liver has been shown to be membrane bound (Guengerich et al., 2009). The equation used to correct for losses in microsomal protein in the preparation process is:

$$MPPGL = \frac{\text{nmol P450 Homogenate } g^{-1}\ liver}{\text{nmol P450 Microsomes } mg^{-1}\ microsomal\ protein} \quad 2.2$$

2.2 Isolation of primary equine hepatocytes

2.2.1 Equipment and reagents

Hank's buffered salt solution (HBSS) without calcium, magnesium or phenol red (Fisher Scientific, UK), Hank's buffered salt solution (HBSS) 10× with calcium and magnesium and without phenol red (Fisher Scientific, UK), Collagenase, Type IV (Fisher Scientific, UK), Williams' Medium E, no phenol red (Gibco®, UK), Autoclaved water, Percoll® (Sigma, UK), Sterile cell strainer 100 µm and nylon mesh 250 µm (Fisher Scientific, UK). The perfusion system consisted of: Peristaltic pump (MasterFlex, Cole-Parmer, USA), Water bath (Fisher Scientific, UK), Jacketed condenser (Fisher Scientific, UK), Bubble trap (CAPIOX® Bubble Traps, Terumo, UK), Büchner

funnel 240 mm (VWR International, UK), Sterile 50 mL conical tubes, Tubing connectors Y-type (Fisher Scientific, UK) and olive tip cannulae (Emst Kratz GmbH, Germany) (Figure 2.2.1a).

2.2.2 Source of liver samples

Samples of horse liver, were obtained from F. Drury and Sons Ltd, Swindon, UK. Liver samples (preferably the left lateral, caudate or Quadratus segment) were excised ex vivo about 20-25 mins after slaughter. The tissue then placed in labelled plastic bag and immersed with cold HBSS (0-2 $^{\circ}$C) and placed on ice in a polystyrene container. The liver sample was then transported to the laboratory, a journey of 2,5-3 hours.

2.2.3 Hepatocyte preparation

The isolation of primary hepatocytes has never been practiced in our lab. Therefore, the development of the protocol to isolate equine hepatocytes with acceptable levels of yield and viability was contained a relatively long optimisation process. Although, the perfusion system simply consists of a pump, autoclavable silastic tubing, water bath and a bubble trap, but finding a proper bubble trap was one of the key issues during optimisation process. Finding a prober bubble trap was not an easy job; hence, three types of bubble traps was tested: the first one was a modified 50 ml Eppendorf tube (fisher, UK), the second was heating coil with built in bubble trap (Radnoti, USA), the third type was adult and paediatric bubble trap from (CAPIOX® Bubble Traps, Terumo, UK). The suitable flow rate was the second issue during optimisation process. Initially, flow rate ranges from 22-44 ml/min/cannula was used to perfuse a liver lob weighing >150 g. This was applied in order to try to obtain a maximum yield and viability with a minimum amount of buffers. Eventually, the optimised protocol was as follows:

As soon as possible after arrival in the laboratory the part of lobe was excised to obtain on the cutting surface at most 2-3 (2-4 mm in diameter) hepatic vessels. The weight of this part was usually about 80 g.

For hepatocytes preparation, a "two-step" perfusion procedure (chelating and collagenase perfusion) was used.

The liver lobe was cannulated and submitted to a blood removal step (Figure 2.2.1b). The size of the used cannulae varies from 1.2-2 mm in diameter. The liver segment was initially perfused with calcium free Hanks-HEPES solution to flush out any remaining blood, at a flow rate of 44 ml/min/cannula for 5 min. The liver lobe was then perfused with Ca^{2+} free-HBSS supplemented with 1 mM EGTA (Chelating step) for 10 min, without recirculation of the perfusate.

This was followed by 0.5 L of HBSS buffer containing 5 mM calcium chloride. Then immediate recirculation of HBSS buffer containing 5 mM calcium chloride and collagenase (0.1% w/v) was performed for 15-25 min at a flow rate of 44 ml/min/cannula.

All perfusion buffers were warmed in a water bath at 40° C. Collagenase solution was kept in another water bath at 37 °C to preserve enzyme activity. The digested liver lobe was then transferred to a 10 cm Petri dish and disrupted gently, using pointed scissors to tear the liver capsule (Figure 2.2.1c).

2.2.4 Purification of the initial cell suspension

The digested liver tissue was dispersed in 100 ml of HBSS buffer containing albumin 0.1% w/v (refer to Table A.I.6) at 4 °C. The resulting cell suspension was twice filtered, first through a 250 µm nylon mesh followed by a 100 µm nylon mesh. Next, HBSS buffer containing albumin was added to the filtered suspension to reach a final volume of 300 ml. Once resuspended, the cell suspension was transferred into 5 ml centrifuge tubes

and centrifuged twice for 3 to 5 min at various centrifugal speeds from 50 to 75 g. The first centrifugation was performed at 75 g for 5 min, therefore, a substantial proportion of cell contaminants was removed. After the final centrifuge step at 50 g for 3 min, the cell pellets were resuspended in HBSS buffer containing albumin and placed on ice.

2.2.5 Determination of hepatocytes yield and viability

The yield and viability of freshly isolated hepatocytes were assessed with Trypan Blue (TB) dye exclusion test (Tennant, 1964). 15 µl TB was mixed with the same volume of cell suspension and stained (non-viable) and unstained (viable) cells were counted in a haemocytometer. Therefore, the viability % can be determined from the percentage of live cells to total cell count.

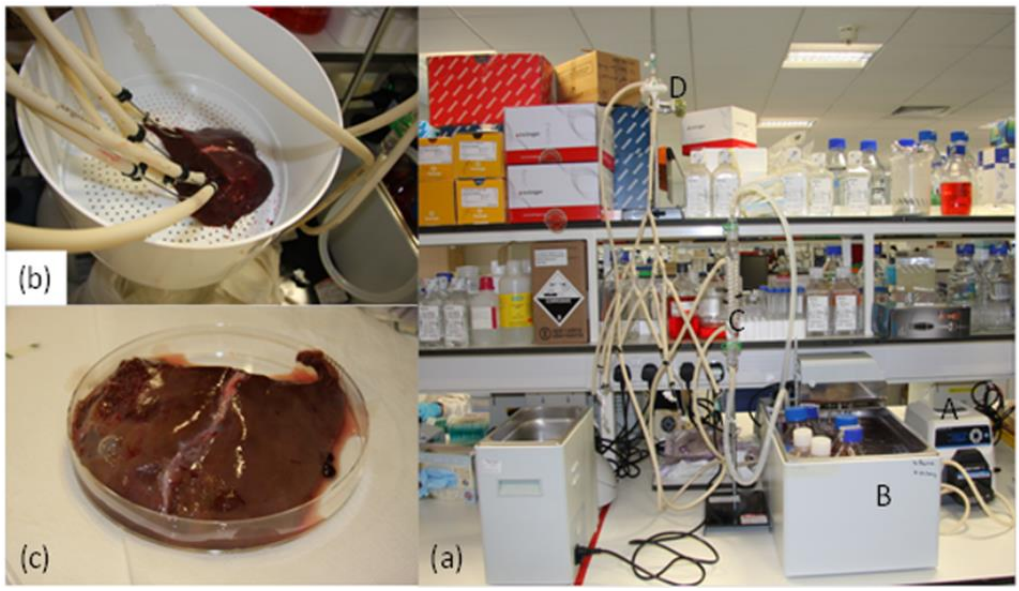


Figure 2.2.1: (a) Perfusion setup. [A] Peristaltic pump, [B] water bath, [C] glass jacketed condenser, [D] bubble trap. (b) Liver piece with curved irrigation cannulae with olive tips inserted in blood vessels on a Büchner funnel. (c) Digested liver tissue: the digested areas appear bulged and pale in colour (left side).

2.2.6 Cryopreservation of equine hepatocytes

Hepatocytes were cryopreserved using the following modified protocol (Adams et al. 1995). Two freezing media were used: 1) is composed of 50%

WME, 40% Foetal calf serum and 10% DMSO; 2) was a commercial freezing medium contain 7.5% DMSO (Sigma, UK). The first medium was prepared fresh at the time of cryopreservation and under sterile conditions.

Cells were pelleted at 50×g for 3 min and resuspended in Falcon tubes with cryopreservation media. After resuspension, the Falcon tubes were placed on ice and the resuspended cells aliquoted into 1.8 ml (1 ml of cell suspension/cryovial at a concentration of 5×10^6 cells/ml. The vials were then transferred to a Styrofoam rack and covered with another Styrofoam rack or transferred to (Mr Frosty®, Freezing Container Fisher, UK) then placed in -80 °C overnight. The cryovials were then transferred to liquid nitrogen cryostat.

2.2.7 Thawing of cryopreserved hepatocytes

Cryopreserved cells were recovered by placing the vials in a 37 °C water bath until all visible ice disappeared using gentle agitation to achieve uniform thawing.

The cells were then diluted 1:10 by dropwise addition to foetal bovine serum containing medium (pre-warmed WEM plus 10% foetal bovine serum). The suspension was centrifuged for 5 minutes at 50×g and 4 °C.

The supernatant was decanted, and the cell pellet was re-suspended in warm culture media.

Hepatocyte yield and viability was determined immediately post-thaw by Trypan Blue exclusion.

2.2.8 Storage

One batch of equine hepatocyte was used to study the effects of the storage time at -196 °C on cryopreserved hepatocytes. Hepatocytes were cryopreserved according to the above protocol (section 2.2.6). A cryovial of this batch was thawed after two days, 1 week, 2 weeks, 3 months, 10 months and 16-month storage at -196 °C. Hepatocytes were thawed rapidly

at 37 °C, and the freezing medium was diluted according to the protocol mentioned in (section 2.2.7). Hepatocyte yield and viability was determined immediately post-thaw by Trypan Blue exclusion. For this analysis, 15 µl of cell suspension was added to 15 µl of Trypan Blue.

2.2.9 Percoll purification

A Percoll density gradient was usually used following thawing of the cells to increase the number of viable cells by separating them from the non-viable cells (Dou et al. 1992). This step has often been performed to get cell viability >70%, which is the minimum viability accepted to perform enzyme kinetic studies *in vitro* (Foster et al., 2011). Two concentrations of Percoll gradient (25% and 30%) were overlaid with the content of one vial of hepatocytes and centrifuged at 110xg at 4 °C for 20 minutes (SciKon Innovation 2010) (Table A.I.7). After centrifugation, the dead cells and the cell debris were located at the interface while viable cells were pelleted. Cell viability was determined as mentioned above.

2.2.10 Measurement of viability in cultured hepatocytes

Cell viability of primarily isolated equine hepatocytes and recovered hepatocytes after cryopreservation was evaluated both before and after seeding. Viability of freshly isolated or recovered cells was determined by Trypan exclusion test. Viability of attached cells was determined with (3-(4,5-Dimethylthiazol-2-yl)-2,5-Diphenyltetrazolium Bromide) (MTT) colorimetric assay. Various cell numbers, i.e. (5000, 8000, 10000, 25000, 50000, 75000, and 100000 viable cells/well) suspended in 100 µl of WE supplemented with 10% FBS were cultured in flat bottomed 96-well tissue culture plate (Table A.I.8). Three wells of media (without cells) were kept, serving as a blank. 10 µl of MTT solution was added into wells, and then the plate was incubated in Heracell 150 Incubator (Thermo Scientific, UK) at 37

°C and 5% CO_2 atmosphere for 4 hours. At the end of the incubation period, the converted dye was solubilised with 100 µl acidic isopropanol (Gibco, UK). The mixture was pipetted up and down several times to make sure the converted dye dissolved completely.

The optical densities (OD) of the formazan solutions in wells were measured at 540 nm by a Microplate Reader model Labtech LT-4000MS Microplate Reader with Manta PC analysis software (Labtech International LTD, UK) (Table A.I.9).

Cell density= OD sample-OD blank (MTT plus acidic isopropanol).

2.2.10.1 Attachment efficiency

The attachment efficiency of primarily isolated equine hepatocytes and recovered hepatocytes after cryopreservation was examined with (MTT) colorimetric assay. Hepatocytes were cultured in 96-well plate at a final density of 5×10^4 viable cells/well in 200 µl of WME supplemented with 10% FBS, antibiotic-antimycotic solution per well into 96 well plates and cultured in Heracell 150 Incubator (Thermo Scientific, UK) at 37 °C and 5% CO_2. Cell attachment was evaluated 24 hours after seeding. The cell culture medium was aspirated off to remove floating dead cells and replaced by 110 µl of WME containing 10 µl filter sterilised MTT (5 mg/ml in BPS). Following a 4 h incubation period with MTT; Formazan crystals dissolved in 100 µl acidified isopropanol for measuring relative percentage viability using Microplate Reader model Labtech LT-4000MS Microplate Reader with Manta PC analysis software (Labtech International LTD, UK). The cell number was determined by comparing the OD of the sample against the standard calibration curve (Figure A.I.1).

2.2.10.2 Determination of horse HPGL

To determine hepatocellularity (HPGL), CYP P450 contents of homogenates and hepatocyte suspensions were measured.

2.2.10.3 Homogenization of hepatocyte suspensions

Cryopreserved hepatocytes were thawed, and the total number of cells was counted. Suspensions were homogenized by freezing thawing cycles. Homogenates were flash frozen in dry ice and stored at -80 °C pending measurement of CYP P450 content.

2.2.10.4 Determination of Hepatocellularity

CYP P450 content method: The CYP P450 content of whole liver homogenates and homogenates of hepatocyte suspensions from 18 equine livers were determined by dithionite difference spectrometry. Equation 2.3 was then used to calculate HPGL values (Wilson et al. 2003):

$$\mathrm{HPGL} = \frac{\text{nmol CYP450}_{\text{homogenate}} \text{ per gram liver}}{\text{nmol CYP450 per } 10^6 \text{cells}} \qquad 2.3$$

Protein method: 97% of liver protein is contained in hepatocytes, and in a suspension of isolated hepatocytes this value is 99% (Worboys et al., 1996). Hence the hepatocellularity can be calculated from the ratio between the liver protein concentration and the protein concentration in the corresponding hepatocyte suspension, corrected by 0.97/0.99.

2.2.10.5 The operator (researcher) influence on estimated values for MPPGL and HPGL

To investigate the effect of the improvement of the researchers' skills in preparation and /or determination of values of MPPGL and HPGL, the all determined values were plotted against the time of preparation.

2.3 Age related alteration in the size of equine hepatocytes

Fragments of liver tissue, drawn after the slaughter of 9 horses divided into three age groups (<9, 10-20 and >20 years) were used in the present study. During routine inspection, no pathological changes were detected in the liver of any horse examined.

2.3.1 Preparation of histological sections

Tissue fragments, obtained from 9 horses aged 1, 3, 5, 10, 16, 19, 21, 23 and 29 years-old, were fixed in 10% formalin for 24 hours at 4 °C. After fixation, samples were processed using routine methods and embedded in paraffin wax. Sections were cut at 5 µm thickness and stained with haematoxylin eosin (H&E). To avoid any biased interpretation each slide was assigned a random number and the investigator was blinded to the identity of the sample. Three non-overlapping slides per horse were photographed in triplicate using 400x magnification (DM5000B, Leica, Germany). The number and size of hepatocytes in a chosen area were counted and measured using Image-Pro® plus Software, Media Cybernetics, USA. For hepatocyte size, the area of 35 cells/image were measured. The average ± SD was calculated using Microsoft Excel (Microsoft Excel 2010, Microsoft Corporation, USA).

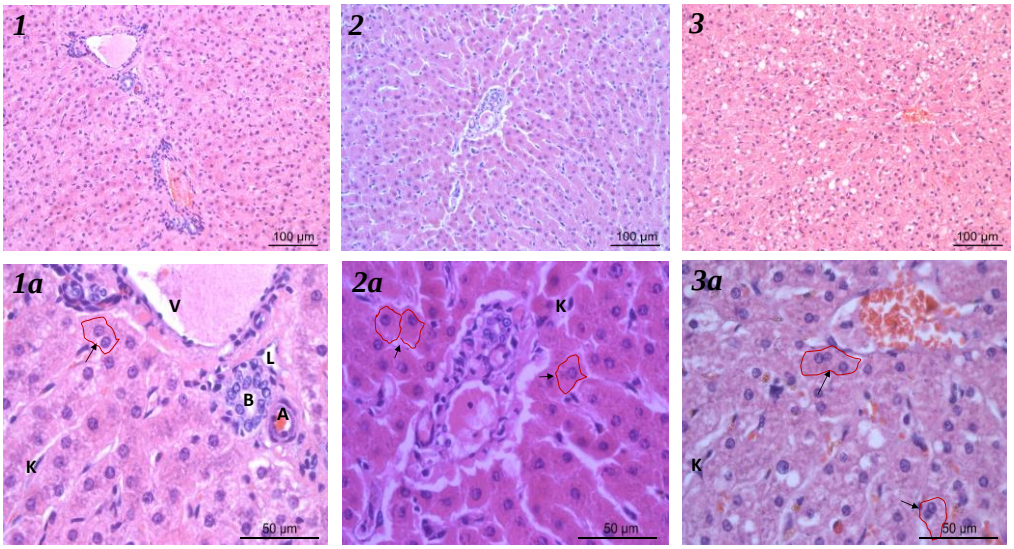


Figure 2.3.1: HE staining, 200X – liver normal structure in 1-year-old (1), 19-year-old (2) and <21-year-old horse (3). High magnification (400X) shows microscopic view of a portal triad; small hepatic arterial (A), portal vein (V), bile duct (B), Lymph vessel (L) (1a), mononuclear, binuclear and polynuclear hepatocytes (arrow) and Kupffer cells (K).

2.4 Determination of Michaelis-Menten parameters for omeprazole, flunixin and phenylbutazone

All incubations were performed in 1.2 ml cluster tubes (Sigma, Dorset, UK) in a 96-well heater block (BioShake iQ, Germany), at 37 °C with a total incubation volume of 1 ml. Drug stocks were prepared in DMSO at 100 x final incubation concentration (from 0.5 to 150 µM).

2.4.1 Linearity of initial reaction rate with respect to mg microsomal protein or number of hepatocytes per ml

To insure appropriate hepatocyte and microsome concentrations were used in incubations, a range of concentrations of the respective in vitro liver system Equine hepatocytes (final concentration 0.1, 0.2, 0.5, 1, 2, 3, 4 x 10^6 cells/ml) and Equine liver microsomes (final concentration 0.1, 0.5, 1, 2, 5 and 10 mg/ml) were incubated with 5 µM (which is below the K_m) of omeprazole, flunixin or phenylbutazone following the respective protocols. The three drugs were selected because they represent the two class of drugs are frequently used in equine medicine. Moreover, omeprazole is used in

human medicine and its metabolism *in vivo* is well characterised in human as well as in horse. Hence, it represents a potential candidate to compare enzyme kinetics in human and horse.

2.4.2 Microsomes

Each incubation contained microsomes at a concentration of 1 mg/ml, drug (10 µl), NADPH 11.3 mM (Roche, Germany) (100 µl) and phosphate buffer (pH 7.4) up to 1 ml. All components of the incubation mixture except NADPH were pre-incubated at 37 ^{o}C for 5 minutes in order to equilibrate. Incubation involved shaking at 500 rpm at 37 ^{o}C incubator. The addition of NADPH immediately started the reaction. At 0, 5, 10, 20 and 60 minutes 100 µl of the incubation was removed and quenched into 200 µl of ice cold methanol. Samples were subsequently frozen at -20 $^{\circ}$C until further analysis. Samples were centrifuged at 31xg for 10 minutes at 4 $^{\circ}$C prior to HPLC analysis. The supernatant was removed and transferred into HPLC vials and analysed. Internal standards were used at a concentration of 10 µM in the quenching methanol to ensure an apparent decrease in substrate concentration was not due to non-specific processes or analysis error.

2.4.3 Fresh hepatocytes

Isolated hepatocytes diluted to 1 million cells/mL, using WEM with 0.125% BSA, were pre-incubated for 30 minutes at 37° C with 5% CO_2. Incubation involved shaking at 750 rpm at 37 $^{\circ}$C in the incubator. The reaction was initiated by adding 10 µl of each drug stock to the cell suspension. Then, 100 µl aliquots were removed at 0, 5, 10, 20 and 30 minutes and quenched in 200 µl of ice cold methanol containing internal standard (10 µM). Samples were subsequently frozen at -20°C until further analysis. Samples were centrifuged at 31xg for 10 minutes at 4° C prior to HPLC analysis. The supernatant was removed and transferred into HPLC vials and analysed.

2.4.4 Cryopreserved hepatocytes

Hepatocytes were thawed using a modified protocol (SciKon Innovation, 2010). Vials of cryopreserved hepatocytes stored in liquid nitrogen were transferred to a 37 °C water bath using dry ice and gently shaken until thawed. 15 ml of 30% Percoll gradient (composed of 9.45 mL WEM, 1.05 mL FCS, 4.05 mL Percoll (Sigma, UK) and 0.45 mL 10x PBS solution) was overlaid with the content of one vial and centrifuged at 110xg at 4°C for 20 minutes (SciKon Innovation 2010). The pellet was resuspended in WEM and kept on ice. Cell viability was determined using TB dye exclusion test, and only suspensions with viability greater than 70% were used for incubations. Incubations were repeated using the fresh hepatocyte protocol, however the heater block was set at 500 rpm.

2.4.5 LC/MS method development

An omeprazole method was developed by the author and undergraduate research student Stefani Pratt (Table A.III.1). All methods were developed on a Micromass Quattro Ultima mass spectrometer using electrospray positive mode with an Agilent 1100 HPLC. The solvent flow rate was kept a constant 0.5 ml/min with an upper pressure limit of 400 bar. Solvent A was 10% methanol, 90% water and 0.002% formic acid and Solvent B was 100% methanol and 0.002% formic acid.

For omeprazole, an MS scan was run in positive ion mode, at cone voltages of 25 eV and 60 eV, and peaks of 346 and 370 mass units were determined for omeprazole and lansoprazole standards, respectively. A nine-minute method was used with an initial gradient of 20% solvent B and 80% solvent A (full method in appendix III). Whereas, methods for flunixin and phenylbutazone were adapted from Orr (2015) (appendix IV).

In addition to substrate depletion, the samples of the three drugs were monitored for the appearance of oxidative metabolites MH+16/Z. These ions

were monitored along with the parent drug ions and methods developed ensured retention times for drug and metabolite varied enough to distinguish between peaks.

2.4.6 LC/MS Analysis

Peak area ratios of omeprazole, flunixin and phenylbutazone to their respective internal standard (lansoprazole, ketoprofen and diclofenac) were determined by integration of chromatograms produced using MassLynx v4.0.

2.4.7 Enzyme Kinetic Analysis

The change in drug substrate concentration was determined using equation 1.42 (section 1.6).

The initial reaction rates (V_0) for the different substrate concentrations were calculated by multiplying the initial substrate concentration with the corresponding K_{dep} value. V_0 is related to the Michealis-Menten constant (K_m) and maximal reaction velocity (V_{max}) via (eq. 1.33).

To determine kinetic parameters, V_0 was plotted against initial substrate concentration to produce a Michaelis-Menten graph using Graph Pad Prism 7. To generate an intrinsic clearance (Cl_{int}), the (equation 1.39) was used. The calculated CL_{int} was corrected for incubational binding (Austin et al., 2002, Austin et al., 2005)

2.4.8 Estimating blood hepatic clearance

The whole liver intrinsic clearance (Liver Cl_{int}) was calculated using (equation 2.4), where the scaling factor is the previously calculated MPPGL or hepatocellularity for microsomes and hepatocytes, respectively. The average mass of an equine liver is 1.5% of the total body weight; 7.5 kg for an average 500 kg horse (Burdas et al., 2003).

$$\boldsymbol{Liver\ CL_{int} = in\ vitro\ CL_{int} \times scaling\ factor \times liver\ weight} \qquad 2.4$$

The blood hepatic clearance (Cl_H) was calculated from the liver Cl_{int} using the well-stirred and parallel tube models (see section 1.7).

2.4.9 Drug-Drug interaction study

A microsomal incubation was conducted using the protocol described in section 2.4.2, with 10 μM omeprazole in all wells, and various concentrations of chloramphenicol (0-150 μM). The inhibitor concentration that results in a 50% decrease in reaction rate (IC_{50}) was determined. Assuming competitive inhibition occurred, the IC_{50} was used to calculate the inhibition constant (K_i) using (equation 1.51), where [S] is the omeprazole concentration.

The effect of the K_i on the area under curve (AUC) was calculated using (equation 2.5).

$$\frac{AUCi}{AUC} = 1 + \left(\frac{[I]}{K_i}\right) \qquad 2.5$$

where [I] is the inhibitor concentration, and AUCi/AUC shows the AUC ratio for the presence and absence of the inhibitor at concentration [I]. The AUC value was obtained from *in vivo* study conducted at the Centre for Racecourse Studies in Newmarket.

2.5 Statistical analysis

All data are presented as average ± standard deviations of the number of samples used. Significant differences between groups were determined using an analysis of variance (ANOVA). Multiple comparisons between groups in each case were performed using a Tukey's honestly significant difference test. Significance of any linear correlations was analysed using the regression slope statistics. Comparison *in vitro* Cl_{int} between freshly isolated, cryopreserved equine hepatocytes and equine liver microsomes for omeprazole, flunixin and phenylbutazone, on the other hand, was performed using a paired, two-tailed Student's test. Level of confidence was set at α=0.05 for all tests, with p-values lower than 0.05 considered statistically

significant. All statistics were carried out using GraphPad Prism version 7.0 (GraphPad Software Inc., San Diego, CA, USA).

Chapter 3

Preliminary studies of cryopreservation and culture of freshly isolated equine hepatocytes

3 Preliminary studies

3.1 Introduction

3.1.1 Why use primary hepatocytes

Isolation and culture of primary hepatocytes have been practiced since more than five decades (Berry and Edwards, 2001). The isolated primary hepatocytes considered as a "gold standard" for evaluating hepatic metabolism and toxicity of drugs and other xenobiotics *in vitro* (Dambach *et al*., 2005; Hewitt et al., 2007b). Despite the fact that freshly isolated hepatocytes have a limited viability in suspension of up to 4 hours, this period is long enough to determine the metabolic stability of a drug and to allow identification of major metabolites (Jouin et al., 2006; Soldatow et al., 2013). The limited availability of fresh cells restrains their use, however, cryopreservation offers an option for long-term storage of hepatocytes providing a continuous and sufficient "off the shelf" supply (Bachmann et al., 2003; Griffin and Houston 2004; Terry et al. 2010).

Fresh equine primary hepatocytes have successfully been isolated and cultured (Bakala et al. 2003; Stefanski et al. 2013). However, there is no literature evidence describing the cryopreservation and recovery of equine hepatocytes and the resulting cell viability and activity of xenobiotic metabolizing enzymes. A better understanding of equine drug metabolism is important for optimal administration regimens of drugs and the resulting effects of the applied treatment. Therefore, equine veterinary surgeons will be better informed with regard to the outcomes of administered drugs and as a result potential drug-drug interaction may be avoided. This will ultimately lead to improved welfare of the horse population. Furthermore, a greater understanding of how drugs are metabolised in the horse, including rates of metabolism and metabolites generated using *in vitro* systems, will

aid the equine sports industry regulate for the abuse of medications and doping substances with a reduction in animal usage and overall costs.

3.1.2 Cryopreservation and recovery of equine hepatocytes

Although hepatocytes from abattoir provide an unlimited source of for cell material, it often happens that only a small portion of these cells is used in a certain experiment and the rest is discarded. Thus, developing a method for cryopreservation of equine hepatocytes is essential, especially that methods for cryopreservation of both animals and human hepatocytes were developed. In this context, several studies were shown that recovered hepatocytes retain the same metabolic enzyme content as freshly isolated hepatocytes (Utesch et al. 1992; Diener et al. 1993). Since CYP P450 enzymes account for ~70% of the metabolism of pharmaceuticals, the major research activity has focused on this family of enzyme (Furge and F. P. 2006). Currently, introduction of recombinant CYP P450s and LMs have made these *in vitro* tools highly valuable for drug metabolism *in vitro*. However, isolated hepatocytes represent the most complex *in vitro* experimental system containing the full complement of enzymes a compound is likely to encounter during first-pass hepatic metabolism.

3.1.3 Comparison of Enzyme activity in fresh and cryopreserved equine hepatocytes

To investigate the effect of cryopreservation on xenobiotic metabolizing enzymes, intrinsic clearance is used as an indicator for the efficiency of metabolism. Moreover, it can be scaled to *in vivo* Cl_{met} with knowledge of physiological parameters such as microsomal protein content, Hepatocellularity, liver weight and a model of hepatic extraction such as the well stirred model (Houston 1994; Naritomi et al. 2001). Using *in vitro* data, notable successes has been reported in determination of *in vivo* clearance for the majority of drug-metabolising enzymes in different species (Lau et

al., 2002; Shibata et al., 2002; Naritomi et al., 2003). Most of these studies assessed *in vitro* metabolism by disappearance of drug substrate, whereas the comprehensive evaluation of the ability of cryopreserved hepatocytes to predict *in vivo* Cl_{int} needs a detailed investigation of the kinetics of metabolite formation of a range of drug substrates. Hence, direct comparisons can be made to fresh hepatocytes.

The main aim of this chapter was to optimise cryopreservation/thawing procedures for equine hepatocytes then compare viability, attachment efficiency and enzymatic activity between freshly isolated and recovered cryopreserved equine hepatocytes.

3.2 Results

3.2.1 Isolation of equine hepatocytes

After a long optimisation process, which lasted more than six months, equine hepatocytes successfully isolated with high yield and viability.

The modified 50 ml centrifuge tube and heating coil bubble trap was not able to stand a high pressure; whereas, adult bubble trap failed to provide stable pressure. In contrast, paediatric bubble trap was able to provide a uniform perfusate. Use of a low flow rate resulted in poor digestion with lower yield and viability; with 22 ml/min/cannula flow rate the total yielded viable cells were $5x\ 10^5$ cells per isolation with viability 44.7%. At 36 ml/min/cannula the total viable cells were 7.2×10^6 cells per isolation with viability of 55%. Best results were obtained using a constant 44ml/min/cannula flow rate. A small part of lobe <100 g cannulated with olive tip cannulae was cost effective option i.e. less perfusate was used with acceptable amount of viable equine hepatocytes was obtained. Eighteen perfusions were performed, and the results of these 18 perfusions are summarised in (Table 3.2.1). The average of total yielded viable hepatocytes was $300\pm214\times10^6$ cells per isolation, which accounted for $3.2\pm2.4\times10^6$ cells per gram of perfused

tissue. Hepatocyte viability was, on average, 84.4±4.6% as determined by Trypan Blue exclusion test.

Table 3.2.1: Overview of the results of the 18 horse liver perfusions

Horse number	**Age at slaughtering in years**	**Liver piece weight in grams**	**Total number of cells×10^6**	**Cell viability using Trypan blue stating in percent**
1	5	90	67.2	97
2	22	80	750	94
3	6	80	140	82.7
4	10	80	413	82.6
5	2	80	300	81.0
6	1	80	400	84.0
7	6	80	150	85.0
8	10	80	250	80.0
9	22	80	180	83.0
10	16	80	56.7	80.0
11	19	100	410	87.7
12	2	90	839.7	83.0
13	18	100	280	84.0
14	3	90	344.7	81.0
15	18	80	129	82.6
16	14	80	189	87.7
17	25	80	352	82.7
18	16	80	152	81.5
Average			**300.2**	**84.4**
SD			**213.6**	**4.6**

3.2.2 Cryopreservation and recovery of equine hepatocytes

The number of viable hepatocytes recovered from cryopreservation was compared for two formulas: 1) 50% Williams medium E, 40% foetal bovine serum and 10% DMSO; 2) Prepared according to the formulation of Waymouth and Varnum (1976), it contains Minimum Essential Medium,

8.7% DMSO and methyl cellulose. However, there were no significant deference between two formulas in terms of post-thaw viability (p=0.24).

3.2.3 Effect of storage in liquid nitrogen

A batch of cryopreserved equine hepatocytes were stored for up to 16 months in liquid nitrogen and no effect on post-thaw viability was observed in that time frame (Figure 3.2.1).

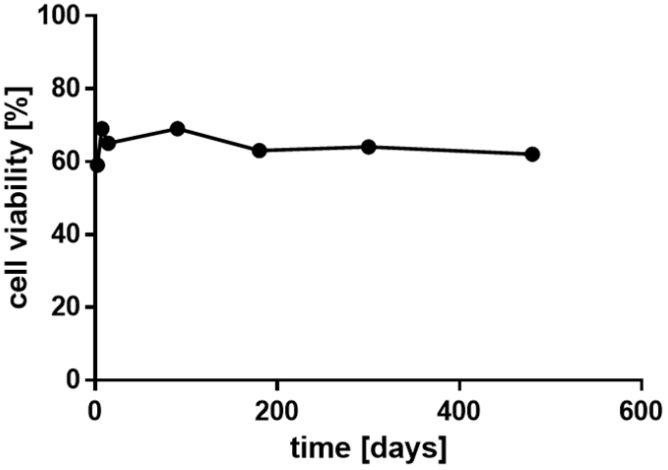


Figure 3.2.1: Effect of storage time on equine hepatocyte post-thaw viability. Cryopreserved hepatocytes were stored in liquid nitrogen from 2 days to 480 days.

3.2.4 Cell viability and attachment

Attachment of isolated hepatocytes is commonly used for the evaluation of their quality. Attachment was assessed following 24 h culture using the MTT assay. The percentage of attached cells was 70.8% and 45±4% (n=3), for fresh and recovered cryopreserved hepatocytes, respectively.

3.2.5 Percoll Purification

Since the average of post-thaw viability was below the acceptable hepatocyte viability for enzyme kinetic studies is >70%, hence Percoll gradient was used to improve the cell viability. Two concentrations of Percoll gradient (25% and 30%) were used in this study to examine its effect on the percentage viability and recovery. A 25% Percoll treatment increased

hepatocyte viability from 52±14 to 62.3±11% with 31.6±6% recovery (n=3). Whereas, the average viability after 30% Percoll treatment was 77±11% with the average recovery of 27±7% (Table 3.2.2).

Table 3.2.2: Summary of equine liver perfusions and Cell viabilities and yield, pre, and post cryopreservation.

Horse	Average viability pre-cryo (%)	Average viability post-cryo with Percoll gradient (%)	Number of viable cells isolated per gram perfused tissue x10^6	Average yield of viable cells post-cryo per vial x10^6
1	87.7	75.0	4.10	2.80
2	83.0	53.5	9.33	3.44
3	81.0	76.2	3.83	1.22
4	83.7	87.7	4.88	2.56
5	82.6	81.3	1.6	3.20
6	87.7	83.3	2.4	3.33
7	82.7	82.1	4.4	2.31
Average	**84.1**	**77.0**	**4.36**	**2.69**
SD	**2.62**	**11.0**	**2.47**	**0.8**

3.2.6 Comparison of intrinsic clearance and metabolite formation between fresh and cryopreserved equine hepatocytes

To compare metabolic activities between fresh and cryopreserved equine hepatocytes, three equine drugs were used. *In vitro* Clint was determined for omeprazole, phenylbutazone and flunixin by measuring their depletion over time at 10^6 cells in both fresh and cryopreserved hepatocytes from an initial substrate concentration of 5 µM.

3.2.7 Optimisation of incubation conditions

Hepatocyte incubation conditions used to study the metabolism of these three substrates were adapted from reported procedures (Griffin and Houston, 2004; McGinnity et al., 2004; Jouin et al., 2006). However, there was a process of optimisation with regard to the experimental conditions.

Eight protocols were examined in the herein study, for optimisation as shown in (Table 3.2.3). However, only method six and eight were used for fresh and cryopreserved hepatocytes, respectively. Freshly isolated and cryopreserved equine hepatocytes showed the optimum metabolism when they were diluted to 1 million cells/ml, using WEM with 0.125% v/v bovine serum albumin (BSA), and pre-incubated for 30 minutes at 37 °C with 5% CO_2. However, the agitation speed of the heater block was different with 750 and 500 rpm for freshly isolated and cryopreserved equine hepatocytes, respectively.

There were no significant differences between Cl_{int} estimated in fresh and cryopreserved equine hepatocytes from 3 horses for each drug (Figure 3.2.2). The average ± SD (n=3) Cl_{int} for omeprazole was 21.3±6.7 and 16.3±0.5 µl/min/10^6 cells, for flunixin 19±6.2 and 18.7±4 µl/min/10^6 cells and for phenylbutazone was 24±12.49 and 16.7±5.5 µl/min/10^6 cells in fresh and cryopreserved hepatocytes, respectively. Oxidation metabolites generated for omeprazole and phenylbutazone in fresh and cryopreserved equine hepatocytes were detected. The mass chromatograms of oxidation metabolites (+16 mass units) generated for omeprazole in fresh (B) and cryopreserved (D) equine hepatocytes are shown in (Figure 3.2.3). Metabolites of omeprazole were characterized by comparison of the negative control chromatogram (0-time point) with the chromatogram of the 30-minute time point. Oxidation metabolite peaks are presented by M1, M2 and M3 with retention times 4.22, 4.96 and 5.57 minutes. The ratio between peak areas of M1, M2 and M3 was 2:1:1, respectively in both fresh and cryopreserved hepatocytes.

A phenylbutazone oxidation metabolite was characterized by comparison of the negative control chromatogram (0-time point) with the chromatogram of the 30-minute time point. This metabolite was identified as oxyphenbutazone since it showed an identical retention time to an authentic

oxyphenbutazone standard. Oxyphenbutazone was detected for both fresh and cryopreserved hepatocytes (Figure 3.2.4 B and D), respectively; however, the intensity, after normalising for internal standard), was 50% lower for the latter which may suggest some degradation in the metabolising enzyme(s).

Whereas no significant oxidation metabolites were observed for flunixin which is known to mainly be conjugated with glucuronic acid in camel (Wasfi et al. 1998). Selected ion monitoring for glucuronide metabolites (+176 M/Z) showed no detectable metabolites.

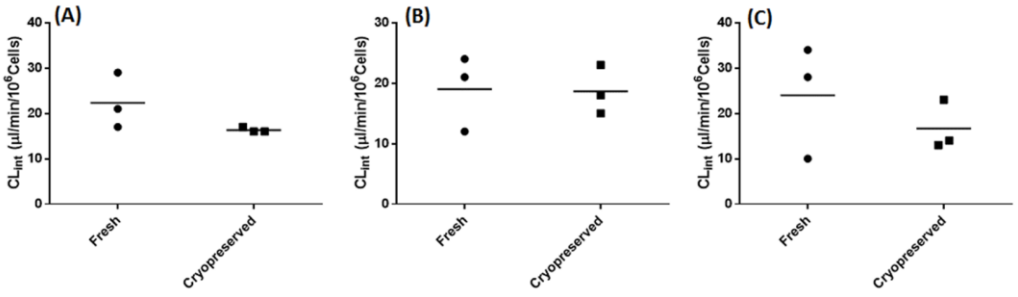


Figure 3.2.2: Comparison of intrinsic clearance between fresh and cryopreserved horse hepatocytes (average presented by dash line) for omeprazole (A), flunixin (B) and phenylbutazone (C) (n=3 horse for each drug). The results show that there is no significant difference between fresh and cryopreserved equine hepatocytes, $p>0.5$.

Table 3.2.3: Kinetic incubation method trialled and outcomes

Method	Speed of heater block (rpm)	Pre-incubation time at 37˚C (minutes)	Media	Metabolism observed
1	300	5 in water bath	WEM	NO
2	900	5 in the incubation tubes	WEM	NO
3	850	5 in the incubation tubes	WEM with 0.125% BSA	Minor metabolism during initial 5 minutes
4	850	30 in the incubation tubes	WEM with 0.125% BSA	Moderate metabolism during initial 5 minutes
5	750	30 in the incubation tubes	WEM with 0.125% BSA	Moderate metabolism during initial 5 minutes
6	750	30 in the incubator at 5% CO_2	WEM with 0.125% BSA	Fresh-Metabolism observed for 60 minutes Cryopreserved-Moderate metabolism during initial 5 minutes
7	400	30 in the incubator at 5% CO_2	WEM with 0.125% BSA	Cryopreserved-Moderate metabolism during initial 10 minutes
8	500	30 in the incubator at 5% CO_2	WEM with 0.125% BSA	Cryopreserved-Metabolism observed for 60 minutes

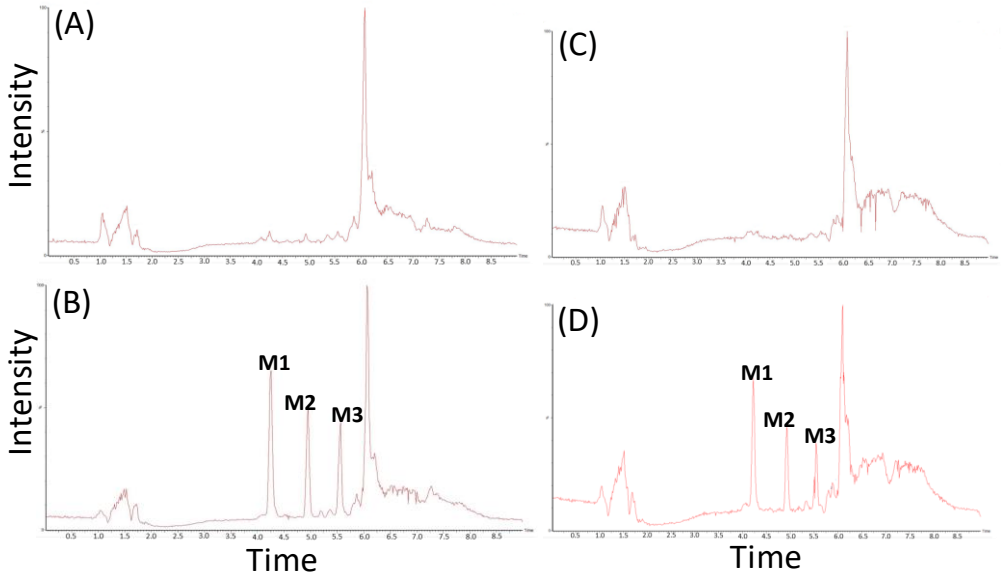


Figure 3.2.3: HPLC–MS chromatograms of oxidation metabolites of omeprazole in extracellular medium of fresh (A=0 min and B=30min) and recovered cryopreserved (C=0 min and D= 30 min) equine hepatocytes. $1x10^6$ freshly isolate and recovered cryopreserved equine hepatocytes/ml were incubated with omeprazole as described under *Materials and Methods* during 30 min. The ratio between the peak areas of M1, M2 and M3 was 2:1:1, respectively in both fresh and cryopreserved hepatocytes.

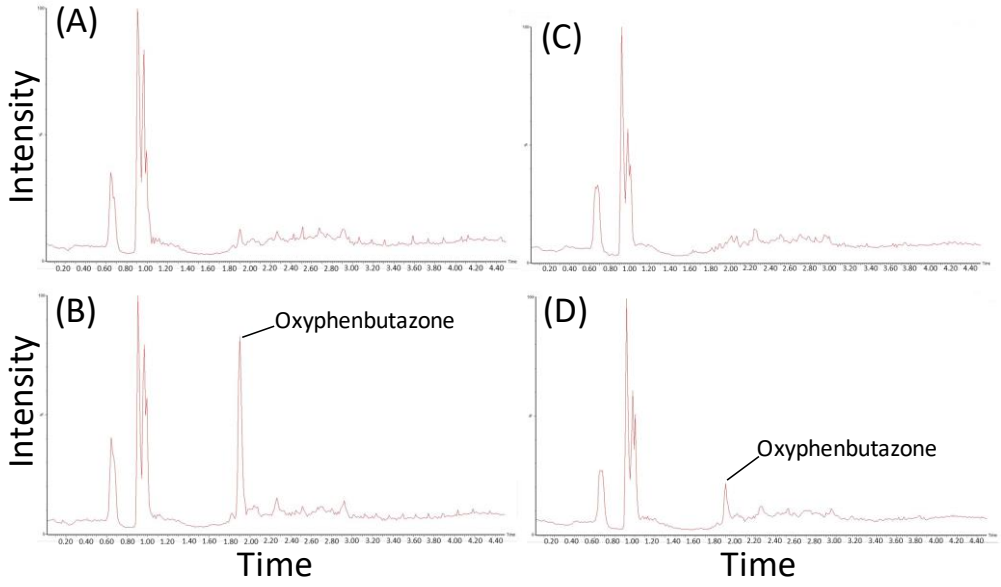


Figure 3.2.4: HPLC–MS chromatogram of metabolites of phenylbutazone in extracellular medium of fresh (A=0 min and B=30min), and recovered cryopreserved (C=0 min and D= 30 min) equine hepatocytes. $1x10^6$ freshly isolated and recovered cryopreserved equine hepatocytes/ml were incubated with omeprazole as described under *Materials and Methods* during 30 min.

3.3 Discussion

This chapter describes a simple method for isolation, cryopreservation and recovery of viable and functional equine hepatocytes. In the present study a protocol adapted from Bakala et al. (2003) and Lee et al. (2013), with slight modification, was used. This protocol enabled high cell yield and viability. Livers processed in this study were immersed in ice cold HBSS, which preserves the liver for extended periods and protects against the decrease in cell viability. Therefore, HBSS appears to be a suitable alternative to other expensive solutions being used for organ preservation such as University of Wisconsin (UW) solution in terms of cell viability and functional integrity.

Livers obtained post mortem from slaughtered horses provide a straightforward way to obtain hepatocytes without the need for large animal operation facilities. Moreover, this source for biological materials allows the reduction of costs and labour. In addition, it represents a suitable alternative to the living animal, hence ethical restrictions can be avoided.

The results of the eighteen liver perfusions show that, there are several variables contributing to high yield and viability. From the literature, the perfusion system consists of a peristaltic pump with appropriate tubing, a water bath and bubble trap; therefore, it is a simple system and there are no potential technical problems. However, it was found that a bubble trap was a critical component. The presences of air bubbles in the system interfered with the final pressure at the cannula, and this may associate with poor yield and viability. In this regard, the present study found that a constant flow rate is very important for successful hepatocyte isolation. Bakala et al. (2003) reported that, a proper constant perfusate flow rate is extremely important for a successful liver perfusion, since the lower flow rate could result in poor tissue dissection by the collagenase.

During the optimisation process, several perfusion speeds (ranging from 22-44 ml/min/cannula) were tested, and the results showed that an average perfusion speed of 44ml/min/cannula is the ideal flow rate. Similarly, a recent study assessed the effect of the perfusion parameters, and found that the average perfusion speed of 44ml/min/cannula is ideal regardless of the liver weight, hence the perfusion speed is adjusted depending on number of cannulae being used (Lee et al., 2013).

The collagenase type and concentration are the key factor in hepatocyte isolation. A concentration of 0.1% of collagenase type VI was used in this study. This concentration resulted in high yield and viability; however, this can vary from batch to batch due to variation of collagenase activity (Berry and Edwards 2001). In this regard, Bakala et al. (2003) reported that use of a concentration at (0.07-0.09%) or higher (0.11-0.12%) of collagenase could result in a higher proportion of damaged cells.

The average yield of hepatocytes was 4.6±2.5 million cells/g of perfused tissue, with an average viability of 84.4±4.6%. This is 5-fold higher than that reported by Stefanski et al. (2013) (n=9). However, the number of hepatocytes isolated per gram of perfused tissue was 5-fold higher in the study by Bakala et al. (2003) than in the present study. Although protocols were similar, they used University of Wisconsin solution for transportation, which may have superior organ preservation capacities, enabling a larger viable cell number to be obtained. Another potential factor is the number of liver samples, which was greater (n=264) in the study by Bakala et al. (2003).

Cryopreservation of hepatocytes has aimed to provide a bank of cells that on recovery, maintain most of the normal enzyme activities. Therefore, the present work used two freezing solutions, the first one is freshly prepared in the lab and consists of: 50% WEM, 40% FCS and 10% DMSO; the second one is a commercial serum free medium containing 7.5% DMSO and methyl

cellulose. The present study found that there was no significant difference between the two formulas in terms of cell viability. Both formulas contained DMSO which has been found to provide a much higher attachment and viability, on thawing, than the other cryoprotectants such as glycerol (Loretz et al. 1989), However, the fresh formula is more cost effective than the commercial one.

The viability of hepatocytes was demonstrated by both Trypan blue exclusion and the MTT assay after the culturing of thawed cryopreserved hepatocytes for 24 hours in a 96-well plate. With both cryopreservation formulas, equine hepatocytes had an average pose-thaw viability of 60%. The results obtained in this study were consistent with data obtained from other species such as rats and human. With rat cryopreserved hepatocytes, the immediate post- thaw viability of 60% has been achieved (Sosef et al., 2005). Meanwhile, Terry et al. (2010) obtained post-thaw viability of 52±9% using cryopreserved human hepatocytes.

For the MTT assay, samples were plated and cultured overnight to assess attachment and viability following 24 hours of culture. Recovery of viable hepatocytes from cryogenic storage was 45±4%, accounting for cellular attachment. This value is comparable with those quoted in the literature (Chesne and Guillouzo 1988; Chesné et al. 1993; Terry et al. 2010). Poor attachment ability of cryopreserved hepatocytes may have occurred due to alterations in the proteins involved in the extracellular matrix adhesion mechanism (Silva et al., 1999; Kunieda, et al., 2010; Arikura et al., 2002; Ostrowska et al., 2000). Furthermore Terry et al. (2007) found that the process of cryopreservation leads to down-regulation of cell adhesion at the gene and the protein level (β1-integrin and E-cadherin, amongst others).

Despite the fact that this method may need improvement since no available data exists with regard to the cryopreservation and thawing of equine hepatocyte, it does provide a simple and robust method for the

cryopreservation and recovery of metabolically competent isolated equine hepatocytes.

The Percoll density gradient has often been used for cell separation and to increase viability by separating live from dead cells (Lloyd et al., 2003). When using a Percoll gradient after thawing, average viability post-cryopreservation was 77±11.0%. This step is a useful procedure since it results in removing dead cells and contaminating debris. Moreover, several studies have found that use of this gradient has an advantage on cell functions, including CYP P450 function and cell attachment (Lawrence and Benford 1991; Dou et al., 1992; Utesch et al., 1992; McGinnity et al., 2004). Intrinsic clearance for three drugs was determined, namely omeprazole, flunixin and phenylbutazone. The results of this preliminary study show that there is no difference between fresh and cryopreserved hepatocytes in terms of enzyme activity; this is consistent with the literature (Diener et al., 1993; McGinnity et al., 2004). Moreover, Griffin and Houston (2004) found that cryopreserved human hepatocytes gave similar high clearances for propranolol and diazepam to fresh hepatocytes. However, a continuous availability of cryopreserved hepatocytes represents a major advantage as a tool for drug screening.

The interval from slaughter process to hepatocyte isolation varies from 4-6 hours and this could lead to variation in the estimated Cl_{int} *in vitro* from both freshly isolated and cryopreserved hepatocytes.

In conclusion, this study has shown that equine hepatocytes can be successfully cryopreserved using a conventional freezing protocol. The use of a Percoll centrifugation after thawing yielded equine hepatocytes, which possess an enzymatic metabolic capability similar to that of freshly isolated hepatocytes. This work is paving the way to establish a bank of cryopreserved equine hepatocytes.

Chapter 4

Determination of Hepatocellularity number and Microsomal scaling factor for *in vitro/ in vivo* extrapolation in the horse

4

4.1 Introduction

Hepatocytes and liver microsomes obtained from several species including human are routinely used to determine the intrinsic clearance (Cl_{int}) of test compounds in the discovery phase of drug development (Smith et al. 2008). The generated *in vitro* Clint values are often extrapolated to *in vivo* using scaling factors such as the hepatocellularity number per gram of liver (HPGL) and the hepatic microsomal protein per gram of liver (MPPGL) (Hakooz et al. 2006). A relatively good correlation has been established between predicted and actual *in vivo* clearance in human and pre-clinical species (Riley et al., 2005). However, an important animal species that has been overlooked regarding *in vitro-in vivo* extrapolation (IVIVE) of drug clearance is the horse.

Microsomal scaling factors and hepatocellularity numbers for human, dog, rabbit, rat and mouse have been estimated using methodologies such as DNA, CYP and protein content (Carlile et al., 1997; Sohlenius-Sternbeck, 2006; Smith et al., 2008). However, horse MPPGL and HPGL have not been investigated.

The present work was performed in order to determine the microsomal protein and the hepatocellularity number for horses. This technique assumes that all the CYP P450 enzymes are located on the smooth endoplasmic reticulum and that their activity is not affected during the preparation process. Therefore, correction for any losses in microsomal protein in the process can be applied to determine an accurate microsomal scaling factor. Microsomal protein per gram of liver and hepatocellularity numbers of human, dog, rabbit, rat and mouse have been estimated using different methodologies, namely, DNA, CYP and protein content. Using CYP P450 content method, a rat hepatocellularity number of 160×10^6 cells/g of liver

and microsomal protein concentration of 61 mg/g of liver was determined (Carlile et al., 1997; Smith et al., 2008). Similarly, a hepatocellularity of 169 (131-207) × 10^6cells/g liver and microsomal protein concentration of 55 (48-62) mg/g liver was reported for dogs (Smith et al., 2008). On the other hand, with protein method, Sohlenius-Sternbeck (2006), calculated a hepatocellularity number of 117±30 and 215±45 × 10^6 cells/g of liver in rats and dogs, respectively.

A human microsomal protein value of 33 (26-54) mg/g liver and hepatocellularity number of 107 (56-185) × 10^6 cells/g of liver were determined using the CYP method (Wilson et al. 2003), whereas the protein method afforded hepatocellularity number of 139±25 × 10^6 (Sohlenius-Sternbeck 2006).

4.1.1 Variability of microsomal protein per gram of liver and the effect of age

The IVIVE of hepatic metabolic drug clearance has been mainly based on average MPPGL and HPGL values for a given species with no estimate of intersubjective variability (Barter at al., 2007). Furthermore, a recent study found that there was up to 19-fold individual variation in values of MPPGL in 128 human livers (Zhang et al., 2015). In this context, many reports have demonstrated specific age-dependent changes in some hepatic parameters, such as decreased protein and bile salt synthesis, and cholesterol metabolism (Tietz et al., 1992; Bertolotti et al., 1993; Schmucker 2005). Moreover, a number of studies have found strong negative correlations between age and hepatic microsomal Phase I drug-metabolising activity in inbred male rats (Schmucker and Wang 1980; Schmucker and Wang 1981; Schmucker and Wang 1983; Yun et al., 2010). However, the results of studies conducted on non-human primates contradict the findings in rat as there was no apparent correlation between age-related changes in the

microsomes and the *in vitro* activities of the constituent drug-metabolizing enzymes (Maloney et al., 1986; Schmucker and Wang 1987).

4.1.2 Age-related alterations in the number and size of equine hepatocytes

Even though the liver is the major site of metabolic activities, unlike the kidney, it does not show well-documented or obvious changes in either structure or function during the aging process. However, several morphological studies have been conducted to study the effect of aging on liver structure (Tauchi 1961; Tauchi and Sato 1962; de al Iglesia et al., 1976; Watanabe and Tanaka, 1982). In the liver of the inbred rat strain Fisher 344 the cell density increased between 1 and 16 months of age and, subsequently, declined while hepatocyte size was similar in immature and senescent animals (Schmucker et al., 1978; Engelmann et al. 1981) . Other changes in hepatocellular structure have been associated with advanced age, which include reduction in the surface area of the smooth endoplasmic reticulum, an increase in the volume of the mitochondrial and microbody compartments and an increase in number of hepatocytes containing two nucleotides (binucleate) or multi-nucleate (polyploidisation) (Tauchi and Sato 1962; Schmucker et al., 1977; Engelmann et al. 1981). Although, none of these age-related changes has a clear role in a significant decline in hepatic function, there are data showing specific age related changes, such as a loss of liver size and a drop in liver perfusion (Schmucker et al., 1977; Schmucker et al., 1978; Watanabe and Tanaka, 1982); both of which may affect certain hepatic functions, including first pass pharmacokinetics (Marchesini et al., 1988; Wynne et al., 1989).

To predict extreme effects in populations and to evaluate risk in horses with different age groups such variability should be assessed. Accordingly, the main aim of this study was to determine levels of MPPGL and HPGL as well as the effect of age on these levels and hepatocyte size in equine liver.

4.2 Results

For the 39 liver samples divided into three age groups (group one 0-9 years n=16, group two 10-20-year n=16 and group three >21-year n=7) (Table 4.2.1), the total protein concentration of the liver homogenates and microsomes was 21.5±5 mg/ml and 31.1±6 mg/ml, respectively. The average value of protein concentration in hepatocyte suspension was 1.0±0.3 mg/10^6 cells (n=14). The CYP P450 concentrations in liver homogenate, equine microsomes and hepatocytes were 29.6±6.6 nmol P450/g liver, 0.510±0.09 nmol P450/mg of microsomal protein and 0.130±0.02 nmol P450/10^6 hepatocytes, respectively.

The CYP P450 content of whole homogenate correlated with that of microsomes (r^2=0.533, p=0.05) (Figure 4.2.1). The ratio of the whole homogenate CYP P450 content to the CYP P450 content for microsomes provided scaling factors for each liver with an average of 57 mg microsomal protein/g liver (CV=15%).

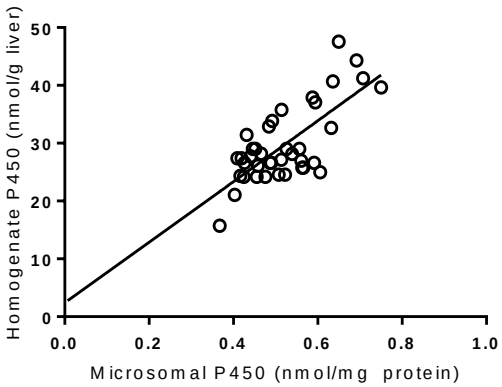


Figure 4.2.1: Relationship between whole homogenate P450 (nanomoles per gram liver) and microsomal P 450 (nanomoles per milligram protein). There is a statistically significant (r^2 = 0.533) (p=0.05) relationship between these metrics.

4.2.1 Hepatocyte scaling factor (Hepatocellularity)

Due to difficulties reported in literature regarding the measurement of CYP P450 concentration in liver homogenates in other species (Sohlenius-Sternbeck 2006), the present study compared CYP P450 method and protein

method. Using the CYP P450 methodology, an average hepatocellularity of 227 x 10^6 cells/g of liver (CV=26%) was determined (Table 4.2.3). For the protein method, the average hepatocellularity was 232×10^6 cells/ g liver (CV=21%) (Table 4.2.4).

The operator i.e. the improvement in sample preparation and /or the technique used for CYP P450 measurements had no considerable influence on estimated values for MPPGL and HPGL as no correlation existed between measurements and time for a 21-month period ($p > 0.05$) (Figure 4.2.2).

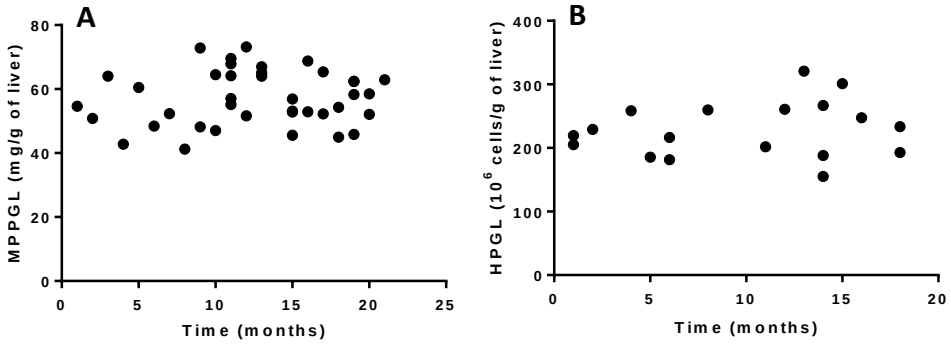


Figure 4.2.2: Effect of operator (researcher) on MPPGL (a) and HPGL (b) values. There was no correlation between measurements and time for a 21-month period ($p > 0.05$).

Table 4.2.1: Determination of Microsomal protein content per gram of liver (MPPGL) using CYP P450 method.

Horse No	Age (years)	Homogenate mg protein/ml of homogenate	Homogenate nmol P450/mg of protein	Homogenate nmol P450/g of liver	Microsomes mg protein/ml of microsomes	Microsomes nmol P450/mg of protein	mg Microsomal protein per g liver
1	1	26.0	0.09	26.1	38.0	0.46	57.3
2	1	32.7	0.09	33.9	33.5	0.49	68.8
3	1.5	17.3	0.14	29.0	32.3	0.43	65.4
4	2	22.2	0.11	26.6	20.8	0.49	54.6
5	2	17.8	0.15	29.0	39.3	0.45	64.3
6	3	18.9	0.13	26.6	34.0	0.40	62.4
7	4	15.5	0.09	15.7	28.4	0.37	42.8
8	5	30.0	0.07	27.6	34.7	0.51	48.4
9	5	22.1	0.10	29.8	26.0	0.61	41.2
10	5	18.1	0.12	24.6	30.0	0.52	47.0
11	6	19.0	0.13	27.0	30.7	0.56	48.5
12	6	16.2	0.18	32.6	25.5	0.63	51.6
13	6	27.0	0.13	39.7	29.3	0.75	52.9
14	6	15.7	0.15	26.6	35.0	0.59	44.9
15	8	17.5	0.12	23.4	23.1	0.48	48.5
16	8	17.6	0.11	21.1	34.1	0.40	52.2
17	10	19.6	0.18	37.9	31.8	0.59	65.0
18	10	17.2	0.15	27.4	30.9	0.41	66.8
19	11	18.3	0.20	40.7	24.2	0.64	64.1
20	12	20.1	0.20	44.3	27.0	0.69	63.8
21	13	29.9	0.10	31.4	34.8	0.43	72.9

Table 4.2.1: Determination of Microsomal protein content per gram of liver (MPPGL) using CYP P450 method.

22	15	17.1	0.18	32.9	34.8	0.48	68.0
23	15	20.2	0.12	25.8	38.3	0.66	45.6
24	15	12.7	0.21	29.0	20.4	0.56	52.1
25	16	19.9	0.19	41.2	29.0	0.71	58.3
26	16	19.0	0.13	27.7	32.4	0.44	62.9
27	17	24.0	0.18	47.5	26.5	0.65	73.2
28	18	19.4	0.13	28.2	18.0	0.54	52.2
29	18	18.0	0.19	37.1	18.5	0.59	62.4
30	19	28.8	0.08	24.2	38.8	0.43	56.9
31	20	19.6	0.17	35.8	32.4	0.51	69.6
32	20	19.6	0.14	29.0	37.8	0.45	65.6
33	22	28.5	0.09	28.2	28.3	0.47	63.1
34	22	28.3	0.08	24.2	33.8	0.46	53.1
35	23	20.5	0.12	27.1	32.1	0.51	52.8
36	23	16.3	0.15	26.6	28.8	0.49	54.3
37	25	16.4	0.16	29.0	32.4	0.53	55.2
38	25	16.1	0.14	24.7	39.6	0.42	58.5
39	29	15.7	0.15	25.8	28.3	0.56	45.8
Average		20.5	0.14	29.6	30.6	0.52	57.2
SD		4.9	0.04	6.6	5.7	0.09	8.5

(n=39)

Table 4.2.2: Determination of hepatocellularity using CYP P450 method

Horse No	Age	P450 nmoles/10^6 hepatocytes	nmol P450/g of liver	Hepatocellularity (10^6 cells/g liver)
1	1	0.14	26.1	181.5
2	2	0.16	29.0	185.6
3	2	0.19	27.4	146.7
4	3	0.14	26.6	188.2
5	5	0.13	27.6	195.7
6	6	0.12	27.0	229.3
7	6	0.15	32.6	216.6
8	10	0.15	37.9	258.5
9	10	0.11	27.4	259.7
10	14	0.12	29.0	247.5
11	16	0.10	25.8	260.7
12	16	0.12	27.7	233.6
13	18	0.11	28.1	266.9
14	18	0.12	37.1	301.2
15	19	0.12	39.7	320.8
16	22	0.14	28.2	205.3
17	22	0.12	24.2	201.8
18	25	0.13	24.4	192.7
Average		0.13	29.8	227.3
SD		0.02	6.00	45.2

(n=18)

Table 4.2.3: Determination of hepatocellularity using protein method.

Horse No	Age	mg protein/ ml	mg protein/10^6 cells	mg protein/g of liver	Hepatocellularity (10^6 cells/g liver)
1	1	1.5	1.5	286.0	208.2
2	2	3.7	0.9	297.0	205.9
3	3	4.0	0.9	213.0	236.7
4	6	2.1	0.8	189.2	214.4
5	10	4.0	0.9	222.2	213.4
6	15	3.5	0.8	139.7	222.6
7	16	2.6	0.9	178.2	261.0
8	18	2.3	0.8	190.3	275.2
9	18	1.8	0.6	172.7	285.3
10	18	2.5	1.0	207.0	253.1
11	19	2.1	0.8	311.0	352.0
12	22	2.7	1.4	313.5	222.7
13	22	1.7	1.4	207.9	225.6
14	25	1.1	1.1	177.1	156.3
Average		2.5	1.0	208.8	232.1
SD		0.9	0.3	49.7	48.6

(n=14)

4.2.2 Inter-Individual Variability of horse MPPGL and HPGL and the effect of age

Levels of hepatic total CYP P450 content per gram of liver increased significantly in the horses aged between 10 and 20 years old relative to the <10 and >20-year-old horses (Figure 4.2.3). On the other hand, the total CYP P450 content in equine liver microsomes per mg protein did not change significantly over the ages examined in this study (Figure 4.2.4). A U-shaped relationship was observed between CYP P450 content per 10^6 hepatocytes and the horse age (Figure 4.2.5). Furthermore, the results of this study show a non-monotonic relationship between age and MPPGL with values increasing from 48 mg/g (1-year-old) of liver to a maximum of 73 mg/g of liver (17-year-old) followed by a gradual decrease in older age (Figure 4.2.6a). There was a significant increase (14.7%) in MPPGL in horses aged 10-20 years old compared to 0-9 years old ($p=0.004$). On the other hand, the MPPGL levels did not change significantly in horses aged >21 years old compared to 10-20 years old (Figure 4.2.6b). Hepatocellularity increased gradually with age to reach the maximum level in 19-year-old horses. Subsequently, hepatocellularity declined until that of 25-year-old horses almost approached the hepatocellularity of those found in the youngest horses, (Figure 4.2.7a). HPGL was significantly higher in horses between 10 and 20-years-old compared to that in horses <10 and >20 years-old (Figure 4.2.7b).

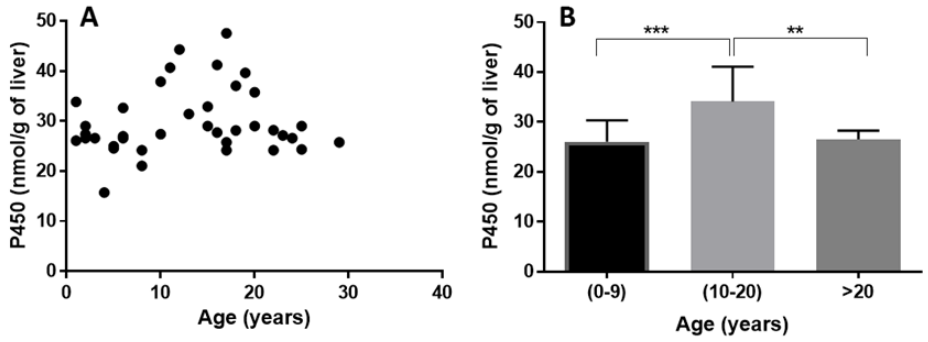


Figure 4.2.3: (A) Relation between nmol P450/g of liver and horse age (n=39). (B) Comparisons of the three different age groups were made using a one-way ANOVA followed by Tukey's multiple comparison test. ** = P<0.05, ***=P<0.01

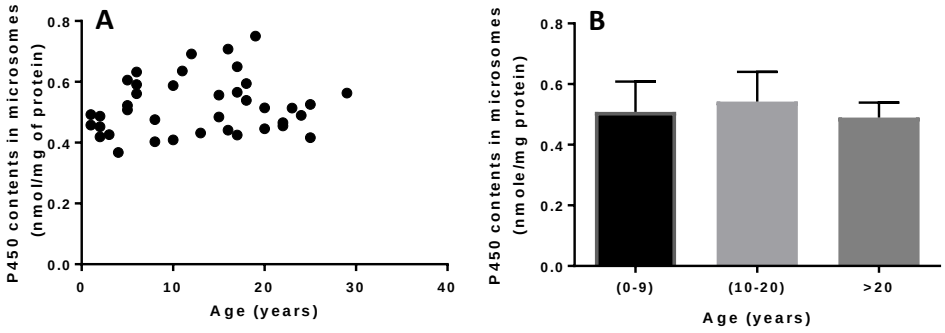


Figure 4.2.4: (A) Relation between nmol P540/mg of liver microsomal protein and horse age. Each value represents the average±SD for triplicate of one horse. (n=39). (B) Comparisons of the three different age groups were made using a one-way ANOVA followed by Tukey's multiple comparison test.

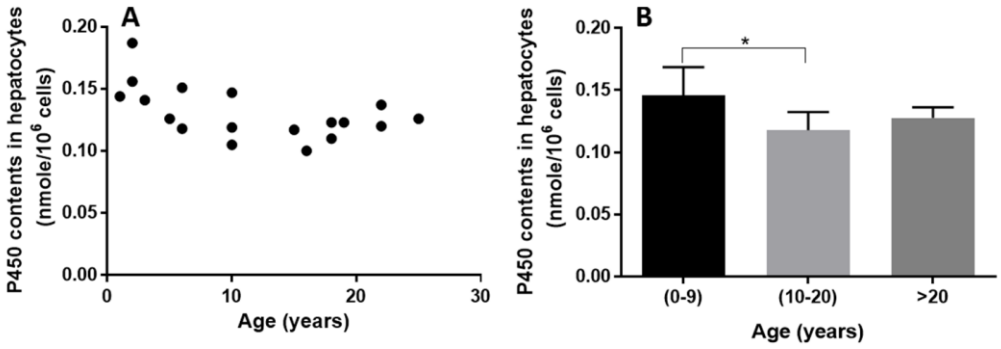


Figure 4.2.5: (A) Correlation between CYP P450 content per 10^6 hepatocytes and horse age. (B) Comparisons of the three different age groups were made using a one-way ANOVA followed by Tukey's multiple comparison test * = P<0.05

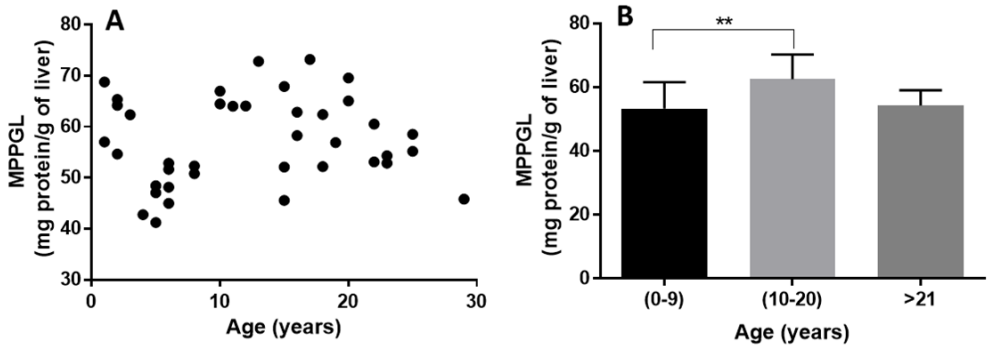


Figure 4.2.6: Effect of increasing age on protein in liver microsomes (A). (n=39). Comparisons of the three different age groups were made using a one-way ANOVA followed by Tukey's multiple comparison test (B). ** = P<0.05.

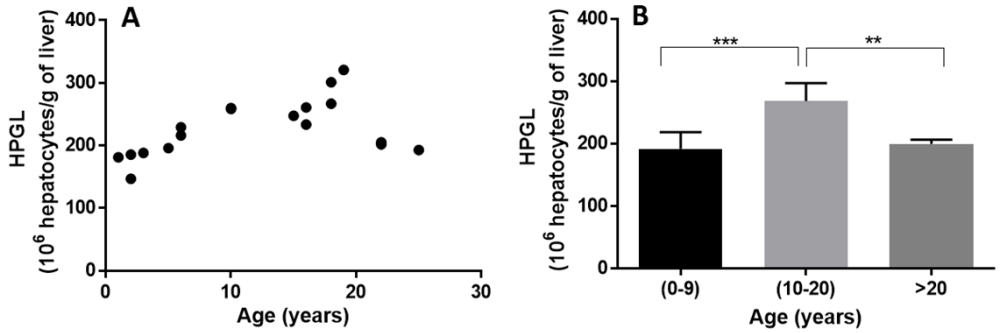


Figure 4.2.7: Relationship between HPGL and horse age. (n=18). Each value represents the average ± SD for 3-9 horses. Comparison of the three different age groups was made using a one-way ANOVA followed by Tukey's multiple comparison test. ** = P<0.05, ***=P<0.01.

There was an inverse relationship between HPGL and CYP P450 content per 10^6 hepatocytes, i.e. the lower the HPGL the higher the CYP P450 content per 10^6 cells (Figure 4.2.8).

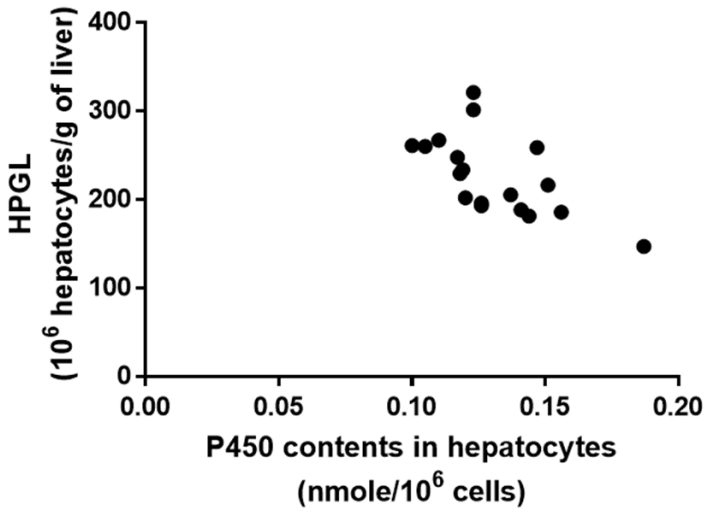


Figure 4.2.8: Relationship between HPGL and CYP P450 content per 10^6 cells for 18 equine livers. There is statistically significant ($p<0.05$) inverse relationship ($r^2 = 0.3926$), between these values.

4.2.3 Age-Related alterations in the size and number of equine hepatocytes

Age-related alterations in the size and number of equine hepatocytes were studied in histological sections of liver samples obtained from 9 horses with age ranging from 1 to 29-years old. The cell size and number per unit area (average± SD) of hepatocytes for each age category is summarised in (Table A.II.1). Between 1 and 20 years of age the cell size of equine hepatocytes decreased in size as age increased. Subsequently, the cell size increased until the hepatocytes of the oldest horses approached the size of those found in the youngest animals. Horses between 10 and 20-years-old contained significantly smaller hepatocytes than horses older than 21-years-old (figure 4.2.9). The number of hepatocytes per unit area increased and decreased inversely with the changes in hepatocyte size over age. There was a significant difference in the number of cells per unit area between 10 to 19 years and <10 and > 20-year-old (Figure 4.2.10).

The HPGL was highly correlated with the number of cells per unit area (r^2 = 0.8294, p=0.0006 and cell size (r^2 = 0.7323, p=0.0032) shown in (Figure 4.2.11A and B), respectively.

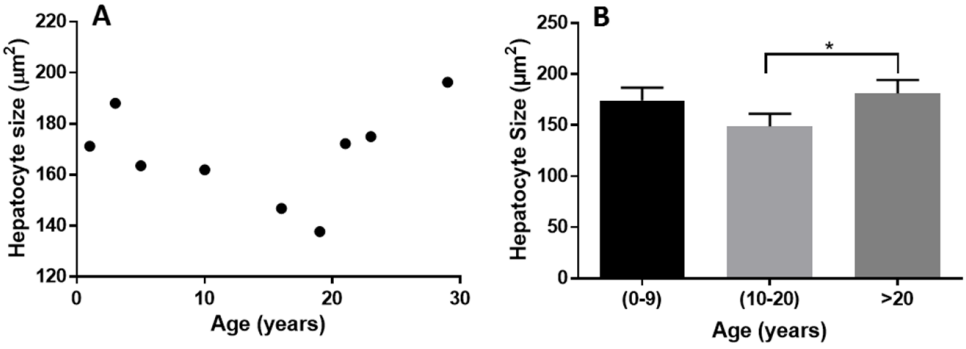


Figure 4.2.9: (A) The age-related changes in the size of hepatocytes is presented in this graph. There is a decline in cell size between 0 and 19 years, followed by a significant increase between 19 and 29 years (p<0.05). Each value represents the average ± SD for 3 horses. (B) Comparison of the three different age groups was made using a one-way ANOVA followed by Tukey's multiple comparison test. *= P<0.05

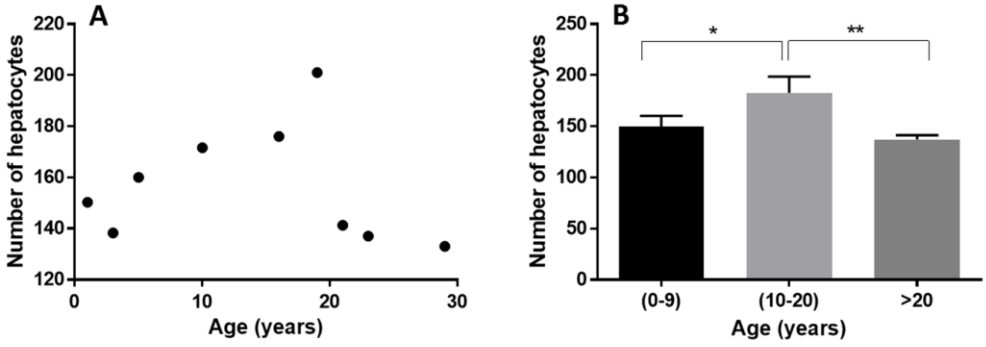


Figure 4.2.10: (A) The age-related changes in the number of cells of hepatocytes per unit area is presented in this graph. There is a significant increase in number of cells between 0 and 19 years, followed by a significant decline between 19 and 29 years (p>0.05) (a). Each value represents the average ± SD for 3 horses. (B) Comparison of the three different age groups was made using a one-way ANOVA followed by Tukey's multiple comparison test. * and ** = P<0.05.

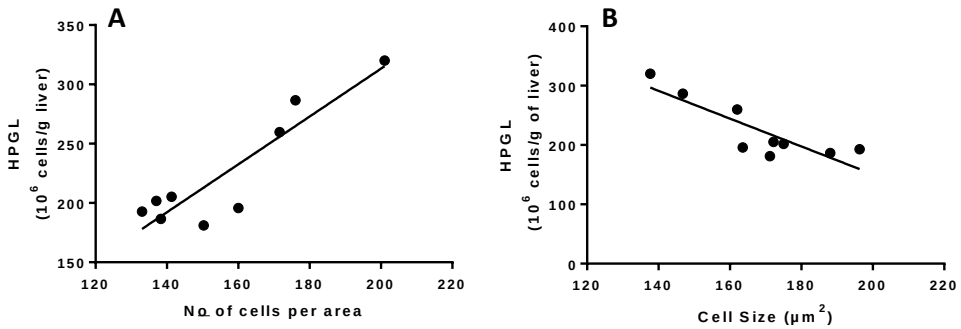


Figure 4.2.11: (A) Relationship between HPGL and number of cells and (B) cell size (b). There is a strong (r^2 = 0.8294 and 0.7323), statistically significant ($p<0.05$) relationship between these values, respectively.

4.3 Discussion

Microsomal protein per gram of liver (MPPGL) and Hepatocellularity (HPGL) are used frequently as scaling factors to predict of the hepatic clearance *in vivo* in human (Houston, 1994). However, there is no information about these scaling factors in horses reported in the literature. In the present study, the MPPGL and HPGL for horse were determined from CYP P450 and protein measurements.

The CYP P450 content in equine liver microsomes was almost double compared to human; in contrast, there was no difference in CYP P450 content in hepatocytes, between horse and human (Seddon et al.,1989).

In the present study, the average values for horse microsomal protein was 57 (41-73) mg/g of liver, and there was no difference in HPGL between the two methods used; CYP P450 content method 227 (146-320) × 10^6 cells/g of liver and protein method 232 (156-352) × 10^6 cells/g of liver. Despite the reports about difficulties in measuring the specific concentration of CYP P450 in liver homogenate (Sohlenius-Sternbeck, 2006), and ease of measuring of protein concentration in both cell suspension and in liver homogenate, no difference was reported between the two methods (Carlile et al., 1997; Bayliss et al., 1999; Wilson et al., 2003; Sohlenius-Sternbeck, 2006). The hepatocellularity number obtained for the horse is higher than for other species. One possible explanation for this may be the diameter of horse hepatocytes (14.6±4.8 μm) being smaller than the diameter of hepatocytes from other species; 19.2±0.6 μm in rat, 18.4±0.8 μm in pigs, and between 20-30 μm in human (Engelmann et al. 1981; Stegemann et al. 2000; Boyer et al., 2017). On the other hand, the microsomal protein value obtained from the horse was similar to values obtained for dog and rat; however, it was higher than that obtained for human (Hakooz et al. 2006; Smith et al. 2008). Furthermore, there is a statistically significant non-monotonic relationship between age and both MPPGL and HPGL in horses.

These findings are consistent with the literature; Basu et al. (1971) studied the effect of the activity of microsomal drug metabolising enzymes with age in rat liver and found that the total microsomal protein increased progressively until the age of 70 days and thereafter it remained more or less constant. Moreover, a study which collated and analysed data from a number of sources found that there was a weak but statistically significant inverse relationship between age and both MPPGL and HPGL in human (Barter et al. 2007). Similarly, Barter et al. (2008) found that values of MPPGL were approximately 36 and 31% lower in new born and elderly (80 years old) individuals than those in a 25-year-old individual. However, recently Zhang et al. (2015), suggested that the variation in content and activity of human liver microsomal protein was due to individual variations rather than an age-dependent variation.

The micrometric measurements of hepatocytes in histological specimens, in the present study, revealed that very young and aged horses possess less and larger hepatocytes than middle age horses. Moreover, there is an inverse relationship between size and number of hepatocyte in a unit area. These findings are in agreement with those reported in the literature; Tauchi (1961) reported that the number of cells in human and rat liver samples decreased to a certain degree with advanced age while hepatocyte size increased. Furthermore, the fall in hepatocyte number with advancing age has been observed in human liver (Wakabayashi et al., 2002).

This increase in hepatocyte size in young subjects may be due to the fast growth demands in this period of age which allows the liver to adapt with a high-energy demand (de la Iglesia et al., 1976). On the other hand, the increase in hepatocyte size in aged subjects may be due to nuclear polyploidisation rather than compensatory hypertrophy (Tauchi and Sato 1962; Watanabe and Tanaka 1982). In the herein study the nuclear polyploidisation was observed in horses over 21 years; however, further

studies are needed on size alterations of both the nuclei and equine hepatocytes in relation to age.

While it has been shown that there is a statistically significant inverse relationship between age and CYP P450 content/mg microsomes in female horses (Nebbia et al. 2004), the present study found that age has no effect on CYP P450 content/mg microsomes. However, the effect of sex could not be studied in the present study due to lack of information regarding the corresponding sex of donor horses. The results of the present study suggest that the increase of MPPGL was due to the increase in the total number of hepatocytes per gram of liver rather than an increase in the expression of CYP P450 resulting from an increase in smooth endoplasmic reticulum (SER) surface area. This cell-size dependent difference in MPPGL content has been reported in human hepatocytes (de la Iglesia et al., 1976). This has been confirmed in this study by the presence of a significant inverse relationship between CYP P450 per 10^6 cells and HPGL which may help horses with low HPGL to maintain their xenobiotic metabolic capacity by having higher levels of CYP P450 per hepatocyte. This observation has also been reported in human hepatocytes (Wilson et al., 2003).

There are several limitations to the present study. Firstly, the corresponding sex of the donor horses was not available, hence it was not possible to study the effect of gender on the CYP P450 content, MPPGL and hepatocellularity number. Secondly, all liver samples used in this study were frozen. A number of studies have found that the freezing of liver samples may have a negative effect on the stability of CYP P450. Smith et al. (2008) found that the average rat and dog CYP P450 content determined from frozen homogenate was almost half of the P450 content of fresh homogenate. However, the activity of CYP P450 in homogenate prepared from fresh and frozen rat liver tissue was assessed using several known P450 substrates, and the results showed that the intrinsic P450 enzyme activity was unaffected by freezing

the homogenate. Hence, calculation of microsomal scaling factors should not be affected by the freezing of liver samples (Smith et al., 2008).

Furthermore, a study that was conducted to examine the stability of CYP P450 in frozen human microsomes found that the concentration of CYP P450 decreased by 20-40% (Pearce et al., 1996). However, freezing human liver tissue had no effect on the stability of CYP P450 which suggests it does not convert to its inactive P420 form, but the accuracy of the P450 assay may have been affected due to contamination of liver tissue fractions with haemoglobin and other haem-containing proteins (Pearce et al., 1996).

In conclusion, this study has established values for equine liver microsomal and hepatocyte number scaling factors of 57 mg microsomal protein per gram liver and 227 x 10^6 per gram liver, respectively. This is the first time that these scaling factors have been determined for the horse. Furthermore, the influence of age was investigated, and the results suggest that MPPGL and HPGL values are dependent on the age of the horse and corrections should be made when predictions of hepatic clearance are carried out using *in vitro-in vivo* extrapolation.

Finally, further investigation is needed regarding the effect of horse gender and breed on MPPGL and HPGL.

Chapter 5

Prediction of equine hepatic metabolic clearance values for omeprazole

5

5.1 Introduction

Omeprazole is a substituted benzimidazole compound originally developed to treat various acid-related gastrointestinal disorders in human such as duodenal ulcer, refractory gastroesophageal reflex disease and zollinger-Ellison syndrome. It is formed by a pyridine moiety and a benzimidazole moiety, linked by a sulfinylmethyl group (Shin et al., 2004) (Figure 5.1.1). Omeprazole decreases gastric acid secretion by specific inhibition of the H+/K+ ATPase enzyme system at the secretory surface of the gastric parietal cell. It is also classified as a proton-pump inhibitor (Shin and Kim. 2013).

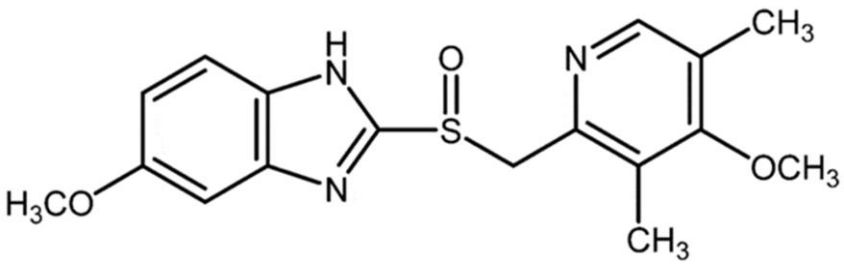


Figure 5.1.1: Structure of omeprazole (Chung et al., 2004)

Environmental stress and prolonged periods of no feed intake with gastric juice pH (<4.0) are considered as major causes of gastric ulcers in human and horses (Murray 1994; Vatistas et al., 1999; Videla and Andrews 2009; Nieto, 2012). Several studies have found that the prevalence of squamous ulceration in racing Thoroughbreds is more than 70% (Hammond et al., 1986; Vatistas et al., 1999; Begg and O'Sullivan 2003). Equine gastric ulcer syndrome (EGUS) has a negative effect on horse health and performance because of associated pain and discomfort (Nieto et al., 2009 ; Videla and Andrews 2009).

As omeprazole is a weak base, it concentrates in the acidic secretory canaliculi within the parietal cell. Here it gains two protons, one on the pyridine nitrogen followed by one on the double-bonded benzimidazole nitrogen, forming a sulphonamide, effectively trapping the drug in the cell. This binds irreversibly via covalent disulphide bonds to the exoplasmic surface of the hydrogen potassium ATPase (H^+/K^+ ATPase) pump. This blocks the ion channel within the pump, preventing ion movement and inhibiting HCl release (Wallmark 1989; Puscas et al., 1999; Ward and Kearns 2013). Consequently, gastric pH increases, allowing ulcer healing.

The pharmacokinetic profile of omeprazole has been characterised in horses (MacAllister et al., 1999; Andrews et al., 2006; Sykes et al., 2015) and a pronounced interindividual variability has been observed: some horses exhibit poor bioavailability regardless of formulation or condition studied. Those horses with poor bioavailability exhibit a wide range of the half-life following intravenous administration (Sykes et al., 2015). This variation in the efficacy of omeprazole has been reported in human and is primarily related to mutations in the CYP2C19 gene and changes in the rate of elimination (Ma et al., 2012; Dean, 2016). Furthermore, several studies found that S-mephenytoin 4'-hydroxylation shows a genetically determined polymorphism and exhibits a marked interethnic difference in the incidence of the poor metabolism phenotype. In vivo studies have the advantage that the whole picture of possible transformation can be considered, however, they require animal experimentation and hence there are additional economical and ethical considerations.

Moreover, the presence of interferences in blood or urine samples such as endogenous metabolites (bilirubin) or interaction between the analyte of interest and the matrix, such as covalent binding to plasma proteins or the enzymatic degradation of a prodrug, may complicate the identification of drug metabolites in urine, and mechanistic studies such as the identification

of the enzymes responsible for metabolism is difficult to conduct (Scarth et al., 2011; Prasain 2012). On the other hand, *in vitro* systems represent a good alternative for animal experimentation; it requires less time, a 'cleaner' extract can be produced, a 'designer' drugs can be studied, and can be easily tailored to study mechanistic aspects (Brandon et al. 2003). Therefore, the aim of this chapter was to determine the intrinsic clearance Cl_{int} and characterise of oxidative metabolism of omeprazole using both fresh and cryopreserved equine hepatocytes as well as equine microsomes. A comparison was made between these three systems with regard to predicting clinical studies in the literature.

5.1.1 Drug-drug interactions

Omeprazole is primarily metabolised by CYP2C19 and CYP3A4 in human (Karam et al., 1996), hence it has been shown to inhibit the metabolism of other drugs, such as diazepam, by competitive inhibition due to its high affinity for CYP2C19 (Blume et al., 2006). Hence, omeprazole is usually the perpetrator drug in interactions; however, as many drugs interact with CYP3A4 and CYP2C19, it is possible omeprazole may become the victim drug. As omeprazole is a long-term therapy there is an increased chance of polypharmacy. For example, chloramphenicol a broad-spectrum bacteriostatic antibacterial is frequently used in equine patients (McElligott et al., 2017). Chloramphenicol is a potent CYP2C19 inhibitor that may affect omeprazole metabolism (Park et al., 2003). Therefore, an interaction study using equine liver microsomes was conducted to prove this hypothesis. Equine liver microsomes was chosen because of their availability and ease of preparation as well as it was reported that microsomes and hepatocytes can be equivalent for determining inhibitory potency for several inhibitors (Brown et al., 2007).

5.2 Results

5.2.1 LCMS method development

An authentic standard confirmed omeprazole's RT at 5.35 minutes, using the developed HPLC-MS method (Figure 5.2.1a). The mass chromatogram obtained for omeprazole and its internal standard lansoprazole is shown in (Figure 5.2.1b). Mass chromatogram analysis demonstrated the omeprazole peak area decreasing and the metabolite peak area increasing over time (Figure 5.2.2).

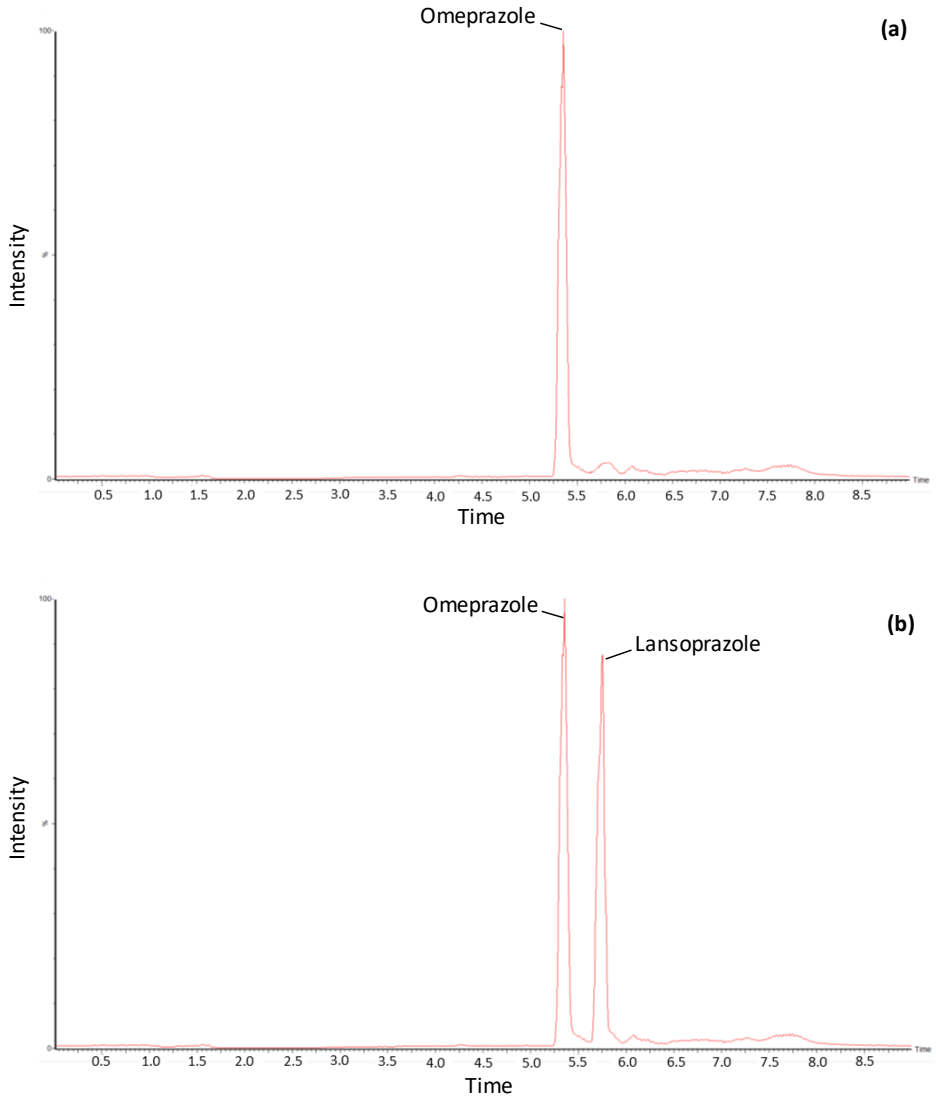


Figure 5.2.1: Mass chromatograms for omeprazole standard (a) and microsomes incubation for 25 µM omeprazole at t=0, with internal standard lansoprazole (b). Peaks were observed at m/z 346 and 370 for omeprazole, lansoprazole, respectively.

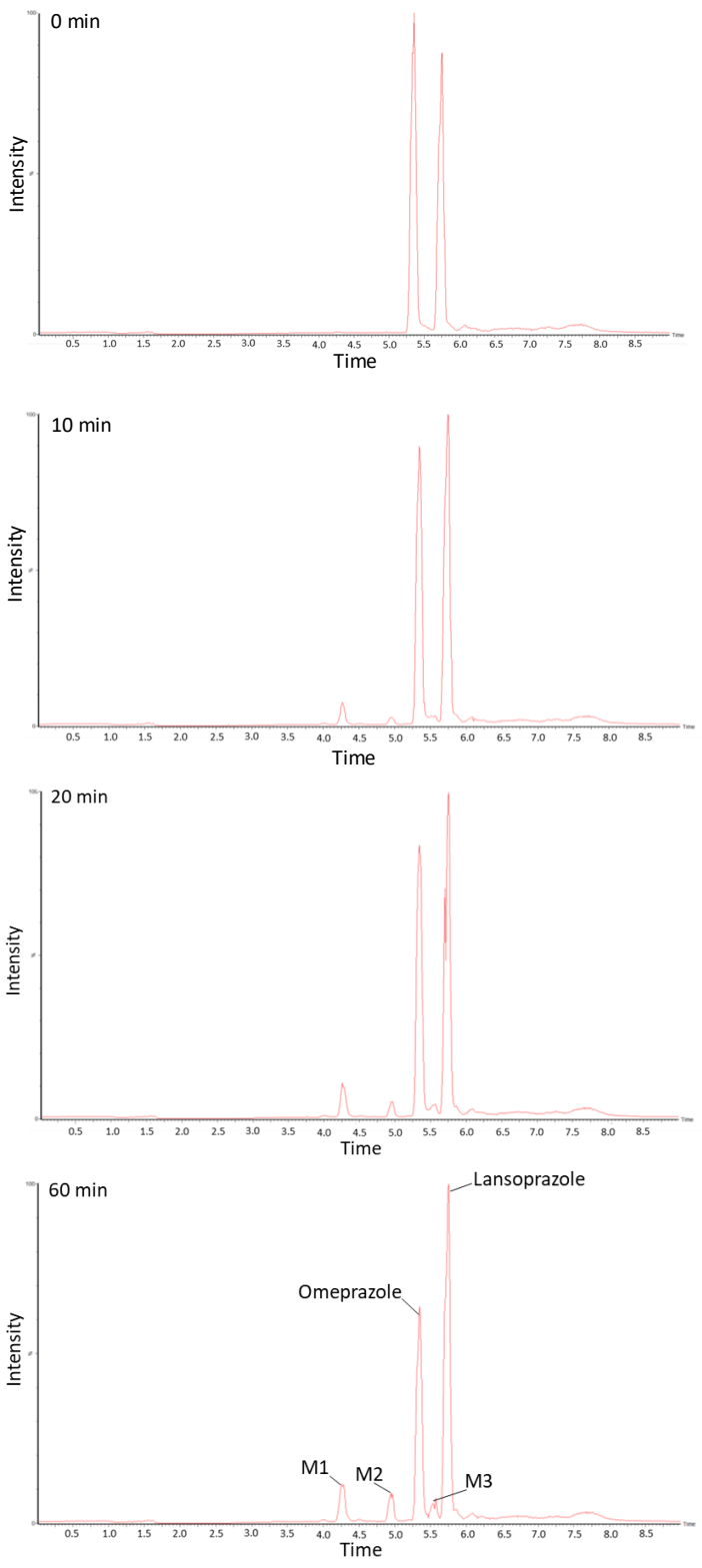


Figure 5.2.2 Mass chromatograms showing omeprazole (m/z 346) disappearance and metabolite (M1, M2 and M3) (m/z 362) appearance with internal standard (lansoprazole) (m/z 370) in microsomes at the following time points; 0, 10, 20 and 60 minutes.

5.2.2 Linearity of initial reaction rate with respect to number of cells or mg microsomal protein

The linearity of enzyme reaction in equine hepatocytes and microsomal incubations was assessed by monitoring the effect of incubation time and hepatocyte and microsomal protein concentrations on omeprazole *in vitro* Cl_{int} values using drug depletion method. At all cell concentrations, depletion over time was linear (Figure 5.2.3A). Similarly, lower microsomal protein concentrations (0.1, 0.5, 1 and 2 mg/ml), the depletion of the three drugs was linear (Figure 5.2.3C); however, at higher microsomal protein concentrations (5, 10 mg/ml) the substrate depletion was not linear (Figure 5.2.3B).

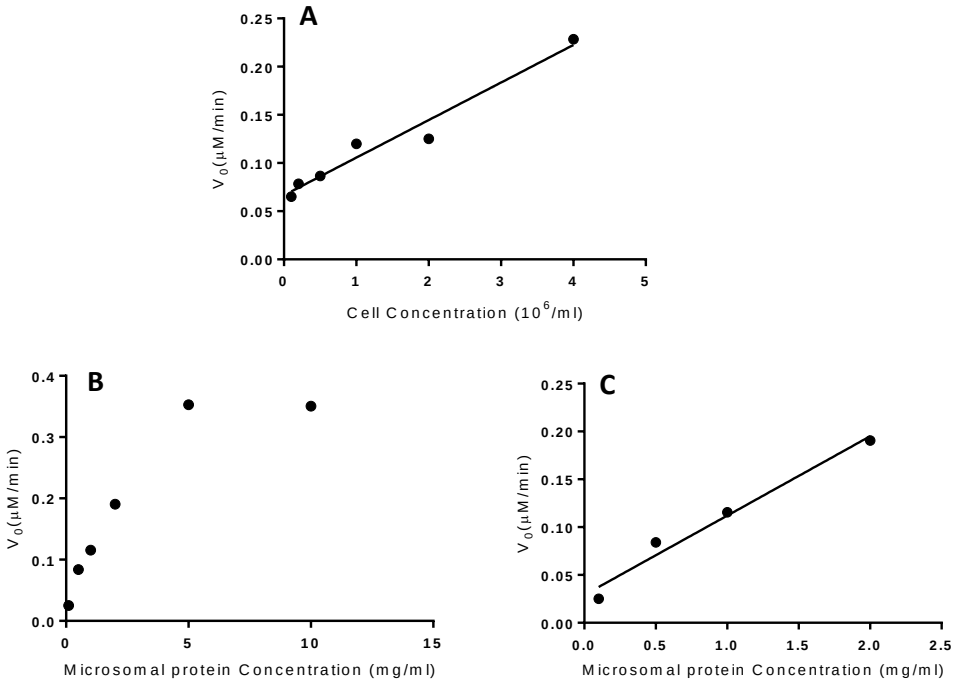


Figure 5.2.3: Linearity of initial reaction rate with respect to number of hepatocytes in 1 ml incubation (A). Linearity of initial reaction rate with respect to microsomal protein concentration in 1 ml incubation (B and C).

5.2.3 Omeprazole Metabolism by Freshly Isolated Equine Hepatocytes

Metabolism was evident for freshly isolated equine hepatocytes with omeprazole across all concentrations (Figure 5.2.4). The V_0 was plotted against drug concentration in a Michaelis-Menten graph (Figure 5.2.5) to determine the kinetic parameters. This data represents hepatocytes from only one of the three donor horses investigated (See appendix III).

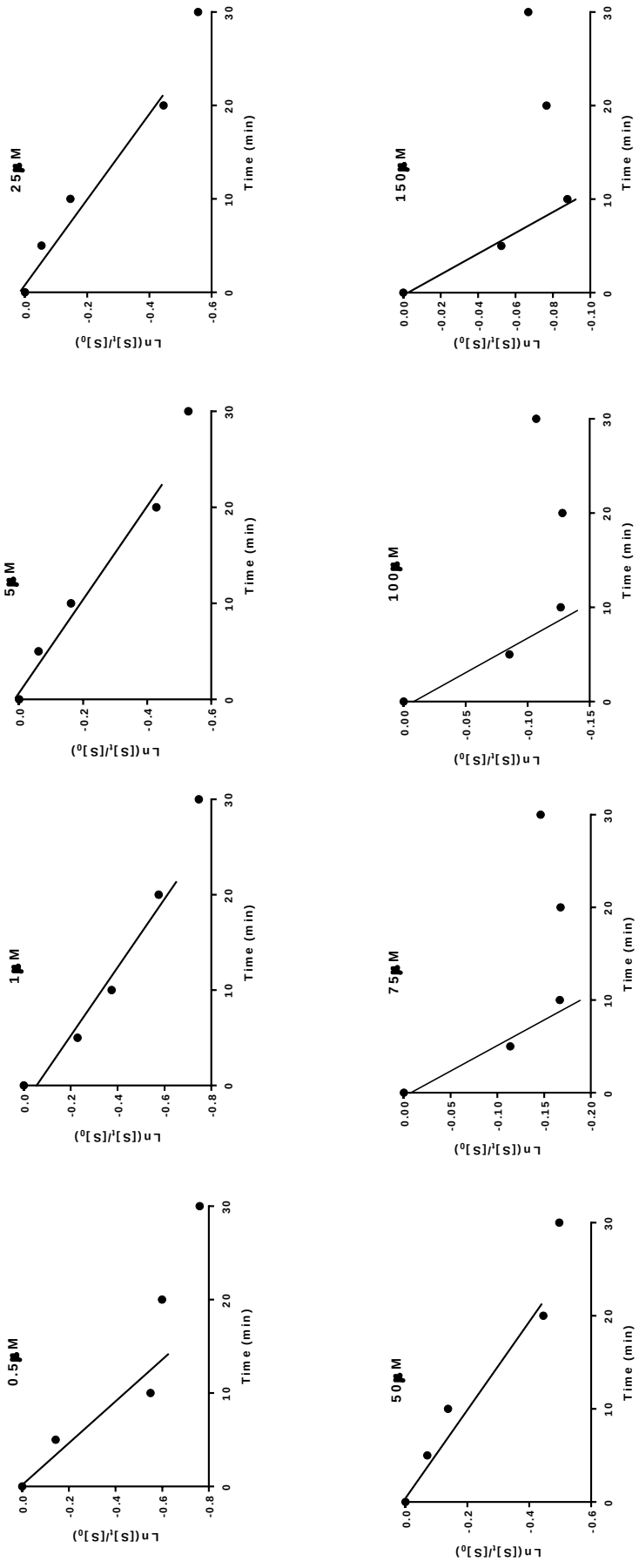


Figure 5.2.4: depletion concentration-time profile in freshly isolated equine hepatocytes. Data was plotted as the natural logarithm (Ln) of substrate concentration over initial concentration against time. Only time points fall within the linear time period of the reaction and allow the assumption of initial rate conditions were chosen. K_{dep} is represented by the slope of the line (refer to table A.III.3, horse 1).

Omeprazole metabolism was observed in the three horses. The V_0 was plotted against drug concentration in a Michaelis-Menten graph (Figure 5.2.6) to determine the kinetic parameters (Table 5.2.1).

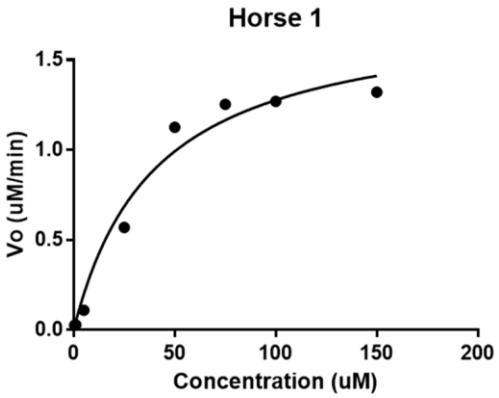


Figure 5.2.5: Michealis-Menten curve for freshly isolated equine hepatocytes with omeprazole. Initial rate (μM/min) is plotted against substrate concentration.

Table 5.2.1: Kinetic parameters from fresh hepatocyte incubations at 1 million cells/mL

	Horse 1	**Horse 2**	**Horse 3**
V_{max} (μM/min)	1.97±0.194	1.84±0.219	1.85±0.182
K_m (μM)	40.25±12.43	45.60±14.61	54.90±13.32
Cl_{int} (μL/min/million cells)	44.50	40.50	33.70

5.2.4 Omeprazole Metabolism by Cryopreserved Equine Hepatocytes

Metabolism was evident for cryopreserved equine hepatocytes with omeprazole across all concentrations (Figure 5.2.6).

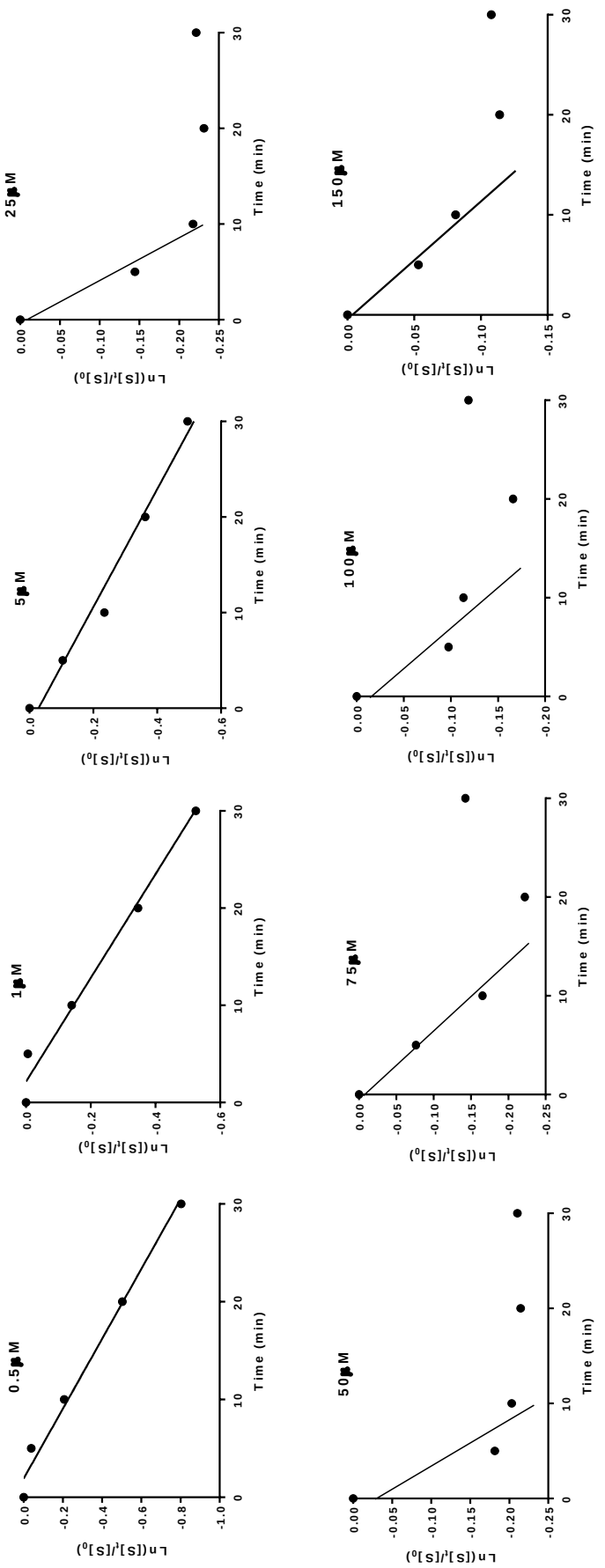


Figure 5.2.6: depletion concentration-time profile in cryopreserved equine hepatocytes. Data was plotted as the natural logarithm (Ln) of substrate concentration over initial concentration against time. Only time points fall within the linear time period of the reaction and allow the assumption of initial rate conditions were chosen. K_{dep} is represented by the slope of the line (refer to table A.III.3, horse 1).

Omeprazole metabolism was observed in the three horses. The V_0 was plotted against drug concentration in a Michaelis-Menten graph (Figure 5.2.7) to determine the kinetic parameters (Table 5.2.2).

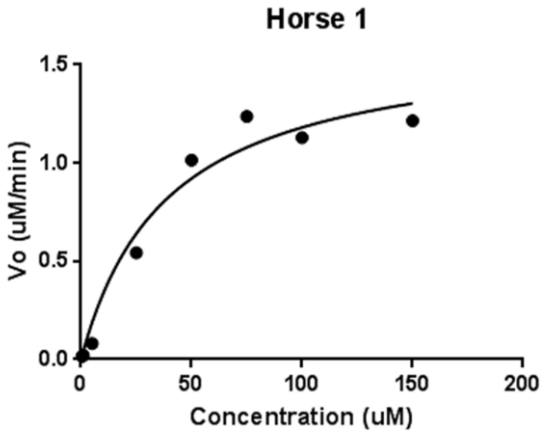


Figure 5.2.7: Michealis-Menten curve for cryopreserved equine hepatocytes with omeprazole. Initial rate (μM/min) is plotted against substrate concentration.

Table 5.2.2: Kinetic parameters from cryopreserved equine hepatocyte incubations at 1 million cells/mL

	Horse 1	**Horse 2**	**Horse 3**
V_{max} (μM/min)	1.65±0.206	1.62±0.074	1.30±0.215
K_m (μM)	39.25±14.22	54.80±6.17	51.60±21.84
Cl_{int} (μL/min/million cells)	41.90	29.60	25.0

5.2.5 Omeprazole Metabolism by Equine Liver Microsomes

Metabolism was evident for equine liver microsomes with omeprazole across all concentrations (Figure 5.2.8).

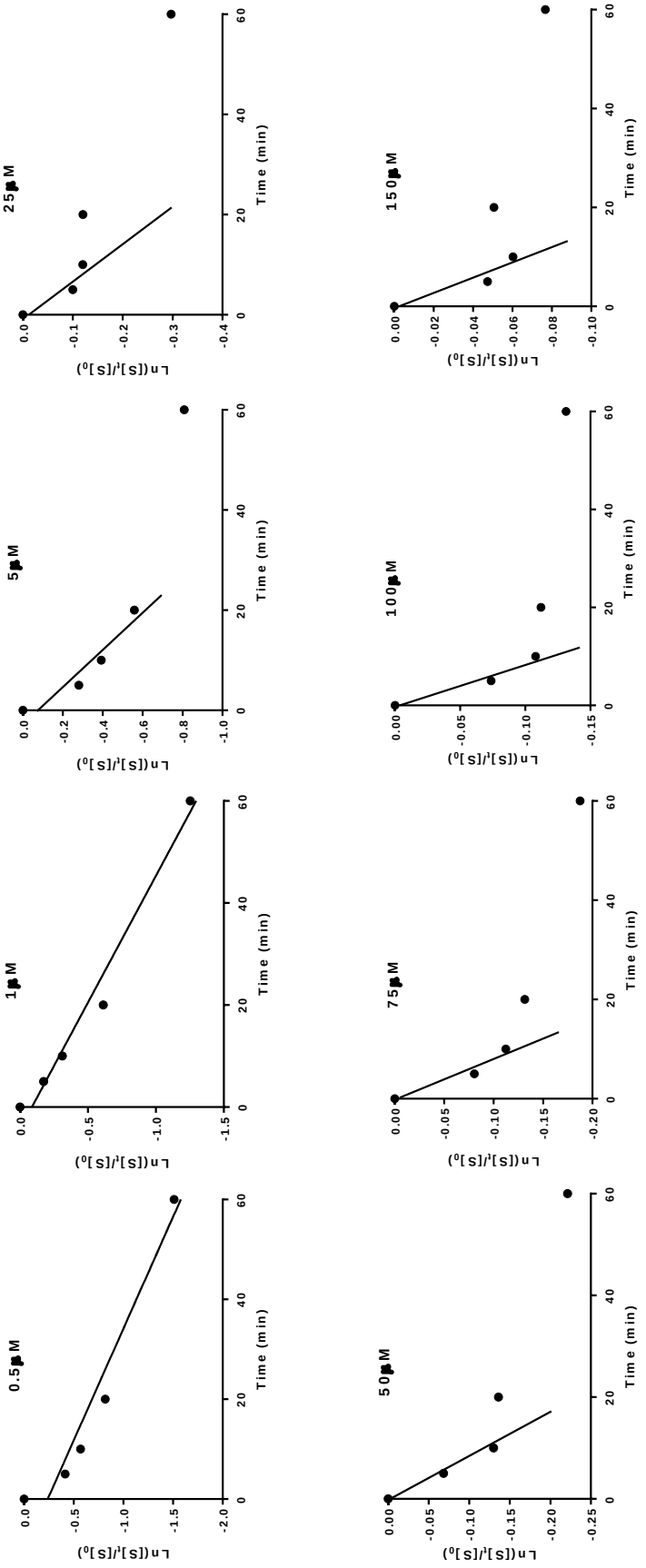


Figure 5.2.8: data gathered using various omeprazole concentrations with equine microsomes. Data was plotted as the natural logarithm (Ln) of substrate concentration over initial concentration against time. Only time points fall within the linear time period of the reaction and allow the assumption of initial rate conditions were chosen. K_{dep} is represented by the slope of the line (refer to table A.III.3, horse 1).

Omeprazole metabolism was observed in the three horses. The V_0 was plotted against drug concentration in a Michaelis-Menten graph (Figure 5.2.19) to determine the kinetic parameters (Table 5.2.3).

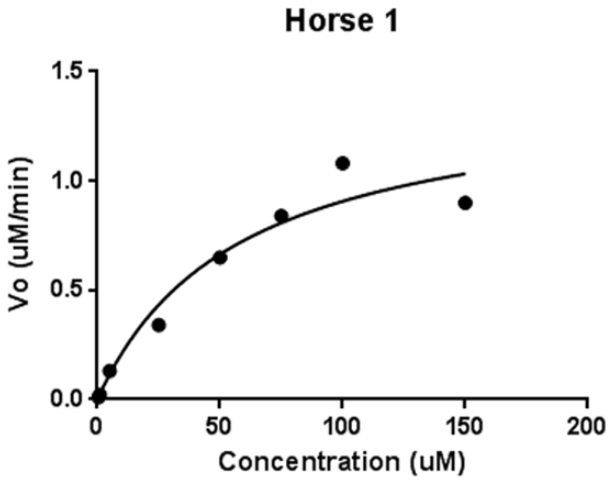


Figure 5.2.9: Michaelis-Menten plot demonstrating omeprazole metabolism by equine microsomes.

Table 5.2.3: Microsome kinetic parameters

	Horse 1	**Horse 2**	**Horse 3**
V_{max} (µM/min)	1.43±0.270	1.96±0.526	0.479±0.025
K_m (µM)	57.6±26.32	94.60±49.50	44.87±6.30
Cl_{int} (µL/min/mg protein)	24.8	20.7	12.6

5.2.6 Metabolite appearance

The appearance of the three oxidation metabolites was observed in fresh and cryopreserved hepatocytes as well as in microsomes (section1.1.1). The appearance (mass spectrum area response) of each of the three metabolites were plotted against time for each concentration to determine the gradient giving, V_0 (Figure 5.2.10) representative of 25 µM omeprazole concentration. V_0 was plotted against initial omeprazole concentration in a Michaelis-Menten graph to determine the K_m (Figure 5.2.11) and (Tables 5.2.4, 5.2.5 and 5.2.6) which were compared to the K_m determined from

omeprazole disappearance (Table 5.2.7) for the corresponding *in vitro* liver system in each horse. No significant difference was observed between the Km from omeprazole disappearance for the three systems and the K_m determined using metabolites formation. However, the K_m of M2 and M3 for microsomes were significantly higher than those for freshly isolated and cryopreserved hepatocytes (Figure 5.2.12).

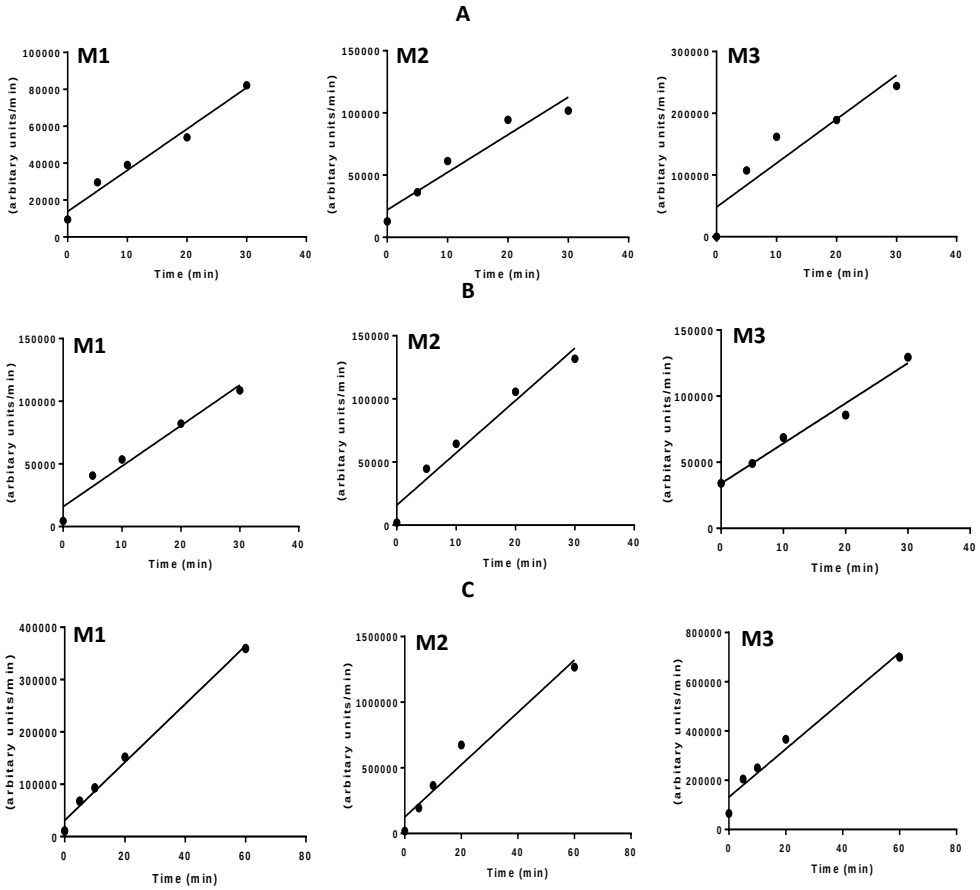


Figure 5.2.10: Omeprazole metabolites appearance in freshly isolated (A), cryopreserved (B) equine hepatocytes and microsomes (C) at 25 µM omeprazole.

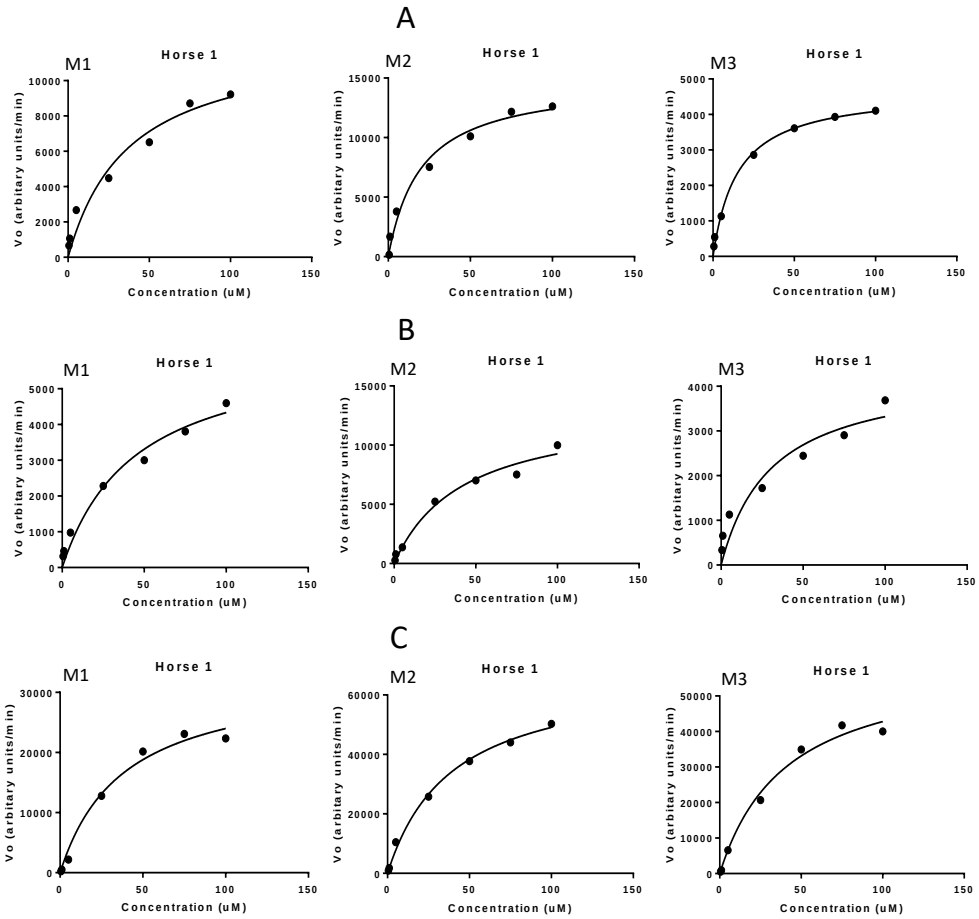


Figure 5.2.11: Michaelis-Menten plots demonstrating omeprazole metabolites appearance in freshly isolated (A), cryopreserved (B) equine hepatocytes and microsomes (C) (Refer to Table A.III.4, horse 1).

Table 5.2.4: K_m determined from metabolite formation in freshly isolated equine hepatocytes for 3 horses.

	K_m determined from metabolite appearance (M1) (uM)	**K_m determined from metabolite appearance (M2) (uM)**	**K_m determined from metabolite appearance (M3) (uM)**
Horse 1	37.5	20.1	15.1
Horse 2	28.0	19.2	16.2
Horse 3	39.7	25.7	28.1
Average ±SD	**35.4±6.4**	**21.7±3.5**	**19.8±7.2**

Table 5.2.5: K_m determined from metabolite formation in cryopreserved equine hepatocytes for 3 horses.

	Km determined from metabolite appearance (M1) (uM)	Km determined from metabolite appearance (M2) (uM)	Km determined from metabolite appearance (M3) (uM)
Horse 1	45.0	42.2	30.8
Horse 2	35.7	47.1	23.7
Horse 3	41.5	48.0	35.9
Average ±SD	**40.7±4.7**	**43.5±7.0**	**30.1±6.1**

Table 5.2.6: K_m determined from metabolite formation in equine liver microsomes for 3 horses.

	Km determined from metabolite appearance (M1) (uM)	Km determined from metabolite appearance (M2) (uM)	Km determined from metabolite appearance (M3) (uM)
Horse 1	38.1	39.2	41.3
Horse 2	86.1	91.7	74.2
Horse 3	32.0	104.3	126.9
Average ±SD	**52.1±29.6**	**79.1±33.3**	**81.0±43.2**

Table 5.2.7: The average of K_m determined from drug disappearance and metabolite formation in microsomes, fresh and cryopreserved hepatocytes (n=3).

	K_m determined from metabolite appearance (µM)			**Km determined from drug disappearance (µM)**
	M1	M2	M3	
Fresh hepatocytes	35.4±6.4	21.7±3.5	19.8±7.2	46.9±7.4
Cryopreserved hepatocytes	40.7±4.7	43.5±7.0	30.1±6.1	48.6±8.2
Microsomes	52.1±29.6	79.1±33.3	81.0±43.2	65.7±25.8

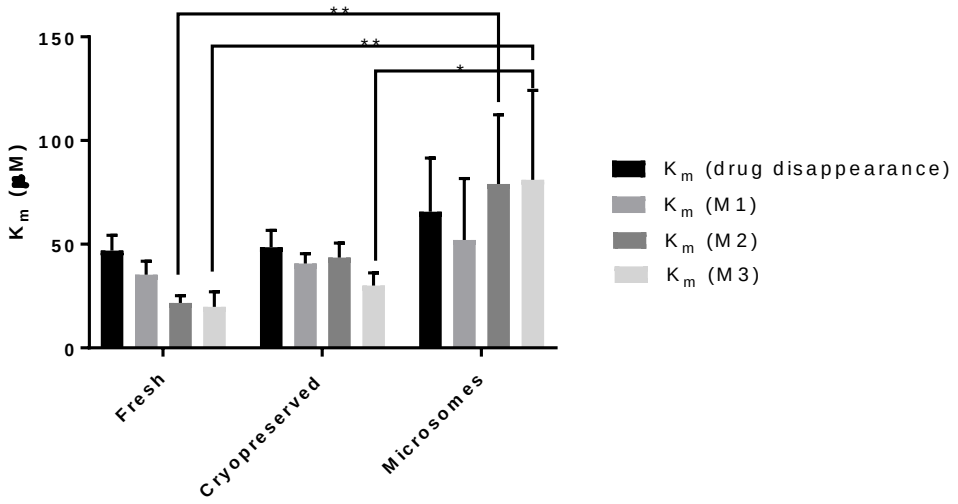


Figure 5.2.12: K_m Values determined using drug disappearance and metabolite formation. Each value represents the average ± SD (n=3). Comparison of the three different systems was made using a two-way ANOVA followed by Tukey's multiple comparison test. *= $p<0.05$, **=$p<0.01$.

5.2.7 *In vitro* comparison of Cl_{int}

The Cl_{int} was corrected for the fraction unbound in the incubation (see section 2.4.7) and the units were standardised using the CYP content in microsomes or hepatocytes for each horse (Table 5.2.8). For horse 3, the average hepatocyte CYP content was used (Table A.III.5).

Table 5.2.8: Cl_{int} correction for unbound fraction in incubation and unit standardisation for equine microsomes, fresh and cryopreserved hepatocytes

	Cl_{int}[1]	Corrected Cl_{int}[1]	Corrected Clint (μL/min/nmol P450)
Fresh			
Horse 1	44.5	54.9	499.0
Horse 2	40.5	50.0	357.1
Horse 3	33.7	41.6	320.0
Cryopreserved			
Horse 1	41.9	51.7	470.0
Horse 2	29.6	36.5	261.0
Horse 3	25.0	30.9	238.0
Microsomes			
Horse 1	24.8	26.3	48.8
Horse 2	20.7	21.3	53.4
Horse 3	10.7	11.3	19.1

[1]Units are μL/min/million cells for hepatocytes and μL/min/mg protein for microsomes.

5.2.8 *In vitro in vivo* extrapolation

The Cl_{int} is scaled to the liver Cl_{int} and then to the CL_H using methodology outlined in (section 1.7) of this thesis, using the unbound fraction in human plasma for omeprazole (the fraction unbound for omeprazole in horse plasma is not evident in literature), and the equine hepatic flow, Q_h= 23.8 ml/min (Tables A.III.6 and 7). Values were from studies completed by Dyke et al., (1998) and Yamazaki and Kanaoka (2004), respectively. For the horse number three the average hepatocellularity was used. The results are summarised in (Table 5.2.9). There was no significant difference between fresh and cryopreserved hepatocytes, whereas there was a significant difference between, both, freshly isolated and cryopreserved hepatocytes and microsomes (Figure 5.2.13).

Table 5.2.9: Hepatic clearance in microsomes, fresh and cryopreserved hepatocytes following scaling to liver Cl_{int} using both models

	Cl_{int}[1]	Liver Cl_{int} (mL/min/liver)	[2]Well-stirred model	[2]Parallel tube model
Fresh				
Horse 1	44.5	178.16	7.56	8.87
Horse 2	40.5	114.33	5.48	6.16
Horse 3	33.7	114.90	5.50	6.19
Cryopreserved				
Horse 1	41.9	167.75	7.25	8.46
Horse 2	29.6	83.56	4.27	4.68
Horse 3	25.0	85.24	4.34	4.77
Microsomes				
Horse 1	24.8	19.42	1.0	1.1
Horse 2	20.1	18.78	1.0	1.0
Horse 3	10.7	7.22	0.40	0.40

[1]Units are µL/min/million cells for hepatocytes and µL/min/mg protein for microsomes
[2]Units are (ml/min/kg)

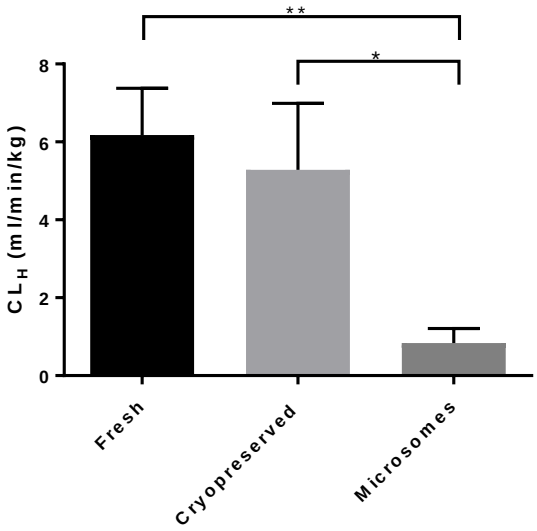


Figure 5.2.13: Hepatic clearances of omeprazole determined from microsomes, fresh and cryopreserved equine hepatocytes (well stirred model). Significant difference between three systems was tested using one-way ANOVA with Tukey's test. *=p < 0.05, **=p<0.01.

The *in vitro* estimated CL_H was displayed with the *in vivo* clearance from equine intravenous studies from literature to enable comparison (Table 5.2.10).

Table 5.2.10: Plasma hepatic clearance for *in vitro* and *in vivo* studies

	[1]Well-stirred model	[1]Parallel tube model
Fresh	6.18 (5.5-7.6)	7.1 (6.2-8.9)
Cryopreserved	5.3 (4.2-7.3)	6.0 (4.7-8.5)
Microsomes	0.8 (0.4-1.0)	0.8 (0.4-1.1)
[*]***In vivo* clearance**	**10.0 (8-17)**	

Data are expressed as the average, followed by the range (n=3)
[1] Units are ml/min/kg
[*] Data from published *in vivo* studies (Toutain and Bousquet-Melou 2004; Sykes et al., 2015)

5.2.9 Drug interaction study

Equine microsomes were tested against chloramphenicol as an inhibitor with omeprazole as the substrate. Chloramphenicol inhibitor concentrations ranged from 0-150 µM. The K_{dep} was determined for each chloramphenicol concentration using a semi-logarithmic graph (Figure 5.2.14). The V_0 was calculated by multiplying the K_{dep} by the omeprazole initial concentration. The IC_{50} was calculated by plotting V_0 as a percentage of V_0 when no inhibitor

was present against the logarithm of the inhibitor concentration (Figure 5.2.15). The average of IC_{50} of the three horses was 17.7±5.8 μM. The obtained IC_{50} values were used to calculate the inhibitor constant K_i using (equation 1.49) (Section1.8.1.1a).

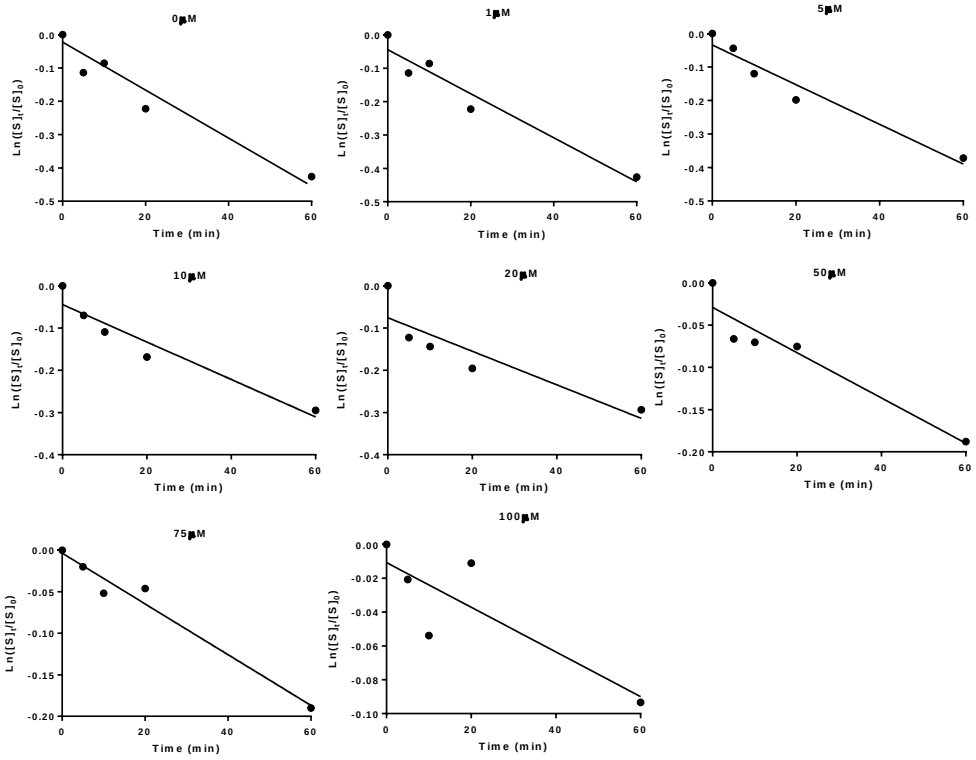


Figure 5.2.14: data gathered using various chloramphenicol concentrations with equine microsomes and omeprazole as the substrate. Data was plotted as the natural logarithm (Ln) of substrate concentration against time. K_{dep} is represented by the slope of the line.

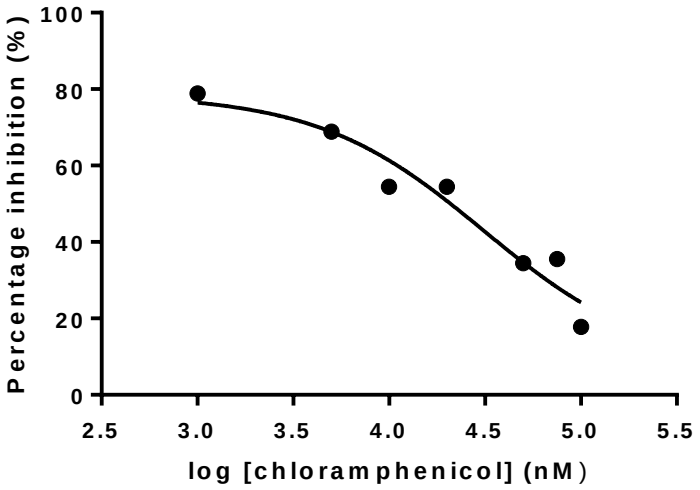


Figure 5.2.15: Dose-response curve demonstrating chloramphenicol inhibition of omeprazole metabolism in microsomes (refer to Table A.III.7).

Table 5.2.11: IC_{50} and K_i determined from an interaction study performed on equine microsomes (n=3)

	Horse 1	**Horse 2**	**Horse 3**	**Average±SD**
IC_{50}	16.5 µM	12.7 µM	24.0 µM	17.7±5.8 µM
K_i	14.3 µM	11.0 µM	20.8 µM	15.4±5 µM

The IC_{50} obtained from the three horses gave an average K_i of 15.4±5 µM (Table 5.2.11), which was used to predict the effect of chloramphenicol on the *in vivo* AUC for omeprazole (Figure 5.2.16) (Table A.III.8). At 10 and 100 µM chloramphenicol the predicted AUC is 1.50 and 7.25-fold larger, respectively, than without the inhibitor.

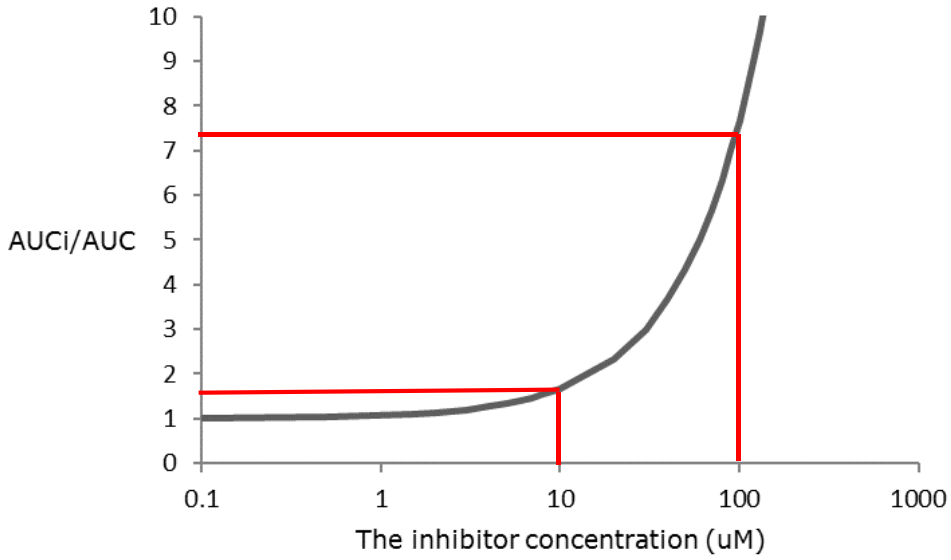


Figure 5.2.16: The predicted effect of increasing concentrations of chloramphenicol on the AUC for *in vivo* omeprazole pharmacokinetics

5.3 Discussion

The pharmacokinetics of omeprazole have been studied *in vivo* in human and horse (Kanazawa et al., 2002; Sykes et al., 2015). These studies found that omeprazole is cleared by phase I metabolism. Furthermore, the major omeprazole metabolites have been identified *in vivo* both in plasma and urine and *in vitro* in human liver microsomes (Chiba et al., 1993). Therefore, the present study investigated the quantitative prediction of equine hepatic metabolic clearance using substrate depletion, from *in vitro* experiments with freshly isolated, cryopreserved equine hepatocytes and liver microsomes focusing on NADPH dependent oxidative metabolism to compare omeprazole metabolism between horse and human.

Despite the presence of variation between studies in literature, the substrate depletion approach is frequently used in the pharmaceutical industry for rapid screening of new drug entities (Jones and Houston 2004; Nath and Atkins 2006).

There was a linear relationship between omeprazole Cl_{int} values and all cell concentrations. Whereas, estimated microsomal *in vitro* Cl_{int} values for

omeprazole reached their peak at 5 mg/ml protein followed by a decline. 1 mg microsomal protein/ml and 1x 10^6 cells/ml were used in the present study, as both of which are in the linear phase.

Initial substrate depletion and metabolite formation studies were performed with omeprazole and a comparison of the predictive ability of microsomal versus hepatocyte substrate depletion data was made using formal scaling procedures (see chapter 2).

The average estimated microsomal liver Cl_{int} for omeprazole was 22 mL/min/kg; which is lower than that reported in human microsomes (98.1 mL/min/kg) (Naritomi et al., 2001). This suggests that the human liver clears omeprazole 4 times greater than in horse. However, *in vivo* studies investigating omeprazole elimination in human and horse determined *in vivo* clearances of 8.40 mL/min/kg and 13.0 mL/min/kg respectively (Obach et al., 2008; Sykes et al., 2015). In this context, hepatic blood flow and plasma protein binding in horse and human should be taken in to account when making a comparison. Hepatic blood flow is similar in both species, whereas, unbound fraction of omeprazole in blood in horses is not available in the literature and needs to be determined.

Predicting the *in vivo* hepatic metabolic clearance of a drug using microsomes requires the assumption that the major metabolic route is via NADPH dependent oxidation (Naritomi et al., 2001). As there is no evidence omeprazole undergoes phase-two metabolism, predictions from microsomes and hepatocytes should be consistent. However, microsome incubations only consider the SER enzymes which rely on NADPH as a cofactor, whereas hepatocytes possess more sophisticated enzyme and transporter activities. Therefore, predictions obtained from freshly isolated and cryopreserved hepatocytes tend to be more accurate than those obtained using microsomes (Houston and Carlile 1997; Ito and Houston 2004; Jones and Houston 2004). It may be that in horse, omeprazole metabolism is more reliant on phase

one enzymes other than NADPH dependent ones, explaining the greater under prediction in equine microsomes compared to human.

Three oxidised metabolites were detected using HPLC-MS with an m/z of 362, sixteen more than omeprazole. RTs of 4.16, 4.89, 5.28 and 5.53 minutes were determined for M1, M2, omeprazole and M3 respectively. This suggests that M1 and M2 are more polar than omeprazole, whereas M3 is less. A previous study determined a RT order of 5-hydroxyomeprazole, omeprazole and then omeprazole sulfone suggesting either M1 or M2 is 5-hydroxyomeprazole and M3 is omeprazole sulfone (Kanazawa et al., 2002). The present study also identified 3-hydroxyomeprazole as a minor metabolite, and although no RT has been published, it is a reasonable assumption that M1 or M2 is 3-hydroxyomeprazole, and the other is 5-hydroxyomeprazole.

There was no significant difference between the K_m from omeprazole disappearance for the three systems and the K_m determined using metabolite formation. However, the K_m of M2 and M3 for microsomes were significantly higher than those for freshly isolated and cryopreserved hepatocytes. In the present study, V_{max} and Cl_{int} could only be determined with arbitrary units, due to the lack of authentic standards for the three metabolites, consequently concentrations were not quantified.

To my knowledge this is the first report describing the metabolism of omeprazole in equine hepatocytes and liver microsomes. However, a study conducted using human liver microsomes has determined two K_m values for the two metabolites (5-Hydroxyomeprazole and omeprazole sulfone) i.e. K_{m1}= 6.0 ± 2.4 and 10.2 ± 7.2 μM and K_{m2}= 106 ± 127 and 482 ± 472 μM, respectively (Chiba et al. 1993). Chiba and his co-workers reported a close correlation ($r= 0.911$, $p < 0.01$) between V_{max1} of 5-hydroxylation and the corresponding parameter V_{max} of S-mephenytoin 4' – hydroxylation. Whereas, K_{m2} and V_{max2} of 5-hydroxylation and all of those of sulfoxination

did not show any significant correlation with the kinetic parameters of S-mephenytoin 4' -hydroxylation. Hence, Chiba et al, concluded that the formation of 5-hydroxyomeprazole and omeprazole sulfone from omeprazole showed a biphasic kinetic behaviour, demonstrating that at least two distinct enzymes are involved in either of metabolic pathways of omeprazole. A similar observation was reported by Shu et al. (2000). Further studies are required to identify the enzymes involved in omeprazole metabolism in horse. However, there are very few recombinant equine enzymes.

Equine microsomes underpredicted the *in vivo* plasma clearance of omeprazole by 16.5-fold compared to the other two liver systems. This result is consistent with human microsomal studies, as underpredictions of 2-fold and 9-fold have been demonstrated in multiple drugs, respectively (Obach 1997; Ito and Houston 2004). However, More IVIVE studies need to be conducted in horse for different drugs to determine if equine microsomes consistently under predict by 16.5-fold.

Predictions of *in vivo* plasma clearance were within 1.6-fold and 1.8-fold using the well stirred model and within 1.3-fold and 1.6-fold using parallel tube model for fresh and cryopreserved hepatocytes, respectively. Parallel tube model was slightly better than well stirred model as expected since omeprazole has a clearance with high extraction efficiency.

Generally, hepatocytes provide more accurate predictions than microsomes with no difference between freshly isolated and cryopreserved hepatocytes. These observations are consistent with the literature for other species (Diener et al., 1993; McGinnity et al., 2004).

Chloramphenicol is a broad-spectrum antibiotic used in horses to treat anaerobic infections (Johns et al., 2011). It was reported in the literature that chloramphenicol interacts with several drugs, such as phenytoin, warfarin, and phenobarbital in human (Park et al., 2003). In the present study, chloramphenicol inhibited omeprazole metabolism in equine

microsomes. Furthermore, as the IC_{50} was greater than 10 μM, chloramphenicol would be considered a weak inhibitor of omeprazole. Significant drug-drug interaction DDIs occur when the AUCi/AUC ratio is greater than two (Blanchard et al., 2004), which is estimated at a chloramphenicol concentration of 30 μM, therefore inhibition is still predicted at high concentrations. A DDI is most likely to occur when chloramphenicol is given orally, since concentrations will be at their highest between absorption in the intestine and first pass metabolism in the liver.

This study also demonstrated that omeprazole and chloramphenicol bind to the same CYP450 enzyme in horse, as a DDI occurred. This may indicate that a CYP2C19 orthologue is present in the horse as chloramphenicol has been shown to have a potent inhibitory effect on CYP2C19 in human (Park et al 2003).

Chapter 6

Prediction of equine hepatic metabolic clearance values for flunixin and phenylbutazone

6

6.1 Introduction

Flunixin and Phenylbutazone are non-steroidal anti-inflammatory drugs (NSAIDs) classified as carboxylic and enolic acids, respectively (Lees and Higgins, 1985; Roy et al., 2015). Generally, the mode of action of NSAIDs is based on inhibition of cyclo-oxygenase (COX) enzymes, hence blocking the formation of COX derived eicosanoid inflammatory mediators, such as Prostaglandins (PGs) which are essential to the acute inflammatory process (Marshall and Blikslager 2011). Both, flunixin and phenylbutazone have been used widely for their anti-inflammatory and analgesic properties to treat musculoskeletal conditions and colic in equine practice (Banse et al., 2015). In equine medicine, flunixin is used in the prevention of endotoxic shock, in musculoskeletal injuries, in the management of colic patients and ocular diseases (Bottoms et al., 1981; Fessler et al. 1982). Moreover, flunixin meglumine is the most efficacious in alleviation of visceral pain and preventing clinical signs of endotoxaemia than phenylbutazone, dipyrone and ibuprofen (Clark and Clark 1999).

Characterisation of flunixin has been established in horses and most studies have found that flunixin has a relatively a short elimination half-life (3.4-4.8 h) and small volume of distribution (Lee and Maxwell 2014; Knych et al. 2015). Flunixin is metabolised by oxidation to 5-hydroxyflunixin (Figure 6.1.1) and by conjugation of the carboxylic acid moiety with glucuronic acid. However, most of the dose is excreted in the urine as flunixin or flunixin glucuronide (Johansson and Anlér 1988; Soma et al., 1988).

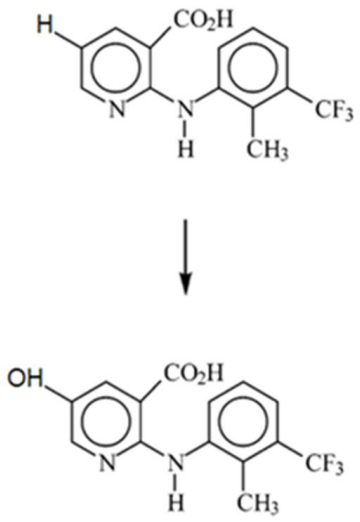


Figure 6.1.1: Metabolism of flunixin to 5'hydroxyflunixin. Adapted from "Determination and confirmation of 5-hydroxyflunixin in raw bovine milk using liquid chromatography tandem mass spectrometry" by Boner et al. (2003).

Phenylbutazone was introduced into human medicine in 1949 and second only to aspirin as one of the oldest NSAIDs. A year later it was introduced into veterinary medical practice and remains one of the most commonly used NSAIDs in the horse (Lees and Higgins 1985; Tobin et al., 1986). Phenylbutazone has been used for the treatment of acute and chronic inflammatory pain caused by various forms of arthritis (Lees and Toutain, 2013). However, by the 1980s, use of phenylbutazone in human was severely restricted because of the recognition that it induces, very rarely, blood dyscrasias including aplastic anaemia, leukopenia, agranulocytosis and thrombocytopenia, in some cases leading to death (Tobin et al., 1986). In contrast, phenylbutazone has been extensively used in equine medicine for more than 50 years and continues to dominate the treatment of pain in equine, especially that associated with joint and muscle conditions (Tobin et al., 1986). Pharmacokinetics of phenylbutazone in the horse have been studied extensively and the elimination-half-life after IV dosing is 4-6 hours (Lees and Higgins 1985; Maitho et al., 1982; Lees and Toutain 2013) . After

oral dosing as granules, paste or bolus formulations phenylbutazone is well absorbed and the bioavailability is in the range of 69-91%. Furthermore, a number of metabolites have been identified; the most important ones are oxyphenbutazone and γ-hydroxyphenylbutazone (Figure 6.1.2) (Lees and Toutain 2013). The importance of these two metabolites comes from their analgesic/anti-inflammatory properties; however, their contribution to pharmacological actions of phenylbutazone is unknown (Lees and Toutain 2013). Both metabolites are detected in plasma and urine with much higher concentrations in urine than those in plasma.

The main objective of the research described herein is to carry out a comprehensive comparison of the three *in vitro* systems used in previous chapter to estimate Cl_{int} values for both drugs. In addition, comparison of two liver models i.e. well stirred and parallel tube model to predict *in vivo* Clint and Cl_H will be explored.

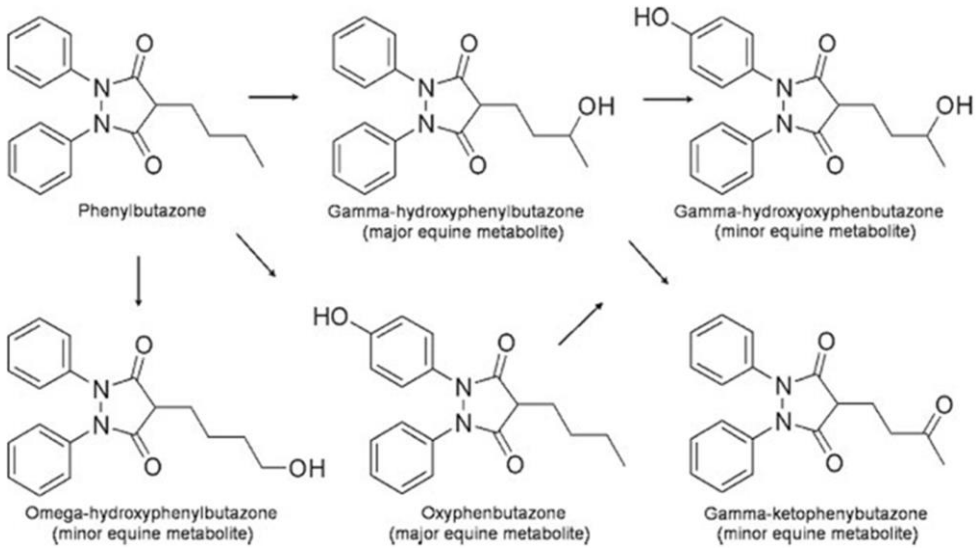


Figure 6.1.2: Phase I metabolism of phenylbutazone in the horse. Adapted from Scarth et al. (2011).

6.2 Results

6.2.1 Flunixin

6.2.1.1 LCMS analysis of flunixin

An authentic standard confirmed flunixin's RT at 4.75 minutes, using the developed HPLC-MS method (Figure 6.2.1).

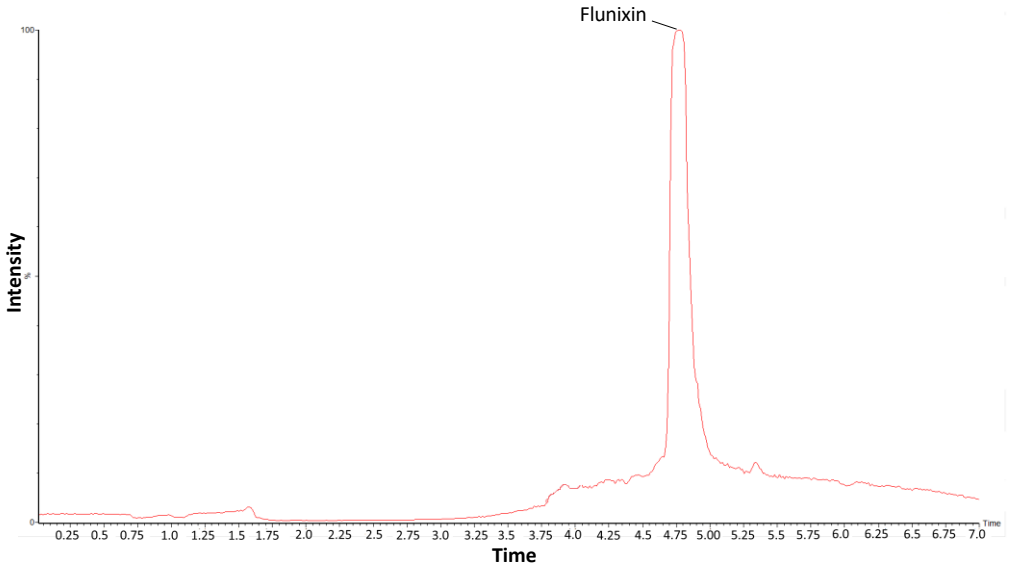


Figure 6.2.1: Chromatogram for monitoring flunixin disappearance. The ion of mass 297.26 was monitored at a retention time of 4.75 minutes.

6.2.1.2 Linearity of initial reaction rate with respect to number of cells or mg microsomal protein

Flunixin Cl_{int} values were determined by measuring their depletion over time at varying cell and microsomal protein concentrations. At all cell concentrations, its depletion over time was linear (Figure 6.2.2 A). However, at higher microsomal protein concentrations (5, 10 mg/ml) the substrate depletion was not linear (Figure 6.2.2 C).

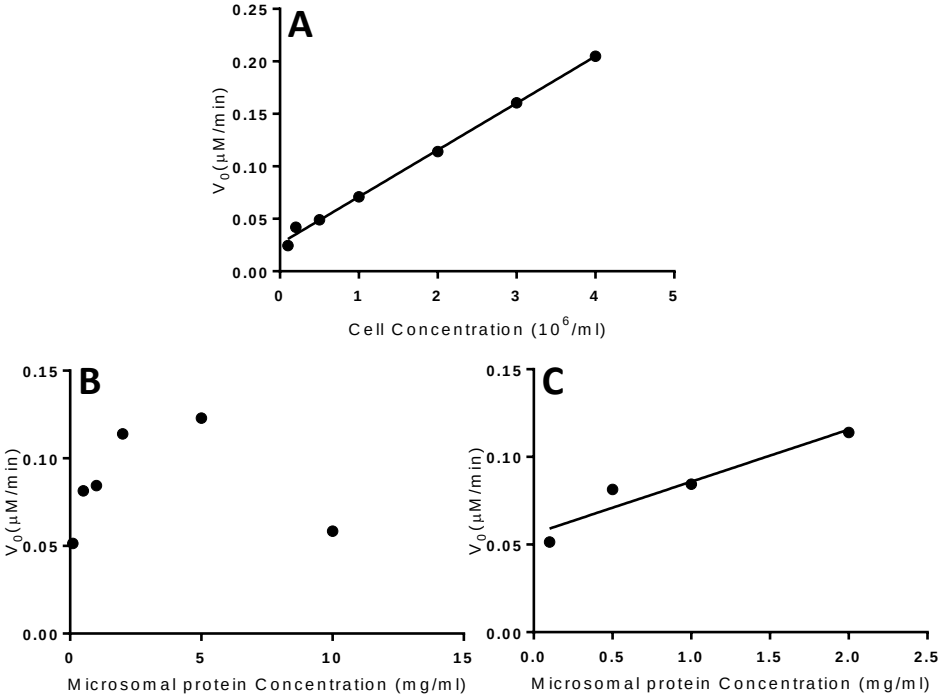


Figure 6.2.2: Linearity of initial reaction rate of flunixin with respect to number of hepatocytes in 1 ml incubation (A). Linearity of initial reaction rate with respect to microsomal protein concentration in 1 ml incubation (B and C).

6.2.1.3 Flunixin metabolism in freshly isolated equine hepatocytes

Metabolism of flunixin was observed with freshly isolated hepatocytes. Drug disappearance was plotted against time for each concentration in a linear semi-logarithmic graph to determine the K_{dep} (Figure 6.2.3). The V_0 was plotted against drug concentration in a Michaelis-Menten graph (Figure 6.2.4) to determine the kinetic parameters (Table 6.2.1). This data represents hepatocytes from only one of the three donor horses investigated (See appendix IV).

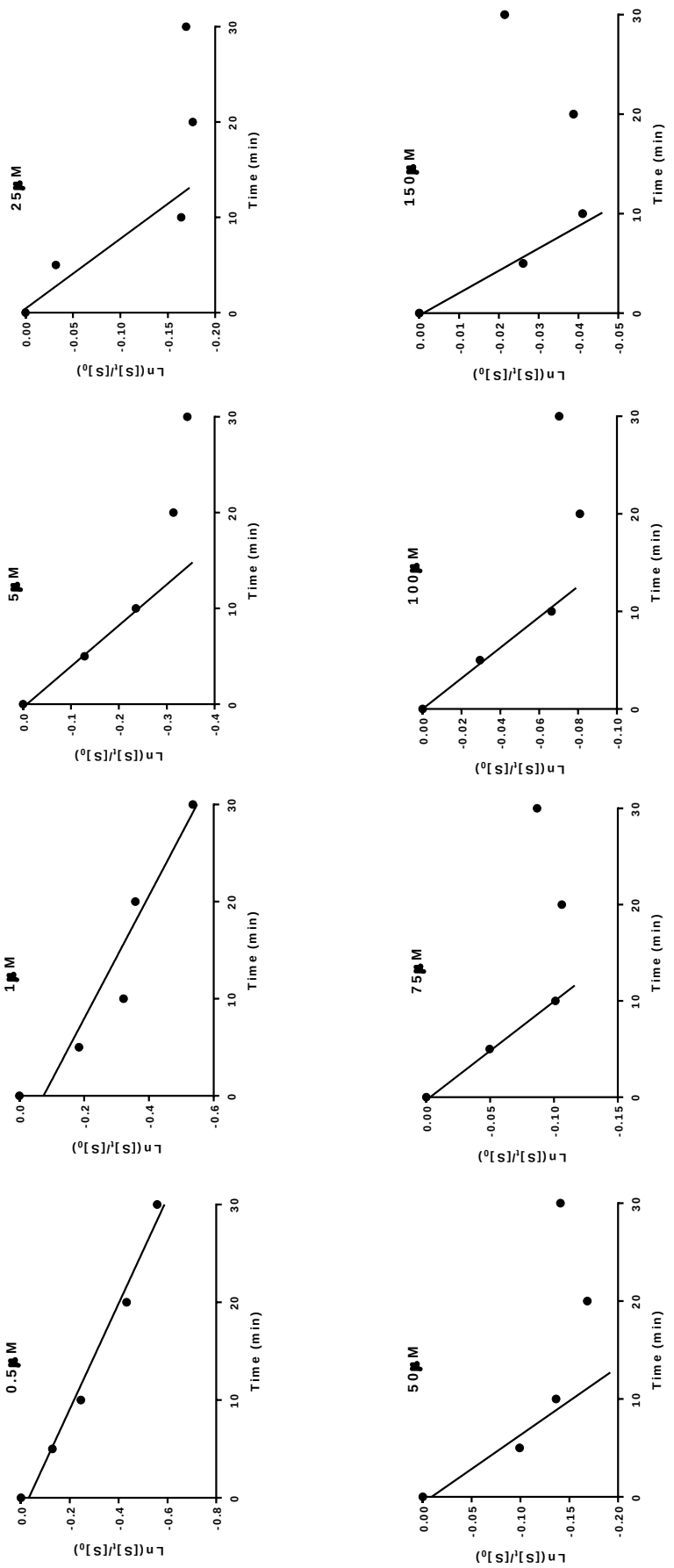


Figure 6.2.3: Metabolism of flunixin by freshly isolated hepatocytes. Data was plotted as the natural logarithm (Ln) of substrate concentration against time. Only time points fall within the linear time period of the reaction and allow the assumption of initial rate conditions were chosen. K_{dep} is represented by the slope of the line (refer to table A.IV.3, horse 1).

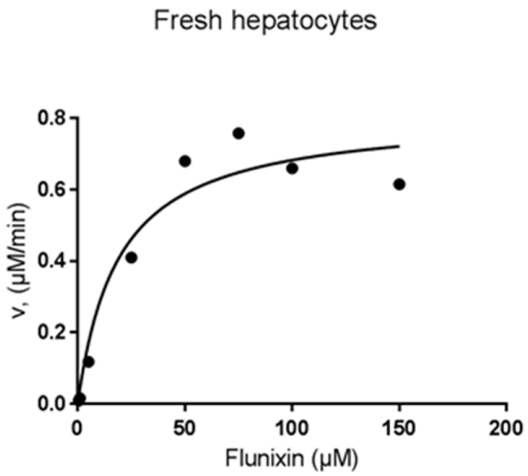


Figure 6.2.4: Michaelis-Menten plot demonstrating flunixin metabolism by fresh hepatocytes

Table 6.2.1: Kinetic parameters from fresh hepatocyte incubations at 1 million cells/mL

	Horse 1	**Horse 2**	**Horse 3**
V_{max} (µM/min)	0.81±0.094	0.75±0.108	0.65±0.070
K_m (µM)	19.0±8.9	31.7±14.5	15.8±7.5
Cl_{int} (µL/min/million cells)	42.7	23.8	41.2

6.2.1.4 Cryopreserved hepatocytes

Metabolism of flunixin was observed with cryopreserved hepatocytes. Drug disappearance was plotted against time for each concentration in a linear semi-logarithmic graph to determine the K_{dep} (Figure 6.2.5). The V_0 was plotted against drug concentration in a Michaelis-Menten graph (Figure 6.2.6) to determine the kinetic parameters (Table 6.2.2). This data represents hepatocytes from only one of the three donor horses investigated (See appendix IV).

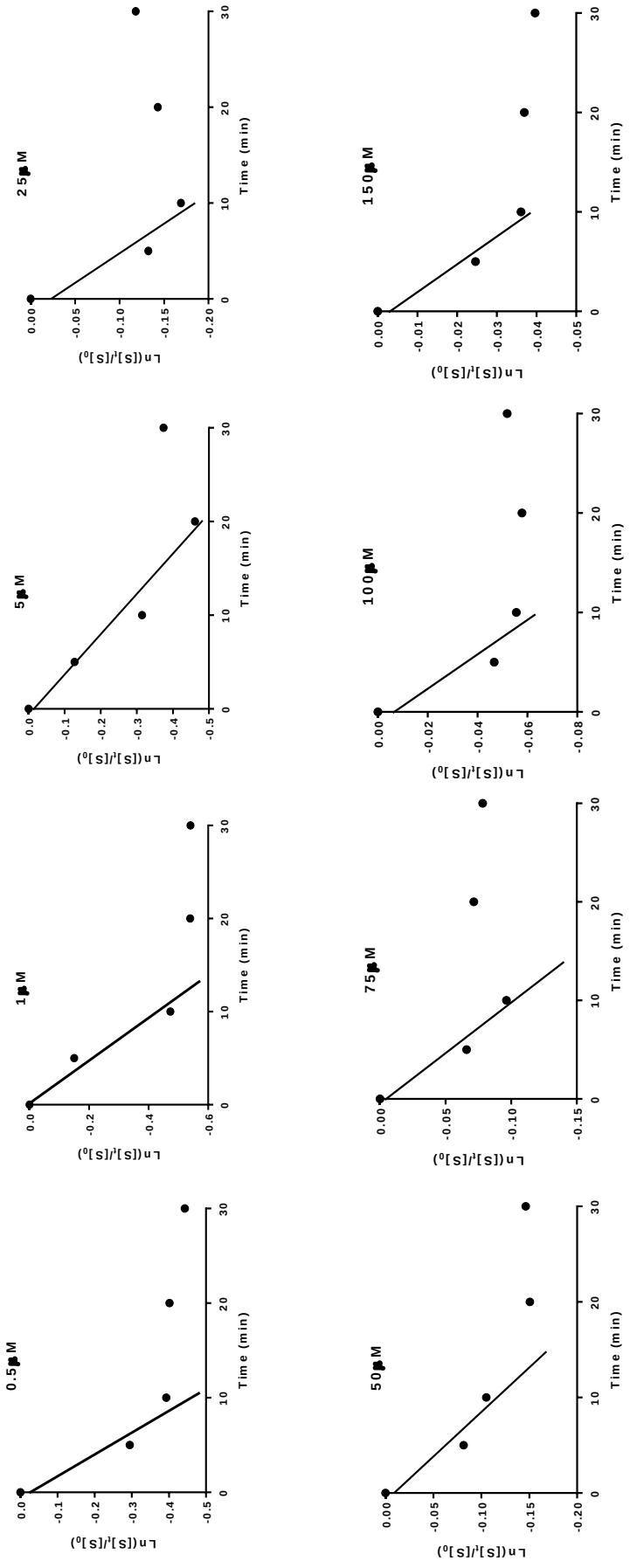


Figure 6.2.5: metabolism of flunixin by cryopreserved hepatocytes. Data was plotted as the natural logarithm (Ln) of substrate concentration against time. Only time points fall within the linear time period of the reaction and allow the assumption of initial rate conditions were chosen. K_{dep} is represented by the slope of the line (refer to table A.IV.1.3, horse 1).

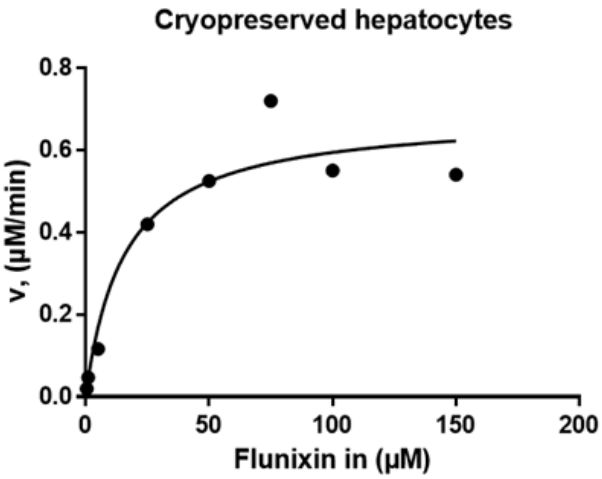


Figure 6.2.6: Michaelis-Menten plot demonstrating flunixin metabolism by cryopreserved hepatocytes

Table 6.2.2: Kinetic parameters from cryopreserved hepatocyte incubations at 1 million cells/mL

	Horse 1	**Horse 2**	**Horse 3**
V_{max} (µM/min)	0.69±0.079	0.74±0.064	0.60±0.049
K_m (µM)	15.6±7.9	20.0±6.8	25.6±7.4
Cl_{int} (µL/min/million cells)	44.0	37.0	23.3

6.2.1.5 Equine liver microsomes

Metabolism of flunixin was observed with equine microsomes. Drug disappearance was plotted against time for each concentration in a linear semi-logarithmic graph to determine the K_{dep} (Figure 6.2.7). However, with increasing substrate concentration, the initial rate firstly increased followed by a decline, therefore the data was fitted to a substrate inhibition curve as in equation 1.51 in (section 1.8.1.4). Hence, the K_m and V_{max} values could not be determined with any certainty and therefore the initial slope of the Michaelis-Menten curve was used to estimate the CL_{int} values (Table 6.2.6.).

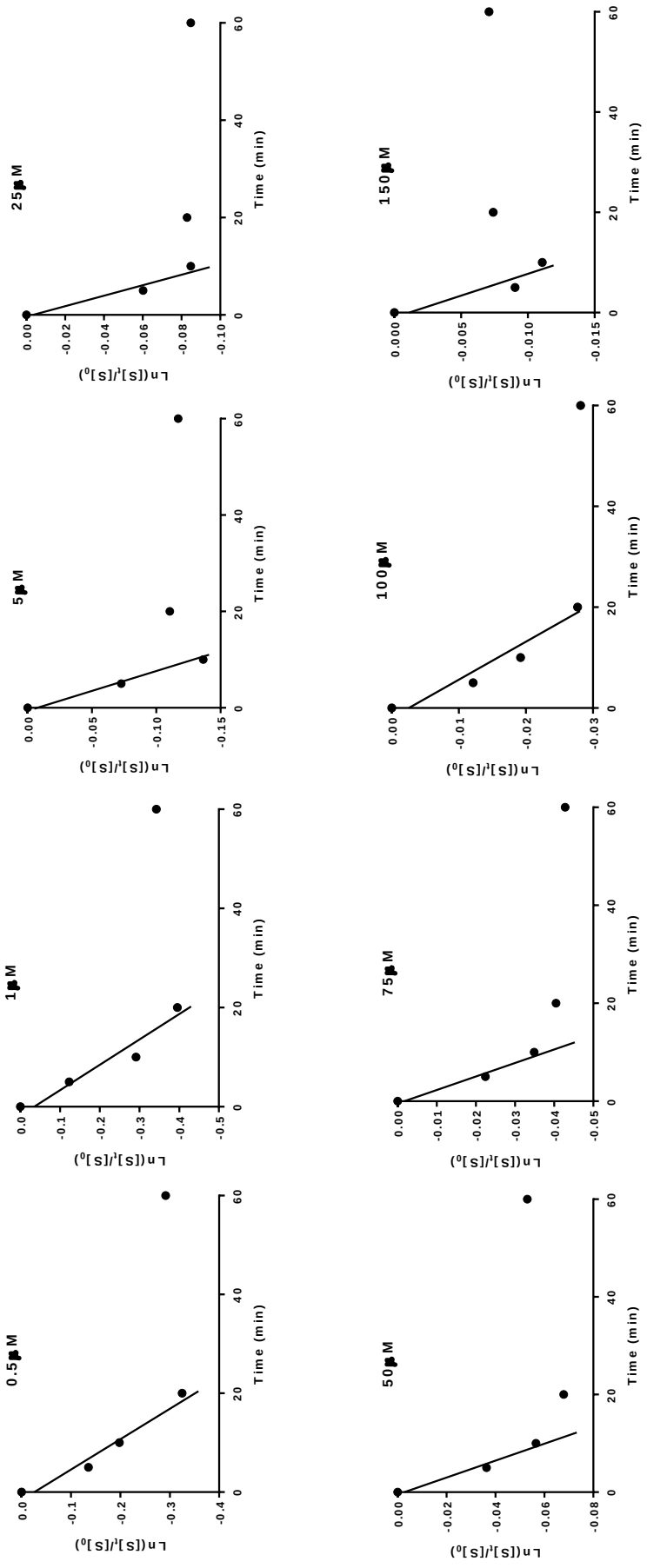


Figure 6.2.7: Metabolism of flunixin by equine liver microsomes. Data was plotted as the natural logarithm (Ln) of substrate concentration against time. Only time points fall within the linear time period of the reaction and allow the assumption of initial rate conditions were chosen. K_{dep} is represented by the slope of the line (refer to table A.IV.1.3, horse 1).

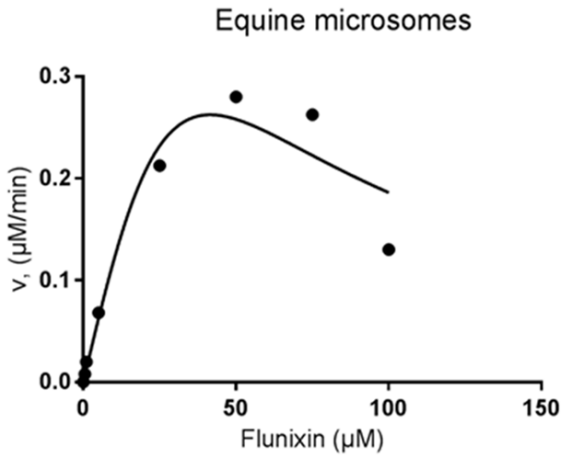


Figure 6.2.8: Michaelis-Menten plot demonstrating flunixin metabolism by equine liver microsomes.

Table 6.2.3: Cl_{int} from equine liver microsome incubations at 1 mg protein/mL

	Horse 1	**Horse 2**	**Horse 3**
Cl_{int} (µL/min/mg protein)	13.0	12.0	17.5

6.2.1.6 Metabolite appearance

Only one metabolite was observed only in microsomes. This metabolite was characterised by comparison of the negative control chromatogram 0 time point with the chromatogram of the 60 min time point (Figure 6.2.9). The appearance of this metabolite mass spec response was plotted against time for each concentration to determine the gradient, which is V_0 (Figure 6.2.10). The initial rate of metabolite formation followed the same pattern. Therefore, the data was fitted to a substrate inhibition curve as in equation 1.51 in section 1.8.1.4 (Figure 6.2.11). Because of substrate inhibition, in addition to the lack of authentic standard of the metabolite V_{max}, K_m and Cl_{int} could not be calculated.

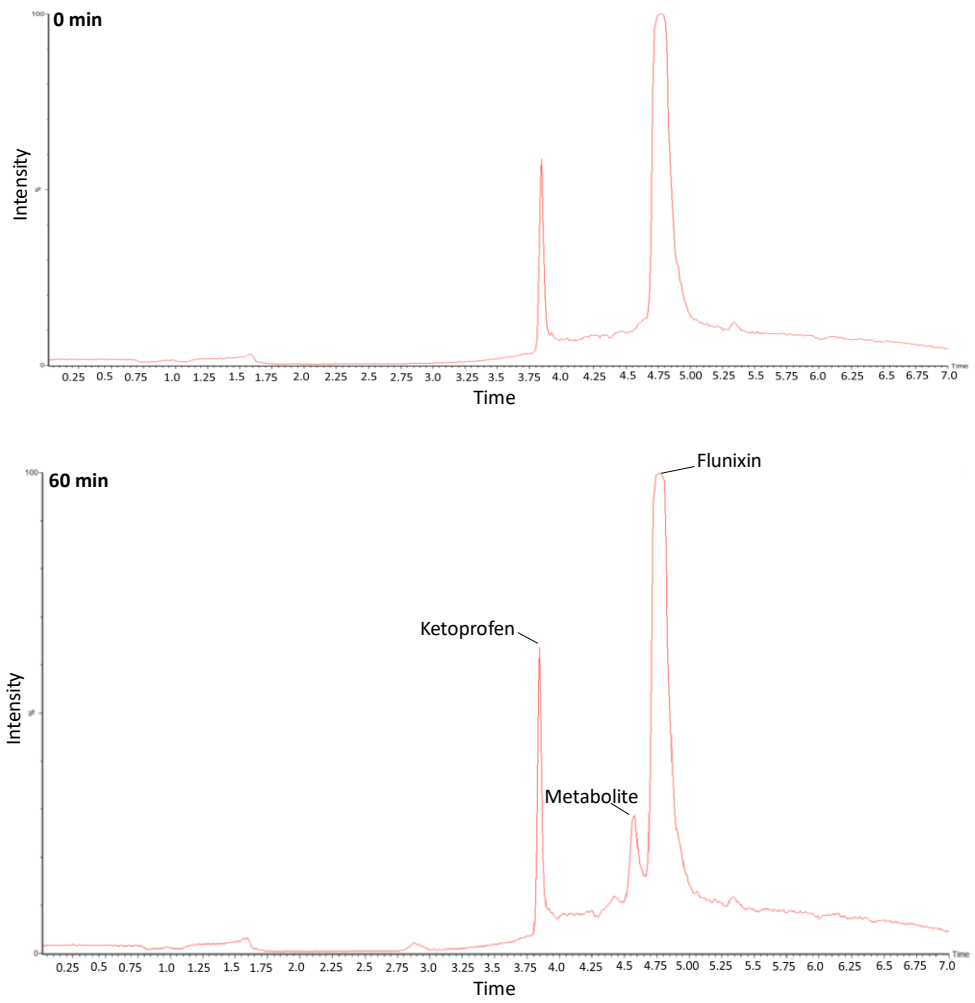


Figure 6.2.9: Graphs derived from flunixin metabolite appearance in equine liver microsomes at 50 μM flunixin

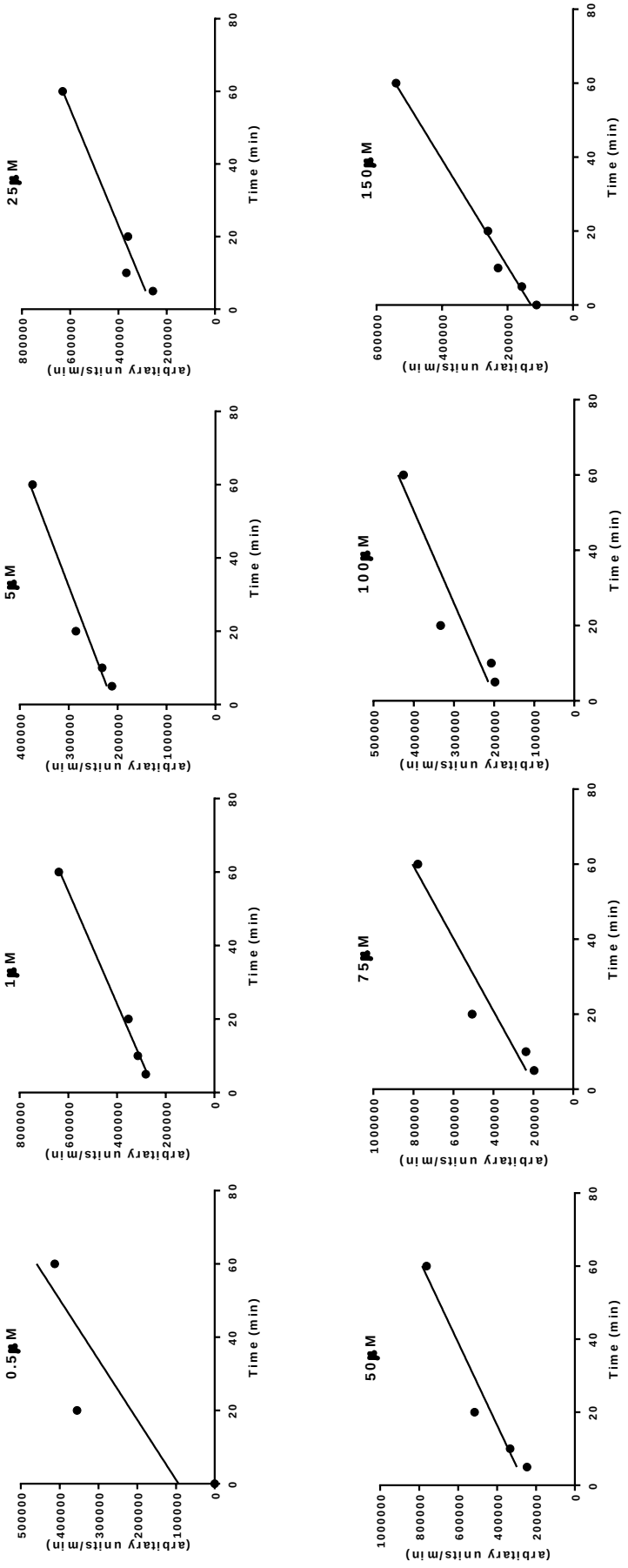


Figure 6.2.10: Flunixin metabolite appearance in microsomes at various flunixin concentrations (refer to A.IV.1.3, horse 1).

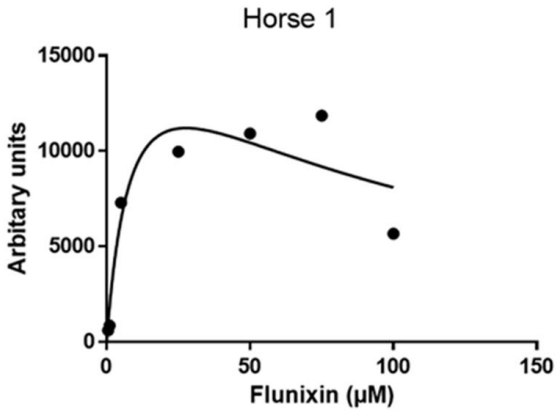


Figure 6.2.11: Michaelis-Menten plot demonstrating flunixin metabolite appearance in microsomes.

6.2.1.7 *In vitro* comparison of Cl_{int}

The Cl_{int} units were standardised using the CYP content in microsomes or hepatocytes for each horse (Table A.IV.1.5). No correction was made for bound drug, assuming that most of the drug was unbound (Table 6.2.4).

Table 6.2.4: Cl_{int} unit standardisation for fresh, cryopreserved hepatocytes and equine liver microsomes

	Cl_{int}[1]	Corrected Cl_{int} (µL/min/nmol P450)
Fresh		
Horse 1	42.7	305.0
Horse 2	23.8	193.5
Horse 3	41.2	352.1
Cryopreserved		
Horse 1	44.0	315.0
Horse 2	37.0	301.0
Horse 3	23.3	199.1
Microsomes		
Horse 1	13.0	32.6
Horse 2	12.0	20.2
Horse 3	17.5	31.4

[1]Units are µL/min/million cells for hepatocytes and µL/min/mg protein for microsomes.

6.2.1.8 *In vitro in vivo* extrapolation

The in vitro Cl_{int} is scaled to the liver Cl_{int} and then to the Cl_H using methodology outlined in section 2.4.9 of this thesis, using the plasma unbound fraction of the drug (0.01) and the hepatic flow, Q_h= 23.8 ml/min (Tables A.IV.1.6 and 7. Plasma unbound fraction of the drug and the hepatic flow values were from studies completed by (Soma et al. 1988) and (Dyke et al. 1998), respectively. The results are summarised in (Table 6.2.5)

There was no significant difference between fresh and cryopreserved hepatocytes, whereas there was a significant difference between, both, freshly isolated and cryopreserved hepatocytes and microsomes (Figure 5.2.12).

Table 6.2.5: Hepatic clearance in microsomes, fresh and cryopreserved hepatocytes following scaling to liver Cl_{int} and Cl_H using both models

	[1]Cl_{int}	Liver Cl_{int} (mL/min /liver)	[2]Well-stirred model	[2]Parallel tube model
Fresh				
Horse 1	42.7	120.5	1.15	1.18
Horse 2	23.7	107.1	1.02	1.10
Horse 3	41.2	153.0	1.43	1.48
Cryopreserved				
Horse 1	44.0	124.2	1.18	1.21
Horse 2	37.0	167.2	1.56	1.61
Horse 3	23.3	79.4	0.83	0.85
Microsomes				
Horse 1	13	12.2	0.12	0.12
Horse 2	12	11.2	0.11	0.11
Horse 3	17.5	13.7	0.14	0.14

[1]Units are µL/min/million cells for hepatocytes and µL/min/mg protein for microsomes
[2]Units are ml/min/kg

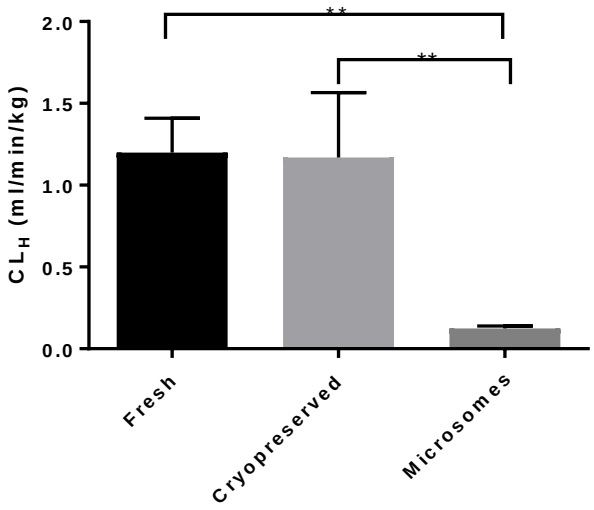


Figure 6.2.12: Hepatic clearances (well stirred model) of flunixin in microsomes, fresh and cryopreserved equine hepatocytes. Significant difference between three systems was tested using one-way ANOVA with Tukey's test. **= $p < 0.05$.

The *in vitro* Cl_H obtained from both models were displayed with the *in vivo* clearance from an equine intravenous study to enable comparison (Table 6.2.6).

Table 6.2.6: Blood and plasma hepatic clearance for *in vitro* and *in vivo* studies

	[1]Well-stirred	[1]Parallel tube
Fresh	1.20 (1.02-1.43)	1.23 (1.10-1.48)
Cryopreserved	1.19 (0.83-1.56)	1.22 (0.85-1.61)
Microsomes	0.12 (0.11-0.14)	0.12 (0.11-0.14)
***In vivo* clearance**	***0.95 (0.52-1.53)**	

Data are expressed as the average, followed by the range (n=3)

[1]Units are ml/min/kg

*(Soma et al. 1988; Lee and Maxwell 2014; Knych et al. 2015)

6.2.2 Phenylbutazone

6.2.2.1 LCMS analysis of phenylbutazone

An authentic standard confirmed phenylbutazone's RT at 2.11 minutes, using the developed HPLC-MS method (Figure 6.2.13).

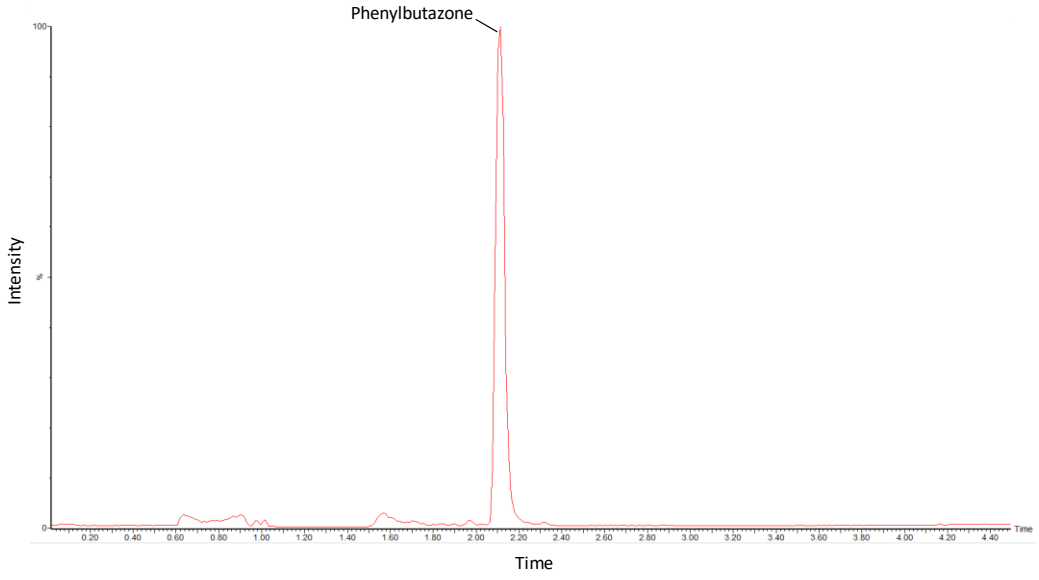


Figure 6.2.13: Chromatogram for monitoring phenylbutazone disappearance. The ion of mass 209.19 was monitored at a retention time of 2.11 minutes.

6.2.2.2 Linearity of initial reaction rate with respect to number of cells or mg microsomal protein

Phenylbutazone Cl_{int} values were determined by measuring their depletion over time at varying cell and microsomal protein concentrations. At all cell concentrations, its depletion over time was linear (Figure 6.2.14A). However, at higher microsomal protein concentrations (5, 10 mg/ml) the substrate depletion was not linear (Figure 6.2.14C).

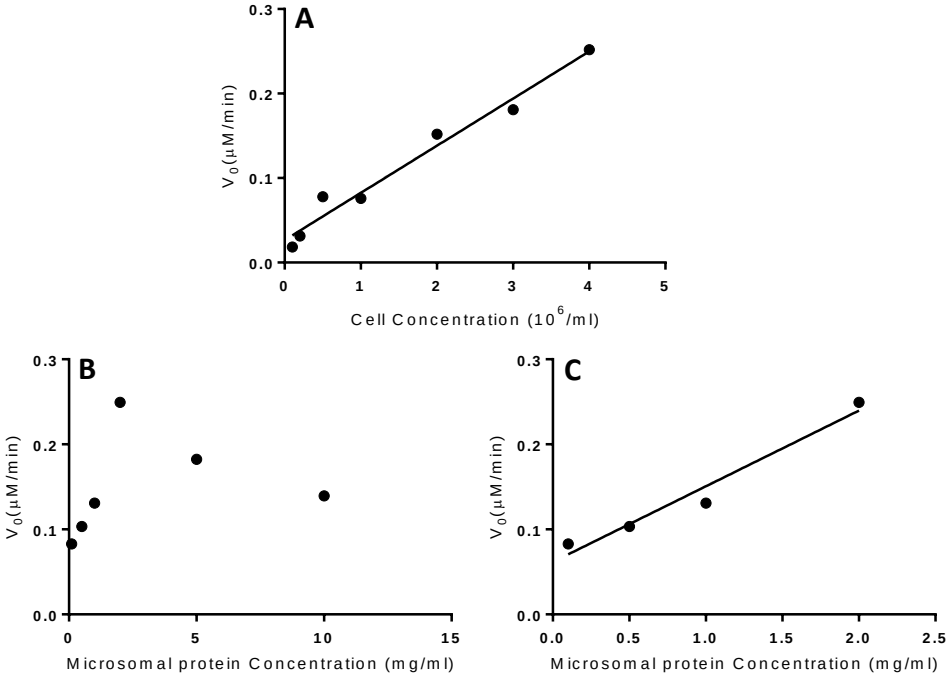


Figure 6.2.14 Linearity of initial reaction rate with respect to number of hepatocytes in 1 ml incubation (A). Linearity of initial reaction rate with respect to microsomal protein concentration in 1 ml incubation (B and C).

6.2.2.3 Phenylbutazone metabolism in freshly isolated equine hepatocytes

Metabolism of phenylbutazone was observed with freshly isolated equine hepatocytes. Drug disappearance was plotted against time for each concentration in a linear semi-logarithmic graph to determine the K_{dep} (Figure 6.2.15). However, with increasing substrate concentration, the initial rate firstly increased followed by a decline, therefore the data was fitted to a substrate inhibition curve as in (equation 1.51) in (section 1.8.1.4) (Figure

6.2.16). Hence, the K_m and V_{max} values could not be determined with any certainty and therefore the initial slope of the Michaelis-Menten curve was used to estimate the CL_{int} values (Table 6.2.7.).

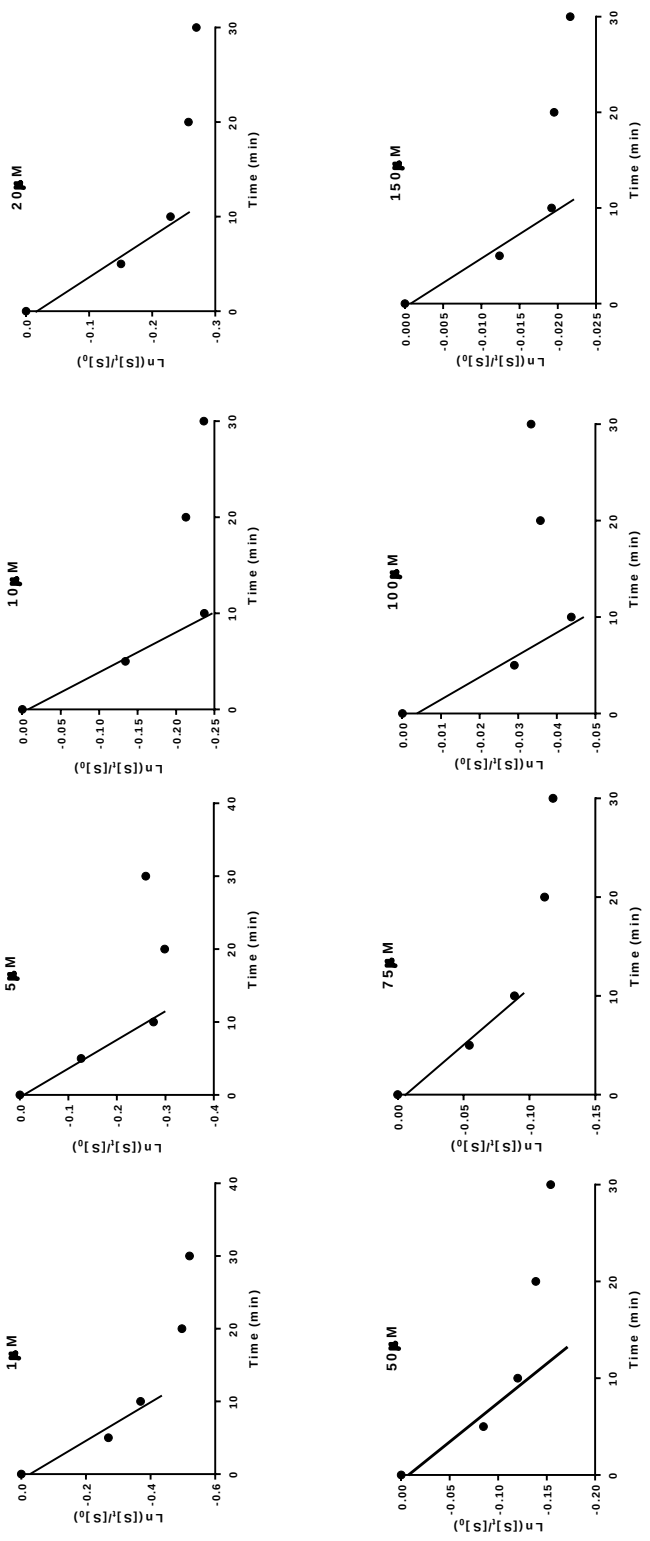


Figure 6.2.15: Metabolism of phenylbutazone by freshly isolated hepatocytes. Data was plotted as the natural logarithm (Ln) of substrate concentration against time. Only time points fall within the linear time period of the reaction and allow the assumption of initial rate conditions were chosen. K_{dep} is represented by the slope of the line (refer to A.IV.2.3, horse 1).

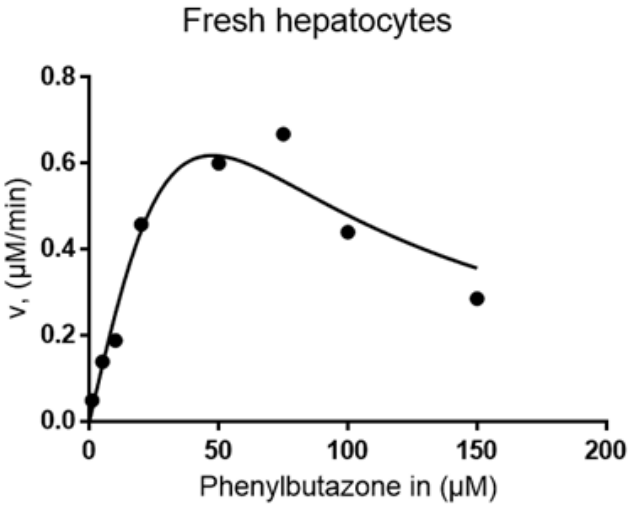


Figure 6.2.16: Michaelis-Menten plot demonstrating phenylbutazone metabolism by fresh hepatocytes

Table 6.2.7: Cl_{int} obtained from freshly isolated hepatocyte incubations at 1 million cells/mL

	Horse 1	**Horse 2**	**Horse 3**
Cl_{int} (µL/min/million cells)	26.0	11.8	28.0

6.2.2.4 Cryopreserved hepatocytes

Metabolism of phenylbutazone was observed with cryopreserved equine hepatocytes. Drug disappearance was plotted against time for each concentration in a linear semi-logarithmic graph to determine the K_{dep} (Figure 6.2.17). However, with increasing substrate concentration, the initial rate firstly increased followed by a decline, therefore the data was fitted to a substrate inhibition curve as in (equation 1.51) in (section 1.8.1.4) (Figure 6.2.18). Hence, the K_m and V_{max} values could not be determined with any certainty and therefore the initial slope of the Michaelis-Menten curve was used to estimate the CL_{int} values (Table 6.2.8).

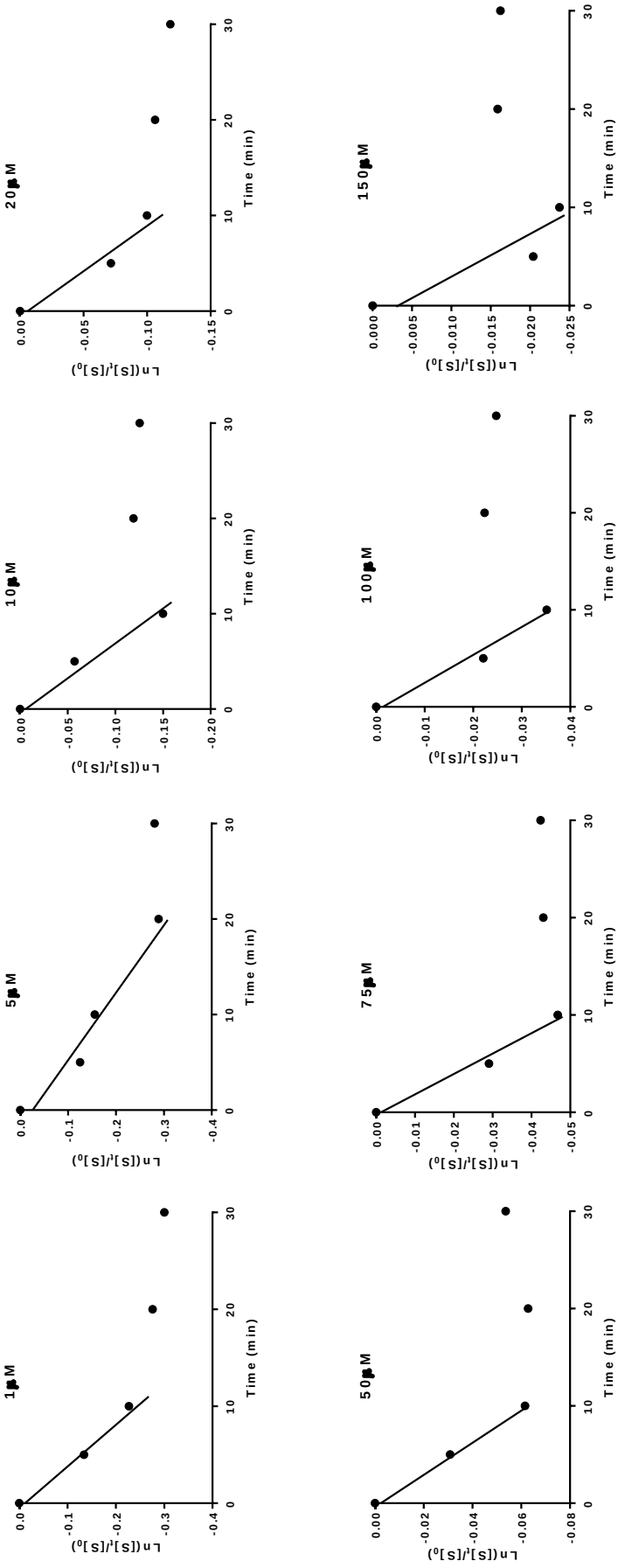


Figure 6.2.17: Metabolism of phenylbutazone by cryopreserved hepatocytes. Data was plotted as the natural logarithm (Ln) of substrate concentration against time. Only time points fall within the linear time period of the reaction and allow the assumption of initial rate conditions were chosen. K_{dep} is represented by the slope of the line (refer to Table. A.IV.2.3, horse 1).

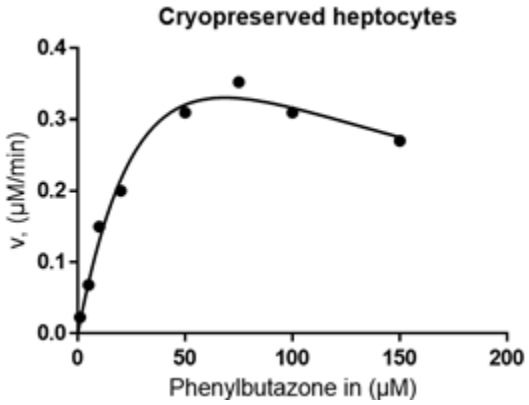


Figure 6.2.18: Michaelis-Menten plot demonstrating phenylbutazone metabolism by cryopreserved hepatocytes.

Table 6.2.8: Cl_{int} obtained from cryopreserved hepatocyte incubations at 1 million cells/mL

	Horse 1	**Horse 2**	**Horse 3**
Cl_{int} (µL/min/million cells)	15.5	11.6	20.8

6.2.2.5 Equine liver microsomes

Metabolism of phenylbutazone was observed with equine liver microsomes. Drug disappearance was plotted against time for each concentration in a linear semi-logarithmic graph to determine the K_{dep} (Figure 6.2.19). However, with increasing substrate concentration, the initial rate firstly increased followed by a decline, therefore the data was fitted to a substrate inhibition curve as in equation 1.51 in (section 1.8.1.4) (Figure 6.2.20). Hence, the K_m and V_{max} values could not be determined with any certainty and therefore the initial slope of the Michaelis-Menten curve was used to estimate the CL_{int} values (Table 6.2.9).

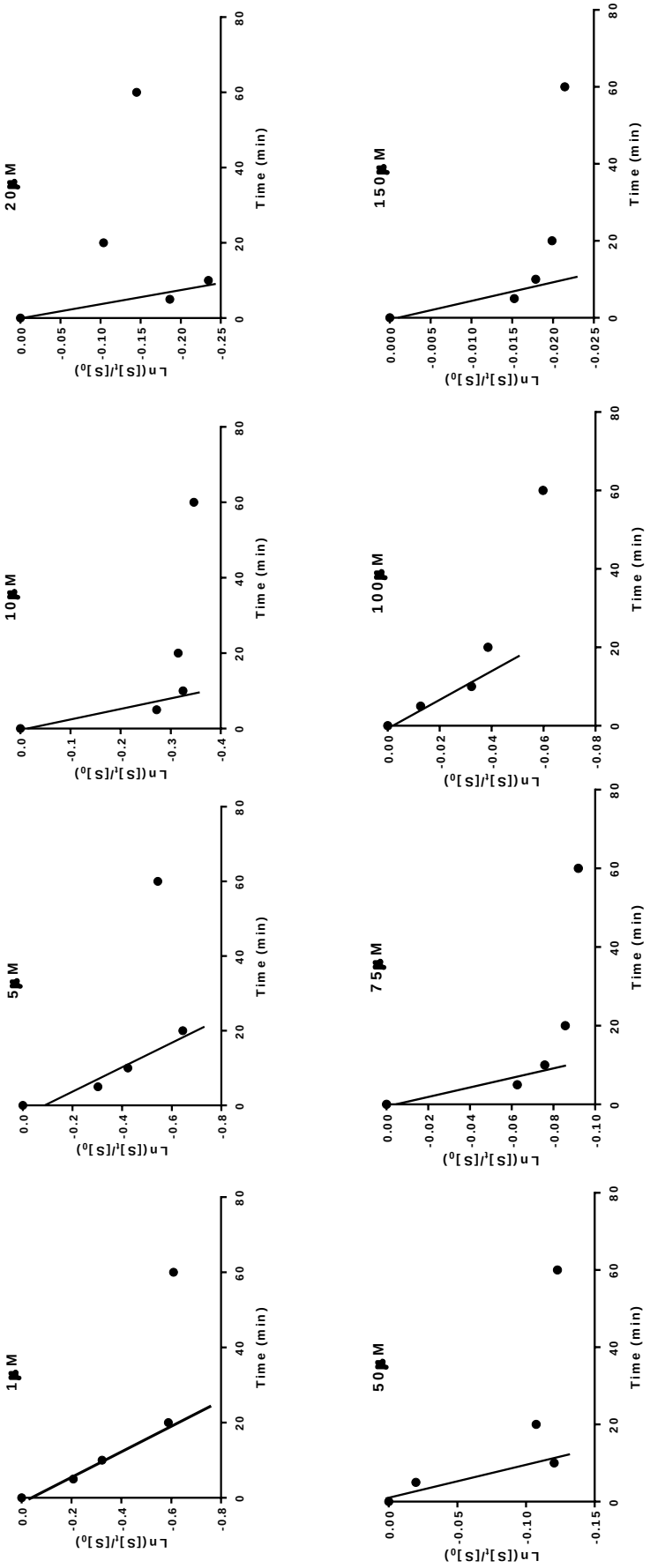


Figure 6.2.19: Metabolism of phenylbutazone by equine liver microsomes. Data was plotted as the natural logarithm (Ln) of substrate concentration against time. Only time points fall within the linear time period of the reaction and allow the assumption of initial rate conditions were chosen. K_{dep} is represented by the slope of the line (refer to table A.IV.2.3, horse 1).

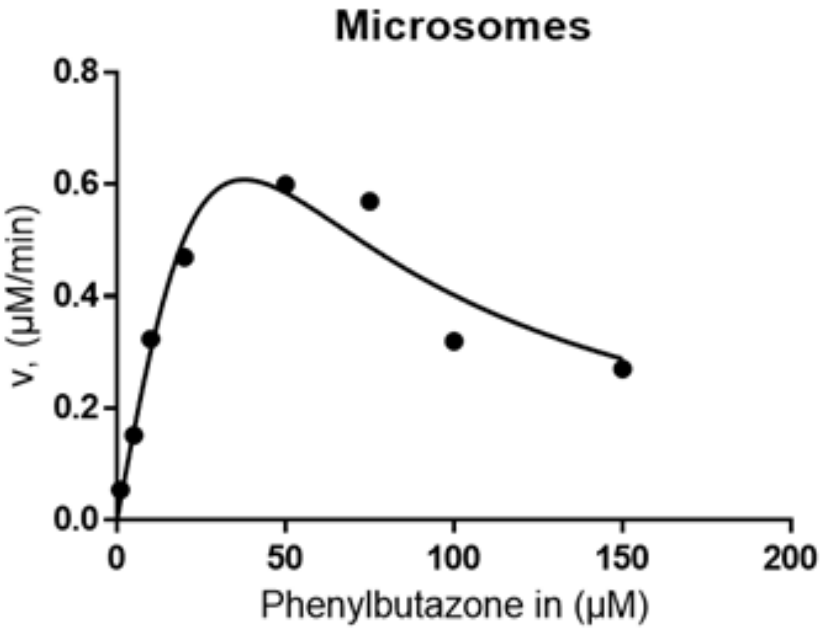


Figure 6.2.20: Michaelis-Menten plot demonstrating phenylbutazone metabolism by equine liver microsomes.

Table 6.2.9: Cl_{int} obtained from equine liver microsome incubations at 1 mg protein/mL

	Horse 1	**Horse 2**	**Horse 3**
Cl_{int} (µL/min/mg protein)	32.2	18.2	24.8

6.2.2.6 Metabolite appearance

The appearance of the metabolite, oxyphenbutazone, was monitored in freshly isolated, cryopreserved equine hepatocytes (section 3.3.1) and in microsomes as well (Figure 6.2.21). Oxyphenbutazone concentration was determined using a stock solution of oxyphenbutazone of known concentration to convert mass spectrometry response into µM.

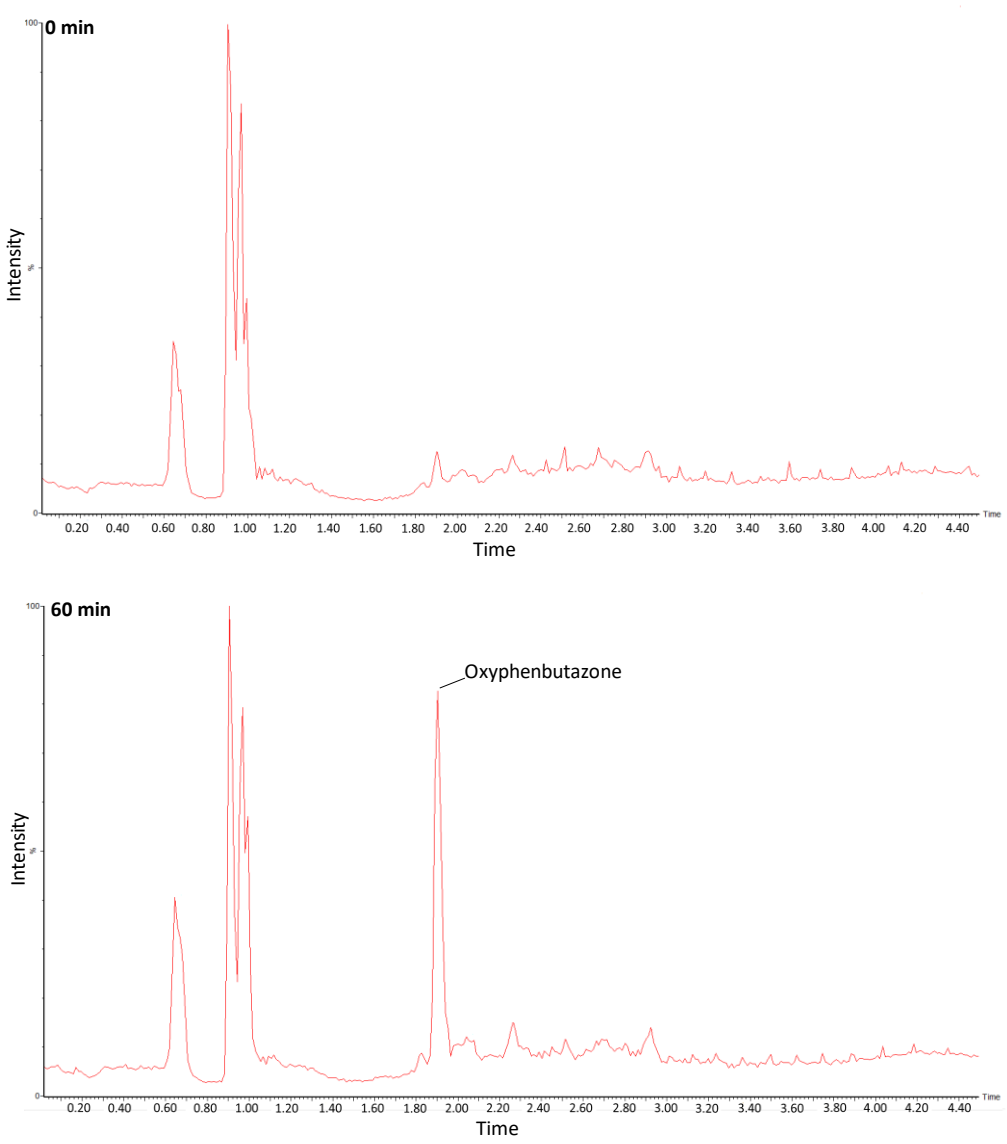


Figure 6.2.21: Graphs derived from phenylbutazone metabolite appearance in equine liver microsomes at 50 µM.

A. Equine hepatocytes

At concentrations 1 and 5 µM no detectable metabolite was produced in both, freshly isolated and cryopreserved equine hepatocytes however, from 10-150 µM significant oxyphenbutazone production was detected (Figures 6.2.22 and 23). Oxyphenbutazone formation by equine hepatocytes followed Michaelis-Menten kinetics with substrate inhibition kinetics. However, the Cl_{int} could not be determined due to lack of data for lower concentrations.

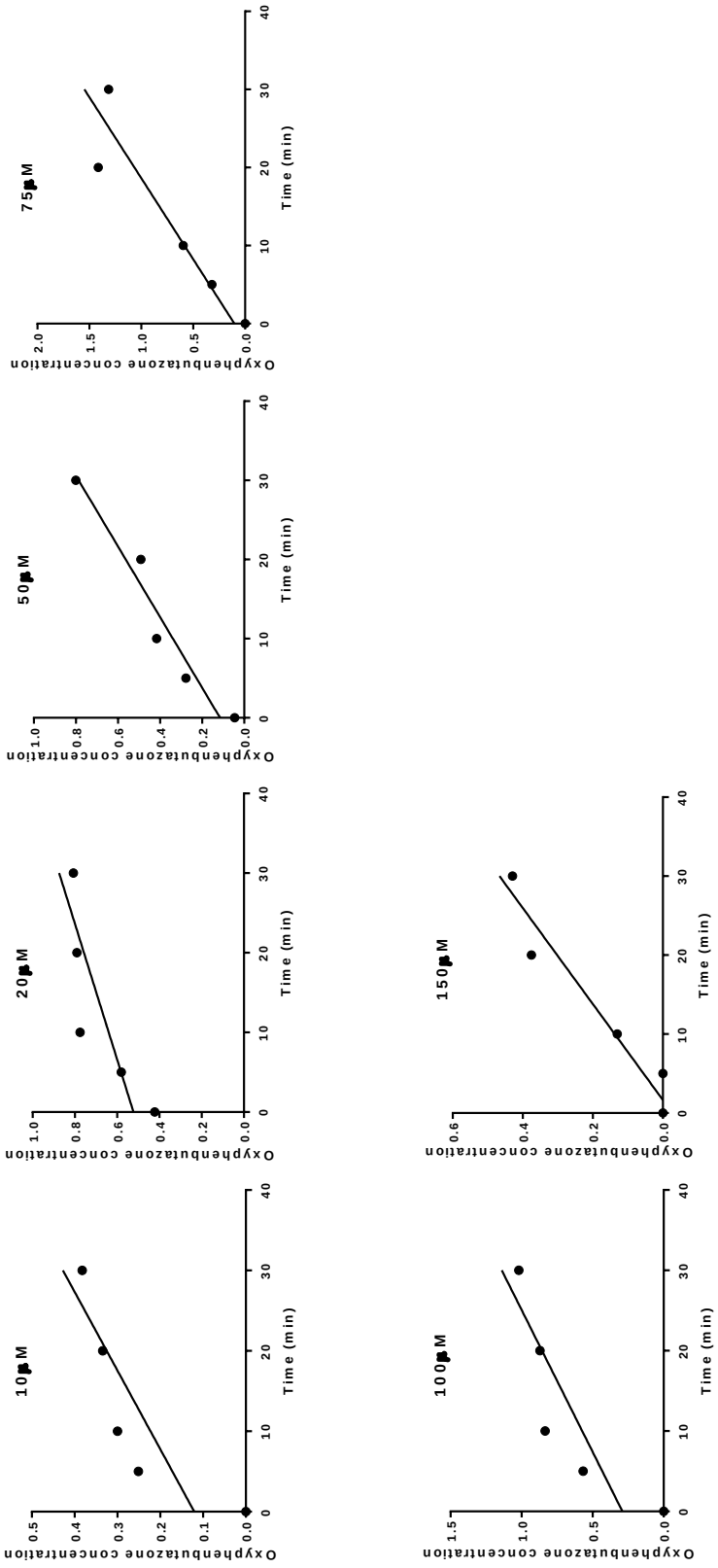


Figure 6.2.22: Data for oxyphenbutazone production with freshly isolated hepatocytes. Concentration was determined using a stock of oxyphenbutazone of known concentration to convert mass spectrometry response into µM. Data was plotted as the concentration (in µM) against time (refer to table A.IV.2.4).

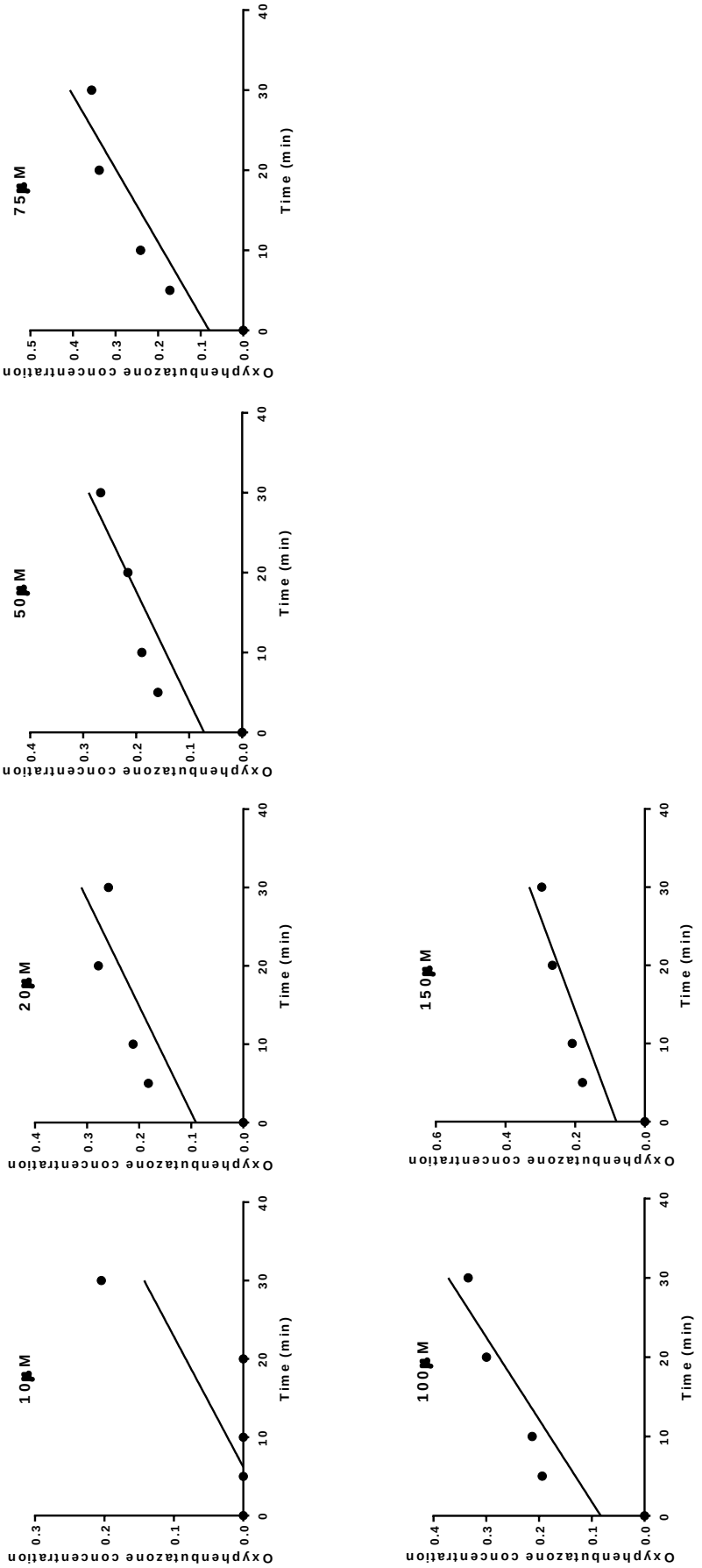


Figure 6.2.23: Data for oxyphenbutazone production with cryopreserved equine hepatocytes. Data was plotted as the concentration (in µM) against time. Concentration was determined using a stock of oxyphenbutazone of known concentration to convert mass spectrometry response into uM (refer to table A.IV.2.4)

B. Equine liver microsomes

A significant oxyphenbutazone production was detected across all concentrations in microsomes in horse 1 and 2 (Figure 6.2.24) and (table A.IV.2.4). Oxyphenbutazone formation by equine liver microsomes followed Michaelis-Menten kinetics with substrate inhibition kinetics. Therefore, the Cl_{int} was determined by fitting the initial rate of oxyphenbutazone formation with phenylbutazone concentrations to a substrate inhibition model (equation 1.51) in (section 1.8.1.4) (Figure 6.2.25). The determined Cl_{int} values are summarised in (Table 6.2.10).

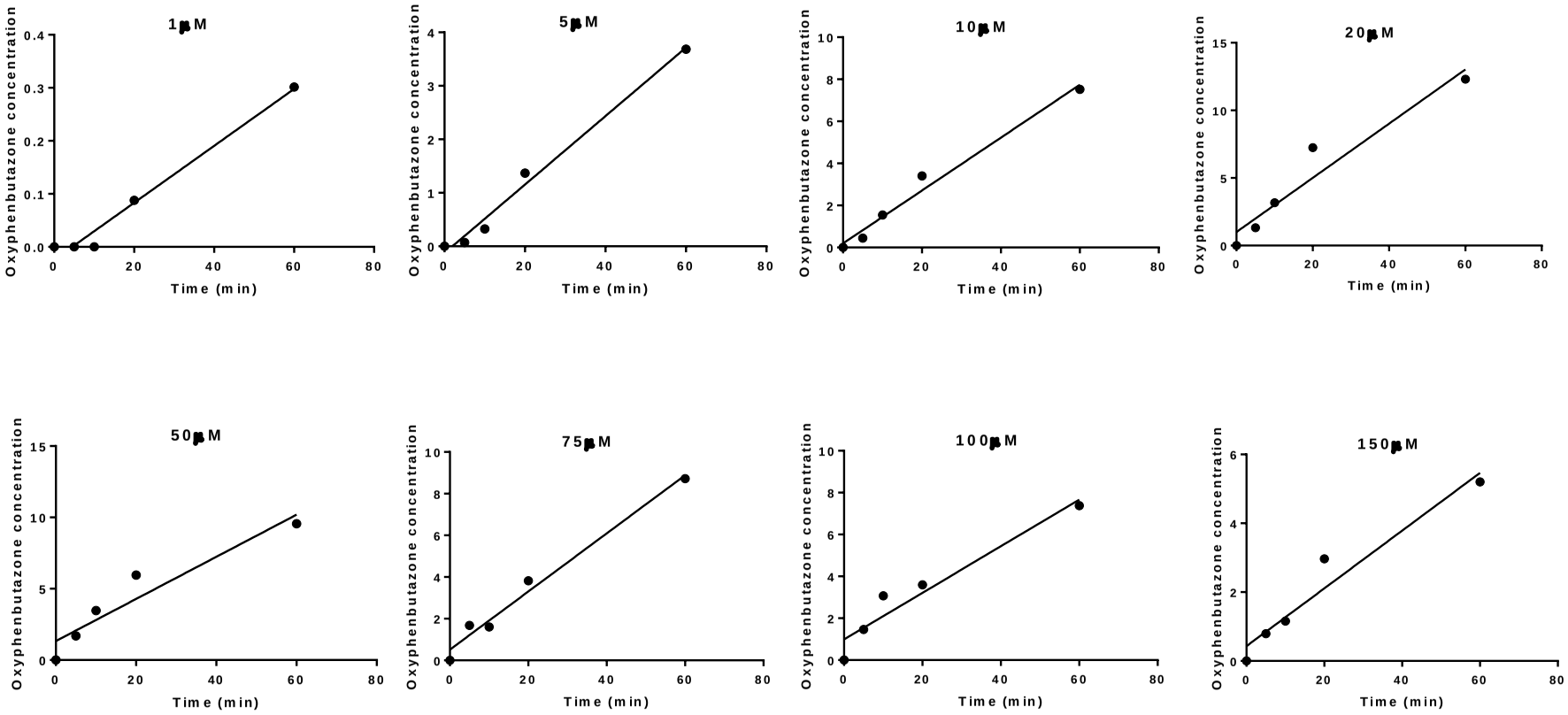


Figure 6.2.24: Data for oxyphenbutazone production with equine liver microsomes. Concentration was determined using a stock of oxyphenbutazone of known concentration to convert mass spectrometry response into μM. Data was plotted as the concentration (in μM) against time (refer to table A.IV.2.4, horse 1).

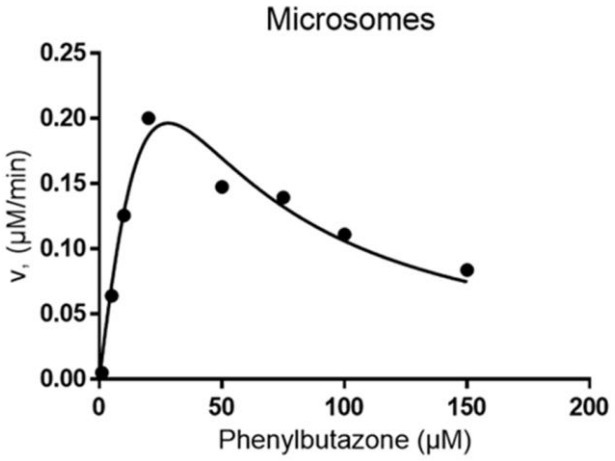


Figure 6.2.25: Velocity obtained from oxyphenbutazone formation by equine liver microsomes as a function of phenylbutazone concentration, fit to a substrate inhibition model.

Table 6.2.10*:* Oxyphenbutazone formation Cl_{int} in liver microsome incubations at 1 mg protein/ml

	Horse 1	**Horse 2**	**Horse 3**
Cl_{int} (µL/min/mg of protein)	15.2	10.4	-

6.2.2.7 *In vitro* comparison of Cl_{int}

i. Drug disappearance

The Cl_{int} units were standardised using the CYP content in microsomes or hepatocytes for each horse (Table A.IV.2.5). No correction was made for bound drug (Table 6.2.11).

Table 6.2.11: Cl_{int} unit standardisation for equine microsomes, fresh and cryopreserved hepatocytes

	Cl_{int}[1]	**Corrected Cl_{int} (µL/min/nmol P450)**
Fresh		
Horse 1	26	211.4
Horse 2	11.8	100.8
Horse 3	28.0	222.2
Cryopreserved		
Horse 1	15.5	126.0
Horse 2	11.6	99.1
Horse 3	20.8	165.1
Microsomes		
Horse 1	32.2	54.2
Horse 2	18.2	32.7
Horse 3	24.8	59.6

[1]Units are µL/min/million cells for hepatocytes and µL/min/mg protein for microsomes.

ii. Metabolite appearance

The Cl_{int} units were standardised using the CYP content in microsomes or hepatocytes for each horse (Table 6.2.12). No correction was made for bound drug.

Table 6.2.12: Cl_{int} unit standardisation for equine microsomes

	Cl_{int}[1]	Corrected Cl_{int} (µL/min/nmol P450)
Horse 1	26	25.6
Horse 2	11.8	18.7
Horse 3	-	-

[1]Unit is µL/min/mg protein.

6.2.2.8 *In vitro in vivo* extrapolation

i. Drug disappearance

The *in vitro* Cl_{int} is scaled to the liver Cl_{int} and then to the Cl_H using methodology outlined in section 1.7 of this thesis, using the plasma unbound fraction of the drug (0.01) and the hepatic flow, Q_h= 23.8 ml/min (Tables A.IV.2.6 and 7). Plasma unbound and hepatic flow values were from studies completed by Tobin et al. (1986) and Dyke et al. (1998), respectively. The results are summarised in (Table 6.2.13). There was no significant difference between fresh and cryopreserved hepatocytes, whereas there was a significant difference between freshly isolated equine hepatocytes and microsomes (Figure 5.2.26).

Table 6.2.13: Hepatic clearance in microsomes, fresh and cryopreserved hepatocytes following scaling to liver Cl_{int} and Cl_H

	Cl_{int}[1]	Liver Cl_{int} (ml/min/liver)	[2]Well-stirred model	[2]Parallel tube model
Fresh				
Horse 1	26	117.46	1.12	1.15
Horse 2	11.8	43.81	0.43	0.43
Horse 3	28	80.93	0.78	0.80
Cryopreserved				
Horse 1	15.5	70.03	0.68	0.69
Horse 2	11.6	43.07	0.42	0.43
Horse 3	20.8	60.12	0.59	0.59
Microsomes				
Horse 1	32.2	30.14	0.30	0.30
Horse 2	18.2	15.56	0.14	0.14
Horse 3	24.8	21.20	0.22	0.22

[1]Units are µl/min/million cells for hepatocytes and µl/min/mg protein for microsomes
[2]Units are ml/min/kg

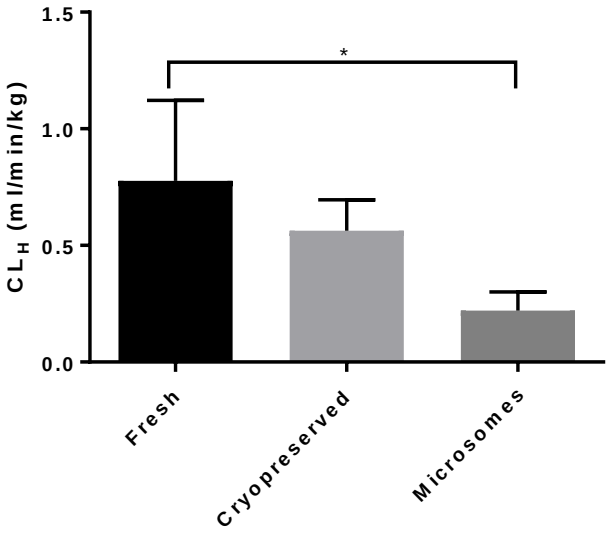


Figure 6.2.26: Hepatic clearances (well stirred model) of phenylbutazone in microsomes, fresh and cryopreserved equine hepatocytes. Significant difference between three systems was tested using one-way ANOVA with Tukey's multiple comparisons test. *= $p < 0.05$.

ii. Metabolite formation

Results for metabolite formation are summarised in (Table 6.2.14).

Table 6.2.14: Enzyme kinetics in microsomes following scaling to liver Cl_{int} and CL_H

	Cl_{int1}	Liver Cl_{int} (mL/min/liver)	[2]Well-stirred model	[2]Parallel tube model
Horse 1	15.2	948.48	0.14	0.14
Horse 2	10.4	542.048	0.08	0.08
Horse 3	-	-	-	-

[1]Unit is µL/min/mg protein
[2]Units are ml/min/kg

The *in vitro* CL_H obtained from both models were displayed with the *in vivo* clearance from an equine intravenous study to enable comparison (Table 6.2.15).

Table 6.2.15: Plasma hepatic clearance for *in vitro* and *in vivo* studies

	[1]Well-stirred	[1]Parallel tube
Fresh	0.78 (0.43-1.12)	0.79 (0.43-1.15)
Cryopreserved	0.56 (0.42-0.68)	0.57 (0.43-0.69)
Microsomes	0.22(0.14-0.30)	0.22 (0.14-0.30)
[√]Microsomes	(0.08-0.14)	(0.08-0.14)
***In vivo* clearance**	**[*]0.42 (0.27-0.70)**	

Data are expressed as the average, followed by the range (n=3)

[1]Units are ml/min/kg

[√]Values predicted from metabolite formation

[*](Jenny et al., 1979; Rose et al., 1982; Maitho et al., 1982; Toutain and Bousquet-Melou 2004; Knych et al., 2016).

6.3 Discussion

The major objective of this research was to investigate the ability of the three-*in vitro* systems i.e. freshly isolated, cryopreserved hepatocytes and equine liver microsomes to determine the *in vitro* Cl_{int} and Cl_H. For this purpose, drug disappearance method was used to determine in vitro Cl_{int} of flunixin and phenylbutazone.

The *in vitro* determination of Cl_{int} values for these compounds in freshly isolated and cryopreserved hepatocytes is not evident in the literature. Whereas, only one study has been carried out to determine the *in vitro* Cl_{int} for flunixin and phenylbutazone in equine microsomes (Orr, 2015). As flunixin is a veterinary-only medication, it is not permitted for use in humans and therefore data relating to its metabolism by human enzyme systems is unavailable.

For flunixin, a one-way ANOVA test showed a significant difference between the average Cl_{int} values determined using microsomes, fresh and cryopreserved hepatocytes test ($p=0.0033$). The microsome Cl_{int} (µl/min/nmol P450) was 17-fold lower than the hepatocyte Cl_{int}. Predicting the *in vivo* clearance of a drug using microsomes requires the assumption that the major metabolic route is via NADPH enzymes (Naritomi et al. 2001). Despite the fact that, microsomes contain several enzymes which use

different cofactors that contribute to metabolism, but phase I metabolism only consider the SER enzymes which rely on NADPH as a cofactor. Thus, microsomes may under predict $Cl_{int,}$ to a greater extent, than hepatocytes.

It is known that horses eliminate flunixin by two pathways. The first one being direct conjugation of flunixin with glucuronic acid (Johansson and Anlér 1988; Soma et al., 1988). The second pathway of elimination is by oxidising flunixin with subsequent elimination. The first pathway seems to be the major one because the relative concentration of free flunixin tends to be greater than that of flunixin metabolite in hydrolysed urine samples (Johansson and Anlér 1988). Furthermore, substrate auto inhibition was noted in the microsomal system. This observation was in agreement with results reported by Orr. (2015).

Only one oxidised metabolite was detected in microsomes using HPLC-MS with an *m/z* of 313, sixteen more than flunixin. A RT of 4.57 minutes was determined for this metabolite. This suggests that it is more polar than flunixin. A previous study determined same RT order of 5-hydroxyflunixin and flunixin in bovine plasma (Jedziniak et al., 2007). Hence, it is a reasonable assumption that the metabolite detected in equine microsomes is 5-hydroxyflunixin. Flunixin metabolism in human is unknown, since this drug is not used in human, however, flunixin metabolism in the horse appears to be very similar to that of niflumic acid in humans and dogs (Jaussaud et al., 1987). In these species, the major metabolites in urine and faeces were isolated and identified as niflumic acid glucuronide, 4'-hydroxyniflumic acid, 5-hydroxyniflumic acid and the glucuronide and sulphate conjugates of 4'-hydroxyniflumic acid and 5-hydroxyniflumic acid (Lan et al., 1973).

Substrate auto inhibition was noted in the microsomal system; hence the K_m could not be determined using either drug disappearance or metabolite formation. Cl_{int} could not be determined using metabolite formation, due to

the lack of an authentic standard for the metabolite and therefore concentrations were not quantified.

For phenylbutazone, one-way ANOVA test showed a significant difference between the average Cl_{int} values determined using microsomes compared to fresh hepatocytes ($p=0.03$). The microsome Cl_{int} (µl/min/nmol P450) was almost 6-fold lower than the hepatocyte Cl_{int}. Despite the fact that no glucuronide metabolites have been reported in the horse (Tobin et al. 1986), one study has found that 4-OH-phenylbutazone, is produced via the cyclo-oxygenase system, and either this metabolite or its glucuronide is therefore the potential metabolite in the horse (Reed et al., 1985). This metabolite has been reported in human (Dieterle et al., 1976).

Substrate auto inhibition (See section 1.8.1.4) was noted in the three systems. This may confirm that phenylbutazone is mainly metabolised by phase I metabolic enzymes. However, further studies are needed to explore all metabolism path ways for this drug.

One oxidised metabolite was detected using HPLC-MS with an m/z of 225.25, sixteen more than phenylbutazone. A RT of 1.9 min was determined for this metabolite. This metabolite was identified as oxyphenbutazone (chapter 3). There was no significant difference between Cl_{int} values determined from the metabolite formation method and those determined from drug disappearance using microsomes.

Equine microsomes underpredicted the *in vivo* plasma clearance of flunixin and phenylbutazone by 5 and 2-fold, respectively. This result is consistent with the previous study for omeprazole (chapter 5). However, IVIVE of microsomal Cl_H for phenylbutazone disappearance was just under the lower range of *in vivo* clearance of 0.27 ml/min/kg. Whereas, microsomal Cl_H for oxyphenbutazone formation was poorly predicted. This could imply that another metabolite (γ-hydroxy phenylbutazone) needs to be monitored to avoid underprediction of Cl_{int} using metabolite formation.

Chapter 7

General Discussion

7 General discussion

As the majority of metabolism occurs in the liver, *in vitro* liver systems such as liver slices, isolated hepatocytes and liver microsomes can be used to study the enzyme kinetics of drug metabolism. The current study aims to develop an *in vitro* approach that mimics the *in vivo* situation for understanding drug metabolism within the horse. Hence, the *in vitro* system which has been used in the present study incorporates isolated equine hepatocytes and liver microsomes.

The research contained in the present thesis has used isolated equine hepatocytes with yield and viability comparable to that reported in the literature for other species (Bakala et al., 2003; Stefanski et al., 2013). However, the number of hepatocytes isolated per gram of perfused tissue was five-fold higher than that reported by Stefanski et al. (2013) but five-fold lower than in the study by Bakala et al. (2003). Although protocols were similar, Bakala et al. (2003) used a University of Wisconsin proprietary solution for transportation, which may have superior organ preservation capacities, enabling a larger viable cell yield to be obtained.

As reported in the literature that applications of freshly isolated hepatocytes have limitations, including: 1) they are not readily available from humans as well as other species; 2) it is difficult to repeat studies or compare studies between laboratories using the same batch (Zhang et al., 2012). Therefore, the current research sought to successfully cryopreserve equine hepatocytes. The cryopreservation of equine hepatocytes is not evident in the literature; however, the cryopreservation method used in the present study was consistently able to have a yield and viability comparable with other species such as human and rats (Sosef et al., 2005; Terry et al., 2010).

Furthermore, the effect of cryopreservation on xenobiotic metabolising enzymes was investigated. Three drugs used frequently in equine medicine,

omeprazole, flunixin and phenylbutazone were used to characterise the activity of freshly isolated and cryopreserved equine hepatocytes. Thawing and incubation protocols were optimised with the goal of creating a standard operating procedure that would produce accurate and reproducible results. A 30% Percoll concentration was used for kinetic studies since it gave a higher post-thaw viability with an acceptable recovery.

No significant difference was reported ($p>0.05$) in intrinsic clearance between fresh and cryopreserved hepatocytes for the three drugs. Moreover, three oxidation metabolites (MH+16/Z) were generated for omeprazole and one metabolite for phenylbutazone in both fresh and cryopreserved equine hepatocytes. However, the intensity, after normalizing for internal standard, was 50% lower for the latter which may suggest some degradation in the metabolising enzymes. The degradation in metabolising enzymes has been reported in the literature (Li et al., 1999; Steinberg et al., 1999; Griffin and Houston 2004). Further studies are required using specific substrates for different enzyme systems.

On the other hand, no significant oxidation metabolites were observed for flunixin in both *in vitro* systems. It is known that horses eliminate flunixin by at least two pathways. The first one being direct conjugation of flunixin with glucuronic acid (Johansson and Anlér 1988; Soma et al., 1988). The second pathway of elimination is by oxidising flunixin with subsequent elimination. However, as discussed earlier in the present thesis (Chapter 6), the first pathway seems to be the main metabolic pathway for flunixin elimination (Johansson and Anlér 1988). Interestingly, an oxidised metabolite was detected in microsomes for flunixin using HPLC-MS with an *m/z* of 313, sixteen more than flunixin (see chapter 6). However, microsome incubations only consider the SER enzymes which rely on NADPH as a cofactor whereas hepatocytes possess more sophisticated enzyme and transporter activities. An attempt was made to study the glucuronidation of

flunixin *in vitro* using equine liver microsomes; however, no metabolism was observed at any significant level. (Natalie Pickwell, PhD Thesis, 2017).

On the other hand, in the present study, no metabolites with MH+176/Z (addition of glucuronic acid) were detected in either hepatocyte system for flunixin. A common metabolite for drugs containing carboxylic acid functionalities is the 1 *β*-*O*-acyl glucuronide (AG); they are unstable compounds at physiological pH and can undergo acyl migration and hydrolysis reactions as well as reacting with endogenous molecules such as proteins via trans acylation and glycation reactions (Potter et al., 2011). Therefore, one possible explanation for not observing a glucuronide metabolite for flunixin, using the hepatocyte systems, may be due to rapid hydrolysis of the glucuronide.

The three drugs have been extensively studied *in vivo* in horses and their metabolites have been detected both in plasma and urine; however, this the first time they have been detected from cryopreserved equine hepatocytes.

The kinetic parameters for the three drugs were determined using freshly isolated, cryopreserved equine hepatocytes and liver microsomes; these kinetic parameters were used to make predictions of *in vivo* clearance. However, knowledge of physiological parameters such as microsomal protein content, hepatocellularity, liver weight, are needed to make these kinds of predictions. The scaling factors for horses are not evident in the literature; thus, microsomal protein per gram of liver (MPPGL) and hepatocellularity (HPGL) were determined in the present study. The microsomal protein value obtained from the horse is similar to values obtained for dog and rat; however, it is higher than that obtained for human (Hakooz et al., 2006; Smith et al., 2008). Whereas, the hepatocellularity number obtained for the horse is higher than other species. Moreover, the micrometric measurements reported in the herein thesis show that the diameter of horse hepatocytes (14.6±4.8 µm) being smaller than the diameter of hepatocytes

from other species; 19.2±0.6 µm in rat, 18.4±0.8 µm in pigs, and between 20-30 µm in human (Engelmann et al., 1981; Stegemann et al., 2000; Boyer et al., 2017). Hence, it is suggested that the higher hepatocellularity number observed for horse liver is due to smaller horse hepatocytes.

On the other hand, the micrometric measurements of hepatocytes in histological specimens revealed that very young and aged horses possess lesser and larger hepatocytes than middle age horses. Moreover, there is an inverse relationship between size and number of hepatocyte in a unit area. These findings are in agreement with those reported in the literature for other species; Tauchi (1961) reported that the number of cells in human and rat liver samples decreased to a certain degree with advanced age while hepatocyte size increased. Furthermore, the fall in hepatocyte number with advancing age has been observed in human liver (Wakabayashi et al., 2002).

This increase in hepatocyte size in young subjects may be due to the fast growth demands in this period of age which allows the liver to adapt with a high-energy demand (De la Iglesia et al., 1976). On the other hand, the increase in hepatocyte size in aged subjects may be due to nuclear polyploidisation rather than compensatory hypertrophy (Tauch and Sato 1962; Watanabe and Tanaka 1982).

While it has been shown that there is a statistically significant inverse relationship between age and CYP P450 content/mg microsomes in female horses (Nebbia et al., 2004), the present study found that age has no effect on CYP P450 content/mg microsomes. However, the effect of sex could not be studied in the present study due to lack of information regarding the corresponding sex of donor horses. However, advances achieved in the molecular genetic field may allow the determination of the donor sex of the cells (McCormack and Bradbury 2014). Hence, further studies may be

performed to determine the sex of the donor horses using cryopreserved hepatocytes.

The results of the present study suggest that the increase of MPPGL was due to the increase in the total number of hepatocytes per gram of liver rather than an increase in the expression of CYP P450 resulting from an increase in smooth endoplasmic reticulum (SER) surface area. This cell-size dependent difference in MPPGL content has been reported in human hepatocytes (de la Iglesia et al. 1976). This has been confirmed in the herein study by the presence of a significant inverse relationship between CYP P450 per 10^6 cells and HPGL which may help horses with low HPGL to maintain their xenobiotic metabolic capacity by having higher levels of CYP P450 per hepatocyte number. This observation has also been reported for human hepatocytes (Wilson et al., 2003).

The Cl_H from the two liver models i.e. well-stirred and parallel tube model, using either freshly isolated, cryopreserved equine hepatocytes or microsomal parameters, were similar, and appears that no one particular model offers any advantages over another. The parallel tube model gave better prediction than the well stirred model for omeprazole, which has a much higher clearance compared to the other drugs. This is in agreement with results from previous studies where the parallel-tube model showed better accuracy than the well-stirred model in predicting *in vivo* intrinsic clearance using isolated hepatocyte suspensions or hepatic microsomes (Ito and Houston 2004; Hallifax et al. 2010; Yin et al., 2013). However, several recent studies have found that hepatocytes specialise as a function based on their position along the porto-central axis of the liver lobule. Consequently, the fate of hepatocytes will be determined as either "periportal" (PP) or "perivenous" (PV) hepatocytes and referred to as Liver zonation (Gebhardt and Matz-soja 2014; Kietzmann 2017). These recent observations are contradicting with the parallel tube model since the latter

is based on the liver being comprised of a series of parallel tubes, each surrounded by hepatocytes of equal drug-metabolizing capacity, through which drug passes at a constant rate. Further studies will be required to study the effect of liver zonation on *in vitro-in vivo* extrapolation using parallel tube model.

On the other hand, the Cl_H predictions obtained, in the present study, from hepatocytes were more accurate than those obtained using microsomes. This is consistent with data reported in the literature (Houston and Carlile 1997; Ito and Houston 2004). This may due to the lack of cellular integrity and certain enzyme and transport activities as a result of "the destructive nature" in the preparation of liver microsomes (Ito and Houston 2004). However, Foster et al., (2011) compared the Cl_{int} (intrinsic clearance) in human liver microsomes and suspended hepatocytes. They reported a four-fold and 1.5 to four-fold underprediction of microsomal Cl_{int} by hepatocytes for high clearance substrates and for the low/medium clearance substrates, respectively. Unlike most of the previous studies, Foster and co-workers used microsomes and hepatocytes from the same donor livers, hence a direct comparison of Cl_{int} between these two systems was made. Further studies using a wide range of substrates are required to investigate the performance of both *in vitro* systems. Moreover, a comparison between the systems i.e. liver microsomes and hepatocytes obtained from both human and horses using drugs frequently used in both species can be made giving more reliable results.

Prediction and extrapolation of pharmacokinetic data between species is a routine practice in the drug discovery process. However comparative studies have shown significant differences in drug metabolism among species including horse (Chauret et al. 1997; Martignoni et al., 2006; Mössner et al., 2011; Zielinski and Mevissen 2015).

Despite the fact that, *in vivo* research does not allow for specific P450 isoforms involved in the metabolism of a drug to be determined, *in vivo* metabolism studies are more frequently used in horses than *in vitro* studies (Scarth et al., 2011).

The herein thesis is the first to optimise conditions for cryopreservation, thawing and enzyme kinetic incubations for equine hepatocytes. In addition to, it has provided an expected range in equine microsomal protein (MPPGL) and hepatocellularity (HPGL) scaling factor values, which was not evident in the literature. Furthermore, the influence of the age was investigated, and the results have demonstrated that, despite MPPGL and HPGL values being dependent on the age of the horse, age of horse has no effect on CYP P450 content per gram of microsomal protein. However, further investigation is needed including the effect of horse gender and breed on MPPGL and HPGL.

The results of *in vitro* kinetic studies for omeprazole show that there is no difference in omeprazole metabolism between human and horse. Moreover, microsomal study described in the present thesis suggests that the oxidative flunixin metabolism in the horse might be similar to that in cattle (Jedziniak et al. 2007). Furthermore, a number of comparative metabolic studies, concluded that oxidative metabolism of flunixin in the horse may be very similar to that of niflumic acid in human and dogs (Lan et al., 1973; Cohen et al., 1974; Jaussaud et al. 1987). However, a recent study found that CYP2B6A subfamily is involved in testosterone metabolism in horse and human but not dog, and sulfaphenazole inhibited metabolism in human more than in horse (Zielinski and Mevissen, 2015). Further studies are required to investigate the species differences in drug metabolism.

Moreover, as mentioned earlier in this thesis, several classes of drugs being used in horses. However, there are a limited information regarding equine metabolism studies available in literature. Most of this published literature obtained from the detection of drug abuse (particularly in horse racing)

(Scarth et al, 2010). According to Scarth et al, (2010), the most important classes of drugs (see introduction section) which that already banned, and/or their use is being regulated in horseracing are regularly monitored. Generally, it was concluded that phase I metabolism pathways in horse are well understood than those of phase II. Moreover, the whole oxidative drug metabolism in horse was reported to be more extensive than in human. On the other hand, a variety of phase II drugs conjugates in equine samples suggests that majority of the phase II enzyme classes present in human may likewise have homologs in horses (Scarth et al, 2010).

In this context, it was reported that drugs or drug metabolites characterised by high polarity and have relatively high molecular weights are more likely to be secreted (Sams 1987). Phase II metabolism glucoronates tend to be highly polar, be ionised and have high molecular weights, hence, they are usually highly cleared in bile; consequently, these drugs or metabolites enter the small intestine and may be reabsorbed (Sams 1987). Despite horses have no gallbladder and bile enters the small intestine continually, but enterohepatic cycling reported in horses and may contributes to persistence of some drugs in the body such as phenylbutazone (Gerring et al., 1981).

The factors which contribute to the fate of equine xenobiotics have not been well characterised. This may explain that disposition of drugs in horse is sometimes unpredictable (Tydén et al., 2009). However, Tydén et al., (2009) found that P-gp is expressed in the cellular membranes in some cells in the intestines, liver, kidney and peripheral blood lymphocytes in horse. They suggested that, the P-gp located in the intestinal epithelial cells may play a key role in determining oral bioavailability of some xenobiotics by pumping the compounds from the inside of the enterocytes back into the lumen of the intestines. Whereas, the suggested role of P-gp at its position in the liver is extrusion of drugs and other compounds from the hepatocytes to the bile. Eventually, extruded substrates would leave the body via the

faeces; hence, generally this would result in a plasma clearing and detoxifying function. Moreover, localization of CYP 3A in villus enterocytes has been reported in horse (Tydén et al. 2004). CYP 3A, is known as a major phase I drug metabolizing enzyme, is present in high levels in the enterocytes in some parts of the intestines and it has been suggested that P-gp and CYP 3A may be functionally linked (Wacher et al., 1995; Watkins 1997). It is documented that P-gp and CYP 3A are induced by various of the same compounds and show a broad overlap in substrate and inhibitor specificities (Wacher et al., 1995; Watkins 1997; Gavhane and Yadav 2012). Therefore, P-gp and CYP 3A may cooperate to limit drug absorption also in horse.

On the other hand, it has been reported that active uptake may be relatively less significant for the majority of highly permeable drugs investigated, to date, in human and pre-clinical species, and may not have had a major effect on predictions (Wu and Benet 2005; Hallifax et al., 2010). Moreover, Hallifax et al. (2012) reported that prediction accuracy was not dependent on the relative permeability demonstrating the absence of a general rate limitation by passive hepatocyte uptake on metabolic clearance. However, Cantrill and Houston (2017) concluded that, with currently available technology, the use of multisystem to comprehensively characterise the hepatic disposition of drugs may unavoidable.

The results presented in this thesis suggest that the use of *in vitro* systems may afford the opportunity to produce qualitative and quantitative data on drug metabolism in horses. According to the new revision of the International Laboratory Accreditation Cooperation (ILAC)-G7 guidelines (Article 16.4) *in vitro* incubations are approved to be used instead of *in vivo* post administration samples (ILAC, 2009). Under these guide lines is not necessary to produce enormous quantities of *in vitro* metabolites that can be isolated and subject for further analysis. Moreover, data obtained from *in*

vitro systems can be used to determine a detection time (DT) which in turn will be used by veterinarians to recommend their own withdrawal time (WT). In the present study, chloramphenicol inhibited omeprazole metabolism in equine liver microsomes. Consequently, omeprazole concentration in the blood may be elevated if it is co-administered with chloramphenicol and it is predicted that an extended DT will be required otherwise the recommended WT will be underestimated. This will have both economical and legal consequences for horse racing, as well as the owner. In this context, microsomes are frequently used in drug interaction studies rather than hepatocytes (Chauret et al., 1997; Jones et al., 2004; Zielinski and Mevissen, 2015). Furthermore, Brown et al (2007) found that there is no difference between microsomes and hepatocytes for the inhibition of 18 pathways of metabolism. Hence, due to their availability and ease of preparation, equine microsomes may represents a suitable candidate to conduct DDI screening studies for drugs used in equine medicine which will reflect positively on horse welfare.

On the other hand, induction of drug metabolism in horse is evident in the literature. Burrows et al. (1989) reported that, the plasma half-life of phenylbutazone was reduced from 4 h to 2.7 h after 4 days treatment with rifampicin at 10 mg/kg BW each day. This is a clear example of a DDI that may affect directly the horse welfare, since the drug e.g. phenylbutazone will be less effective and the horse may not be fully healed. Therefore, it is necessary to introduce drug induction studies as a routine procedure for horse medications. In this context, various complex culture systems have been developed including sandwich cultures, and 3D models such as scaffold-based systems and bioreactors to extend the life span of equine hepatocyte in vitro (Bachmann et al., 2015; Bell et al., 2016). These culture systems can be used for equine hepatocytes to perform further metabolic studies such as phase II metabolism and drug induction studies, providing

an approach to perform further comparative metabolic studies between horse and human. This, also, allow the cells to maintain transporter protein levels for several days and both uptake and biliary efflux can be accessed through modulation of calcium ions (Hoffmaster et al., 2004; Bi et al., 2006; Kim et al., 2010; Swift et al., 2010). Furthermore, with a tremendous growth in the interest of allometric scaling in the last decades, the predicted Cl_{int} in this study can be used to perform interspecies allometric scaling (Mahmood 2007). Consequently, the Cl_{int} values and scaling factors determined in the present study may represent a forward step in improvement of interspecies allometric scaling by integrating more *in vitro* data into these type of calculations (Lave et al., 1995; Lave et al., 1997). Hence, drug development process may be improved including the first-in-human and animal dose selection by adding more species during process of clearance predictions.

Appendices

Appendix I. Preparation of equine hepatocyte isolation solutions

Table A.I.1 Preparation of Hanks HEPES Buffer (1x) (solution 1)

Hanks balanced salt solution (10x)	100 ml
HEPES 1mM	20 ml
Sodium bicarbonate 7.5%	4.7 ml
Sterile distilled water	Up to 1L

Stored at 4°C.

1.1.1 Preparation of perfusate buffer (EGTA chelating buffer)

Table A.I.2: Preparation of Hanks HEPES buffer (10x) (without sodium bicarbonate/glucose)

NaCl (Sigma, UK)	1.37 M (8 g)
KCL (Sigma, UK)	54 mM (402.58 mg)
KH_2PO_2 (Sigma, UK)	4.4 mM (59.87 mg)
Na_2HPO_4. $12H_2O$ (Sigma, UK)	3.6 mM (128.92 mg)
HEPES (Sigma, UK)	200 mM (4.77 g)
NaOH (Sigma, UK)	100 mM (399.97 mg)
Sterile distilled water	100 ml

- Filter sterilised and stored at 4°C.
- To make up 1x buffer, diluted with sterile water and stored at 4°C.

Table A.I.3 Preparation of 100mM EGTA solution

EGTA (Sigma, UK)	1.92g
Sterile Hanks HEPES (1x) (no sodium bicarbonate/glucose)	25 ml
NaOH (Sigma, UK)	5 ml

Made up to 50 ml with 1x HanksHEPES buffer, filter sterilised and stored at 4°C.

To prepare EGTA chelating buffer (solution 2), 10 ml of 100mM EGTA solution was added to 990 ml of solution 1 and store at stored at 4°C.

1.3 Preparation of calcium chloride solution (Solution 3)

Table A.I.4 Preparation of 0.5 M CaCl2 solution

Sterile Hanks HEPES (1x) with calcium chloride	5.50 g
Sterile distilled water	100 ml

Filter sterilise and stored at stored at 4°C

To prepare solution 3, 10 ml of 0.5 M $CaCl_2$ was added to 990 ml of solution 1 and store at stored at 4°C.

Table A.I.5 Preparation of collagenase perfusate buffer (solution 4)

Solution 3	1000 ml
Collagenase type iv	0.1% W/V

Table A.I.6 Preparation of solution 5

NaCl (Sigma, UK)	120 mM (7.013 g)
HEPES (Sigma, UK)	10 mM (2.383 g)
$CaCl_2$ dihydrate (Sigma, UK)	0.9mM (0.099 g)
KCL (Sigma, UK)	6.2 mM (0.462 g)
Albumin	0.1% W/V (1g)
Sterile distilled water	1000 ml

Table A.I.7: Optimisation of the effect of Percoll on viability and recovery of equine hepatocytes

Percoll Gradient	COLD WEM	FCS	Percoll	PBS 10x
25%	10 ml	1.25 ml	3.375 ml	0.375
30%	9.54 ml	1.05 ml	4.05 ml	0. 45 ml

1.6 Evaluation of equine hepatocyte attachment efficiency

Table.A.I.8 Standard curve

Step	Cell concentration	Stock	WEM (ml)
1	1000000	1 x 10^6 cells/ml	2.5
2	100000	100 µl from step 1	0.1
3	75000	75 µl from step 1	0.125
4	50000	50 µl from step 1	0.150
5	25000	25 µl from step 1	0.175
6	15000	15 µl from step 1	0.185
7	10000	10 µl from step 1	0.190
8	5000	5 µl from step 1	0.195

Table.A.I.9

No of cells	OD 450nm 1	OD 450nm 2	OD 450nm 3	OD Average
5000	0.233777	0.245587	0.246847	0.242070333
8000	0.249435	0.264351	0.246847	0.253544333
10000	0.273004	0.274267	0.281209	0.27616
15000	0.323234	0.334199	0.335815	0.331082667
25000	0.401769	0.394563	0.384546	0.393626
50000	0.613217	0.565305	0.571265	0.583262333
75000	0.754594	0.770252	0.760289	0.761711667
100000	0.852259	0.866941	0.873956	0.864385333
Blank	0.216625	0.218726	0.23155	0.222300333

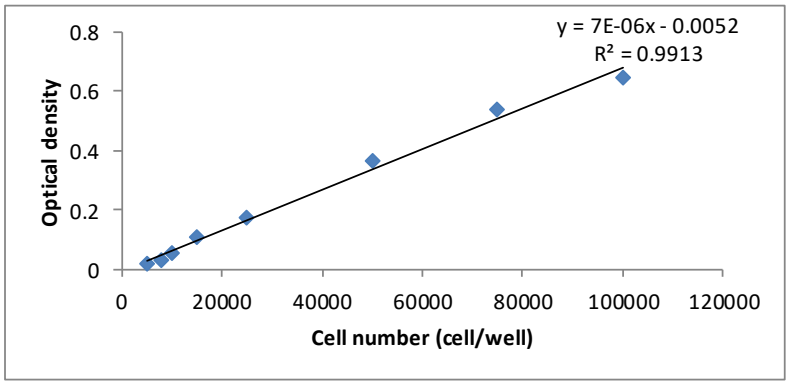


Figure A.I.1: Hepatocyte in suspension were seeded into flat-bottomed 96-well tissue culture plate. Good linearity was observed (R^2>0.9) between cell number and signal produced when cells were seeded at 5000, 10000, 15000, 25000, 50000, 75000 and 100000 viable cells per well as determined by the Trypan blue exclusion assay.

Table A.II.1: Hepatocyte size and number in equine liver at different ages

	0-9 years			10-20 years			>20 years		
	1	**3**	**5**	**10**	**18**	**19**	**21**	**23**	**29**
Cell size (μm^2)	171.2 ± 16.9	188.1 ± 22.3	163.6 ± 23.7	162.0 ± 12.4	146.8 ± 16.3	137.7 ± 15.0	172.2 ± 18.5	175.0 ± 24.4	196.3± 13.7
No of cells/unit area	25.7± 1.3	23.0 ± 1.7	26.5± 1.1	29.4± 3.5	29.3± 2.2	33.5± 2.0	23.8± 1.0	22.7± 2.3	22.1 ± 1.2

Values expressed as average ± SD, measurements performed in triplicate for each liver sample.

A.III.1 Omeprazole HPLC-MS detection method

Initial conditions- 80% solvent A and 20% solvent B

Table A.III.1. LC method for detecting omeprazole concentrations in the *in vitro* study

Time (minutes)	Solvent A (%)	Solvent B (%)	Flow (mL/min)	Pressure (bar)
0.00	80.0	20.0	0.500	400
2.00	50.0	50.0	0.500	400
4.00	0.00	100	0.500	400
5.00	0.00	100	0.500	400
5.20	80.0	20.0	0.500	400
9.00	80.0	20.0	0.500	400

Table A.III.2. Mass spectrometry method for omeprazole, lansoprazole and omeprazole metabolites

Drug	Ionised Mass (M/Z)	Dwell (seconds)	Cone (volts)	~ Retention time, min
Omeprazole	346	0.200	25.0	5.28
Lansoprazole	370	0.200	60.0	5.70
M1	362	0.200	25.0	4.16
M2	362	0.200	25.0	4.89
M3	362	0.200	25.0	5.53

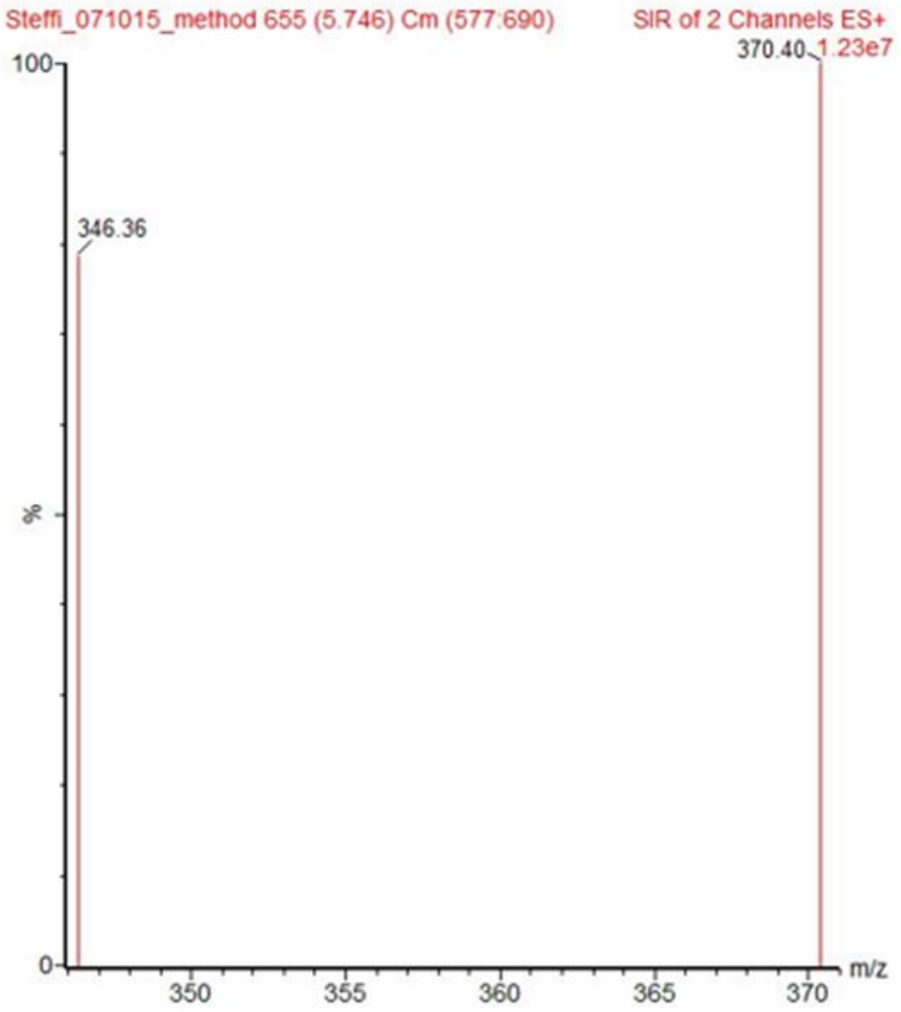


Figure A.III.1: Mass spectrum showing omeprazole and lansoprazole at *m/z* 346 and 370, respectively.

A.III.2 Calculated K_{dep} and V_0 data for omeprazole

Table A.III.3: K_{dep} and V_0 data for microsomes, fresh and cryopreserved hepatocyte incubations for omeprazole disappearance

Horse	*In vitro* liver model	Omeprazole concentration (µM)	K_{dep} (µM)	V_0 (µM/min)
1	Fresh Hepatocytes	0.500	0.055	0.0275
		1.00	0.0278	0.0278
		5.00	0.0219	0.1095
		25.0	0.0228	0.57
		50.0	0.0225	1.125
		75.0	0.0165	1.2525
		100	0.0127	1.27
		150	0.0088	1.32
	Cryopreserved hepatocytes	0.500	0.0304	0.0152
		1.00	0.0205	0.0205
		5.00	0.0162	0.081
		25.0	0.0217	0.5425
		50.0	0.0203	1.015

		75.0	0.0165	1.2375
		100	0.0113	1.13
		150	0.0081	1.215
	Microsomes	0.500	0.0223	0.01115
		1.00	0.0201	0.0201
		5.00	0.0262	0.131
		25.0	0.0136	0.340
		50.0	0.013	0.650
		75.0	0.0112	0.840
		100	0.0108	1.080
		150	0.006	0.900
2	Fresh Hepatocytes	0.500	0.0358	0.0179
		1.00	0.0414	0.0414
		5.00	0.029	0.145
		25.0	0.0203	0.5075
		50.0	0.0211	1.055
		75.0	0.0169	1.2675
		100	0.0129	1.29
		150	0.0087	1.305
	Cryopreserved hepatocytes	0.500	0.033	0.0165
		1.00	0.0173	0.0173
		5.00	0.0161	0.0805
		25.0	0.0216	0.54
		50.0	0.0156	0.78
		75.0	0.0124	0.93
		100	0.0103	1.03
		150	0.008	1.2
	Microsomes	0.500	0.0174	0.0087
		1.00	0.0128	0.0128
		5.00	0.0152	0.076
		25.0	0.0106	0.265
		50.0	0.0141	0.705
		75.0	0.0115	0.8625
		100	0.0122	1.22
		150	0.0071	1.065
3	**Fresh Hepatocytes**	0.500	0.0344	0.0172
		1.00	0.0408	0.0408
		5.00	0.0174	0.087
		25.0	0.0223	0.5575
		50.0	0.017	0.85
		75.0	0.0149	1.1175
		100	0.013	1.3
		150	0.0084	1.26
	Cryopreserved hepatocytes	0.500	0.0259	0.01295
		1.00	0.0285	0.0285
		5.00	0.0179	0.0895
		25.0	0.0136	0.34
		50.0	0.0131	0.655
		75.0	0.0105	0.7875
		100	0.01	1
		150	0.0056	0.84
	Microsomes	0.500	0.0316	0.0158
		1.00	0.021	0.021
		5.00	0.0103	0.0515
		25.0	0.0067	0.1675

	50.0	0.005	0.25
	75.0	0.0039	0.2925
	100	0.0035	0.35
	150	0.0024	0.36

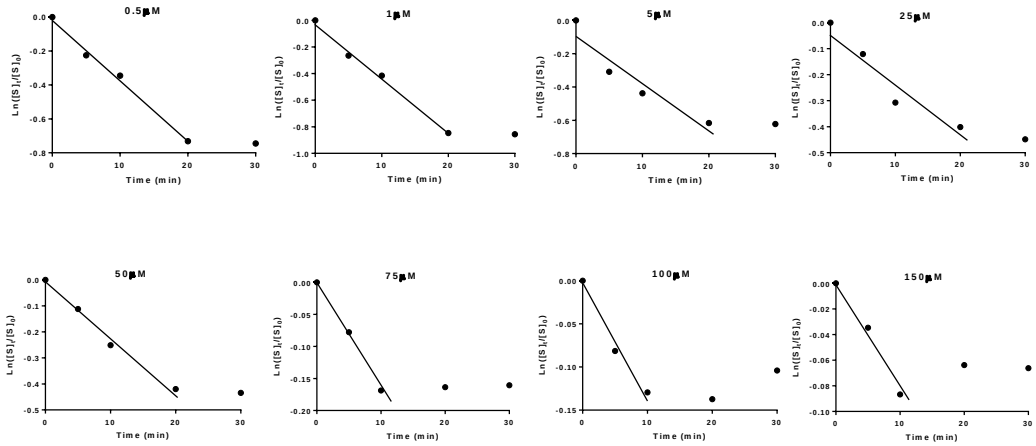


Figure A.III.2: data gathered using various omeprazole concentrations with freshly isolated equine hepatocytes. Data was plotted as the natural logarithm (Ln) of substrate concentration against time. K_{dep} is represented by the slope of the line (refer to table A.III.3, horse 2).

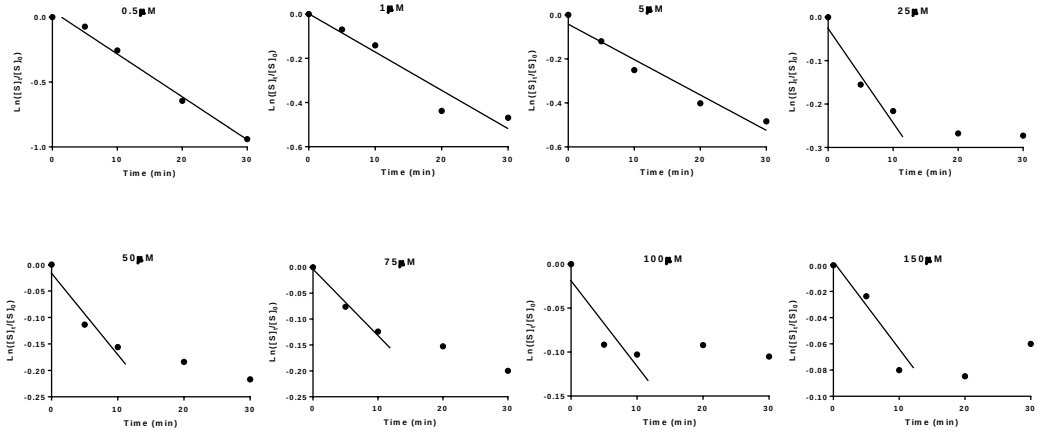


Figure A.III.3: data gathered using various omeprazole concentrations with cryopreserved equine hepatocytes. Data was plotted as the natural logarithm (Ln) of substrate concentration against time. K_{dep} is represented by the slope of the line (refer to table A.III.3, horse 2).

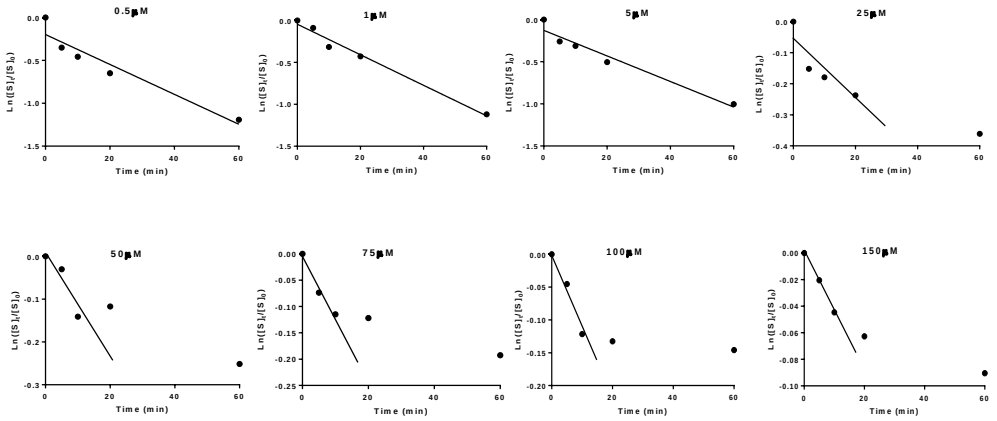


Figure A.III.4: data gathered using various omeprazole concentrations with equine microsomes. Data was plotted as the natural logarithm (Ln) of substrate concentration against time. K_{dep} is represented by the slope of the line (refer to table A.III.3, horse 2).

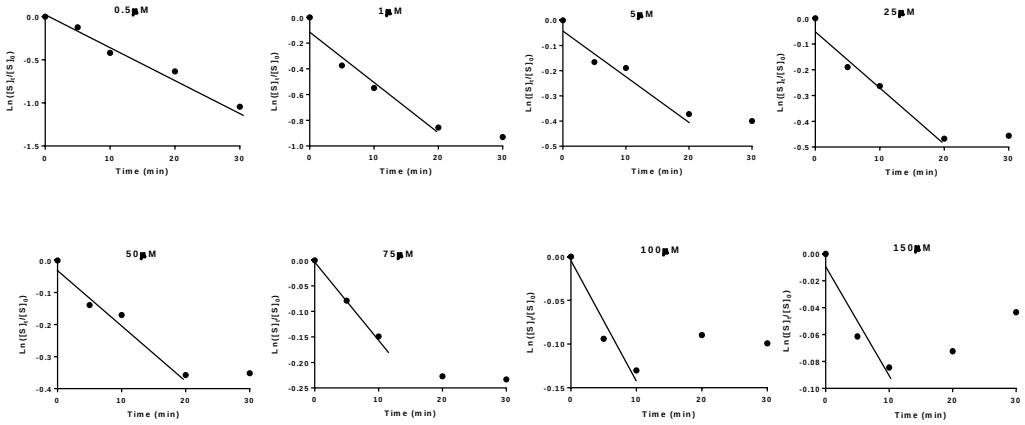


Figure A.III.5: data gathered using various omeprazole concentrations with freshly isolated equine hepatocytes. Data was plotted as the natural logarithm (Ln) of substrate concentration against time. K_{dep} is represented by the slope of the line (refer to table A.III.3, horse 3).

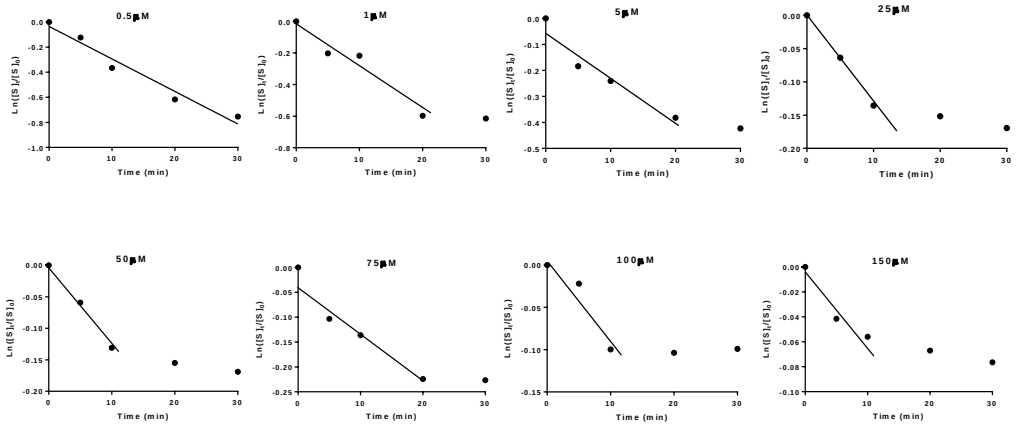


Figure A.III.6: data gathered using various omeprazole concentrations with cryopreserved equine hepatocytes. Data was plotted as the natural logarithm (Ln) of substrate concentration against time. K_{dep} is represented by the slope of the line (refer to table A.III.3, horse 3).

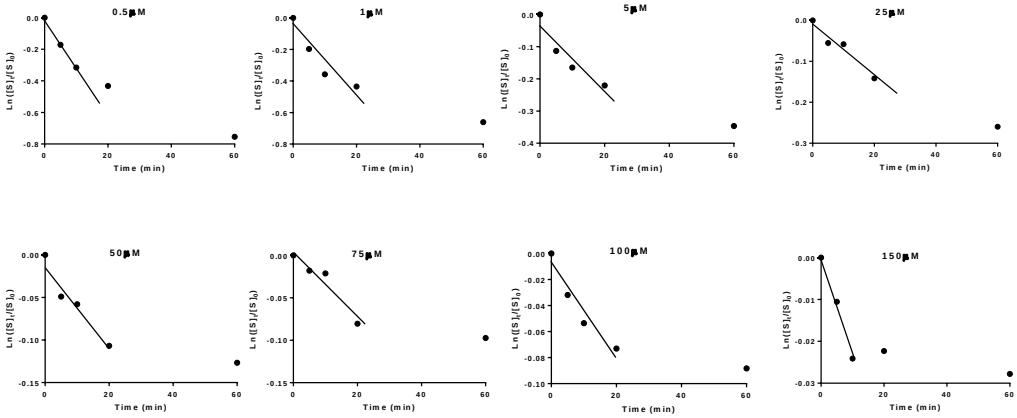


Figure A.III.7: data gathered using various omeprazole concentrations with equine microsomes. Data was plotted as the natural logarithm (Ln) of substrate concentration against time. K_{dep} is represented by the slope of the line (refer to table A.III.3, horse 3).

Table A.III.4: V_0 data for microsomes, fresh and cryopreserved hepatocyte incubations for metabolite appearance

Horse	*In vitro* liver model	Omeprazole concentration (µM)	V_0 (arbitraryunits/min)		
			M1	M2	M3
1	**Fresh Hepatocytes**	0.500	663	150	281
		1.00	1065	1677	542
		5.00	2669	3797	1131.5
		25.0	4477	7534	2858.9
		50.0	6509	10107	3610.7
		75.0	8714	12169	3931.3
		100	9217	12619	4107.7
		150	-	-	-
	Cryo. hepatocytes	0.500	316	263.3	333.9
		1.00	459.3	783.1	654
		5.00	977	1370.3	1127.7
		25.0	2282	5231.2	1720.9
		50.0	3000	7016.2	2444.2
		75.0	3806.3	7515.4	2906
		100	4596.5	9996.4	3686.2
		150	-	-	-
	Microsomes	0.500	240.5	915	541
		1.00	508.3	1753	937.3
		5.00	2181	10482	6574
		25.0	12797	25797	20687
		50.0	20159	37700	34929
		75.0	23084	44033	41737
		100	22343	50298	40035
		150	-	-	-
2	**Fresh Hepatocytes**	0.500	148.8	311.2	147.4
		1.00	421.5	696.2	1725.7
		5.00	1022.7	1760.5	3842.6
		25.0	2237.7	3020.9	7121
		50.0	2889.3	4771.6	10128
		75.0	3228.1	4990	12413
		100	4023.5	5136.1	12577
		150	4126.4	5820.3	11341
	Cryo. hepatocytes	0.500	643	298	460.3
		1.00	907.4	898.9	1024.2
		5.00	1950	1052.3	1829
		25.0	3237.8	4145.1	2447.9
		50.0	5141.6	5176	3781.4
		75.0	6037.2	8041.8	4952.1
		100	6483.5	8900.7	5392.2
		150	7472.3	8351.7	5062.7
	Microsomes	0.500	619.5	701.93	694
		1.00	1362.3	1306.7	1322
		5.00	4249.3	7166.1	4664.4
		25.0	5562.5	19927	9779.8
		50.0	9079.7	34177	18474
		75.0	12580	50475	27430
		100	17809	57941	24290
		150	16741	62083	31496

3	Fresh Hepatocytes	0.500	601.7	588.9	281.2
		1.00	1233	870.9	1513.1
		5.00	1644	2943	2578.8
		25.0	2171	5019	3614.3
		50.0	3208	5941	5881.1
		75.0	4138	7038	6749.7
		100	4291	9562	7649.7
		150	5396	9082	8046.4
	Cryo. hepatocytes	0.500	487	339.9	328.1
		1.00	771.8	956.3	1002.3
		5.00	2052	1375	2555.7
		25.0	3338	4533	3855.2
		50.0	4841	7131	4704.5
		75.0	6961	8042	5823.4
		100	7485	9367	6347.4
		150	7598	10368	8412.2
	Microsomes	0.500	846.7	1587.3	1519.3
		1.00	1668.9	2933	2406.6
		5.00	4377.5	12797	5959.3
		25.0	6079.2	32409	23203
		50.0	9619.3	56340	32931
		75.0	10286	67217	44920
		100	11486	83778	50787
		150	14244	100901	67727

Table A.III.5: Summary of scaling values for the three horses used for omeprazole study

Horse No	Hepatocytes		Microsomes	
	P450 nmoles/10^6 hepatocytes	Hepatocellularity (10^6cells/g liver)	nmol P450/mg of protein	mg Microsomal protein per g liver
1	0.110	266.9	0.539	52.2
2	0.140	188.2	0.399	62.3
3	*0.130	*227.3	0.591	45.0

* The average of the 18 livers.

Table A.III.6: *In vitro in vivo* extrapolation

Well Stirred Model		Hepatocytes									
Drug	Clint Heps per million cells	HPGL Horse	Clint per gram of liver	Size of liver	Weight of horse	Clint per liver	fuinc	Fup	Corrected Clint per liver	Hepatic blood flow horse	Hepatic Clearance
Omeprazole	ul/min/million cells	million cells per gram liver	ul/min/gram	grams	kilograms	ml/min/kg			ml/min/kg	ml/min/kg	ml/min/kg
Fresh	44.5	266.90	11877.05	7500	500	178.15575	0.8	0.05	11.13473438	23.5	7.555024242
	40.5	188.2	7622.1	7500	500	114.3315	0.8	0.05	7.14571875	23.5	5.479538333
	33.7	227.3	7660.01	7500	500	114.90015	0.8	0.05	7.181259375	23.5	5.500412915
Cryo	41.9	266.9	11183.11	7500	500	167.74665	0.8	0.05	10.48416563	23.5	7.249784941
	29.6	188.2	5570.72	7500	500	83.5608	0.8	0.05	5.22255	23.5	4.272946692
	25	227.3	5682.5	7500	500	85.2375	0.8	0.05	5.32734375	23.5	4.342841269
Parallel Tube Model		Hepatocytes									
	Clint Heps per million cells	HPGL Horse	Clint per gram of liver	Size of liver	Weight of horse	Clint per liver	fuinc	Fup	Corrected Clint per liver	Hepatic blood flow horse	Hepatic Clearance
	ul/min/million cells	million cells per gram liver	ul/min/gram	grams	kilograms	ml/min/kg			ml/min/kg	ml/min/kg	ml/min/kg
Fresh	44.5	266.90	11877.05	7500	500	178.15575	0.8	0.05	11.13473438	23.5	8.868423941
	40.5	188.2	7622.1	7500	500	114.3315	0.8	0.05	7.14571875	23.5	6.16153779
	33.7	227.3	7660.01	7500	500	114.90015	0.8	0.05	7.181259375	23.5	6.18774009
Cryo	41.9	266.9	11183.11	7500	500	167.74665	0.8	0.05	10.48416563	23.5	8.457707802
	29.6	188.2	5570.72	7500	500	83.5608	0.8	0.05	5.22255	23.5	4.682933494
	25	227.3	5682.5	7500	500	85.2375	0.8	0.05	5.32734375	23.5	4.766657783

Table A.III.7: *In vitro in vivo* extrapolation

Well Stirred Model		Microsomes									
Drug	Clint microsomes	MPPGL Horse	Clint per gram of liver	Size of liver	Weight of horse	Clint per liver	fuinc	Fup	Corrected Clint per liver	Hepatic blood flow horse	Hepatic Clearance
	ul/min/mg protein	mg per gram liver	ul/min/gram	grams	kilograms	ml/min/kg			ml/min/kg	ml/min/kg	ml/min/kg
Omeprazole	24.8	52.20	1294.56	7500	500	19.4184	0.9	0.05	1.0788	23.8	1.032020837
	20.1	62.30	1252.23	7500	500	18.78345	0.9	0.05	1.043525	23.8	0.999692878
	10.7	45.00	481.5	7500	500	7.2225	0.9	0.05	0.40125	23.8	0.394597386

Parallel Tube Model		Microsomes									
Drug	Clint microsomes	MPPGL Horse	Clint per gram of liver	Size of liver	Weight of horse	Clint per liver	fuinc	Fup	Corrected Clint per liver	Hepatic blood flow horse	Hepatic Clearance
	ul/min/mg protein	mg per gram liver	ul/min/gram	grams	kilograms	ml/min/kg			ml/min/kg	ml/min/kg	ml/min/kg
Omeprazole	24.8	52.20	1294.56	7500	500	19.4184	0.9	0.05	1.0788	23.8	1.054715491
	20.1	62.30	1252.23	7500	500	18.78345	0.9	0.05	1.043525	23.8	1.020978735
	10.7	45.00	481.5	7500	500	7.2225	0.9	0.05	0.40125	23.8	0.397886543

Table A.III.7: K_{dep} and V_0 data for the drug interaction study between omeprazole and chloramphenicol completed in microsomes from horse 2 and 3

Chloramphenicol concentration (μM)		Omeprazole concentration (μM)	K_{dep} (μM)	V_0 (μM/min)
H1	**0**	10.0	0.0086	0.086
	1	10.0	0.0066	0.066
	5	10.0	0.0059	0.059
	10	10.0	0.0044	0.044
	20	10.0	0.004	0.04
	50	10.0	0.0027	0.027
	75	10.0	0.0031	0.031
	100	10.0	0.0015	0.015
	150	10.0	0.0035	0.035
H2	**0**	10.0	0.0081	0.081
	1	10.0	0.0066	0.066
	5	10.0	0.0059	0.059
	10	10.0	0.0054	0.054
	20	10.0	0.0054	0.054
	50	10.0	0.0047	0.047
	75	10.0	0.0035	0.035
	100	10.0	0.0039	0.039
	150	10.0	0.0031	0.031
H3	**0**	10.0	0.01	0.1
	1	10.0	0.0099	0.099
	5	10.0	0.0076	0.076
	10	10.0	0.0078	0.078
	20	10.0	0.0073	0.073
	50	10.0	0.0072	0.072
	75	10.0	0.006	0.06
	100	10.0	0.0043	0.043
	150	10.0	0.0048	0.048

Table A.III.8: Calculation of the effect of the Ki on the AUC.

Inhibitor Conc.	I/Ki	I/Ki + 1	(I/Ki + 1) x AUC
0.1	0.006494	1.006494	4831.169
0.5	0.032468	1.032468	4955.844
1.5	0.097403	1.097403	5267.532
2	0.12987	1.12987	5423.377
3	0.194805	1.194805	5735.065
4	0.25974	1.25974	6046.753
5	0.324675	1.324675	6358.442
6	0.38961	1.38961	6670.13
7	0.454545	1.454545	6981.818
8	0.519481	1.519481	7293.506
9	0.584416	1.584416	7605.195
10	0.649351	1.649351	7916.883
20	1.298701	2.298701	11033.77
30	1.948052	2.948052	14150.65
40	2.597403	3.597403	17267.53
50	3.246753	4.246753	20384.42
60	3.896104	4.896104	23501.3
70	4.545455	5.545455	26618.18
80	5.194805	6.194805	29735.06
90	5.844156	6.844156	32851.95
100	6.493506	7.493506	35968.83
110	7.142857	8.142857	39085.71
120	7.792208	8.792208	42202.6
130	8.441558	9.441558	45319.48
140	9.090909	10.09091	48436.36
150	9.74026	10.74026	51553.25
160	10.38961	11.38961	54670.13
170	11.03896	12.03896	57787.01
180	11.68831	12.68831	60903.9
190	12.33766	13.33766	64020.78
200	12.98701	13.98701	67137.66
400	25.97403	26.97403	129475.3
600	38.96104	39.96104	191813
800	51.94805	52.94805	254150.6
1000	64.93506	65.93506	316488.3
1200	77.92208	78.92208	378826
1400	90.90909	91.90909	441163.6
1600	103.8961	104.8961	503501.3
1800	116.8831	117.8831	565839
2000	129.8701	130.8701	628176.6
2200	142.8571	143.8571	690514.3
2400	155.8442	156.8442	752851.9
2600	168.8312	169.8312	815189.6
2800	181.8182	182.8182	877527.3
3000	194.8052	195.8052	939864.9
3200	207.7922	208.7922	1002203
3400	220.7792	221.7792	1064540
3600	233.7662	234.7662	1126878
3800	246.7532	247.7532	1189216
4000	259.7403	260.7403	1251553
5000	324.6753	325.6753	1563242
6000	389.6104	390.6104	1874930

7000	454.5455	455.5455	2186618
8000	519.4805	520.4805	2498306
9000	584.4156	585.4156	2809995
10000	649.3506	650.3506	3121683
11000	714.2857	715.2857	3433371
12000	779.2208	780.2208	3745060
13000	844.1558	845.1558	4056748
14000	909.0909	910.0909	4368436
15000	974.026	975.026	4680125
20000	1298.701	1299.701	6238566
25000	1623.377	1624.377	7797008
30000	1948.052	1949.052	9355449
35000	2272.727	2273.727	10913891
40000	2597.403	2598.403	12472332
45000	2922.078	2923.078	14030774
50000	3246.753	3247.753	15589216
55000	3571.429	3572.429	17147657
60000	3896.104	3897.104	18706099

Appendix IV.1 Flunixin HPLC-MS detection method

Initial conditions- 50% solvent A and 50% solvent B

Table A.IV.1.1: LC method for detecting flunixin concentrations

Time (minutes)	Solvent A (%)	Solvent B (%)	Flow (mL/min)	Pressure (bar)
0.00	50.0	50.0	0.500	400
2.00	0.00	10.0	0.500	400
4.00	0.00	100	0.500	400
5.00	50.0	50.0	0.500	400
7.50	50.0	50.0	0.500	400

Table A.IV.1.2: Mass spectrometry method for flunixin, ketoprofen and flunixin metabolite in microsomes

Drug	Ionised Mass (M/Z)	Dwell (seconds)	Cone (volts)	~ Retention time, min
Flunixin	297.26	0.200	40.0	4.75
Ketoprofen	332.6 (MW+ formic acid +methanol)	0.200	15.0	3.85
Metabolite		0.200	40.0	4.55

Table A.IV.1.3: K_{dep} and V_0 data for microsomes, fresh and cryopreserved hepatocyte incubations for flunixin disappearance

Horse	*In vitro* liver model	Flunixin concentration (µM)	K_{dep} (µM)	V_0 (µM/min)
1	**Fresh Hepatocytes**	0.500	0.0185	0.0093
		1.00	0.0158	0.0158
		5.00	0.0236	0.118
		25.0	0.0164	0.410
		50.0	0.0136	0.680
		75.0	0.0101	0.758
		100	0.0066	0.660
		150	0.0041	0.615
	Cryopreserved hepatocytes	0.500	0.0393	0.0197
		1.00	0.0473	0.0473
		5.00	0.0233	0.1165
		25.0	0.0168	0.4200
		50.0	0.0105	0.5250
		75.0	0.0096	0.7200
		100	0.0055	0.5500
		150	0.0036	0.5400
	Microsomes	0.500	0.0155	0.0078
		1.00	0.0199	0.0199
		5.00	0.0136	0.0680
		25.0	0.0085	0.2125
		50.0	0.0056	0.2800

		75.0	0.0035	0.2625
		100	0.0013	0.1300
		150	-	-
2	**Fresh Hepatocytes**	0.500	0.0221	0.01105
		1.00	0.0207	0.0207
		5.00	0.012	0.06
		25.0	0.011	0.275
		50.0	0.01	0.5
		75.0	0.0086	0.645
		100	0.0055	0.55
		150	0.0037	0.555
	Cryopreserved hepatocytes	0.500	0.06	0.03
		1.00	0.0275	0.0275
		5.00	0.0184	0.092
		25.0	0.0169	0.4225
		50.0	0.0105	0.525
		75.0	0.009	0.675
		100	0.0062	0.62
		150	0.0039	0.585
	Microsomes	0.500	0.0184	0.0092
		1.00	0.0234	0.0234
		5.00	0.0113	0.0565
		25.0	0.0055	0.1375
		50.0	0.0032	0.16
		75.0	0.0021	0.1575
		100	0.001	0.1
		150	0.0009	0.135
3	**Fresh Hepatocytes**	0.500	0.0184	0.0092
		1.00	0.0279	0.0279
		5.00	0.0213	0.1065
		25.0	0.0152	0.38
		50.0	0.0112	0.56
		75.0	0.0086	0.645
		100	0.0052	0.52
		150	0.0034	0.51
	Cryopreserved hepatocytes	0.500	0.0205	0.01025
		1.00	0.0185	0.0185
		5.00	0.0148	0.074
		25.0	0.0108	0.27
		50.0	0.0083	0.415
		75.0	0.0067	0.5025
		100	0.0047	0.47
		150	0.0031	0.465
	Microsomes	0.500	0.0244	0.0122
		1.00	0.022	0.022
		5.00	0.0126	0.063
		25.0	0.0117	0.2925
		50.0	0.0073	0.365
		75.0	0.0048	0.36
		100	0.0012	0.12
		150	0.0010	0.15

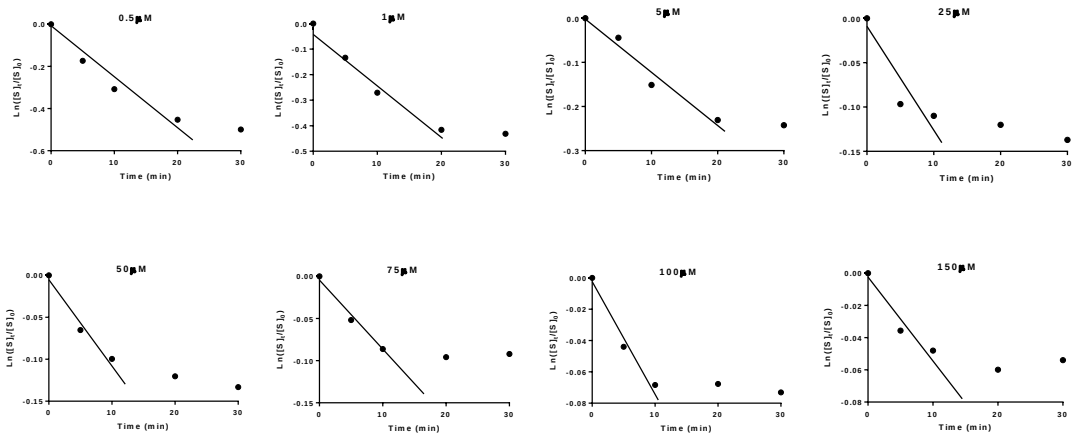


Figure A.IV.1.1: data gathered using various flnixin concentrations with freshly isolated equine hepatocytes. Data was plotted as the natural logarithm (Ln) of substrate concentration against time. K_{dep} is represented by the slope of the line (refer to table 1, horse 2).

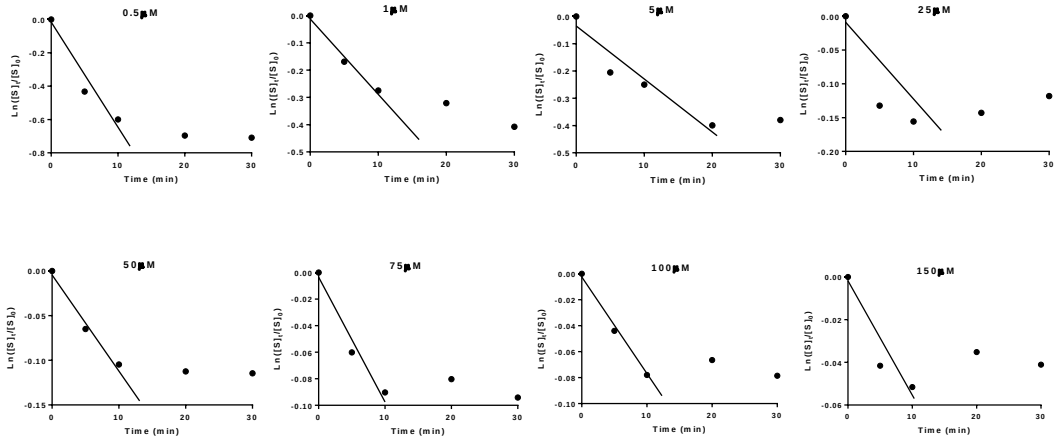


Figure A.IV.1.2: data gathered using various flunixin concentrations with cryopreserved equine hepatocytes. Data was plotted as the natural logarithm (Ln) of substrate concentration against time. K_{dep} is represented by the slope of the line (refer to table 1, horse 2).

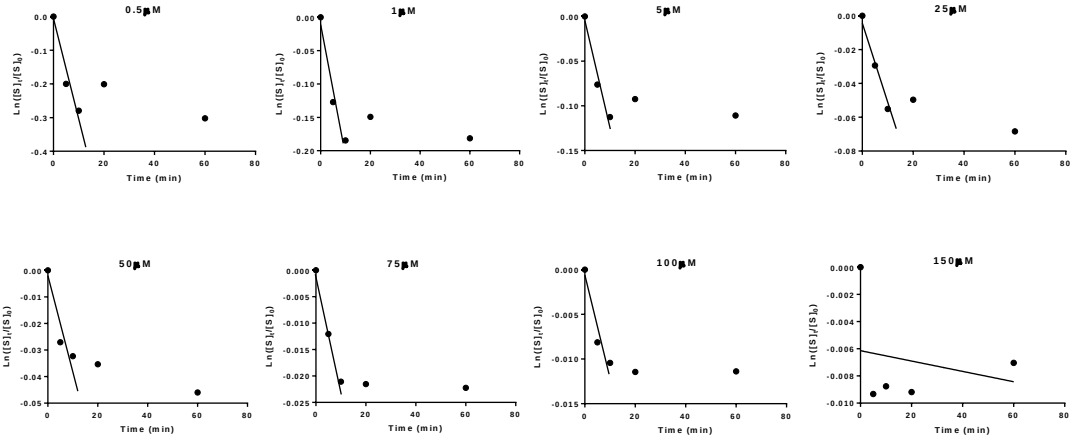


Figure A.IV.1.3: data gathered using various flunixin concentrations with equine microsomes. Data was plotted as the natural logarithm (Ln) of substrate concentration against time. K_{dep} is represented by the slope of the line (refer to table 1, horse 2).

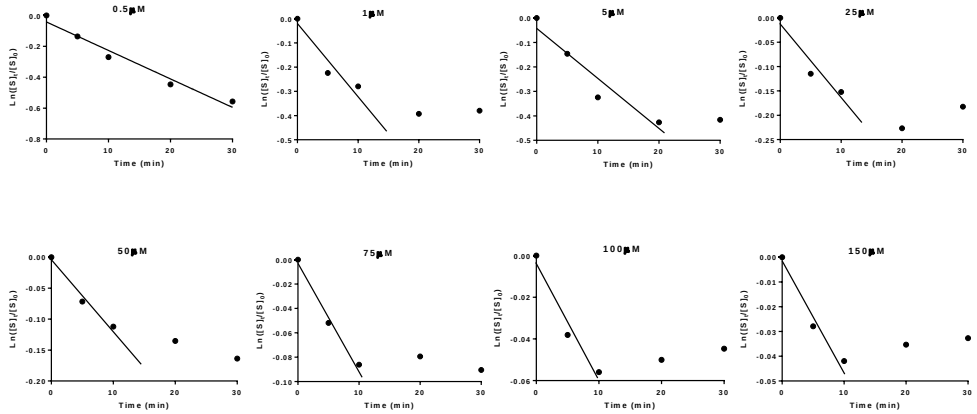


Figure A.IV.1.4: data gathered using various flnixin concentrations with freshly isolated equine hepatocytes. Data was plotted as the natural logarithm (Ln) of substrate concentration against time. K_{dep} is represented by the slope of the line (refer to table 1, horse 3).

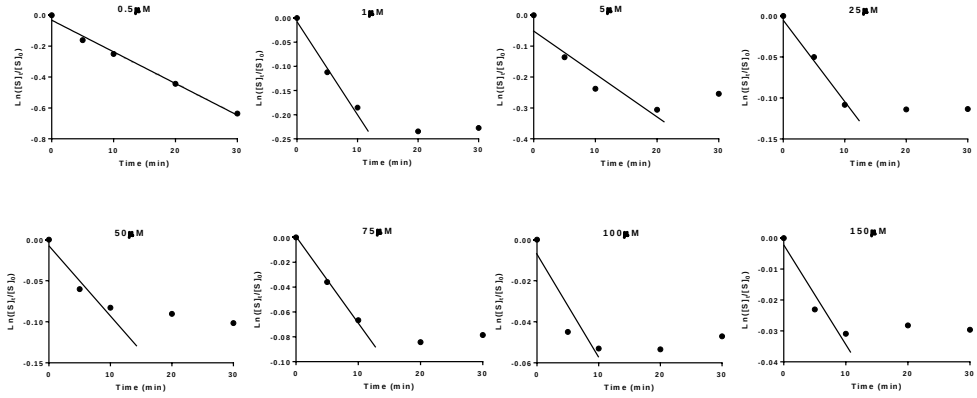


Figure A.IV.1.5: data gathered using various flunixin concentrations with cryopreserved equine hepatocytes. Data was plotted as the natural logarithm (Ln) of substrate concentration against time. K_{dep} is represented by the slope of the line (refer to table 1, horse 3).

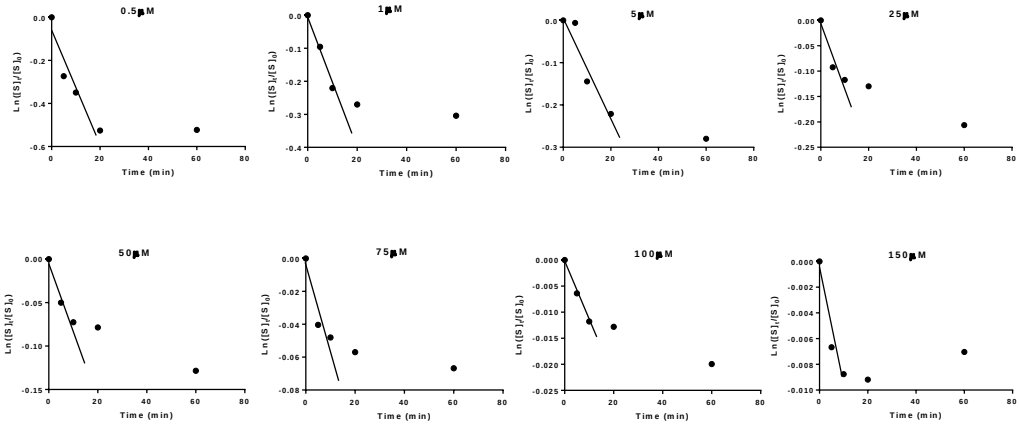


Figure A.IV.1.6: data gathered using various flunixin concentrations with equine microsomes. Data was plotted as the natural logarithm (Ln) of substrate concentration against time. K_{dep} is represented by the slope of the line (refer to table 1, horse 3).

Table A.IV.1.4: V_0 data for microsomes incubations for metabolite appearance

Horse	*In vitro* liver model	Flunixin concentration (µM)	V_0 (arbitrary units/min)
1	Microsomes	0.500	610.16
		1.00	852.7
		5.00	7288.1
		25.0	9968.2
		50.0	10921
		75.0	11857
		100	5670.8
		150	6918.3
2	Microsomes	0.500	-
		1.00	-
		5.00	12261
		25.0	27570
		50.0	14141
		75.0	18231
		100	8571.9

		150	10293
3	Microsomes	0.500	487
		1.00	578
		5.00	5581.4
		25.0	34830
		50.0	25552
		75.0	18875
		100	6747.4
		150	9418.3

Table A.III.1.5: Summary of scaling values for the three horses used for flunixin study

Horse No	Hepatocytes		Microsomes	
	P450 nmoles/10^6 hepatocytes	Hepatocellularity (10^6cells/g liver)	nmol P450/mg of protein	mg Microsomal protein per g liver
1	0.140	188.2	0.599	62.4
2	0.123	301.2	0.394	62.4
3	0.117	247.5	0.557	52.1

Table A.IV.1.6: *In vitro in vivo* extrapolation

Well Stirred Model		Hepatocytes								
Drug	Clint Heps per million cells	HPGL Horse	Clint per gram of liver	Size of liver	Weight of horse	Clint per liver	Fup	Corrected Clint per liver	Hepatic blood flow horse	Hepatic Clearance
Flunixin	ul/min/million cells	million cells per gram liver	ul/min/gram	grams	kilograms	ml/min/kg		ml/min/kg	ml/min/kg	ml/min/kg
Fresh	42.7	188.20	8036.14	7500	500	120.5421	0.01	1.205421	23.8	1.147312009
	23.7	301.2	7138.44	7500	500	107.0766	0.01	1.070766	23.8	1.0246661
	41.2	247.5	10197	7500	500	152.955	0.01	1.52955	23.8	1.437186606
Cryo	44	188.2	8280.8	7500	500	124.212	0.01	1.24212	23.8	1.180509318
	37	301.2	11144.4	7500	500	167.166	0.01	1.67166	23.8	1.56195191
	23.3	247.5	5766.75	7500	500	86.50125	0.01	0.8650125	23.8	0.834676143
Parallel Tube Model		Hepatocytes								
	Clint Heps per million cells	HPGL Horse	Clint per gram of liver	Size of liver	Weight of horse	Clint per liver	Fup	Corrected Clint per liver	Hepatic blood flow horse	Hepatic Clearance
	ul/min/million cells	million cells per gram liver	ul/min/gram	grams	kilograms	ml/min/kg		ml/min/kg	ml/min/kg	ml/min/kg
Fresh	42.7	188.20	8036.14	7500	500	120.5421	0.01	1.205421	23.8	1.175403855
	23.7	301.2	7138.44	7500	500	107.0766	0.01	1.070766	23.8	1.047036228
	41.2	247.5	10197	7500	500	152.955	0.01	1.52955	23.8	1.481436548
cryo	44	188.2	8280.8	7500	500	124.212	0.01	1.24212	23.8	1.210263528
	37	301.2	11144.4	7500	500	167.166	0.01	1.67166	23.8	1.614303808
	23.3	247.5	5766.75	7500	500	86.50125	0.01	0.8650125	23.8	0.849481757

Table A.IV.1.7: *In vitro in vivo* extrapolation

Well Stirred Model		Microsomes									
Drug	Clint microsomes	MPPGL Horse	Clint per gram of liver	Size of liver	Weight of horse	Clint per liver	fuinc	Fup	Corrected Clint per liver	Hepatic blood flow horse	Hepatic Clearance
Flunixin	ul/min/mg protein	mg per gram liver	ul/min/gram	grams	kilograms	ml/min/kg			ml/min/kg	ml/min/kg	ml/min/kg
	13	62.40	811.2	7500	500	12.168	0.9	0.01	0.12168	23.8	0.121061063
	12	62.4	748.8	7500	500	11.232	0.9	0.01	0.11232	23.8	0.111792415
	17.5	52.1	911.75	7500	500	13.67625	0.9	0.01	0.1367625	23.8	0.135981109

Parallel Tube Model		Microsomes									
Drug	Clint microsomes	MPPGL Horse	Clint per gram of liver	Size of liver	Weight of horse	Clint per liver	fuinc	Fup	Corrected Clint per liver	Hepatic blood flow horse	Hepatic Clearance
	ul/min/mg protein	mg per gram liver	ul/min/gram	grams	kilograms	ml/min/kg			ml/min/kg	ml/min/kg	ml/min/kg
	13	62.40	811.2	7500	500	12.168	0.9	0.01	0.12168	23.8	0.121369479
	12	62.4	748.8	7500	500	11.232	0.9	0.01	0.11232	23.8	0.112055379
	17.5	52.1	911.75	7500	500	13.67625	0.9	0.01	0.1367625	23.8	0.136370311

Appendix IV.2 Phenylbutazone HPLC-MS detection method

Initial conditions- 50% solvent A and 50% solvent B

Table A.IV.2.1: LC method for detecting phenylbutazone concentrations

Time (minutes)	Solvent A (%)	Solvent B (%)	Flow (mL/min)	Pressure (bar)
0.00	50.0	50.0	1.00	400
1.00	0.00	100	1.00	400
3.00	0.00	100	1.00	400
4.00	50.0	50.0	1.00	400
5.00	50.0	50.0	1.00	400

Table A.III.2.2: Mass spectrometry method for phenylbutazone and diclofenac and phenylbutazone metabolite (oxyphenbutazone)

Drug	Ionised Mass (M/Z)	Dwell (seconds)	Cone (volts)	~ Retention time, min
Phenylbutazone	309.19	0.200	50.0	2.11
Diclofenac	296.19	0.200	35.0	2.35
Oxyphenbutazone	325.19	0.200	50.0	1.9

Table A.IV.2.3: K_{dep} and V_0 data for microsomes, fresh and cryopreserved hepatocyte incubations for phenylbutazone disappearance

Horse	*In vitro* liver model	Phenylbutazone concentration (µM)	K_{dep} (µM)	V_0 (µM/min)
1	**Fresh Hepatocytes**	1	0.0482	0.0482
		5	0.0276	0.1380
		10	0.0188	0.188
		20	0.0229	0.4580
		50	0.0120	0.600
		75	0.0089	0.668
		100	0.0044	0.440
		150	0.0019	0.285
	Cryopreserved hepatocytes	1	0.0227	0.0227
		5	0.0136	0.068
		10	0.0150	0.150
		20	0.010	0.200
		50	0.006	0.310
		75	0.005	0.353
		100	0.003	0.310
		150	0.002	0.270
	Microsomes	1	0.054	0.054
		5	0.030	0.152
		10	0.032	0.324
		20	0.024	0.470
		50	0.012	0.600
		75	0.008	0.570
		100	0.003	0.320
		150	0.002	0.270

2	**Fresh Hepatocytes**	1	0.034	0.034
		5	0.01	0.05
		10	0.0104	0.104
		20	0.0106	0.212
		50	0.0054	0.27
		75	0.0046	0.345
		100	0.0024	0.24
		150	0.0014	0.21
	Cryopreserved hepatocytes	1	0.0124	0.0124
		5	0.0127	0.0635
		10	0.0114	0.114
		20	0.0099	0.198
		50	0.0069	0.345
		75	0.006	0.45
		100	0.0031	0.31
		150	0.0018	0.27
	Microsomes	1	0.044	0.044
		5	0.02	0.1
		10	0.0229	0.229
		20	0.0155	0.31
		50	0.0114	0.57
		75	0.0102	0.765
		100	0.0076	0.76
		150	0.0032	0.48
3	**Fresh Hepatocytes**	1	0.0471	0.0471
		5	0.0338	0.169
		10	0.0285	0.285
		20	0.019	0.38
		50	0.0107	0.535
		75	0.0089	0.668
		100	0.0046	0.46
		150	0.0026	0.39
	Cryopreserved hepatocytes	1	0.0208	0.0208
		5	0.0233	0.1165
		10	0.0164	0.164
		20	0.0136	0.272
		50	0.0075	0.375
		75	0.0056	0.42
		100	0.0034	0.34
		150	0.002	0.3
	Microsomes	1	0.0388	0.0388
		5	0.021	0.105
		10	0.0179	0.179
		20	0.0176	0.352
		50	0.0074	0.37
		75	0.0061	0.4575
		100	0.0042	0.42
		150	0.002	0.3

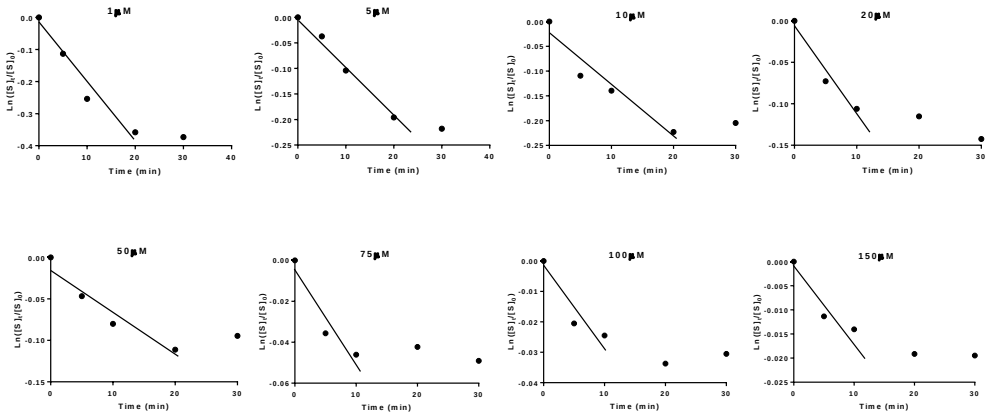


Figure A.IV.2.1: data gathered using various phenylbutazone concentrations with freshly isolated equine hepatocytes. Data was plotted as the natural logarithm (Ln) of substrate concentration against time. K_{dep} is represented by the slope of the line (refer to table A.IV.2.3, horse 2).

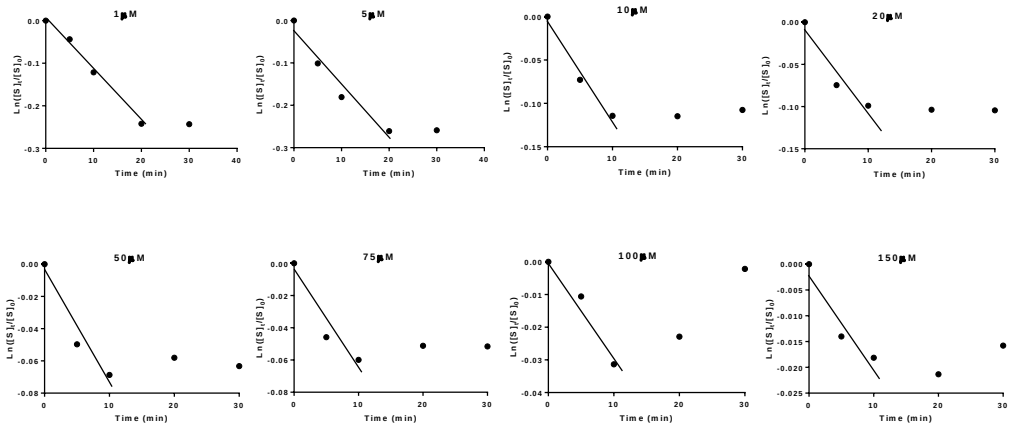


Figure A.IV.2.2: data gathered using various phenylbutazone concentrations with cryopreserved equine hepatocytes. Data was plotted as the natural logarithm (Ln) of substrate concentration against time. K_{dep} is represented by the slope of the line (refer to table A.IV.2.3, horse 2).

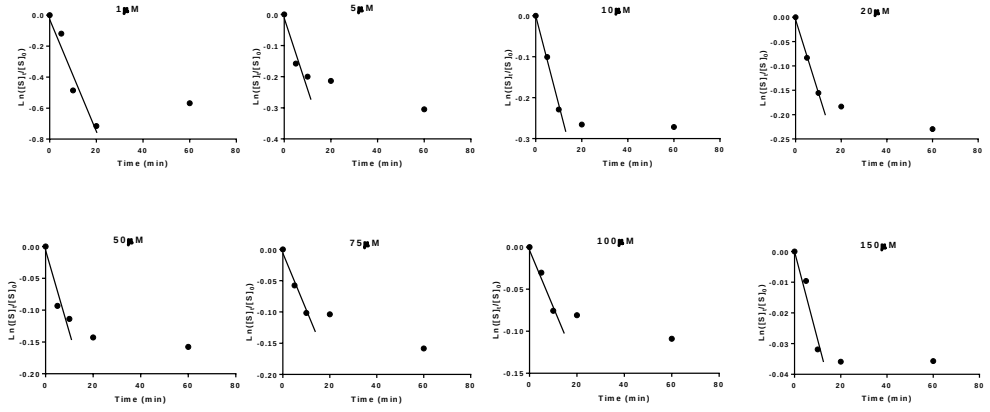


Figure A.IV.2.3: data gathered using various phenylbutazone concentrations with equine microsomes. Data was plotted as the natural logarithm (Ln) of substrate concentration against time. K_{dep} is represented by the slope of the line (refer to table A.IV.2.3, horse 2).

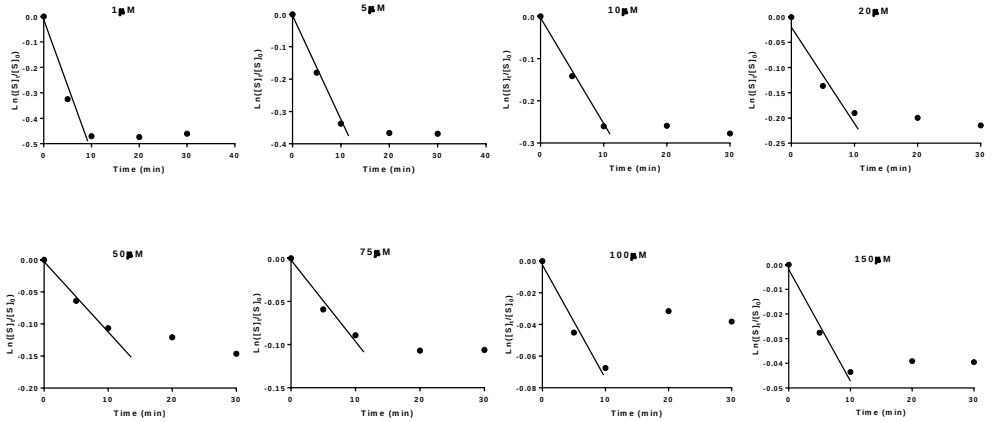


Figure A.IV.2.4: data gathered using various phenylbutazone concentrations with freshly isolated equine hepatocytes. Data was plotted as the natural logarithm (Ln) of substrate concentration against time. K_{dep} is represented by the slope of the line (refer to table A.IV.2.3, horse 3).

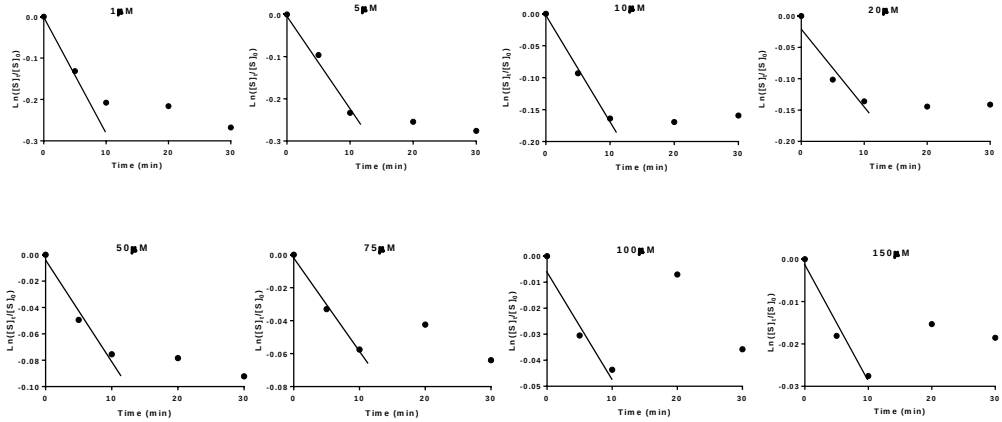


Figure A.IV.2.5: data gathered using various phenylbutazone concentrations with cryopreserved equine hepatocytes. Data was plotted as the natural logarithm (Ln) of substrate concentration against time. K_{dep} is represented by the slope of the line (refer to table A.IV.2.3, horse 3).

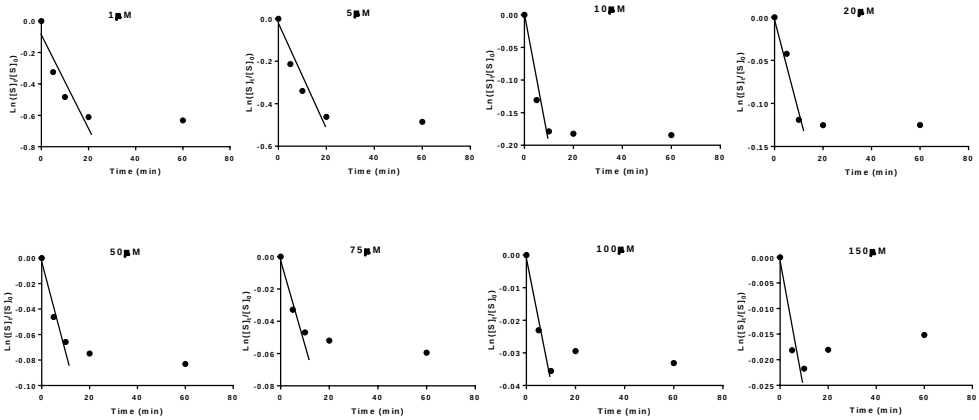


Figure A.IV.2.6: data gathered using various phenylbutazone concentrations with equine microsomes. Data was plotted as the natural logarithm (Ln) of substrate concentration against time. K_{dep} is represented by the slope of the line (refer to table A.IV.2.3, horse 3).

Table A.IV.2.4: $K_{appearance}$ and V_0 data for microsomes incubations for oxyphenbutazone appearance

Horse	*In vitro* liver model	Phenylbutazone concentration (µM)	$K_{appearnce}$ (µM)	V_0 (µM/min)
1	**Fresh hepatocytes**	1	-	-
		5	-	-
		10	0.0102	0.102
		20	0.0212	0.424
		50	0.0224	1.12
		75	0.0482	3.615
		100	0.0283	2.83
		150	0.0172	2.58
1	**Cryo. hepatocytes**	1	-	-
		5	-	-
		10	0.0068	0.068
		20	0.0073	0.146
		50	0.0073	0.365
		75	0.0109	0.8175
		100	0.0096	0.96
		150	0.0083	1.245
1	**Microsomes**	1	0.0051	0.0051
		5	0.0640	0.320
		10	0.1257	1.257
		20	0.2004	4.008
		50	0.1477	7.385
		75	0.1395	10.4625
		100	0.1112	11.12
		150	0.0839	12.585
2	**Microsomes**	1	0.0115	0.0115
		5	0.0497	0.2485
		10	0.0785	0.785

		20	0.1781	3.562
		50	0.2055	10.275
		75	0.1926	14.445
		100	0.1392	13.92
		150	0.0891	13.365
3	**Microsomes**	1	-	-
		5	0.016	0.08
		10	0.02	0.2
		20	0.025	0.494
		50	0.032	1.62
		75	0.019	1.39
		100	0.017	1.69
		150	0.013	2.01

Table A.III.2.5: Summary of scaling values for the three horses used for phenylbutazone study

Horse No	Hepatocytes		Microsomes	
	P450 nmoles/10^6 hepatocytes	Hepatocellularity (10^6cells/g liver)	nmol P450/mg of protein	mg Microsomal protein per g liver
1	0.123	301.2	0.594	62.4
2	0.117	247.5	0.557	52.1
3	0.126	192.7	0.416	58.5

Table A.IV.2.6: *In vitro in vivo* extrapolation

Well Stirred Model		Hepatocytes								
Drug	Clint Heps per million cells	HPGL Horse	Clint per gram of liver	Size of liver	Weight of horse	Clint per liver	Fup	Corrected Clint per liver	Hepatic blood flow horse	Hepatic Clearance
Phenylbutazone	ul/min/million cells	million cells per gram liver	ul/min/gram	grams	kilograms	ml/min/kg		ml/min/kg	ml/min/kg	ml/min/kg
Fresh	26	301.19	7830.94	7500	500	117.4641	0.01	1.174641	23.8	1.1193937
	11.8	247.5	2920.5	7500	500	43.8075	0.01	0.438075	23.8	0.430157304
	28	192.7	5395.6	7500	500	80.934	0.01	0.80934	23.8	0.78272282
Cryo	15.5	301.19	4668.445	7500	500	70.026675	0.01	0.70026675	23.8	0.680251722
	11.6	247.5	2871	7500	500	43.065	0.01	0.43065	23.8	0.422996081
	20.8	192.7	4008.16	7500	500	60.1224	0.01	0.601224	23.8	0.586410387

Parallel Tube Model		Hepatocytes								
	Clint Heps per million cells	HPGL Horse	Clint per gram of liver	Size of liver	Weight of horse	Clint per liver	Fup	Corrected Clint per liver	Hepatic blood flow horse	Hepatic Clearance
	ul/min/million cells	million cells per gram liver	ul/min/gram	grams	kilograms	ml/min/kg		ml/min/kg	ml/min/kg	ml/min/kg
Fresh	26	301.19	7830.94	7500	500	117.4641	0.01	1.174641	23.8	1.146125049
	11.8	247.5	2920.5	7500	500	43.8075	0.01	0.438075	23.8	0.434067907
	28	192.7	5395.6	7500	500	80.934	0.01	0.80934	23.8	0.795733509
Cryo	15.5	301.19	4668.445	7500	500	70.026675	0.01	0.70026675	23.8	0.690065085
	11.6	247.5	2871	7500	500	43.065	0.01	0.43065	23.8	0.426777188
	20.8	192.7	4008.16	7500	500	60.1224	0.01	0.601224	23.8	0.593693629

Table A.IV.2.7: *In vitro in vivo* extrapolation

Well Stirred Model		Microsomes								
Drug	Clint microsomes	MPPGL Horse	Clint per gram of liver	Size of liver	Weight of horse	Clint per liver	Fup	Corrected Clint per liver	Hepatic blood flow horse	Hepatic Clearance
	ul/min/mg protein	mg per gram liver	ul/min/gram	grams	kilograms	ml/min/kg		ml/min/kg	ml/min/kg	ml/min/kg
Phenylbutazone	32.2	62.40	2009.28	7500	500	30.1392	0.01	0.301392	23.8	0.297623042
	18.2	52.10	948.22	7500	500	14.2233	0.01	0.142233	23.8	0.14138804
	24.8	58.50	1450.8	7500	500	21.762	0.01	0.21762	23.8	0.215648178
Parallel Tube Model		Microsomes								
Drug	Clint microsomes	MPPGL Horse	Clint per gram of liver	Size of liver	Weight of horse	Clint per liver	Fup	Corrected Clint per liver	Hepatic blood flow horse	Hepatic Clearance
	ul/min/mg protein	mg per gram liver	ul/min/gram	grams	kilograms	ml/min/kg		ml/min/kg	ml/min/kg	ml/min/kg
	32.2	62.40	2009.28	7500	500	30.1392	0.01	0.301392	23.8	0.299491687
	18.2	52.10	948.22	7500	500	14.2233	0.01	0.142233	23.8	0.141808841
	24.8	58.50	1450.8	7500	500	21.762	0.01	0.21762	23.8	0.2166281

Table A.IV.2.7: *In vitro in vivo* extrapolation

Well Stirred Model		Microsomes								
Drug	Clint microsomes	MPPGL Horse	Clint per gram of liver	Size of liver	Weight of horse	Clint per liver	Fup	Corrected Clint per liver	Hepatic blood flow horse	Hepatic Clearance
Oxyphenbutazone	ul/min/mg protein	mg per gram liver	ul/min/gram	grams	kilograms	ml/min/kg		ml/min/kg	ml/min/kg	ml/min/kg
	15.2	62.41	948.632	7500	500	14.22948	0.01	0.1422948	23.8	0.141449108
	10.4	52.12	542.048	7500	500	8.13072	0.01	0.0813072	23.8	0.081030378
		58.51	0	7500	500	0	0.01	0	23.8	

Parallel Tube Model		Microsomes								
Drug	Clint microsomes	MPPGL Horse	Clint per gram of liver	Size of liver	Weight of horse	Clint per liver	Fup	Corrected Clint per liver	Hepatic blood flow horse	Hepatic Clearance
	ul/min/mg protein	mg per gram liver	ul/min/gram	grams	kilograms	ml/min/kg		ml/min/kg	ml/min/kg	ml/min/kg
	15.2	62.41	948.632	7500	500	14.22948	0.01	0.1422948	23.8	0.141870272
	10.4	52.12	542.048	7500	500	8.13072	0.01	0.0813072	23.8	0.081168474
		58.51	0	7500	500	0	0.01	0	23.8	0

References

Acikgöz, A., Giri S., Cho M. G., and Bader A. 2013. 'Morphological and Functional Analysis of Hepatocyte Spheroids Generated on Poly-HEMA-Treated Surfaces under the Influence of Fetal Calf Serum and Nonparenchymal Cells'. *Biomolecules* 3 (1): 242–69.

Alsanosi, S. M. M., Skiffington C., and Padmanabhan S. 2014. *Pharmacokinetic Pharmacogenomics*. *Handbook of Pharmacogenomics and Stratified Medicine*. Elsevier Inc.

American Pharmaceutical Association. 1972. *Guidelines for Biopharmaceutical Studies in Man*. Washington, DC: American Pharmaceutical Association.

Andrews, F. M., Frank N., Sommardahl C. S., Buchanan B. R., Elliott S. B., and Allen V. A. 2006. 'Effects of Intravenously Administrated Omeprazole on Gastric Juice pH and Gastric Ulcer Scores in Adult Horses.' *Journal of Veterinary Internal Medicine / American College of Veterinary Internal Medicine* 20 (5): 1202–6.

Animals in Science Regulation Unit. 2014. 'Code of Practice for the Housing and Care of Animals Bred, Supplied or Used for Scientific Purposes.'

Ansede, J. H., Smith W. R., Perry C. H., St. Claire III R. L., and Brouwer K. R. 2010. 'An In Vitro Assay to Assess Transporter-Based Cholestatic Hepatotoxicity Using Sandwi ... Page 1 of 1 An In Vitro Assay to Assess Transporter- Based Cholestatic Hepatotoxicity Using Sandwich-Cultured Rat Hepatocytes'. *In Vitro* 38 (2): 2010–2010.

Arikura, J., Kobayashi N., Okitsu T., Noguchi H., Totsugawa T., Watanabe T., Matsumura T., et al. 2002. 'UW Solution: A Promising Tool for Cryopreservation of Primarily Isolated Rat Hepatocytes'. *Journal of Hepato-Biliary-Pancreatic Surgery* 9 (6): 742–49.

Astashkina, A., Mann B., and Grainger D. W. 2012. 'A Critical Evaluation of in Vitro Cell Culture Models for High-Throughput Drug Screening and Toxicity.' *Pharmacology & Therapeutics* 134 (1). Elsevier Inc.: 82–106.

Austin, R. P., Barton P., Cockroft S. L., Wenlock M. C., and Riley R. J. 2002. 'The Influence of Nonspecific Microsomal Binding on Apparent Intrinsic Clearance, and Its Prediction from Physicochemical Properties'. *Drug Metabolism and Disposition* 30 (12): 1497–1503.

Bachmann, A., Moll M., Gottwald E., Nies C., Zantl R., Wagner H., Burkhardt B., et al. 2015. '3D Cultivation Techniques for Primary Human Hepatocytes'. *Microarrays* 4: 64–83.

Bachmann, K., Byers J., and Ghosh R. 2003. 'Prediction of in Vitro Hepatic Clearance from in Vitro Data Using Cryopreserved Human Hepatocytes'. *Xenobiotica* 33: 475–83.

Badyal, D. K., and Dadhich A. P. 2001. 'Cytochrome P450 and Drug Interactions'. *Indian Journal of Pharmacology* 33: 248–59.

Bailey, S. R., Katz L. M., Berhane Y., Samuels T., De Brauvere N., Marr C. M., and Elliott J. 2003. 'Seasonal Changes in Plasma Concentrations of Cecum-Derived Amines in Clinically Normal Ponies and Ponies Predisposed to Laminitis'. *American Journal of Veterinary Research* 64 (9): 1132–38.

Bakala, A., Karlik W., and Wiechetek M. 2003. 'Preparation of Equine Isolated Hepatocytes'. *Toxicology in Vitro* 17 (5–6): 615–21.

Banse, H. E., La D., and Cribb A. E. 2015. 'Review of Nonsteroidal Anti-Inflammatory Drug Selection in Horses' 61.

Barragry, T. 2006. 'Doping and Drug Detection Times in Horses: New Data for Therapeutic Agents'. *Irish Veterinary Journal* 59 (7): 394–98.

Barter, Z. E., Chowdry J. E., Harlow J. R., Sanwder J. E., and Lipscomb J. C. 2008. 'Covariation of Human Microsomal Protein Per Gram of Liver with Age : Absence of Influence of Operator and Sample'. *Drug Metabolism and Disposition* 36 (12): 2405–9.

Barter, Z., Bayliss M., Beaune P., Boobis A., Carlile D., Edwards R., Houston J.B., et al. 2007. 'Scaling Factors for the Extrapolation of In Vivo Metabolic Drug Clearance From In Vitro Data: Reaching a Consensus on Values of Human Micro-Somal Protein and Hepatocellularity Per Gram of Liver'. *Current Drug Metabolism* 8 (1): 33–45.

Barthová, J., Pecka M., and Leblová S. 1977. 'The Function of Sulfhydryl Groups in Lactate Dehydrogenase Isolated from Soy Bean Seedlings Using Blue Dextran-Sepharose'. *Collection of Czechoslovak Chemical Communications* 42 (12): 3705–11.

Basu, T. K., Dickerson J. W. T., and Parke D. V. W. 1971. 'Effect of Development on the Activity of Microsomal Drug-Metabolizing Enzymes in Rat Liver'. *Biochem. J.* 124: 19–24.

Bayliss, M. K., Bell J. A., Jenner W. N., Park G. R., and Wilson K. 1999. 'Utility of Hepatocytes to M Odel Species Diå Erences in the M Etabolism of Loxtidine and to Predict Pharm Acokinetic Param Eters in Rat , Dog and M an Evidence for the Presence of a Glucuronide Metabolite Was Observed . Model for the Prediction of Xenobi'.

Xenobiotica 29 (3): 253–68.

Begg, L. M., and O'Sullivan C. B. 2003. 'The Prevalence and Distribution of Gastric Ulceration in 345 Racehorses'. *Australian Veterinary Journal* 81 (4): 199–201.

Bell, C. C., Hendriks D. F. G., Moro S. M. L., Ellis E., Walsh J., Renblom A., Puigvert L. F., et al. 2016. 'Characterization of Primary Human Hepatocyte Spheroids as a Model System for Drug-Induced Liver Injury , Liver Function and Disease'. *Nature Publishing Group*. Nature Publishing Group.

Berry, M. N., and A. M. Edwards. 2001. *The Hepatocyte Review*. Edited by Michael N. Berry and Anthony M. Edwards. First. Dordrechet, The Netherlands: Kluwer academic Publisher.

Bertolotti, M., N. Abate, S. Bertolotti, P. Loria, M. Concari, R. Messora, F. Carubbi, A. Pinetti, and N. Carulli. 1993. 'Effect of Aging on Cholesterol 7a-Hydroxylation in Humans'. *J. of Lipid Res.* 34: 1001–7.

Bi, Y. A., Kazolias D., and Duignan D. B. 2006. 'Use of Cryopreserved Human Hepatocytes in Sandwich Culture to Measure Hepatobiliary Transport' 34 (9): 1658–65.

Biosciences, Amersham. 2013. *Percoll: Methodology and Applications*.

Bisswanger, H. 2008. *Enzyme Kinetics. Principles and Methods*. Second. Weinheim: WILEY-VCH.

Blanca, J., Muñoz R., Muñoz P., Aranda Á., Díaz R., and de Pozuelo M. M. 2013. 'Analysis of Phenylbutazone Residues in Horse Muscle'.

Blanchard, N., Richert L., Coassolo P., and Lave T. 2004. 'Qualitative and Quantitative Assessment of Drug-Drug Interaction Potential in Man, Based on Ki, IC50 and Inhibitor Concentration'. *Current Drug Metabolism* 5 (2): 147–56.

Boison, J. O., Dowling T., and Kinar J. 2016. 'Analysis of Phenylbutazone Residues in Horse Tissues with and without Enzyme-Hydrolysis by LC-MS / MS'. *Drug Testing and Analysis* 8 (April): 535–38.

Bonate, P. L. 2010. 'A Brief Introduction to Monte Carlo Simulation'. *Clinical Pharmacokinetics* 40 (1): 15–22.

Boner, P. L, Liu D. D. W., Feely W. F., Wisocky M. J., and Wu J. 2003. 'Determination and Confirmation of 5-Hydroxyflunixin in Raw Bovine Milk Using Liquid Chromatography Tandem Mass Spectrometry'. *Journal of Agricultural and Food Chemistry* 51: 3753–59.

Bottoms, G. D., Fessler J. F., Roesel O. F., Moore A. B., and Frauenfelder H. C. 1981. 'Endotoxin-Induced Hemodynamic Changes in Ponies:

Effects of Flunixin Meglumine'. *American Journal of Veterinary Research* 42 (9): 1514–18.

Boyer, T. D., Sanyal A. J., Lindor K. D., and Terrault N. A. 2018. *Zakim and Boyer's Hepatology: A Textbook of Liver Disease*. Edited by Arun J. Sanyal, Keith D. Lindor, Thomas D. Boyer, and Norah A. Terrault. 7th ed. Philadelphia: Elsevier.

Bradford, M. M. 1976. 'A Rapid and Sensitive Method for the Quantitation of Microgram Quantities of Protein Utilizing the Principle of Protein-Dye Binding.' *Analytical Biochemistry* 72 (May): 248–54.

Bragulla, H., Burdas K. D., Ćerveny C., König H. E., and Liebich H. G. 2004. *Veterinary Anatomy of Domestic Mammals*. Edited by Liebich H. -G. könig H. E. First. stuttgart, Germany: Schattauer GmbH.

Brandon, E.F. A., Raap C.D, Meijerman I., Hbeijnen J., and Mschellens J. H. 2003. 'An Update on in Vitro Test Methods in Human Hepatic Drug Biotransformation Research: Pros and Cons'. *Toxicology and Applied Pharmacology* 189 (3): 233–46.

Breslin, S., and O'Driscoll L. 2013. 'Three-Dimensional Cell Culture: The Missing Link in Drug Discovery.' *Drug Discovery Today* 18 (5–6). Elsevier Ltd: 240–49.

British Horseracing Autority. 2013. 'Economic Impact of British Racing 2013'.

Brown, H. S., Chadwick A., and Houston J. B. 2007. 'Use of Isolated Hepatocyte Preparations for Cytochrome P450 Inhibition Studies: Comparison with Microsomes for Ki Determination'. *Drug Metabolism and Disposition* 35 (11): 2119–26.

Brown, H. S., Griffin M., and Houston J. B. 2007. 'Evaluation of Cryopreserved Human Hepatocytes as an Alternative in Vitro System to Microsomes for the Prediction of Metabolic Clearance'. *Drug Metabolism and Disposition* 35 (2): 293–301.

Brunton, L. L., Chabner B. A., and Knollmann B. C. 2012. *Goodman & Gilman's The Pharmacological Basis of Threabutics*. Twelfth. Mcgraw-Hill Proffessional's MediaCenter.

Burdas, KD, Sack W. O., and Rock S. 2003. *Anatomy of the Horse*. 4th ed. Germany, Schlütersche.

Burrows, G. E., MacAllister C. G., Tripp P., and Black J. 1989. 'Interactions between Chloramphenicol, Acepromazine, Phenylbutazone, Rifampin and Thiamylal in the Horse'. *Equine Veterinary Journal* 21 (1): 34–38.

Cantrill, C., and Houston J. B. 2017. 'Understanding the Interplay Between

Uptake and Efflux Transporters Within In Vitro Systems in Defining Hepatocellular Drug Concentrations'. *Journal of Pharmaceutical Sciences* 106 (9): 2815–25.

Carlile, D. J., Zomorodi K., and Houston J. B. 1997. 'Scaling Factors to Relate Drug Metabolic Clearance in Hepatic Microsomes , Isolated Hepatocytes, and the Intact Liver' 25 (8): 903–11.

Chang, R. 2005. *Physical Chemistry for the Biosciences*. Sausalito: University Science Books.

Chapman, G. B., and Eagles D. A. 2007. 'Ultrastructural Features of Glisson's Capsule and the Overlying Mesothelium in Rat, Monkey and Pike Liver.' *Tissue & Cell* 39 (5): 343–51.

Chauret, N., Gauthier A., Martin J., and Nicoll-griffith D. A. 1997. 'In Vitro Comparison of Cytochrome P450-Mediated Metabolic Activities in Human , Dog , Cat , and Horse'. *Drug Metabolism & Disposition* 25 (10): 1130–36.

Chay, S., Woods W. E., Nugent T., Blake J. M., and Tobin T. 1982. 'The Pharmacology of Nonsteroidal Anti-Inflammatory Drugs in the Horse:Flunixin Meglumine(Banamine)'. *Equine Practice* 4 (10): 16–23.

Chesné, C., and Guillouzo A. 1988. 'Cryopreservation of Isolated Rat Hepatocytes: A Critical Evaluation of Freezing and Thawing Conditions'. *Cryobiology* 25 (4): 323–30.

Chesné, C., Guyomard C., Fautrel A., Frémond B., Poullain M-G, Fremond B., De Jong H., and Guillouzo A. 1993. 'Viability and Function in Primary Culture of Adult Hepatocytes from Various Animal Species and Human Beings after Cryopreservation'. *Hepatology* 18: 406–414.

Chiba, K., Kobayashi K., Manabe K., Tani M., Kamataki T., and Ishizaki T. 1993. 'Oxidative Metabolism of Omeprazole in Human Liver Microsomes: Cosegregation with S-Mephenytoin 4'-hydroxylation'. *Pharmacol Exp Ther* 266 (1): 52–59.

Chung, E. W., Ho E. N. M., Leung D. K. K., Tang F. P. W., Yiu K. C. H., and T. S. M.. Wan. 2004. 'Detection of Anti-Ulcer Drugs and Their Metabolites in Horse Urine by Liquid Chromatography - Mass Spectrometry'. *Chromatographia* 59 (S1): S29–38.

Clark, J. O., and Clark T. P. 1999. 'Analgesia'. *Veterinary Clinics of North America - Equine Practice* 15: 705–23.

Cohen, C. 1987. 'The Case for the Use Animals in Biomedical Research'. *The England Journal of Medicine* 315 (26): 858–67.

Cohen, I., Weliky I., Lan S-j, and Levine D. 1974. 'Metabolism of [14C]

Niflumic Acid Isolation and Identification of Metabolites from Human Urine'. *Biomedical Mass Spectrometry* 1: 1–4.

Cornish-Bowden, A. 2012. *Fundamentals of Enzyme Kinetics*. Fourth. London: Wiley–Blackwell.

Coundouris, J. A., Grant H. M., Engeset J., Petric J. C., and Hawksworth G. M. 1993. 'Cryopreservation of Human Adult Hepatocytes for Use in Drug Metabolism and Toxicity Studies'. *Xenobiotica* 23: 1399–1409.

Dambach, D. M., Andrews B. A., and Moulin F. 2005. 'New Technologies and Screening Strategies for Hepatotoxicity: Use of in Vitro Models.' *Toxicologic Pathology* 33 (1): 17–26.

De Bartolo, L., Morelli S., Piscioneri A., Lopez L. C., Favia P., D'Agostino R., and Drioli E. 2007. 'Novel Membranes and Surface Modification Able to Activate Specific Cellular Responses'. *Biomolecular Engineering* 24 (1 SPEC. ISS.): 23–26.

De Bartolo, L., Salerno S., Curcio E., Piscioneri A., Rende M., Morelli S., Tasselli F., Bader A., and Drioli E. 2009. 'Human Hepatocyte Functions in a Crossed Hollow Fiber Membrane Bioreactor'. *Biomaterials* 30 (13). Elsevier Ltd: 2531–43.

de la Iglesia, F. A., Sturgess J. M., McGuire E. J., and Feuer G. 1976. 'Quantitative Microscopic Evaluation of the Endoplasmic Reticulum in Developing Human Liver'. *American Journal of Pathology* 82 (1): 61–70.

De Loecker, W., Koptelov V. A., Grischenko V. I., and De Loecker P. 1998. 'Effects of Cell Concentration on Viability and Metabolic Activity during Cryopreservation'. *Cryobiology* 37 (2): 103–9.

Dean, L. 2016. 'Omeprazole Therapy and CYP2C19 Genotype Drug Class : Proton Pump Inhibitors Drug : Omeprazole'. In *Medical Genetics Summaries*, edited by Victoria Pratt, Howard McLeod, Laura Dean, Adriana Malheiro, and Wendy Rubinstein, 233–40. National Center for Biotechnology Information.

Dickins, M., Elcombe C. R., Moloney S. J., Netter K. J., and Bridges J. W. 1979. 'Further Studies on the Dissociation of the Isosafrole Metabolite-Cytochrome P-450 Complex'. *Biochemical Pharmacology* 28 (2): 231–38.

Diener, B., Dietmar U., Beer N., Heike D., and Oesch F. 1993. 'A Method for the Cryopresrvation of Liver Parenchymal Cells for Studies of Xenobiotics'. *Cryobiology* 30: 116–27.

Dieterle, W., Faigle J. W., Früh F., Mory H., Theoblad W., Alt K. O., and

Richter W. J. 1976. 'Metabolism of Phenylbutazone in Man'. *Arzneimittelforschung* 26: 572-.

Dittrich, P. S., and Manz A. 2006. 'Lab-on-a-Chip: Microfluidics in Drug Discovery.' *Nature Reviews. Drug Discovery* 5 (3): 210–18.

Dou, M., de Sousa G., Lacarelle B., Placidi M., Lechene P., Domingo M., Lafont H., and Rahmani R. 1992. 'Thawed Human Hepatocytes in Primary Culture'. *Cryobiology* 469 (1992): 454–69.

Dowling, P. M. 2002. 'Drug Withdrawal Times for Performance Horses and Horses Intended for Food'. *Clinical Techniques in Equine Practice* 1 (2): 68–73.

Dyke, T. M., Hubbell J. A., Sams R. A., and Hinchcliff K. W. 1998. 'Hepatic Blood Flow in Horses during the Recuperative Period from Maximal Exercise.' *Amarecan Journal of Veterinary Research* 59 (11): 1476–80.

Endres, Christopher J., Peng Hsiao, Francisco S. Chung, and Jashvant D. Unadkat. 2006. 'The Role of Transporters in Drug Interactions'. *European Journal of Pharmaceutical Sciences* 27 (5): 501–17.

Engelmann, G. L., Richardson A., Katz A., and Fierer J. A. 1981. 'Age-Related Changes in Isolated Rat Hepatocytes. Compansation of Size, Morphology, Binucleation, and Protein Content'. *Mechanisms of Aging and Development* 16: 385–95.

Federation, Equestre Internationale. 2017. '2018 Equine Prohibited Substances List'.

Ferdowsian, H. R, and Beck N. 2011. 'Ethical and Scientific Considerations Regarding Animal Testing and Research.' *PloS One* 6 (9): e24059.

Fersht, A. 1999. *Structure and Mechanism in Protein Science: A Guide to Enzyme Catalysis and Protein Folding*. Second. Washington, DC: W. H. Freeman and Company.

Fessler, J. F., Bottoms G. D., Roesel O. F., Moore A. B., Frauenfelder H. C., and Boon G. D. 1982. 'Endotoxin-Induced Change in Hemograms, Plasma Enzymes, and Blood Chemical Values in Anesthetized Ponies: Effects of Flunixin Meglumine'. *American Journal of Veterinary Research* 43 (1): 140–44.

Foster, J. A., Houston J B., and Hallifax D. 2011. 'Comparison of Intrinsic Clearances in Human Liver Microsomes and Suspended Hepatocytes from the Same Donor Livers: Clearance-Dependent Relationship and Implications for Prediction of in Vivo Clearance.' *Xenobiotica; the Fate of Foreign Compounds in Biological Systems* 41 (2): 124–36.

Friebe, M., Schumacher S., Stahl J., and Kietzmann M. 2013. 'Synovial

Distribution Of "systemically" administered Acetylsalicylic Acid in the Isolated Perfused Equine Distal Limb.' *BMC Veterinary Research* 9 (January).

Furge, L. L., and Guengerich F. P. 2006. 'Cytochrome P450 Enzymes in Drug Metabolism and Chemical Toxicology: An Introduction'. *Biochemistry and Molecular Biology Education* 34 (2): 66–74.

Garré, B., Shebany K., Gryspeerdt A., Baert K., van der Meulen K., Nauwynck H., Deprez P., De Backer P., and Croubels S. 2007. 'Pharmacokinetics of Acyclovir after Intravenous Infusion of Acyclovir and after Oral Administration of Acyclovir and Its Prodrug Valacyclovir in Healthy Adult Horses.' *Antimicrobial Agents and Chemotherapy* 51 (12): 4308–14.

Gavhane Y. N. and Yadav A. V. 2012. 'Loss of Orally Administered Drugs in GI Tract'. *Saudi Pharmaceutical Journal* 20 (4). King Saud University: 331–44.

Gebhardt, R., Hengstler J. G., Müller D., Glöckner R., Buenning P., Laube B., Schmelzer E., et al. 2003. 'New Hepatocyte in Vitro Systems for Drug Metabolism: Metabolic Capacity and Recommendations for Application in Basic Research and Drug Development, Standard Operation Procedures.' *Drug Metabolism Reviews* 35 (2–3): 145–213.

Gebhardt, R., and Matz-soja M. 2014. 'Liver Zonation : Novel Aspects of Its Regulation and Its Impact on Homeostasis'. *World Journal of Gastroenterology* 20 (26): 8491–8504.

Gerring, E. L., Lees P., and Taylor J. B. 1981. 'Pharmacokinetics of Phenylbutazone and Its Metabolites in the Horse'. *Equine Veterinary Journal* 13 (3): 152–57.

Gibson, G., and Sket P. 2001. 'Introduction to Drug Metabolism'. Edited by Gordon Gibson G. and Paul Sket. Cheltenham: Nelson Thornes.

Godoy, P., Hewitt N. J., Albrecht U., Andersen M. E., Ansari N., Bhattacharya S., Bode J. G., et al. 2013. 'Recent Advances in 2D and 3D in Vitro Systems Using Primary Hepatocytes, Alternative Hepatocyte Sources and Non-Parenchymal Liver Cells and Their Use in Investigating Mechanisms of Hepatotoxicity, Cell Signaling and ADME.' *Archives of Toxicology* 87 (8): 1315–1530.

Gray, H. B., and Winkler J. R. 1996. 'Electron Transfer in Proteins'. *Annu. Rev. Biochem.* 65: 537–61.

Griffin, J. S., and Houston J B. 2004. 'Comparison of Fresh and Cryopreserved Rat Hepatocyte Suspensions for The Prediction of In

Vitro Intrinsic Clearance'. *Drug Metabolism and Disposition* 32: 552–58.

Grijalva, J., and Vakili K. 2013. 'Neonatal Liver Physiology.' *Seminars in Pediatric Surgery* 22 (4). Elsevier: 185–89.

Grondin, M., Hamel F., Averill-Bates D. A., and Sarhan F. 2009. 'Wheat Proteins Enhance Stability and Function of Adhesion Molecules in Cryopreserved Hepatocytes.' *Cell Transplantation* 18 (1): 79–88.

Groneberg, D. A., Grosse-Siestrup C., and Fischer A. 2002. 'In Vitro Models to Study Hepatotoxicity'. *Toxicologic Pathology* 30 (3): 394–99.

Guengerich, F. P., Martin M. V., Sohl C. D., and Cheng Q. 2009. 'Measurement of Cytochrome P450 and NADPH-Cytochrome P450 Reductase.' *Nature Protocols* 4 (9): 1245–51.

Gupta, S. 2000. 'Hepatic Polyploidy and Liver Growth Control.' *Seminars in Cancer Biology* 10 (3): 161–71.

Hakooz, N., Ito K., Rawden H., Gill H., Lemmers L., Boobies A. R., Edwards R. J., Carlile D. J., Lake B. G., and Brian H. J. 2006. 'Determination of a Human Hepatic Microsomal Scaling Factor for Predicting in Vivo Drug Clearance'. *Pharmaceutical Research* 23: 533–39.

Hallifax, D., Foster J. A., and Houston J. B. 2010. 'Prediction of Human Metabolic Clearance from in Vitro Systems: Retrospective Analysis and Prospective View'. *Pharmaceutical Research* 27 (10): 2150–61.

Hallifax, D., Turlizzi E., Zanelli U., and Houston J. B. 2012. 'Clearance-Dependent Underprediction of in Vivo Intrinsic Clearance from Human Hepatocytes: Comparison with Permeabilities from Artificial Membrane (PAMPA) Assay, in Silico and Caco-2 Assay, for 65 Drugs'. *European Journal of Pharmaceutical Sciences* 45 (5): 570–74.

Hammond, C. J., Mason D. K., and Watkins K. L. 1986. 'Gastric Ulceration in Mature Thoroughbred Horses'. *Equine Veterinary Journal* 18 (4): 284–87.

Harris, C. L., Toner M., Hubel A., Cravalho E. G., Yarmush M. L., and Tompkins R. G. 1991. 'Cryopreservation of Isolated Hepatocytes: Intracellular Ice Formation under Various Chemical and Physical Conditions'. *Cryobiology* 28 (5): 436–44.

Hediger, M. A., Romero M. F., Peng J. B., Rolfs A., Takanaga H., and Bruford E. A. 2004. 'The ABCs of Solute Carriers: Physiological, Pathological and Therapeutic Implications of Human Membrane Transport Proteins'. *Pflugers Archiv European Journal of Physiology* 447 (5): 465–68.

Hewitt, N. J., Lechón M. J.G., Houston J. B., Hallifax D., Brown S. H., Maurel P., Kenna J. G., et al. 2007. 'Primary Hepatocytes: Current Understanding of the Regulation of Metabolic Enzymes and Transporter Proteins, and Pharmaceutical Practice for the Use of Hepatocytes in Metabolism, Enzyme Induction, Transporter, Clearance, and Hepatotoxicity Studies'. *Drug Metabolism Reviews* 39 (1): 159–234.

Hewitt, N. J., de Kanter R., and LeCluyse E. 2007. 'Induction of Drug Metabolizing Enzymes: A Survey of in Vitro Methodologies and Interpretations Used in the Pharmaceutical Industry--Do They Comply with FDA Recommendations?' *Chemico-Biological Interactions* 168 (1): 51–65.

Ho, E. N. M., Leung D. K.K., Wan T. S. M., and Yu N. H. 2005. 'Metabolic Studies of Methenolone Acetate in Horses'. *Analytica Chimica Acta* 540 (1): 111–19.

Ho, E. N.M, Kwok W. H., Leung D.K K., Wan T. S. M., and Wong A. S Y. 2007. 'Metabolic Studies of Turinabol in Horses'. *Analytica Chimica Acta* 586 (1–2 SPEC. ISS.): 208–16. doi:10.1016/j.aca.2006.09.053.

Hoffmaster, K. A., Turncliff R. Z., LeCluyse E. L., Kim R. B., Meier P. J., and Brouwer K. L. R. 2004. 'P-Glycoprotein Expression, Localization, and Function in Sandwich-Cultured Primary Rat and Human Hepatocytes: Relevance to the Hepatobiliary Disposition of a Model Opioid Peptide.' *Pharmaceutical Research* 21 (7): 1294–1302.

Hollenberg, P. F. 2002. 'Characteristics and Common Properties of Inhibitors, Inducers, and Activators of CYP Enzymes.' *Drug Metabolism Reviews* 34 (1–2): 17–35.

Houston, J. B. 1994. 'Utility of In Vitro Drug Metabolism Data in Predicting In Vivo Metabolic Clearance'. *Biochemical Pharmacology* 47 (9): 1469–79.

Houston, J. B., and Carlile D. J. 1997. 'Prediction of Hepatic Clearance from Microsomes, Hepatocytes, and Liver Slices.' *Drug Metabolism Reviews* 29 (4): 891–922.

Houston, J. B., Rowland-Yeo K., and Zanelli U. 2012. 'Evaluation of the Novel in Vitro Systems for Hepatic Drug Clearance and Assessment of Their Predictive Utility'. *Toxicology in Vitro* 26 (8). Elsevier Ltd: 1265–71.

Howard, R. B., Christensen A. K., Gibbs F. A., and Pesch L. A. 1967. 'The Enzymatic Preparation of Isolated Intact Parenchymal Cells From Rat

Liver'. *Journal of Cell Biology* 35: 675–84.

Hu, M., Ling J., Lin H., and Chen J. 2004. *Use of Caco-2 Cell Monolayers to Study Drug Absorption and Metabolism*. Edited by Yan Z and Caldwell G W. *Methods in Pharmacology and Toxicology Otimization in Drug Discoveery: In Vitro Methods*. Towowa, NJ: Humana Press Inc.

ILAC. 2009. 'Accreditation Requirements and Operating Criteria for Horseracing Laboratories'.

Ionescu, C., and Caira M. R. 2005. *Drug Metabolism*. Dordrecht: Springer.

Ishibashi, H., Nakamura M., Komori A., Migita K., and Shimoda S. 2009. 'Liver Architecture, Cell Function, and Disease.' *Seminars in Immunopathology* 31 (3): 399–409.

Ishikawa, M., Sekine K., Okamura A., Zheng Y-W, Ueno Y., Koike N., Tanaka J., and Taniguchi H. 2011. 'Reconstitution of Hepatic Tissue Architectures from Fetal Liver Cells Obtained from a Three-Dimensional Culture with a Rotating Wall Vessel Bioreactor.' *Journal of Bioscience and Bioengineering* 111 (6). The Society for Biotechnology, Japan: 711–18.

Ito, K., and Houston J. B. 2004. 'Comparison of the Use of Liver Models for Predicting Drug Clearance Using in Vitro Kinetic Data from Hepatic Microsomes and Isolated Hepatocytes'. *Pharmaceutical Research* 21 (5): 785–92.

Ito, K., Iwatsubo T., Kanamitsu S., Ueda K., Suzuki H., and Sugiyama Y. 1998. 'Prediction of Pharmacokinetic Alterations Caused by Drug-Drug Interactions: Metabolic Interaction in the Liver.' *Pharmacological Reviews* 50 (3): 387–412.

Iwatsubo, T., Hirota N., Ooie T., Suzuki H., Shimada N., Chiba K., Ishizaki T., Green C. E., Tyson A., and Sugiyama Y. 1997. 'Prediction of In Vivo Drug Metabolism in the Human Liver from In Vitro Metabolism Data'. *Pharmacology & Therapeutics* 73 (2): 147–71.

Jambhekar, S. S., and Breen P. J. 2009. *Basic Pharmacokinetic*. First. London: Royal Pharmaceutical Society of Great Britain.

Jaussaud, Ph., Courtot D., Guyot J. L., and Paris J. 1987. 'Identification of a Flunixin Metabolite in the Horse by Gas Chromatography-Mass Spectrometry'. *Journal of Chromatography B: Biomedical Sciences and Applications* 423 (C): 123–30.

Jedziniak, P., Szprengier-Juszkiewicz T., Olejnik M., and Jaroszewski J. 2007. 'Determination of Flunixin and 5-Hydroxyflunixin in Bovine Plasma with HPLC-UV Method Development, Validation and

Verification'. *Bulletin of the Veterinary Institute in Pulawy* 51: 261–66.

Jenny, E., Steinijans V. W., and Seifert P. 1979. 'Pharmacokinetic Interaction of Isopropylaminophenazone and Phenyl- Butazone in the Horse'. *J. Vet. Pharmacol. Therap* 2: 101–8.

Jigorel, E., and Houston J. B. 2012. 'Utility of Drug Depletion-Time Profiles in Isolated Hepatocytes for Accessing Hepatic Uptake Clearance: Identifying Rate-Limiting Steps and Role of Passive Processes'. *Drug Metabolism and Disposition* 40 (8): 1596–1602.

Johansson, M., and Anlér E. L. 1988. 'Gas Chromatographic Analysis of Flunixin in Equine Urine after Extractive Methylation'. *Journal of Chromatography B: Biomedical Sciences and Applications* 427 (C): 55–66.

Johns, I. C., Baxter K., Booler H., Hicks C., and Menzies-Gow N. 2011. 'Conjunctival Bacterial and Fungal Flora in Healthy Horses in the UK'. *Veterinary Ophthalmology* 14 (3): 195–99.

Jones, H. M., Hallifax D., and Houston J. B. 2004. 'Quantitative Prediction of the in Vivo Inhibition of Diazepam Metabolism by Omeprazole Using Rat Liver Microsomes and Hepatocytes'. *Drug Metabolism and Disposition* 32 (5): 572–80.

Jones, H. M., and Houston J B. 2004. 'Substrate Depletion Approach for Determining in Vitro Metabolic Clearance: Time Dependencies in Hepatocyte and Microsomal Incubations'. *Drug Metabolism and Disposition* 32 (9): 973–82.

Jouin, D., Blanchard N., Alexandre E., Delobel F., David-Pierson P., Lavé T., Jaeck D., Richert L., and Coassolo P. 2006. 'Cryopreserved Human Hepatocytes in Suspension Are a Convenient High Throughput Tool for the Prediction of Metabolic Clearance'. *European Journal of Pharmaceutics and Biopharmaceutics* 63 (3): 347–55.

Kanazawa, H., Okada A., Matsushima Y., Yokota H., Okubo S., Mashige F., and Nakahara K. 2002. 'Determination of Omeprazole and Its Metabolites in Human Plasma by Liquid Chromatography-Mass Spectrometry'. *Journal of chromatography.A* 949 (1–2): 1–9.

Kasai, S., and Mito M. 1993. 'Large Scale Cryopreservation of Isolated Dog Hepatocytes.pdf'. *Cryobiology* 30: 1–11.

Kemmer, Gerdi, and Sandro Keller. 2010. 'Nonlinear Least-Squares Data Fitting in Excel Spreadsheets'. *Nature Protocols* 5 (2). Nature Publishing Group: 267–81.

Khetani, S. R., and Bhatia S. N. 2007. 'Microscale Culture of Human Liver

Cells for Drug Development'. *Nature Biotechnology* 26 (1): 120–26.

Kietzmann, T. 2017. 'Metabolic Zonation of the Liver : The Oxygen Gradient Revisited'. *Redox Biology* 11: 622–30.

Kim, Mihye, Ji Youn Lee, Caroline N. Jones, Alexander Revzin, and Giyoong Tae. 2010. 'Heparin-Based Hydrogel as a Matrix for Encapsulation and Cultivation of Primary Hepatocytes'. *Biomaterials* 31 (13). Elsevier Ltd: 3596–3603.

Klingenberg, M. 1958. 'Pigments of Rat Liver Microsomes'. *Archives of Biochemistry and Biophysics* 75 (2): 376–86.

Knych, H. K., Arthur R. M., Mckemie D. S., and Chapman N. 2015. 'Pharmacokinetics and Effects on Thromboxane B2 Production Following Intravenous Administration of Flunixin Meglumine to Exercised Thoroughbred Horses'. *Journal of Veterinary Pharmacology and Therapeutics* 38 (4): 313–20.

Knych, H. K., Stanley S. D., Arthur R. M., and McKemie D. S. 2016. 'Disposition of the Anti-Ulcer Medications Ranitidine, Cimetidine, and Omeprazole Following Administration of Multiple Doses to Exercised Thoroughbred Horses'. *Journal of Veterinary Pharmacology and Therapeutics* 40 (1): 92–96.

Knych, H. K., S. D. Stanley, K. N. Seminoff, D. S. McKemie, and P. H. Kass. 2016. 'Pharmacokinetics of Methocarbamol and Phenylbutazone in Exercised Thoroughbred Horses'. *Journal of Veterinary Pharmacology and Therapeutics* 39 (5): 469–77.

Kollias-Baker, C. 2005. 'NSAIDS in Equine Medicine: Best Practice'. In *The North American Veterinary Conference*, 206–8. Orlando, Florida.

Komori, M., Higami A., Imai Y., Imaoka S., and Funae Y. 1993. 'Purification and Characterization of a Form of P450 from Horse Liver Microsomes.' *Journal of Biochemistry* 114 (3): 445–48.

Kunieda, T., Maruyama M., Okitsu T., Shibata N., Takesue M., Totsugawa T., Kosaka Y., et al. 2010. 'Cryopreservation of Primarily Isolated Porcine Hepatocytes with UW Solution'. *World Journal of Gastroenterology* 16 (1): 1–14.

Kwak, H. C., Kim H. C., Oh S. J., and Kim S. K. 2014. 'Effects of Age Increase on Hepatic Expression and Activity of Cytochrome P450 in Male C57BL/6 Mice.' *Archives of Pharmacal Research*, July.

Lan, S. J., Chando T. J., Weliky I., and Schreiber E. C. 1973. 'Metabolism of Niflumic Acid-14C: Absorption, Excretion and Biotransformation by Human and Dog'. *J. Pharmacol. Exp. Ther.* 186: 323–30.

Lau, Y. Y., Sapidou E., Cui X., White R. E., Cheng K., and Plough S. 2002. 'Development of a Novel In Vitro Model to Predict Hepatic Clearance Using Fresh, Cryopreserved, and Sandwhich-Cultured Hepatocytes'. *Drug Metabolism & Disposition* 30 (12): 1446–54.

Lave, T., Dupin S., Schmitt C., Chou R.C., Jaeck D., and Coassolo P. 1997. 'Integration of in Vitro Data into Allometric Scaling to Predict Hepatic Metabolic Clearance in Man: Application to 10 Extensively Metabolized Drugs'. *Journal of Pharmaceutical Sciences* 86 (5): 584–90.

Lave, T., Schmitt-Hoffmann A. H., Coassolo P., Valles B., Ubeaud G., Brandt B. R., and Chou R. C. 1995. 'A New Extrapolation Method from Animals to Man: Application to a Metabolized Compound, Mofarotene.' *Life Sciences* 56 (26): 473-8.

Lawrence, J. N., and Benford D. J. 1991. 'Development of an Optimal Method for the Cryopreservation of Hepatocytes and Their Subsequent Monolayer Culture'. *Toxicology in Vitro* 5 (1): 39–50.

Lee, C. D., and Maxwell L. K. 2014. 'Effect of Body Weight on the Pharmacokinetics of Flunixin Meglumine in Miniature Horses and Quarter Horses'. *Journal of Veterinary Pharmacology and Therapeutics* 37 (1): 35–42.

Lee, S. M.L, Schelcher C., Demmel M., Hauner M., and Thasler W. E. 2013. 'Isolation of Human Hepatocytes by a Two-Step Collagenase Perfusion Procedure.' *Journal of Visualized Experiments* 79: 1–9.

Lees, P., and Higgins A. J. 1985. 'Clinical Pharmacology and Therapeutic Uses of Non-steroidal Anti-inflammatory Drugs in the Horse'. *Equine Veterinary Journal* 17: 83–96.

Lees, P., and Toutain P-L. 2013. 'Pharmacokinetics, Pharmacodynamics, Metabolism, Toxicology and Residues of Phenylbutazone in Humans and Horses.' *Veterinary Journal* 196 (3): 294–303.

Leite, S. B., Teixeira A. P., Miranda J. P., Tostões R. M., Clemente J. J., Sousa M. F., Carrondo M. J.T, and Alves P. M. 2011. 'Merging Bioreactor Technology with 3D Hepatocyte-Fibroblast Culturing Approaches: Improved in Vitro Models for Toxicological Applications'. *Toxicology in Vitro* 25 (4): 825–32.

Li, A. P. 2007. 'Human Hepatocytes: Isolation, Cryopreservation and Applications in Drug Development.' *Chemico-Biological Interactions* 168 (1): 16–29.

Li, A. P., Lu C., Brent J. A., Pham C., Fackett A., Ruegg C. E., and Silber P. M. 1999. 'Cryopreserved Human Hepatocytes: Characterization of

Drug-Metabolizing Activities and Applications in Higher Throughput Screening Assays for Hepatotoxicity, Metabolic Stability, and Drug-Drug Interaction Potential'. *Chemico-Biological Interactions* 121 (1): 17–35.

Li, A. P., Gorycki P. D., Hengstler J. G., Kedderis G. L., Koebe H. G., Rahmani R., de Sousas G., Silva J. M., and Skett P. 1999. 'Present Status of the Application of Cryopreserved Hepatocytes in the Evaluation of Xenobiotics: Consensus of an International Expert Panel.' *Chemico-Biological Interactions* 121 (1): 117–23.

Lin, J. H., and Lu A. Y. 1998. 'Inhibition and Induction of Cytochrome P450 and the Clinical Implications.' *Clinical Pharmacokinetics* 35 (5): 361–90.

Lloyd, T. D.R., Orr S., Skett P., Berry D. P., and Dennison A. R. 2003. 'Cryopreservation of Hepatocytes: A Review of Current Methods for Banking.' *Cell and Tissue Banking* 4 (1): 3–15.

Loretz, L. J., Li A. P., Flye M. W., and Wilson A. G. E. 1989. 'Optimization of Cryopreservation Procedures for Rat and Human Hepatocytes'. *Xenobiotica* 19: 489–98.

Lu, C., and Li A. P. 2010. *Enzyme Inhibition in Drug Discovery and Development: The Good and the Bad*. John Wiley and Sons.

Ma, J. D., Lee K. C., and Kuo G. M. 2012. 'Clinical Application of Pharmacogenomics'. *Journal of Pharmacy Practice* 25 (4): 417–27.

MacAllister, C. G., Sifferman R. L., McClure S. R., White G. W., Vatistas N. J., Holste J. E., Ericcson G. F., and Cox J. L. 1999. 'Effects of Omeprazole Paste on Healing of Spontaneous Gastric Ulcers in Horses and Foals: A Field Trial.' *Equine Veterinary Journal. Supplement* 29 (29): 77–80.

Madan, A., Dehaan R., Mudra D., Carroll K., Lecluyse E., and Parkinson A. 1999. 'Effect of Cryopreservation on Cytochrome P-450 Enzyme Induction in Cultured Rat Hepatocytes'. *Drug Metabolism and Disposition* 27 (3): 327–35.

Mahmood, I. 2007. 'Application of Allometric Principles for the Prediction of Pharmacokinetics in Human and Veterinary Drug Development'. *Advanced Drug Delivery Reviews* 59 (11): 1177–92.

Maitho, T. E., Lees P., and Taylor J. . 1982. 'Absorption and Pharmacokinetics of Phenylbutazone in Welsh Mountain Ponies'. *J. Vet. Pharmacol. Therap* 9: 26–39.

Maloney, A. G., Schmucker D. L., Vessay D. S., and Wang R. K. 1986. 'The

Effects of Aging on the Hepatic Microsomal Mixed- Function Oxidase System of Male and Female Monkeys'. *Hepatology* 6 (2): 282–87.

Marasovi, M., T. Marasovi, and M. Miloš. 2017. 'Robust Nonlinear Regression in Enzyme Kinetic Parameters Estimation'. *Journal of Chemistry* 2017: 1–12.

Marchesini, G, Bua V., Brunori A., Bianchi G., Pisi P., Fabbri A., Zoli M., and Pisi E. 1988. 'Galactose Elimination Capacity and Liver Volume in Aging Man.' *Hepatology (Baltimore, Md.)* 8 (5): 1079–83.

Marshall, J. F., and Blikslager A. T. 2011. 'The Effect of Nonsteroidal Anti-Inflammatory Drugs on the Equine Intestine'. *Equine Veterinary Journal* 43 (SUPPL.39): 140–44.

Martignoni, M., Groothuis G. MM., and de Kanter R. 2006. 'Species Differences between Mouse, Rat, Dog, Monkey and Human CYP-Mediated Drug Metabolism, Inhibition and Induction'. *Expert Opinion on Drug Metabolism & Toxicology* 2 (6): 875–94.

Marttinez-Hernandez, A, and Amenta P. S. 1995. 'The Extracellular Matrix in Hepatic Regeneration'. *The FASEB Journal* 9: 1401–10.

Matsubara, T., Koike M., Touchi A., Tochino Y., and Sugeno K. 1976. 'Determination of Cytochrome in Rat Liver Homogenate'. *Analytical Biochemistry* 603: 596–603.

Mazzoleni, G., and Steimberg N. 2012. 'New Models for the In Vitro Study of Liver Toxicity : 3D Culture Systems and the Role of Bioreactors'. In *The Continuum of Health Risk Assessments*, edited by Michael G Tyshenko, 194. In Tech.

McElligott, E. M., Sommardahl C. S., and Cox S. K. 2017. 'Pharmacokinetics of Chloramphenicol Base after Oral Administration in Adult Horses'. *Journal of the American Veterinary Medical Association* 251 (1): 90–94.

McGinnity, D. F., Soars M. G., Urbanowicz R. A., and Riley R. J. 2004. 'Evaluation of Fresh and Cryopreserved Hepatocytes as in Vitro Drug Metabolism Tools for the Prediction of Metabolic Clearance'. *Drug Metabolism and Disposition* 32 (11): 1247–53.

Mckinnon, R. A., Sorich M. J., and Ward M. B. 2008. 'Cytochrome P450 Part 1 : Multiplicity and Function' 38 (1): 55–57.

Mohan, C., Long K. D., and Mutneja M. 2013. *An Introduction to Inhibitors and Their Biological Applications*. *EMD Millipore Corporation*. First Edit. Darmstadt, Germany: EMD Millipore.

Mooij, M. G., Nies A. T., Knibbe C. A.J., Schaeffeler E., Tibboel D., Schwab

M., and de Wildt S. N. 2016. 'Development of Human Membrane Transporters: Drug Disposition and Pharmacogenetics'. *Clinical Pharmacokinetics* 55 (5). Springer International Publishing: 507–24.

Mössner, L. D., Schmitz A., Theurillat R., Thormann W., and Mevissen M. 2011. 'Inhibition of Cytochrome P450 Enzymes Involved in Ketamine Metabolism by Use of Liver Microsomes and Specific Cytochrome P450 Enzymes from Horses, Dogs, and Humans'. *American Journal of Veterinary Research* 72 (11): 1505–13.

Motulsky, H., and Christopoulos A. 2003. *Fitting Models to Biological Data Using Linear and Nonlinear Regression*. GraphPad Software Inc.

Mukoyoshi, M., S. Nishimura, S. Hoshide, S. Umeda, M. Kanou, K. Taniguchi, and H. Muroga. 2008. 'In Vitro Drug-Drug Interaction Studies with Febuxostat, a Novel Non-Purine Selective Inhibitor of Xanthine Oxidase: Plasma Protein Binding, Identification of Metabolic Enzymes and Cytochrome P450 Inhibition'. *Xenobiotica* 38 (5): 496–510.

Murray, M. J. 1994. 'Equine Model of Inducing Ulceration in Alimentary Squamous Epithelial Mucosa'. *Digestive Diseases and Sciences* 39 (12): 2530–35.

Naritomi, Y., Terashita S., Kagayama A., and Sugiyama Y. 2003. 'Utiliy of Hepatocytes in Predicting Drug Metabolism: Comparision of Hepatic Clearance in Rats and Humans in Vivo and in Vitro'. *Drug Metabolism and Disposition* 31 (5): 580–88.

Naritomi, Y., Terashita S., Kimura S., Suzuki A., Kagayama A., and Sugiyama Y. 2001. 'Prediction of Human Hepatic Clearance from in Vivo Animal Experiments and in Vitro Metabolic Studies with Liver Microsomes from Animals and Humans'. *Drug Metab Dispos* 29 (10): 1316–24.

Nath, A., and Atkins W. M. 2006. 'Short Communication A Theoretical Validation of the Substrate Depletion Approach to Determining Kinetic Parameters'. *Drug Metab Dispos* 34 (9): 1433–35.

Nebbia, C. 2001. 'Biotransformation Enzymes as Determinants of Xenobiotic Toxicity in Domestic Animals.' *Veterinary Journal* 161 (3): 238–52.

Nebbia, C., Dacasto M., Rossetto Giaccherino A., Giuliano Albo A., and Carletti M. 2003. 'Comparative Expression of Liver Cytochrome P450-Dependent Monooxygenases in the Horse and in Other Agricultural and Laboratory Species'. *The Veterinary Journal* 165 (1): 53–64.

Nebbia, C., Dacasto M., and Carletti M. 2004. 'Postnatal Development of Hepatic Oxidative, Hydrolytic and Conjugative Drug-Metabolizing Enzymes in Female Horses'. *Life Sciences* 74 (13): 1605–19.

Nelatury, S. R., Nelatury C. F., and Vagula M. C. 2014. 'Parameter Estimation in Different Enzyme Reactions'. *Advances in Enzyme Research* 2 (March): 14–26.

Nieto, J. 2012. 'Diagnosing and Treating Gastric Ulcers in Horses'. *Center of Equine Health Horse Report*.

Nieto, J. E, Snyder J. R., Vatistas N. J., and Jones J. H. 2009. 'Responses To Exercise in Horses' 70 (6): 787–95.

Nikolic, K., and Agababa D. 2009. 'Prediction of Hepatic Microsomal Intrinsic Clearance and Human Clearance Values for Drugs.' *Journal of Molecular Graphics & Modelling* 28 (3): 245–52.

Nussler, A. K., Wang A., Neuhaus P., Fischer J., Yuan J., Liu L., Zeilinger K., Gerlach J., Arnold P. J., and Albrecht W. 2001. 'The Suitability of Hepatocyte Culture Models to Study Various Aspects of Drug Metabolism.' *Altex* 18 (2): 91–101.

Obach, R. S. 1999. 'Prediction of Human Clearance of Twenty-Nine Drugs From Hepatic Microsomal Intrinsic Clearance Data : An Examination of in Vitro Half-Life Approach and Nonspecific Binding To Microsomes'. *Drug Metab Dispos* 27 (11): 1350–59.

Obach, R. S., Lombardo F., and Waters N. J. 2008. 'Trend Analysis of a Database of Intravenous Pharmacokinetic'. *Pharmacology* 36 (7): 1385–1405.

Obach, R S. 1996. 'The Importance of Nonspecific Binding in in Vitro Matrices, Its Impact on Enzyme Kinetic Studies of Drug Metabolism Reactions, and Implications for in Vitro-in Vivo Correlations'. *Drug Metab Dispos* 24: 1047–49.

Obach, R Scott. 1997. 'Nonspecific Binding to Microsomes: Impact on Scale-up of'. *Pharmacology* 25 (12): 1359–69.

Ogu, C. C., and Maxa J. L. 2000. 'Drug Interactions due to Cytochrome P450.' *Proceedings (Baylor University. Medical Center)* 13 (4): 421–23.

Orr, C. 2015. 'Characterisation of Equine Cytochrome P450s'. The University of Nottingham.

Ostrowska, A., Bode C, D., Pruss J., Bilir B., Smith G. D., and Zeisloft S. 2000. 'Investigation of Functional and Morphological Integrity of Freshly Isolated and Cryopreserved Human Hepatocytes.' *Cell and*

Tissue Banking 1 (1): 55–68.

Pang, K. S., and Rowland M. 1977. 'Hepatic Clearance of Drugs . I . Theoretical Considerations of a " Well-Stirred " Model and a " Parallel Tube " Model . Influence of Hepatic Blood Flow , Plasma and Blood Cell Binding , and the Hepatocellular Enzymatic Activity on Hepatic Drug Clearance I'. *Journal of Pharmacokinetics and Biopharmaceutics* 5 (6).

Park, J-y, Kim K-Ah., and Kim Su-L. 2003. 'Chloramphenicol Is a Potent Inhibitor of Cytochrome P450 Isoforms CYP2C19 and CYP3A4 in Human Liver Microsomes These Include : Chloramphenicol Is a Potent Inhibitor of Cytochrome P450 Isoforms CYP2C19 and CYP3A4 in Human Liver Microsomes'. *Antimicrobial Agents and Chemotherapy* 47 (11): 3464–69.

Pearce, R. E., Mcintyre C. J., Madan A., Sanzgiri U., Draper A. J., Bullock P. L., Cook D. C., et al. 1996. 'Effects of Freezing , Thawing , and Storing Human Liver Microsomes on Cytochrome P450 Activity'. *Archives of Biochemistry and Biophysics* 331 (2): 145–69.

Penner, N., Woodward C., and Prakash C. 2012. 'Drug Metabolizing Enzymes and Biotransformation Reactions'. In *ADME-Enabling Technologies in Drug Design and Development*, edited by Donglu Zhang and Sekhar Surapaneni, First Edit, 545–65. John Wiley & Sons, Inc.

Pertoft, H., Laurent C. T., Låås T., and Kågedal L. 1978. 'Density Gradients Prepared from Colloidal Silica Particles Coated by Polyvinylpyrrolidone (Percoll)'. *Analytical Biochemistry* 88 (1): 271–82.

Plant, N. 2004. 'Strategies for Using in Vitro Screens in Drug Metabolism.' *Drug Discovery Today* 9 (7): 328–36.

Potter, T., Lewis R., Luker T., Bonnert R., Thom S., Wenlock M., and Paine S. 2011. 'In Silico Prediction of Acyl Glucuronide Reactivity'. *J Comput Aided Mol Des* 25: 997–1005.

Prasain, J. K. 2012. *Tandem Mass Spectrometry – Applications and Principles*. First. Rijeka: In Tech.

Prot, J. M., Videau O., Brochot C., Legallais C., Bénech H., and Leclerc E. 2011. 'A Cocktail of Metabolic Probes Demonstrates the Relevance of Primary Human Hepatocyte Cultures in a Microfluidic Biochip for Pharmaceutical Drug Screening'. *International Journal of Pharmaceutics* 408 (1–2): 67–75.

Puscas, I., Coltau M., Baican M., and Domuta G. 1999. 'Omeprazole Has a Dual Mechanism of Action : It Inhibits Both H+ K+ ATPase and Gastric

Mucosa Carbonic Anhydrase Enzyme in Humans (In Vitro and In Vivo Experiments)' 290 (2): 530–34.

Ramadori, G., Moriconi F., Malik I., and Dudas J. 2008. 'Physiology and Pathophysiology of Liver Inflammation, Damage and Repair.' *Journal of Physiology and Pharmacology : An Official Journal of the Polish Physiological Society* 59 Suppl 1 (August): 107–17.

Reed, GA, Griffin IO., and Eling TE. 1985. 'Inactivation of Prostaglandin H Synthase and Prostacyclin Synthase by Phenylbutazone. Requirement for Peroxidative Metabolism'. *Mol Pharmacol* 27: 109–14.

Rehman, Z. U., Ashraf M., Khan M. A., Jabbar M. A., and Rasheed M. A. 2012. 'Pharmacokinetics of Ketoprofen in Healthy Horses in Pakistan'. *The Journal of Animal & Plant Sciences* 22 (3): 584–87.

Reid, L. M., Fiorino A. S., Sigal S. H., Brill S., and Holst P. A. 1992. 'Extracellular Matrix Gradients in the Space of Disse: Relevance to Liver Biology.' *Hepatology (Baltimore, Md.)* 15 (6): 1198–1203.

Rijntjes, P. J., Moshage H. J., Van Gemert P. J., De Waal R., and Yap S. H. 1986. 'Cryopreservation of Adult Human Hepatocytes. The Influence of Deep Freezing Storage on the Viability, Cell Seeding, Survival, Fine Structures and Albumin Synthesis in Primary Cultures.' *Journal of Hepatology* 3 (1): 7–18.

Riley, R. J., Mcginnity D. F., and Austin R. P. 2005. 'A Unified Model for Predicting Human Hepatic , Metabolic Clearance from In Vitro Intrinsic Cearance Data in Hepatocytes and Microsomes'. *Pharmacology* 33 (9): 1304–11.

Riley, R. J., Grime K., and Weaver R. 2007. 'Time-Dependent CYP Inhibition.' *Expert Opinion on Drug Metabolism & Toxicology* 3 (1): 51–66.

Rose, R. J., Kohnke J. R., and Baggot J. D. 1982. 'Bioavailability of Phenylbutazone Preparations in the Horse'. *Equine Veterinary Journal* 14 (3): 234–37.

Roy, O., Brianceau P., Thiry J., Catala M., Montreuil C., and Fournier R. 2015. 'Comparative Efficacy of Flunixin on Prostaglandin E2 Synthesis in a Bovine Tissue Cage Model of Acute Inflammation'. *Revue Méd Vét* 166: 185–91.

Sai, Y., and Tsuji A. 2004. 'Transporter-Mediated Drug Delivery: Recent Progress and Experimental Approaches'. *Drug Discovery Today* 9 (16): 712–20.

Sams, R. A. 1987. 'Principles of Drug Disposition in the Horse'. *Veterinary*

Clinics of North America - Equine Practice 3 (1): 221–50.

Sams, R. A., Gerken D. F., and Ashcraft S. M. 1999. 'Detection and Identification of Flunixin after Multiple Intravenous and Intramuscular Doses to Horses'. *Journal of Analytical Toxicology* 23 (5): 372–79.

Scarth, J. P., Clarke A. D., Teale P., and Pearce C. M. 2010. 'Comparative in Vitro Metabolism of the "Designer" Steroid Estra-4,9-Diene-3,17-Dione between the Equine, Canine and Human: Identification of Target Metabolites for Use in Sports Doping Control'. *Steroids* 75 (10): 643–52.

Scarth, J. P., Spencer H A., Timbers S. E., Hudson S. C., and Hillyer L. L. 2010. 'The Use of in Vitro Technologies Coupled with High Resolution Accurate Mass LC-MS for Studying Drug Metabolism in Equine Drug Surveillance'. *Drug Testing and Analysis* 2 (1): 1–10.

Scarth, J. P., Teale P., and Kuuranne T. 2011. 'Drug Metabolism in the Horse: A Review.' *Drug Testing and Analysis* 3 (1): 19–53.

Schinkel, A. H., and Jonker J. W. 2003. 'Mammalian Drug Efflux Transporters of the ATP Binding Cassette (ABC) Family: An Overview'. *Advanced Drug Delivery Reviews* 55 (1): 3–29.

Schmelzer, E., Mutig K., Schrade P., Bachmann S., Gerlach J. C., and Zeilinger K. 2009. 'Effect of Human Patient Plasma Ex Vivo Treatment on Gene Expression and Progenitor Cell Activation of Primary Human Liver Cells in Multi-Compartment 3D Perfusion Bioreactors for Extra-Corporeal Liver Support'. *Biotechnology and Bioengineering* 103 (4): 817–27.

Schmitz, A., Zielinski J., and Dick B. 2014. 'In Vitro Metabolism of Testosterone in the Horse Liver and Involvement of Equine CYPs 3A89 , 3A94 and 3A95'. *J. Vet. Pharmacol. Therap* 37: 338–47.

Schmucker, D. L., J. S. Mooney, and A. L. Jones. 1978. 'Stereological Analysis of Hepatic Fine Structure in the Fischer 344 Rat. Influence of Sublobular Location and Animal Age'. *Journal of Cell Biology* 78 (2): 319–37.

Schmucker, Douglas L. 2005. 'Age-Related Changes in Liver Structure and Function: Implications for Disease?' *Experimental Gerontology* 40 (8–9): 650–59.

Schmucker, Douglas L., and Rose K Wang. 1980. 'Effects of Animal Age and Phenobarbital on Rat Liver Glucose-6-Phospahte Activity'. *Experimental Gerontology* 15: 249–61.

Schmucker, Douglas L. 1981. 'Effect of Aging and Phenobarbital on the Rat

Liver Microsomal Drug-Metabolizing System'. *Aging Dev* 4: 81–92.

Schmucker, Douglas L. 1983. 'Age-Dependent Alteration in Rat Liver Microsomal NADPH Cytochrome c (P-450) Reductase: A Qualitative and Quantitative Analysis'. *Aging Dev* 21: 137–56.

Schmucker, Douglas L. 1987. 'Effects of Aging on the Properties of Rhesus Monkey Liver Microsomal NADPH-Cytochrome c (P-450) Reductase.' *Drug Metabolism and Disposition* 15: 225–32.

Schmucker, L. D., Mooney J. S., and Albert J. L. 1977. 'Age-Related Changes in the Hepatic Endoplasmic Reticulum: A Quantitive Analysis'. *Science* 197: 1005–8.

SciKon Innovation, Inc. 2010. 'SciKon Mouse Hepatocyte Care Manual SciKon'. http://scikoninnovation.com/wp-content/ uploads/ 2011/ 10/Mouse-Hepatocyte-Care-Manual.pdf.

Seddon, T., Michelle I., and Chenery R. J. 1989. 'Comparative Drug Metabolism of Diazepam in Hepatocytes Isolated From Man, Rat, Monkey and Dog'. *Biochemical Engineering Journal* 38: 1657–65.

Segel, I. H. 1975. *Enzyme Kinetics : Behavior and Analysis of Rapid Equilibrium and Steady State Enzyme Systems*. Illustrate. New York: Wiley.

Selgen, P.O. 1976. 'Preparation of Isolated Rat Liver Cells'. *Methods in Cell Biology* 13: 29–83.

Shah, K., McCormack C. E., and Bradbury N. A. 2014. 'Do You Know the Sex of Your Cells?' *American Journal of Physiology. Cell Physiology* 306 (1): 3-18.

Sharma, R. 2012. 'Enzyme Inhibition : Mechanisms and Scope'. *Enzyme Inhibition and Bioapplications*, 3–36.

Shibata, Y., Takahashi H., Chiba M., and Ishii Y. 2002. 'PREDICTION OF HEPATIC CLEARANCE AND AVAILABILITY BY CRYOPRESERVED HUMAN HEPATOCYTES : AN APPLICATION OF SERUM INCUBATION METHOD'. *DRUG METABOLISM AND DISPOSITION* 30 (8): 892–96.

Shin, J. M., and Kim N. 2013. 'Pharmacokinetics and Pharmacodynamics of the Proton Pump Inhibitors'. *Journal of Neurogastroenterology and Motility* 19 (1): 25–35.

Shin, J. M., Cho Y. M., and Sachs G. 2004. 'Chemistry of Covalent Inhibition of the Gastric (H + , K +) -ATPase by Proton Pump Inhibitors'. *J. AM. CHEM. SOC.* 126: 7800–7811.

Shitara, Y, Sugiyama Y., Itoh T., Sato A. P. L., and Sugiyama Y. 2003. 'Inhibition on the Transporter-Mediated Hepatic Uptake as a

Mechanism of Drug-Drug Interaction'. *Japanese Pharmacology and Therapeutics* 30 (SUPPL. 2): 610–16.

Shu, Y., Wang L. S., Xu Z. H., He N., Xiao W. M., Wang W., Huang S. L., and Zhou H. H. 2000. '5-Hydroxylation of Omeprazole by Human Liver Microsomal Fractions from Chinese Populations Related to CYP2C19 Gene Dose and Individual Ethnicity.' *The Journal of Pharmacology and Experimental Therapeutics* 295 (2): 844–51.

Silva, Jose M., Stephen H. Day, and Deporah A. Nicoll-Griggith. 1999. 'Induction of Cytochrome-P450 in Cryopreserved Rat and Human Hepatocytes'. *Chemico-Biological Interactions* 121: 49–63.

Smith, R., Jones R. D. O., Ballard P. G., and Graffiths H. H. 2008. 'Determination of Microsome and Hepatocyte Scaling Factors for in Vitro/in Vivo Extrapolation in the Rat and Dog'. *Xenobiotics* 38 (11): 1386–98.

Soars, Mathew G., Peter J.H. Webborn, and Robert J. Riley. 2009. 'Impact of Hepatic Uptake Transporters on Pharmacokinetics and Drug-Drug Interactions: Use of Assays and Models for Decision Making in the Pharmaceutical Industry'. *Molecular Pharmaceutics* 6 (6): 1662–77.

Sohlenius-Sternbeck, A-K. 2006. 'Determination of the Hepatocellularity Number for Human, Dog, Rabbit, Rat and Mouse Livers from Protein Concentration Measurements'. *Toxicology in Vitro* 20 (8): 1582–1586.

Soldatow, V. Y., Lecluyse E. L., Griffith L. G., and Rusyn I. 2013. 'In Vitro Models for Liver Toxicity Testing'. *Toxicology Research* 2 (1): 23–39.

Soma, L. R., Behrend E., Rudy J., and Sweeney R. 1988. 'Disposition and Excretion of Flunixin Meglumine in Horses'. *American Journal of Veterinary Research* 49: 1894–98.

Sosef, M. N., Baust J. N., Sugimachi K., Fowler A., Tompkins R. G., and Toner M. 2005. 'Cryopreservation of Isolated Primary Rat Hepatocytes Enhanced Survival and Long-Term Hepatospecific Function'. *Annals of Surgery* 241 (1): 125–32.

Stefanski, A., Mevissen M., Möller A-M., Kuehni-Boghenbor K., and Schmitz A. 2013. 'Induction of Cytochrome P450 Enzymes in Primary Equine Hepatocyte Culture.' *Toxicology in Vitro : An International Journal Published in Association with BIBRA* 27 (7). Elsevier Ltd: 2023–30.

Stegemann, J. P., Raina S., Nicholson D. T., Jimenez P., Shah L., Cain S., Chandler B., Pitkin Z., Mullon C., and Custer L. 2000. 'Comparison of Analytical Methods for Quantitation of Isolated Porcine Hepatocyte Yields.' *Tissue Engineering* 6 (3): 253–64.

Steinberg, P., Fischer T., Kiulies S., Biefang K., Platt K-L., Oesch F., Ottger T. B., Bulitta C., Kempf P., and Hengstler J. 1999. 'Drug Metabolizing Capacity of Cryopreserved Human , Rat , and Mouse Liver Parenchymal Cells In Suspension'. *Drug Metab Dispos* 27 (12): 1415–22.

Stéphenne, X., Najimi M, and Sokal E. M. 2010. 'Hepatocyte Cryopreservation : Is It Time to Change the Strategy ?' *World Journal of Gastroenterol* 16 (1): 1–14. doi:10.3748/wjg.v16.i1.World.

Sugano, K., Kansy M., Artursson P., Avdeef A., Bendels S., Di L., Ecker G. F., et al. 2010. 'Coexistence of Passive and Carrier-Mediated Processes in Drug Transport'. *Nature Reviews Drug Discovery* 9 (8): 597–614.

Swift, B., Pfeifer N. D., and Brouwer K. L.R. 2010. 'Sandwich-Cultured Hepatocytes: An In Vitro Model to Evaluate Hepatobiliary Transporter-Based Drug Interactions and Hepatotoxicity'. *Drug Metabolism Reviews* 42 (3): 446–71.

Sykes, B. W., Underwood C., Mcgowan C. M., and Mills P. C. 2015. 'Pharmacokinetics of Intravenous, Plain Oral and Enteric-Coated Oral Omeprazole in the Horse'. *Journal of Veterinary Pharmacology and Therapeutics* 38 (2): 130–36.

Tauchi, H. 1961. 'On the Fundamental Morhology of the Senile Changes'. *Nagoya Journal of Medical Science* 24: 97–132.

Tauchi, H., and Sato T. 1962. 'Some Micromeasuring Studies of Hepatic Cells in Senility'. *Journal of Gerontology* 17 (3): 254–59.

Tauchi, H. 1961. 'On the Fundamental Morhology of the Senile Changes'. *Nagoya Journal of Medical Science* 24: 97–132.

Tennant, J. R. 1964. 'Evaluation of the Trypan Blue Technique for Determination of Cell Viability'. *Transplantation* 2 (6): 685–93.

Terry, C., Dhawan A., Mitry R. R., Lehec S. C., and Hughes R. D. 2010. 'Optimization of the Cryopreservation and Thawing Protocol for Human Hepatocytes for Use in Cell Transplantation.' *Liver Transplantation : Official Publication of the American Association for the Study of Liver Diseases and the International Liver Transplantation Society* 16 (2): 229–37.

Terry, C., Hughes R. D., Mitry R. R., Lehec S. C., and Dhawan A. 2007. 'Cryopreservation-Induced Nonattachment of Human Hepatocytes: Role of Adhesion Molecules'. *Cell Transplantation* 16 (6): 639–47.

Tietz, N. W., Shuey D. F., and Wekstein D. R. 1992. 'Laboratory Values in

Fit Aging Individuals - Sexagenarians through Centenarians'. *Clinical Chemistry* 38 (6): 1167–85.

Tilles, A. W., Baskaran H., Roy P., Yarmush M. L., and Toner M. 2001. 'Effects of Oxygenation and Flow on the Viability and Function of Rat Hepatocytes Cocultured in a Microchannel Flat-Plate Bioreactor'. *Biotechnology and Bioengineering* 73 (5): 379–89.

Tobin, T. 1986. 'Uncertainty in the " Detection Times " for Drugs in Horses'. *Journal of Equine Veterinary Science* 6 (3): 124–28.

Tobin, T., Chay S., Kamerling S., Woods W. E., Weckman T. J., Blake J. W., and Lees P. 1986. 'Phenylbutazone in the Horse: A Review'. *J. Vet. Pharmacol. Therap* 9: 1–25.

Tompkins, L. M., and Wallace A. D. 2007. 'Mechanisms of Cytochrome P450 Induction.' *Journal of Biochemical and Molecular Toxicology* 21 (4): 176–81.

Toutain, P. L. 2010a. 'How to Extrapolate a Withdrawal Time from an EHSLC Published Detection Time: A Monte Carlo Simulation Appraisal'. *Equine Veterinary Journal* 42 (3): 248–54.

Toutain, P. L. 2010b. 'Veterinary Medicines and Comppetition Animals: The Question of Medication Versus Doping Control'. In *Comparative and Veterinary Pharmacology*, edited by F. Cunningham, 391–314. Berlin: Springer.

Toutain, P. L., and Bousquet-Melou A. 2004. 'Plasma Clearance'. *J. Vet. Pharmacol. Therap* 27: 415–25.

Toutain, P. L., and Lassourd V. 2002. 'Pharmacokinetic/pharmacodynamic Approach to Assess Irrelevant Plasma or Urine Drug Concentrations in Postcompetition Samples for Drug Control in the Horse.' *Equine Veterinary Journal* 34 (3): 242–49.

Tydén, E., Tallkvist J., TjÄlve H., and Larsson P. 2009. 'P-Glycoprotein in Intestines, Liver, Kidney and Lymphocytes in Horse'. *Journal of Veterinary Pharmacology and Therapeutics* 32 (2): 167–76.

Tydén, E., Olsén L., Tallkvist J., Larsson P., and Tjälve H. 2004. 'CYP3A in Horse Intestines.' *Toxicology and Applied Pharmacology* 201 (2): 112–19.

Ullrich, V., and Schnabel K. H. 1973. 'Formation and Binding of Carbanions by Cytochrome P-450 of Liver Microsomes.' *Drug Metabolism and Disposition: The Biological Fate of Chemicals* 1 (1): 176–83.

Ulvestad, M., Björquist P., Molden E., Sberg A., and Andersson T. B. 2011. 'OATP1B1/1B3 Activity in Plated Primary Human Hepatocytes over

Time in Culture'. *Biochemical Pharmacology* 82 (9): 1219–26.

Umehara, K. I., T. Iwatsubo, K. Noguchi, and H. Kamimura. 2007. 'Functional Involvement of Organic Cation transporter1 (OCT1/Oct1) in the Hepatic Uptake of Organic Cations in Humans and Rats'. *Xenobiotica* 37 (8): 818–31.

Utesch, D., Diener B., Molitor E., Oesch F., and Platt K. L. 1992. 'Characterization of Cryopreserved Rat Liver Parenchymal Cells by Metabolism of Diagnostic Substrates and Activities of Related Enzymes'. *Biochemical Pharmacology* 44 (2): 309–15.

Van Summeren, A., Renes J., Lizarraga D., Bouwman F. G., Noben J. P., van Delft J. H. M., Kleinjans J. C. S., and Mariman E. C. M. 2013. 'Screening for Drug-Induced Hepatotoxicity in Primary Mouse Hepatocytes Using Acetaminophen, Amiodarone, and Cyclosporin a as Model Compounds: An Omics-Guided Approach.' *Omics : A Journal of Integrative Biology* 17 (2): 71–83.

Vasiliou, V., Vasiliou K., and Nebert D. W. 2009. 'Human ATP-Binding Cassette (ABC) Transporter Family'. *Human Genomics* 3 (3): 281–90.

Vatistas, N. J., Nieto J. E., Snyder J. R., and Thompson D. 1999. 'Clinical Trial to Determine the Effect of Omeprazole given Once or Twice Daily on Gastric Ulceration'. *Equine Gastric Ulceration* 29: 87–90.

Vekemans, K., and Braet F. 2005. 'Structural and Functional Aspects of the Liver and Liver Sinusoidal Cells in Relation to Colon Carcinoma Metastasis.' *World Journal of Gastroenterology* 11 (33): 5095–5102.

Videla, R., and Andrews F. M. 2009. 'New Perspectives in Equine Gastric Ulcer Syndrome'. *Veterinary Clinics of North America - Equine Practice* 25 (2): 283–301.

Vinci, B., .Duret C, Klieber S., Gerbal-Chaloin S., Sa-Cunha A., Laporte S., Suc B., Maurel P., Ahluwalia A., and Daujat-Chavanieu M. 2011. 'Modular Bioreactor for Primary Human Hepatocyte Culture: Medium Flow Stimulates Expression and Activity of Detoxification Genes'. *Biotechnology Journal* 6 (5): 554–64.

Wacher, V. J., Wu C. Y., and Benet L. Z. 1995. 'Overlapping Substrate Specificities and Tissue Distribuion of Cytochrome P450 3A and P-Glycoprotein: Implications for Drug Delivery and Activity in Cancer Chemotherapy'. *Molecular Carcinogenesis* 13: 129–34.

Wakabayashi, H., Nishiyama Y., Ushiyama T., Maeba T., and Maeta H. 2002. 'Evaluation of the Effect of Age on Functioning Hepatocyte Mass and Liver Blood Flow Using Liver Scintigraphy in Preoperative

Estimations for Surgical Patients: Comparison with CT Volumetry.' *The Journal of Surgical Research* 106 (2): 246–53.

Wallmark, B. 1989. 'Omeprazole: Mode of Action and Effect on Acid Secretion in Animals.' *Scandinavian Journal of Gastroenterology. Supplement* 166: 12–18.

Ward, R. M., and Kearns G. L. 2013. 'Proton Pump Inhibitors in Pediatrics: Mechanism of Action, Pharmacokinetics, Pharmacogenetics, and Pharmacodynamics'. *Pediatric Drugs* 15 (2): 119–31.

Wasfi, I. A., Boni N. S., Elghazali M., Zorob O., and Hadi A. 1998. 'Pharmacokinetics , Metabolism and Urinary Detection Time of Flunixin after Intravenous Administration in Camels'. *Journal of Veterinary Pharmacolgy and Therabutics* 21: 203–8.

Watanabe, T., and Tanaka Y. 1982. 'Age-Related Alterations in the Size of Human Hepatocytes'. *Virchows Archive B* 39: 9–20.

Watkins, P. B. 1997. 'The Barrier Function of CYP3A4 and P-Glycoprotein in the Small Bowel'. *Advanced Drug Delivery Reviews* 27 (2–3): 161–70.

Waymouth, C., and Varnum D. S. 1976. 'Simple Freezing Procedure for Storage in Serum-Free Media of Cultured and Tumor Cells of Mouse'. *TCA Manual / Tissue Culture Association* 2 (1): 311–313.

Wilkinson, G. N. 1961. 'Statistical Estimations in Enzyme Kinetics'. *Biochem. J.* 80: 324–32.

Wilkinson, G. R., and Shand D. G. 1975. 'A Physiological Approach to Hepatic Drug Clearance'. *Clinical Pharmacology & Therapeutics* 18 (4): 377–90.

Williams, P. A., Cosme J., Vinkovic D. M., Ward A., Angore H. C., Day P. J., Vonrhein C., Tickle I. J., and Jhoti H. 2004. 'Crystal Structures of Human Cytochrome P450 3A4 Bound to Metyrapone and Progesterone'. *Science* 305 (5684): 683–86.

Wilson, Z. E., Rostami-Hodjegan A., Burn J. L., Tooley A., Boyle J., Ellis S. W., and Tucker G. T. 2003. 'Inter-Individual Variability in Levels of Human Microsomal Protein and Hepatocellularity per Gram of Liver.' *British Journal of Clinical Pharmacology* 56 (4): 433–40.

Wisse, E., Braet F., De Zanger R., Jans D., Crabbe E., and Vermoesen A. 1996. 'Structure and Function of Sinusoidal Lining Cells in the Liver'. *Toxicologic Pathology* 24 (1): 100–111.

Worboys, P.D., Bradbury A., and Houston J.B. 1996. 'Kinetics of Drug Metabolism in Rat Liver Slices. II. Comparison of Clearance by Liver Slices and Freshly Isolated Hepatocytes'. *Drug Metabolism and*

Disposition 24: 676–81.

Wu, C. Y., and Benet L. Z. 2005. 'Predicting Drug Disposition via Application of BCS: Transport/absorption/ Elimination Interplay and Development of a Biopharmaceutics Drug Disposition Classification System'. *Pharmaceutical Research* 22 (1): 11–23.

Wu, L., Sun J., Wang L., Wang C., Woodman K., Koutalistras N., Horvat M., and Sheil A. G. R. 2000. 'Cryopreservation of Primary Porcine Hepatocytes for Use in Bioartificial Liver Support Systems'. *Transplantation Proceedings* 32 (7): 2271–72.

Wynne, H. A., Cope L. H., Mutch E., Rawlins M. D., Woodhouse K. W., and James O. F. W. 1989. 'The Effect of Age upon Liver Volume and Apparent Liver Blood Flow in Healthy Man.' *Hepatology (Baltimore, Md.)* 9 (2): 297–301.

Xu, R., Zhang Z., and Wang F. S. 2012. 'Liver Fibrosis: Mechanisms of Immune-Mediated Liver Injury.' *Cellular & Molecular Immunology* 9 (4). Nature Publishing Group: 296–301. doi:10.1038/cmi.2011.53.

Yamazaki, K., and Kanaoka M. 2004. 'Computational Prediction of the Plasma Protein-binding Percent of Diverse Pharmaceutical Compounds'. *Journal of Pharamaceutical Sciences* 93 (6): 1480–94.

Yin, J., Qiu H., Dai J., Lu Y., Zhao R., Chen L., and Meng Q. 2013. 'Prediction of Hepatic Plasma Clearance in Vivo from Gel-Entrapped Rat and Human Hepatocytes'. *Canadian Journal of Physiology and Pharmacology* 91 (2): 178–86.

Yun, K. U., Oh S. J., Oh J. M., Kang K. W., Myung C. S., Song G. Y., Kim B. H., and Kim S. K. 2010. 'Age-Related Changes in Hepatic Expression and Activity of Cytochrome P450 in Male Rats.' *Archives of Toxicology* 84 (12): 939–46.

Zamek-Gliszczynski, M. J., Hoffmaster K. A., Nezasa K. I., Tallman M. N., and Brouwer K. L.R. 2006. 'Integration of Hepatic Drug Transporters and Phase II Metabolizing Enzymes: Mechanisms of Hepatic Excretion of Sulfate, Glucuronide, and Glutathione Metabolites'. *European Journal of Pharmaceutical Sciences* 27 (5): 447–86.

Zeilinger, K., Holland G., Sauer I. M., Efimova E., Kardassis D., Obermayer N., Liu M., Neuhaus P., and Gerlach J. C. 2004. 'Time Course of Primary Liver Cell Reorganization in Three- Dimensional High-Density Bioreactors for Extracorporeal Liver Support: An Immunohistochemical and Ultrastructural Study'. *Tissue Engineering* 10 (7): 1113–24.

Zhang, D., Luo G., Ding X., and Lu C. 2012. 'Preclinical Experimental

Models of Drug Metabolism and Disposition in Drug Discovery and Development'. *Acta Pharmaceutica Sinica B* 2 (6). Elsevier: 549–61..

Zhang, H., Gao N., Tian X., Liu T., Fang Y., Zhou J., Wen Q., et al. 2015. 'Content and Activity of Human Liver Microsomal Protein and Prediction of Individual Hepatic Clearance in Vivo.' *Scientific Reports* 5. Nature Publishing Group: 1–12.

Zheng, H. X., Huang Y., Frassetto L. A., and Benet L. Z. 2009. 'Elucidating Rifampin's Inducing and Inhibiting Effects on Glyburide Pharmacokinetics and Blood Glucose in Healthy Volunteers: Unmasking the Differential Effects of Enzyme Induction and Transporter Inhibition for a Drug and Its Primary Metabolite'. *Clinical Pharmacology and Therapeutics* 85 (1): 78–85.

Zielinski, J., and Mevissen M. 2015. 'Inhibition of in Vitro Metabolism of Testosterone in Human, Dog and Horse Liver Microsomes to Investigate Species Differences'. *Toxicology in Vitro* 29 (3): 468–78.

Zou, P., Yu Y., Zheng N., Yang Y., Paholak H. J., Yu L. X., and Sun D. 2012. 'Applications of Human Pharmacokinetic Prediction in First-in-Human Dose Estimation'. *The AAPS Journal* 14 (2): 262–81.